

**Structural evolution and tectonostratigraphy of the Kheis Orogen
and its relationship to
the south western margin of the Kaapvaal Craton.**

by

Paul Hilliard

Submitted in partial fulfilment of the requirements for the degree of
Doctor of Philosophy
in the Department of Geology of the Faculty of Science
at the University of Durban-Westville.

Promoter
Prof. S. McCourt

May 1999

Declaration

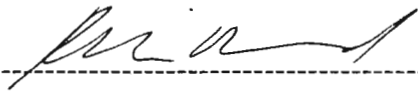
The Registrar (Academic)
University of Durban-Westville

Dear Sir

I, Paul Hilliard (registration number: 9509664), hereby declare that the dissertation entitled:

“Structural evolution and tectonostratigraphy of the Kheis Orogen and its relationship to the south western margin of the Kaapvaal Craton.”

is the result of my own investigation and research and that it has not been submitted in part, or in full, for any other degree or to any other University.



9 MAY 1999

Abstract

The focus of this project was the Early Proterozoic Kheis orogenic belt, situated in the Northern Cape Province, South Africa. A predominantly field-based study, it documents the evolution of the south-western margin of the Kaapvaal Craton, the sequence of geological events that led to deposition of the Olifantshoek Supergroup and subsequent deformation to produce the Kheis orogen.

A U-Pb single zircon (SHRIMP) radiometric age of 2853 ± 4 Ma is presented for the Draghoender granite that allows crustal growth of the Kaapvaal Craton, along its south-western margin, to be constrained between 2.83 and 2.72 Ga.

The Griqualand West Supergroup unconformably overlies the >2.72 Ga Zeekoebaart Formation and was deposited during a period of relative cratonic stability between 2.65 and 2.22 Ga. New structural evidence is presented that indicates that the Griqualand West Supergroup was deformed to produce north-south trending periclinal folds prior to, not after, deposition of the manganese rich sediments of the Voelwater Subgroup. This observation allows correlation of the Voelwater Subgroup with the iron and manganese rich Wolhaarkoorn and Manganore Formations. These economically important sediments are disconformably overlain by the Olifantshoek Supergroup.

The stratigraphy and sedimentology of the 1.93 Ga Olifantshoek Supergroup, as documented during this study, records the development of an extensional basin that developed in response to rifting of the Kaapvaal Craton, thermal subsidence and the development of the passive continental margin. Recognition of two volcano-sedimentary cycles in the Olifantshoek Supergroup indicates that two phases of rifting and thermal subsidence occurred. The rift stage of each phase was characterised by the deposition of proximal conglomerates and immature clastic sediments and was accompanied by mafic volcanism. Sedimentary rocks associated with each thermal subsidence stage record the transition from the high energy, fluvial environment of the fault controlled rift stage to marine sedimentation as the new ocean basin developed. A suite of gabbro-norite sills was recognised that intruded the Olifantshoek Supergroup prior to the Kheis orogeny.

Collisional tectonics, associated with the Kheis orogeny, along the western margin of the Olifantshoek Supergroup depository resulted in the formation of an eastward vergent fold and thrust belt termed the Kheis belt. Structural observations indicate that the Kheis orogeny was a progressive event, initiating with layer-parallel shortening, leading to the development of upright folds, followed by continuing shortening resulting in overturning of folds to the east and thrusting. A previously unrecognised thrust fault system, responsible for significant tectonic thickening of the Olifantshoek Supergroup and the Voelwater Subgroup was documented. The fold and thrust geometry of the Kheis belt suggests that tectonic inversion of pre-existing, rift related extensional faults played a significant role in the development of the Kheis belt. Hydrothermal fluids that utilised thrust sense shear zones as conduits resulted in the formation of small copper deposits on the south-eastern margin of the Kheis belt.

Previous workers have suggested that the Kheis belt is of similar age, and possibly an extension of, the Zimbabwean Magondi belt. A U-Pb single zircon (SHRIMP) radiometric age of 1997 ± 3 Ma determined during this study for the syn-Magondi orogeny Urungwe granite indicates that the two belts cannot be correlated.

Orogenesis associated with the 1.20 to 1.05 Ga extended Namaqua orogeny has strongly overprinted the south-western portion of the Kheis belt. The Spioenkop Formation, a metamorphosed sedimentary unit in the highly deformed zone was previously considered to be part of the 3.0 Ga Marydale Group. Structural and lithological data is presented to support a correlation with the Olifantshoek Supergroup. Structural elements related to the extended Namaqua orogeny are documented and compared with those recognised by previous workers in the south-western part of the Kheis belt and the Namaqua belt.

TABLE OF CONTENTS

	Page
1. INTRODUCTION	1
1.1 LOCATION OF THE STUDY AREA AND REGIONAL SETTING	1
1.2 AIMS OF THIS STUDY	2
1.3 TERMINOLOGY	6
1.4 METHODOLOGY	7
1.5 STRUCTURE OF THIS THESIS	8
2. PREVIOUS WORK	10
2.1 LITHOSTRATIGRAPHY, CHRONOSTRATIGRAPHY AND DEPOSITIONAL ENVIRONMENT	10
2.1.1 The Marydale Group.	10
2.1.2 The Draghoender granite	12
2.1.3 The Skalkseput granite	13
2.1.4 The Zeekoebaart Formation	13
2.1.5 The Griqualand West Supergroup	14
2.1.5.1 The Schmidtsdrif Subgroup	15
2.1.5.2 The Campbellrand Subgroup	15
2.1.5.3 The Asbestos Hills Subgroup	15
2.1.5.4 The Koegas Subgroup	17
2.1.5.5 The Makganyene Formation	17
2.1.5.6 The Ongeluk Formation	17
2.1.5.7 The Voelwater Subgroup	17
2.1.5.8 The Wolhaarkop and Manganore Formations	18
2.1.6 The Olifantshoek Supergroup	21
2.1.6.1 The Mapedi Formation	23
2.1.6.2 The Lucknow Formation	24
2.1.6.3 The Hartley Formation	24
2.1.6.4 The Volop Group	25
2.1.6.5 The Groblershoop Formation	26

2.1.7 Stratigraphic units of uncertain correlation in the Kheis belt and the Kaaiken domain	26
2.1.7.1 <i>The Kaaiken Group</i>	26
2.1.7.2 <i>The Wilgenhoutsdrif Group</i>	27
2.2 STRUCTURAL STUDIES OF THE BLACKRIDGE THRUST SYSTEM	28
2.3 THE NAMAQUA BELT	29
2.1 STRUCTURAL AND METAMORPHIC STUDIES OF THE SOUTH-WESTERN MARGIN OF THE KHEIS BELT, THE KAAIKEN DOMAIN AND THE EASTERN PART THE NAMAQUA BELT	31
3. THE GEOLOGY OF THE KORANNABERGE-LANGBERGE	36
3.1 LITHOSTRATIGRAPHY	36
3.1.1 The Voelwater Subgroup	37
3.1.2 The Mapedi Formation	39
3.1.3 The Lucknow Formation	40
3.1.4 The Hartley Formation	41
3.1.5 The Matsap Formation	45
3.1.5.1 <i>The Fuller member</i>	45
3.1.5.2 <i>The Ellies Rus member</i>	48
3.1.5.3 <i>The Glen Lyon member</i>	48
3.1.6 The Brulsand Formation	49
3.1.6.1 <i>The Verwater member</i>	49
3.1.6.2 <i>The Top Dog member</i>	49
3.1.7 Mafic sills	53
3.2 STRUCTURAL GEOLOGY	55
3.2.1 Fold geometry	55
3.2.2 Fold cleavage and foliations	64
3.2.3 Thrust sense shear zones	69
3.2.4 The Molopo River area	74
3.3 SUMMARY	76
3.3.1 Stratigraphy and depositional environment	76
3.3.2 The Kheis orogeny	79

4. THE GEOLOGY OF THE BOEGOEBERG DAM AREA	80
4.1 LITHOSTRATIGRAPHY	80
4.1.1 The Zeekoebaart Formation	80
4.1.2 The Griqualand West Supergroup	82
4.1.2.1 <i>The Schmidtsdrif Subgroup</i>	82
4.1.2.2 <i>The Campbellrand Subgroup</i>	85
4.1.2.3 <i>The Asbestos Hills Subgroup</i>	85
4.1.2.4 <i>The Koegas Subgroup</i>	86
4.1.2.5 <i>The Makganyene Formation</i>	86
4.1.2.6 <i>The Ongeluk Formation</i>	87
4.1.2.7 <i>The Voelwater Subgroup</i>	87
4.1.3 The Olifantshoek Supergroup	91
4.1.3.1 <i>The Mapedi Formation</i>	91
4.1.3.2 <i>The Lucknow Formation</i>	93
4.1.3.3 <i>The Hartley Formation</i>	94
4.1.3.4 <i>The Matsap Formation</i>	97
4.1.4 Mafic intrusions	98
4.2 STRUCTURAL GEOLOGY	100
4.2.1 Pre-Olifantshoek Supergroup deformation	101
4.2.2 The Kheis Orogeny	105
4.2.2.1 <i>Folding</i>	105
4.2.2.2 <i>Bedding sub-parallel simple shear</i>	110
4.2.2.3 <i>Brittle-ductile, thrust sense shear zones</i>	119
4.2.3 The extended Namaqua Orogeny	121
4.2.3.1 <i>NNW trending folds</i>	121
4.2.3.2 <i>The Doringberg fault</i>	123
4.3 SUMMARY	126
4.3.1 Stratigraphy and depositional environment	126
4.3.2 Structural geology	129
4.3.2.1 <i>Pre-Voelwater Subgroup folding</i>	129
4.3.2.2 <i>The Kheis Orogeny</i>	130

4.3.2.3 <i>The extended Namaqua Orogeny</i>	130
5. THE GEOLOGY OF THE MARYDALE BASEMENT HIGH	131
5.1 LITHOLOGY, RELATIVE AGES AND GEOCHRONOLOGY	131
5.1.1 The Marydale Group	131
5.1.2 The Draghoender granite	132
5.1.3 The Skalkseput granite	132
5.1.4 The Zeekoebaart Formation	137
5.2 STRUCTURAL GEOLOGY	139
5.3 SUMMARY	141
6. THE STRUCTURAL GEOLOGY OF THE SOUTHERN PART OF THE KAAIEN DOMAIN	143
6.1 THE MARYDALE AREA	144
6.1.1 Lithology	144
6.1.2 Structural geology	146
6.1.2.1 <i>Low strain zones</i>	146
6.1.2.2 <i>High strain zones</i>	148
6.2 THE PRIESKA POORT AREA	153
6.2.1 Locality 6.2	153
6.2.2 Locality 6.3	153
6.3 THE BLAAUWPUTS AREA	157
6.4 DISCUSSION	162
6.4.1 Correlation of structural elements observed in the Kaaien domain	162
6.4.2 Stratigraphic correlations	165
7. THE MAGONDI BELT	167
7.1 REGIONAL SETTING	167
7.2 EXISTING AGE CONSTRAINTS ON THE DEPOSITION OF THE MAGONDI SUPERGROUP AND THE TIMING OF THE MAGONDI OROGENY	170
7.3 THE URUNGWE GRANITE	170

7.4 U-Pb SINGLE ZIRCON SHRIMP DATING OF THE URUNGWE GRANITE	171
8. DISCUSSION	175
8.1 THE MARYDALE BASEMENT HIGH	175
8.2 THE ZEEKOEBAART FORMATION	176
8.3 THE GRIQUALAND WEST SUPERGROUP	177
8.4 PRE-VOELWATER SUBGROUP FOLDING OF THE GRIQUALAND WEST SUPERGROUP	178
8.5 THE VOELWATER SUBGROUP	179
8.6 THE OLIFANTSHOEK SUPERGROUP DEPOSITORY	181
8.7 THE SIGNIFICANCE OF THE MAFIC INTRUSIVES	186
8.8 THE KHEIS OROGENY	187
8.9 THE EXTENDED NAMAQUA OROGENY	199
8.10 CORRELATIONS BETWEEN THE KHEIS BELT, THE OKWA BASEMENT COMPLEX AND THE MAGONDI BELT	201
9. CONCLUSION	206
ACKNOWLEDGEMENTS	208
REFERENCES	209
LIST OF FIGURES	216
LIST OF TABLES	225
LIST OF MAPS	227

1. INTRODUCTION

1.1 Location of the study area and regional setting

The study area is situated on the western margin of an Archaean crustal block known as the *Kaapvaal Craton* (Figure 1.1). In this area, the basement rocks that form the Kaapvaal Craton are largely covered by the *Griqualand West Supergroup* (Figure 1.2), a Late-Archaean to Early-Proterozoic intracratonic supracrustal sequence (SACS¹, 1980, 1994; Beukes, 1986; Walraven and Martini, 1995). Archaean basement rocks of the Kaapvaal Craton (the Marydale Group, the Draghoender granite and the Skalkseput granite) are exposed in a north-west trending “basement window” situated west of Prieska (Figure 1.2). The granite-greenstone terrane exposed in this window is referred to as the Marydale basement high. The map pattern of the granite-greenstone terrane forming the Marydale basement high is truncated in the north by that of the enigmatic Zeekoebaart Formation, a meta-volcanic sequence of uncertain age, internal stratigraphy and stratigraphic correlation (Vajner, 1974; Smit, 1977; Altermann and Halbach, 1990, 1991).

The Zeekoebaart Formation and the Griqualand West Supergroup are overlain by the Early-Proterozoic *Olifantshoek Supergroup* (SACS, 1980; Cornell *et al.*, 1998), a regionally north-south striking, westward dipping dominantly sedimentary sequence. Deformation of this sequence, together with the older rocks in its immediate footwall, occurred during a craton-vergent orogenic event termed the *Kheis orogeny* (Stowe, 1986; Beukes and Smit, 1987), resulting in the formation of an eastward vergent fold and thrust belt. This fold and thrust belt is referred to as the *Kheis belt* (Hartnady *et al.*, 1985) and forms the focus of this investigation.

Subsequent to the Kheis orogeny, collisional tectonics along the south-western margin of the combined Kaapvaal Craton-Kheis belt resulted in the $\approx 1.20\text{--}1.05$ Ga (Thomas *et al.*, 1994) *extended Namaqua orogeny*. The Zonderhuis Formation and the Kaaien Group (Figure 1.2) are thought to represent highly deformed equivalents of the Olifantshoek Supergroup that were strongly overprinted during the north-east vergent, extended Namaqua orogeny (Botha *et al.*, 1976; Smit, 1977; Stowe, 1986). The age and stratigraphic correlation of the Spioenkop Formation is unclear from previous studies (SACS, 1980; Coward and Potgieter, 1983; Cornell *et al.*, 1986; Stowe, 1986; Scott, 1987; Humphreys *et al.*, 1988; SAGS², 1995). The eastern part of the *Namaqua belt* (Figure 1.1 and 1.2) consists of a ≈ 1.3 Ga volcanic

¹ SACS: South African Committee for Stratigraphy

² SAGS: South African Geological Survey

arc complex (the Areachap Group) that has been thrust north-eastwards over the Kheis belt and intruded by 1.2-1.1 Ga orogenic granitoids of the Keimoes suite (Thomas *et al.*, 1994).

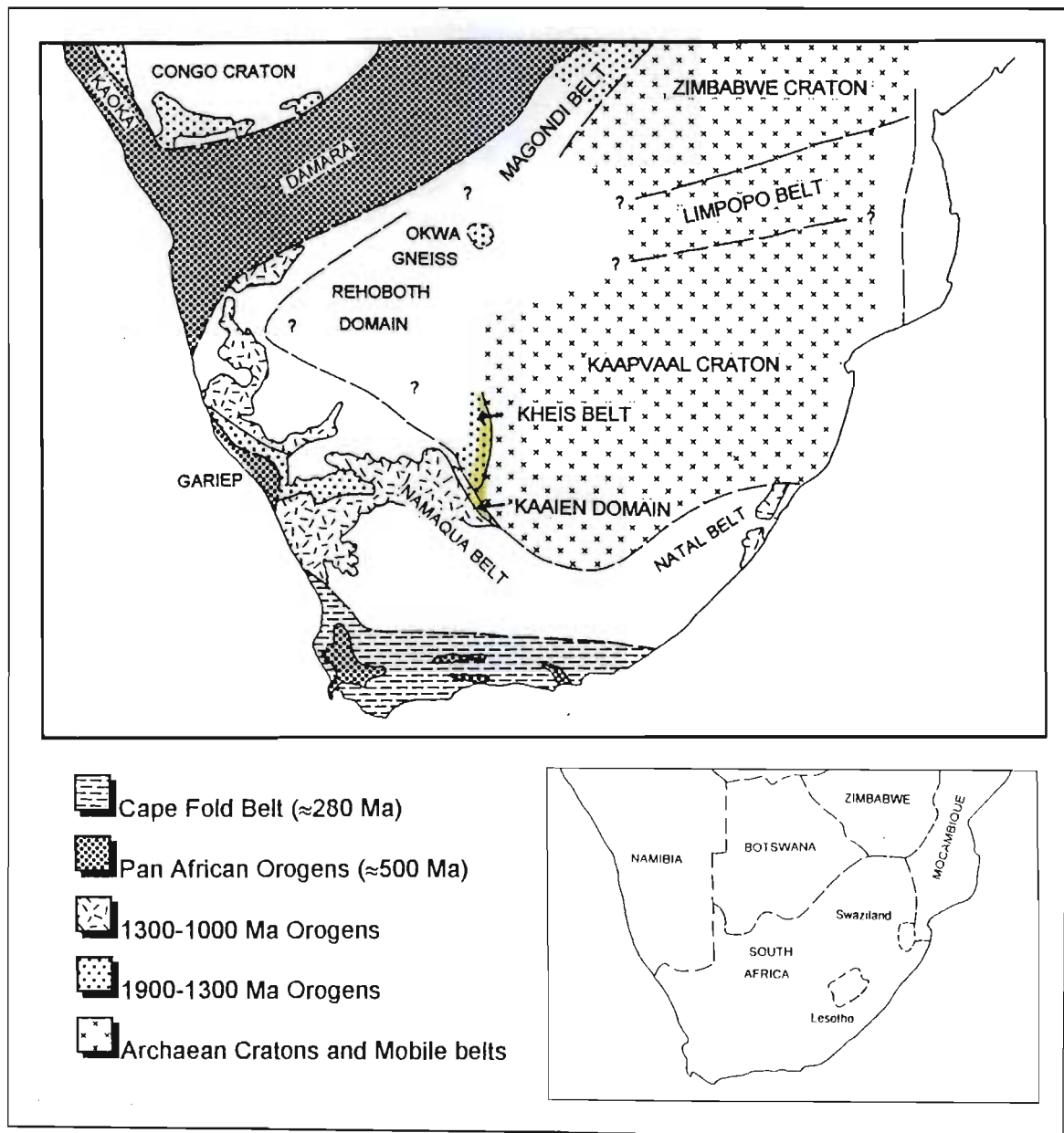


Figure 1.1: The crustal architecture of southern Africa (modified after Thomas *et al.*, 1993). The study area is indicated in colour.

1.2 Aims of this study

The principal aim of this project was to investigate the geology and geometry of the eastern margin of the Kheis belt and to determine the relationship between the Olifantshoek Supergroup, the Griqualand West Supergroup and the Kaapvaal Craton.

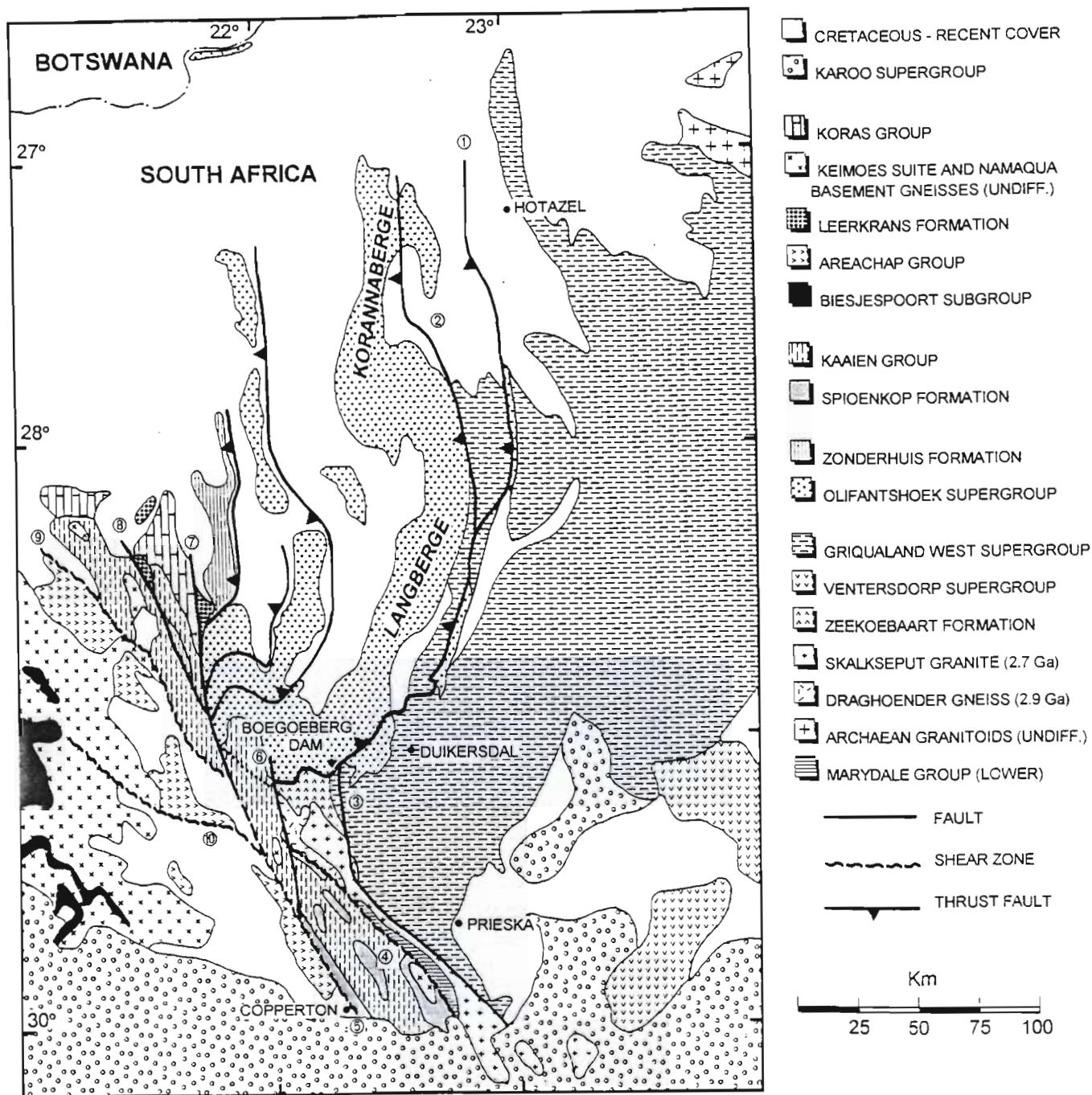


Figure 1.2: Simplified geological map of the SW part of the Kaapvaal Craton, the Kheis belt and the eastern part of the Namaqua belt. ①= Blackridge thrust; ②= Korannaberg thrust; ③= Doringberg fault; ④= Doornberg s.z (shear zone); ⑤= Copperton s.z.; ⑥= Brulpan fault; ⑦= Brakbos fault; ⑧= Dagbreek fault; ⑨= Straussberg s.z.; ⑩= Boven-Rugzeer s.z. The approximate eastern boundary of the Kheis belt is marked by ①. The boundary between the Kheis belt and the Kaaiken domain is formed by ④, ⑥, dotted line and ⑦. The boundary between the Kaaiken domain and the Namaqua belt is marked by ⑤ and ⑨. An additional copy of this Figure is located in the front map-pocket.

The tectonic setting of the Olifantshoek Supergroup depository is unclear from the published literature (Cooper, 1978; Jansen, 1983; Hartnady *et al.*, 1985; Stowe, 1986; Cornell, 1987, 1998; Cheney *et al.*, 1990). The relationship between the Griqualand West Supergroup and the Olifantshoek Supergroup is important as it represents the transition from the intracratonic Griqualand West basin to the Olifantshoek Supergroup depository. The stratigraphy and sedimentology of the upper part of the Griqualand West Supergroup, and the lower part of the Olifantshoek Supergroup, was studied in order to better constrain the nature of this transition and the tectonic setting of the Olifantshoek Supergroup depository. In order to understand this transition, it was essential to determine the structural history of the Griqualand West Supergroup prior to deposition of the Olifantshoek Supergroup.

Previous studies of the structural geology of the Kheis belt have concentrated on its south-western extremity (Figure 1.2: the area north-west of Boegoeberg Dam), where structural elements related to the Kheis orogeny have been strongly overprinted, and re-orientated, by tectonism associated with the extended Namaqua orogeny (Vajner, 1974; Smit, 1977; Botha *et al.*, 1976, 1977; Coward and Potgieter, 1983; Stowe, 1986; Scott, 1987; Humphreys and Van Bever Donker, 1987; Humphreys *et al.*, 1988). Although detailed studies of the Blackridge thrust have been made (Van Wyk, 1980; Beukes and Smit, 1987), no study of the structural geology of the Olifantshoek Supergroup rocks that form the Langberge-Korannaberge (Figure 1.2) has previously been undertaken. The structural geology of the Olifantshoek Supergroup rocks that form the Langberge-Korannaberge and the underlying Griqualand West Supergroup strata was documented in order to constrain the fold and thrust geometry of the eastern part of the Kheis belt.

The map pattern of the Zeekoebaart Formation, the Griqualand West Supergroup and the Olifantshoek Supergroup all converge in the vicinity of Boegoeberg dam (Figure 1.2). The published maps, stratigraphy and structural geology of this area are inconsistent (Vajner, 1974; Smit, 1977; Stowe, 1986; Altermann and Halbich, 1990, 1991; SAGS, 1995). The Boegoeberg dam area was studied in an effort to clarify these inconsistencies and also as the area offers a unique opportunity to study the tectono-stratigraphic relationships between the Zeekoebaart Formation, the Griqualand West Supergroup and the Olifantshoek Supergroup.

When compared to other granite-greenstone terranes of the Kaapvaal Craton, very little attention has been focused on the Marydale basement high. The only field-based study of the northern part of the Marydale basement high was undertaken by Vajner (1974), prior to distinction in the published literature between Kheis and Namaqua orogenesis. The northern part of the Marydale basement high and the Zeekoebaart

Formation were examined during this study to document any structural elements that developed during the Kheis and Namaqua orogenies.

Radiometric age constraints for the Marydale Group, although characterised by large errors, suggest that it is ≈ 3.0 Ga in age (Burger and Coertze, 1973). The Marydale Group is intruded by the Draghoender granite (Vajner, 1974). No reliable radiometric ages have been published for the Draghoender granite. The Draghoender granite was dated during this study using the single zircon, U-Pb SHRIMP (Scanning high resolution ion microprobe) technique in an effort to determine its absolute age and to provide a reliable minimum age for the Marydale Group.

The stratigraphy of the Zeekoebaart Formation is unclear from previous work (Vajner, 1974; Smit, 1977; Altermann and Halbach, 1990, 1991). Vajner (1974) and Smit (1977) have correlated the Zeekoebaart Formation with the Pniel Group of the Ventersdorp Supergroup. The age of the Pniel Group is bracketed between 2709 ± 4 Ma and 2643 ± 2 Ma (Armstrong *et al.*, 1991, Pers. Comm. R.A. Armstrong). A U-Pb whole rock age of $2135 (+74, -71)$ Ma (Armstrong, 1987) for the Zeekoebaart Formation suggests that it is considerably younger than the Pniel Group. The Zeekoebaart Formation was studied on a regional basis to determine its stratigraphy. U-Pb SHRIMP dating of the Zeekoebaart Formation was undertaken in an effort to determine its absolute age.

The age, correlation and structural geology of the Spioenkop Formation is unclear in the published geological data-base (Botha *et al.*, 1976, 1977; Coward and Potgieter, 1983; Stowe, 1986; Scott, 1987; Humphreys and Van Bever Donker, 1987; Humphreys *et al.*, 1988; SAGS, 1995). The Kaaiken Group has been tentatively correlated with the Olifantshoek Supergroup (Botha *et al.*, 1977). The Spioenkop Formation and the Kaaiken Group were studied in the southern part of the Kaaiken domain to determine their structural history and to enable suggestions to be made regarding possible stratigraphic correlations of these units. One of the aims of this study of the Kaaiken domain was to determine whether Kheis-age, thrust sense shear zones could be traced from the Olifantshoek Supergroup, around the north-west margin of the Marydale basement high, into the Kaaiken Group and Spioenkop Formation as suggested by Coward and Potgieter (1983).

The geometry, and relative timing, of structural elements produced during the extended Namaqua orogeny in the south-western part of the Kheis belt formed a subsidiary, but important part of the study. In particular, the eastern extent of structural elements related to the extended Namaqua orogeny was to be determined.

The northern and western extensions of the Kheis belt are unclear in terms of the existing geological database. Various proposals have been made as regards possible correlations between the Kheis belt, the Okwa block (Figure 1.1) and the Magondi belt (e.g. Stowe *et al.*, 1984; Carney *et al.*, 1994). These correlations are re-evaluated in light of the new data from the Kheis belt and the Magondi belt that is presented in this thesis.

1.3 Terminology

The term *belt* is used in terrane analysis (Howell, 1995) to describe a distinct assemblage of rocks that are aligned in a linear pattern. In South African literature (e.g. McCourt and Vearncombe, 1987), the term belt is generally used to indicate a linear zone of deformation of a certain age but does not imply that the rocks in that zone of deformation form a distinct assemblage. A good example of this is the Limpopo belt (Figure 1.1), which is a term used to describe a zone of deformation and metamorphism that includes the central zone (a lithologically distinct terrane) as well as the deformed margins of both the Kaapvaal and Zimbabwe Cratons.

In this thesis, the term *Kheis belt* is used to describe the approximately north-south trending fold and thrust belt situated on the western margin of the Kaapvaal Craton. The term belt is used here in the South African sense, implying only that it is a linear zone of deformation of a certain age. The eastern margin of the Kheis belt, as applied here, is defined by the eastern limit of Kheis age deformation on the Kaapvaal Craton and its Late-Archaeon to Early-Proterozoic cover-sequences.

Stowe *et al.* (1984) and Hartnady *et al.* (1985) classified the Kheis belt as a Subprovince as they considered it to form part of a much larger, Eburnian age (2.0-1.8 Ga) “Kgalagadi Province” (that also included the Okwa gneiss and the Magondi belt: Figure 1.1), situated along the western margin of the combined Kaapvaal-Zimbabwe Cratons. The Kheis belt has also been referred to as the Kheis Province (Thomas *et al.*, 1993).

In terrane analysis, Province is a general term used to describe a region characterised by either a particular structural style, a distinct stratigraphy, a unique geophysical signature or a combination of these characteristics (Howell, 1995). The term Province is used in North American literature (e.g. Hoffman, 1989) to describe Archaean cratonic blocks, that are bounded by Proterozoic orogenic belts. These Proterozoic orogenic belts are referred to by Hoffman (1989) as orogens. The use of the terms Kheis Province and Kheis Subprovince is misleading and will not be followed in this thesis.

The south-western part of the Kheis belt, that has been strongly overprinted by the extended Namaqua orogeny, is here termed the *Kaaie domain*. Structural elements in the Kaaie domain have a dominant north-west trend, parallel to that in the eastern part of the Namaqua belt. The eastern boundary of the Kaaie domain as applied here is shown on Figure 1.2. No Kheis belt sequences or structures can be recognised west of the combined Copperton-Straussburg shear zone and this lineament defines the boundary between the Kaaie domain and the Namaqua belt.

1.4 Methodology

In order to satisfy the aims of this project, as outlined above, mapping areas were selected along the length of the Korannaberge-Langberge. Four approximately east-west orientated traverses (Traverses 1-4: located inside the back cover) were made across the Langberge-Korannaberge (Map 1: located inside front cover) and, where possible, onto the Griqualand West Supergroup in the east. Traverse 1 was made across the Korannaberge to the west of Hotazel. Isolated outcrops of the Olifantshoek Supergroup in the Molopo River valley on the South Africa-Botswana border were also investigated (Map 1). Traverse 2 and 3 were made in the Olifantshoek area, Traverse 4 was made across the Langberge to the north of Volop. Mapping of the traverses was done on $\approx 1:50\,000$ scale aerial photographs, $1:50\,000$ scale topographic maps were used for ground control.

An area 23×13 km was mapped in the Boegoeberg dam area (Map 2: located inside back cover) on $\approx 1:50\,000$ scale aerial photographs, using $1:50\,000$ scale topographic maps for ground control. The Zeekoebaart Formation and the granitoids and greenstones of the Marydale basement high were investigated on a regional scale.

The Kaaie Group and Spioenkop Formation were studied in three areas (Map 1): To the east of Putsonderwater, to the west of Marydale and in road-cuttings between Copperton and Prieska.

Transmitted-light microscopy formed by far the most important component of the laboratory work during this study. Thin-sections were studied in order to determine sample lithology, as well as to study micro-fabrics associated with deformation events. Ore microscopy was utilised to determine the composition of mineralised samples. Limited use was made of an X-Ray diffraction analyser to determine the mineralogy of samples where transmitted-light microscopy proved unsuccessful.

Several rock types were selected for radiometric dating. Zircons were separated from samples and analysed by Dr R.A. Armstrong at the Australian National University using the SHRIMP.

A field trip to the Magondi Belt was undertaken with Dr H. Munyanyiwa (University of Zimbabwe) in order to collect samples for radiometric dating.

1.5 Structure of this thesis

The existing geological database relating to the study area is summarised in Chapter 2.

Chapter 3 deals with the tectonostratigraphy of the upper part of the Griqualand West Supergroup, and the Olifantshoek Supergroup rocks that form the Langberge-Korannaberge, as documented in Traverses 1-4 and Molopo River areas. Two major volcano-sedimentary cycles are identified in the Olifantshoek Supergroup. A previously unrecognised thrust system, responsible for significant tectonic thickening of the Olifantshoek and Griqualand West Supergroups, as well as the overall geometry of the Langberge-Korannaberge, is described.

The results of mapping in the Boegoeberg dam area are summarised in Chapter 4. The local stratigraphy of the Griqualand West and Olifantshoek Supergroups is presented, as well as evidence for pre-Olifantshoek Supergroup deformation of the Griqualand West Supergroup. A stratigraphic unit, previously unrecognised in the area, with associated iron and manganese mineralisation is described. The two volcano-sedimentary cycles in the Olifantshoek Supergroup, described in Chapter 3, have also been identified in the Boegoeberg dam area. The geometry and style of deformation features produced during the Kheis orogeny, including the southern extension of the Blackridge thrust system, and the effects of overprinting by the extended Namaqua Orogeny are documented.

In Chapter 5 the results of a regional study of the Archaean basement granitoids and greenstones and the Zeekoebaart Formation are presented. The results of U-Pb single zircon SHRIMP radiometric dating of the Draghoender granite are given and their implications for the crustal evolution of the south-western margin of the Kaapvaal Craton are discussed. The uncertain stratigraphy of the Zeekoebaart Formation is resolved and new observations indicating that the Skalkseput Granite is younger than the Zeekoebaart Formation are documented. Shear zone geometry in this area indicates that deformation of the basement occurred during both the Kheis and the extended Namaqua Orogeny.

Chapter 6 deals with the geology of the Kaaie Group and Spioenkop Formation in the Kaaie domain. Structural elements recognised are correlated with those documented (both during this study and by previous workers) from the Kheis belt and the Namaqua belt. Suggestions are made regarding the age and stratigraphic correlation of the Kaaie Group and the Spioenkop Formation.

In Chapter 7, the reader is introduced to the regional geology of the Magondi belt in north-west Zimbabwe. New U-Pb single zircon SHRIMP radiometric data is presented that constrains the timing of the Magondi orogeny.

In Chapter 8 the results of this study are discussed. The pre-Olifantshoek Supergroup, geological evolution of the western parts of the Kaapvaal Craton is described. Possible tectonic settings for the Olifantshoek Supergroup depository are examined. The geometry of the Kheis belt is discussed and compared with fold and thrust belts of similar geometry that have been described in the literature. Possible stratigraphic correlations of units in the south-western part of the Kheis belt and the Kaaie domain are examined in terms of the overall structural framework of the Kheis belt and the subsequent overprint during the extended Namaqua orogeny. Possible extensions of the Kheis belt and correlations with the Okwa block and Magondi belt are examined in light of the new data presented in this thesis and regional airborne magnetic imagery.

The main results of this study are concluded in Chapter 9.

2. PREVIOUS WORK

In the following section previous work dealing with the litho- and chrono-stratigraphy of the geology along the south-western margin of the Kaapvaal Craton (including the Kheis belt and the Kaaiken domain) is summarised. Where established models exist for the environment of deposition, or extrusion, of a particular stratigraphic unit, these are cited. In section 2.2 the results of structural studies of the Blackridge thrust are described. The reader is introduced to the eastern part of the Namaqua belt in section 2.3, prior to a summary of the published database concerning the structural geology and metamorphism of its foreland (viz. the south-western part of the Kheis belt and the Kaaiken domain) in section 2.4.

2.1 Lithostratigraphy, chronostratigraphy and depositional environment

Table 2.1 summarises the stratigraphy and available age constraints of the major litho-stratigraphic units in the study area. Possible correlations of units of uncertain age and stratigraphic equivalent are included in the two right hand columns.

2.1.1 The Marydale Group

The Marydale Group (SACS, 1980) crops out between the Doringberg fault and the Copperton shear zone in the area west of Prieska (Map 1). SACS (1980) subdivided the Marydale Group as shown in Table 2.2. Note that the Prieskaspoort and Doornfontein Subgroups only outcrop east of the Doornberg shear zone whereas the Spioenkop Formation only occurs west of the Doornberg shear zone (Map 1).

Burger and Coertze (1973) obtained a conventional U-Pb bulk zircon age of 2940 ± 140 Ma for the Steenkop Formation, Barton *et al.* (1986) report Pb-Pb (whole rock) minimum ages of 2915 (+120,-130) Ma for a meta-basalt in the Perdeput Formation and 3010 (+260,-300) Ma for a banded ironstone in the Modderfontein Formation. These radiometric ages, although characterised by large errors, suggest that the Prieskaspoort and Doornfontein Subgroups are approximately 3.0 Ga in age.

Xenoliths of mafic material in the ≈ 2.9 Ga Draghoender granite were correlated with the Marydale Group by Vajner (1974), supporting a Swazian age (3750-2870 Ma: SACS, 1980) for the Marydale Group. The correlation of these mafic xenoliths with the Marydale Group remains uncertain however (SACS, 1980; Barton *et al.*, 1986).

Age (Ga)	Supergroup	Group	Sub-group	Formation	Possible Correlate	Correlation Proposed by
c. 1.93	Olifantshoek	Volop		Grobbershoop	Zonderhuis Formation ¹	Smit (1977)
				Brulsand	Kaaie Group	Botha <i>et al.</i> (1976)
				Matsap		
				Hartley		
				Lucknow (upper)		
				Lucknow (lower)		
				Mapedi	Mapedi Formation	This study
c. 2.22	Griqualand West	Postmasburg	Voelwater			
				Ongeluk		
		Ghaap		Makganyene	Wolhaarkop and Manganore Fm's	Button (1976)
					Wolhaarkop and Manganore Fm's	Beukes (1978)
c. 2.45			Koegas		Wolhaarkop and Manganore Fm's	Visser (1944)
c. 2.55			Asbestos Hills		Wolhaarkop and Manganore Fm's	
c. 2.65			Campbellrand			
			Schmidtsdrif			
c. 3.00		Marydale		Zeekoebaart	Pniel Group (Ventersdorp Supergroup)	Vajner (1974)
					Spioenkop Fm ²	SACS (1980)
				Doornfontein		
			Prieskaspoot			

Table 2.1: An overview of the stratigraphy of the study area including available age constraints and proposed correlations of units of uncertain stratigraphic position.

1: The Zonderhuis Formation is the lower part of the Wilgenhoutsdrif Group. The Leerkrans Formation (upper Wilgenhoutsdrif Group) has been excluded from this table.

2: Scott (1987) proposed that the Spioenkop Formation be correlated with the Kaaie Group. SACS (1995) interpret the Spioenkop Formation to have a Mokolian metamorphic age (2070-1180Ma) but an uncertain depositional age.

The Spioenkop Formation (SACS, 1980) consists of quartzite, quartz-mica schist, quartz-feldspar gneiss and amphibolite (SACS, 1980; SACS, 1995). SACS (1980) states: "...this formation apparently overlies the Uitzigt formation conformably but the boundaries with the Doornfontein Subgroup (of which the Uitzigt Formation forms the uppermost unit) and the Korannaland Sequence (Areachap Group) are unknown". Coward and Potgieter (1983), Cornell *et al.* (1986), Stowe (1986) and Humphreys *et al.* (1988) consider the Spioenkop Formation to be part of the ≈ 3.0 Ga Marydale Group greenstone succession. Scott (1987) suggested that the Spioenkop Formation is part of the Kaaie Group. SACS

(1995) consider the Doornfontein and Prieskaspoort Subgroups to be Archaean greenstone rocks but interpret the Spioenkop Formation to be part of the Namaqua Metamorphic Province with a Mokolian metamorphic age (2070-1180 Ma: SACS, 1980) but an uncertain depositional age.

Group	Subgroup	Formation	Lithology
Marydale		Spioenkop	Immature quartzite, quartz-sericite schist with subordinate massive and streaky amphibolite
	Doornfontein	Uitzigt	Massive amphibolite (garnetiferous) and streaky amphibolite.
		Modderfontein	Banded iron-formation, dolomite, amphibolite, quartzite, greenstone.
	Prieskaspoort	Perdeput	Amygdaloidal basaltic lava, tuff, feldspathic quartzite, minor ultramafic layers, amphibolite.
		Steenkop	Conglomerate, grit, sub-greywacke, volcanoclastics, minor intercalated lava, quartzite.

Table 2.2: The lithostratigraphy of the Marydale Group after SACS (1980).

In summary, it is generally accepted that the Prieskaspoort and Doornfontein Subgroups of the Marydale Group are ≈ 3.0 Ga greenstone remnants. The age and the stratigraphic position of the Spioenkop Formation remains unclear.

2.1.2 The Draghoender granite

Vajner (1974) identified two granitoid intrusions in the area east of Marydale (Map 1) viz.: the Draghoender granite and the Skalkseput granite. The Draghoender granite comprises biotite-muscovite granite and adamellite and has a strong foliation in places, defined by layers of biotite (Vajner, *op. cit.*).

A sample described as a granitoid volcanic breccia, that was correlated by Vajner (1974) with the Draghoender granite, has been dated at ≈ 2.9 Ga (Kent, 1971: Conventional U-Pb bulk zircon). The radiometric age calculated from the analysis of the bulk zircon sample could conceivably have been influenced by the presence of inherited and xenocrystic zircons and is deemed unreliable

2.1.3 The Skalkseput Granite

The Skalkseput granite is exposed, between the Doringberg fault and the Draghoender granite, in the area east of Marydale and its outcrop pattern continues southward, west of the Doringberg fault (Map 1). Vajner (1974) described the Skalkseput granite as a light-grey, medium to coarse grained muscovite-granite. Xenoliths of biotite granitoid, resembling the Draghoender granite, occur within the Skalkseput granite, suggesting that the Skalkseput granite is younger than the Draghoender granite (Vajner, 1974).

The Skalkseput granite has been dated at 2718 ± 8 Ma using single zircon, U-Pb SHRIMP geochronology (Pers. comm. R.A. Armstrong).

2.1.4 The Zeekoebaart Formation

The Zeekoebaart Formation (SACS, 1980) is exposed in a roughly triangular map pattern to the north of the Draghoender and Skalkseput granitoids, smaller outcrops occur to the east of the Doringberg fault (Map 1).

Vajner (1974) subdivided the Zeekoebaart Formation as shown in Table 2.3. The Geelbeksdam Porphyry member, consisting of a rhyodacitic quartz porphyry lava, was interpreted to be the base of the Zeekoebaart Formation. This member only occurs to the east of the Doringberg fault (Vajner, *op. cit.*). Vajner (1974) interpreted the Waterval member (consisting of andesitic lava and pyroclastics, with interbedded conglomerate, quartzite and phyllite) to be the base of the Zeekoebaart Formation in the main outcrop area (i.e. west of the Doringberg fault). The Waterval member has subsequently been correlated with the Hartley Formation of the Olifantshoek Supergroup (Smit, 1977). Vajner (1974) described the Skalkseput conglomerate bed as a granite pebble conglomerate that unconformably overlies the Draghoender and Skalkseput granitoids. Vajner (*op. cit.*) interpreted the Skalkseput conglomerate bed to be a lateral equivalent of the Waterval member. The Blinkfontein volcanic member of Vajner (1974) consists of andesitic lava with minor tuffaceous and carbonate layers.

The uppermost unit of the Zeekoebaart Formation that was recognised by Vajner (1974) is the Witvlei conglomerate member, a poorly sorted, clast supported conglomerate only observed immediately below the Schmidtsdrif Subgroup on the eastern side of the Doringberg fault.

Member		Thickness (m)	
Witvlei conglomerate		<100	
Blinkfontein volcanic		600-900	
Waterval	Skalkseput conglomerate	400-700	0-2m
Geelbeksdam porphyry		<50	

Table 2.3: Stratigraphic subdivisions of the Zeekoebaart Formation (after Vajner, 1974).

Vajner (1974) considered the Zeekoebaart Formation to be younger than the Skalkseput granite and suggested that it is a correlate of the Pniel Group, the uppermost unit of the Ventersdorp Supergroup. Smit (1977) supported this correlation.

Armstrong (1987) obtained a U-Pb whole rock age of 2135 (+74; -71) Ma and a Rb-Sr whole rock age of 2745 ± 628 Ma for the Zeekoebaart Formation lavas. Neither of these ages are deemed to be reliable (Pers. comm. R. A. Armstrong).

2.1.5 The Griqualand West Supergroup

The Transvaal and Griqualand West Supergroups (SACS, 1980, 1994) are considered broadly equivalent in age (Walraven and Martini, 1995) and depositional environment (Button, 1976; Beukes, 1986). These lithostratigraphic and chronostratigraphic correlations have led some workers to use the same stratigraphic name for both Supergroups (viz.: Transvaal Supergroup) contrary to the formal stratigraphic nomenclature of SACS (1980, 1994). The stratigraphy of the Griqualand West Supergroup is currently under review.

The stratigraphy and sedimentology of the Griqualand West Supergroup has been intensively studied by Beukes (1978, 1979, 1980a, 1980b) and is summarised in Beukes (1983, 1984, 1986) and Beukes and Smit (1987). Authors of recent publications dealing with the Griqualand West Supergroup have utilised either the formal SACS (1980) stratigraphic subdivisions (e.g. Walraven and Martini, 1995) or the informal subdivisions proposed by Beukes (1986) and Beukes and Smit (1987) (e.g. Sumner and Bowring, 1996). The informal stratigraphy of Beukes and Smit (1987) shall be used here as: (a) it takes into account unconformities and major sedimentary facies changes and (b) it rectifies a fundamental error in the SACS (1980) stratigraphy which resulted in the inclusion of part of the Olifantshoek Supergroup within the middle of the Griqualand West Supergroup (Beukes and Smit, 1987).

Table 2.4 shows the stratigraphy of the Griqualand West Supergroup as proposed by Beukes and Smit (1987). The map pattern of the basal Schmidtsdrif Subgroup (Map 1) delimits the margin of the preserved Griqualand West Basin. The Schmidtsdrif Subgroup unconformably overlies Archaean basement granitoids to the north-east of Kuruman, the Ventersdorp Supergroup near the confluence of the Vaal and Orange rivers (Beukes, 1986) and the Zeekoebaart Formation in the vicinity of the Doringberg fault (Vajner, 1974).

2.1.5.1 The Schmidtsdrif Subgroup

The Schmidtsdrif Subgroup consists of interbedded siliclastic and carbonate sedimentary rocks, with minor volcanic units, deposited in a fluvial to shallow marine palaeo-depositional environment (Beukes, 1986). A volcanic horizon in the basal Vryburg Formation has been dated at 2643 ± 2 Ma (Pers. comm. R. A. Armstrong: U-Pb single zircon SHRIMP) constraining the onset of Griqualand West Supergroup deposition.

2.1.5.2 The Campbellrand Subgroup

The Campbellrand Subgroup conformably overlies the Schmidtsdrif Subgroup and consists of dolomite with subordinate shale, chert, limestone and volcanics. The proximal facies dolomites of the Campbellrand Subgroup are thought to have been deposited in a carbonate platform environment, the more distal facies as carbonate turbidites in deeper water (Beukes, 1986). A layered tuff from the Campbellrand Subgroup, sampled 150m below the contact with the overlying Asbestos Hills Subgroup, has been dated at 2552 ± 12 Ma (Barton *et al.*, 1994: U-Pb single zircon SHRIMP). Another volcanic horizon some 50m below the Asbestos Hills Subgroup has been dated at 2521 ± 3 Ma (Sumner and Bowring, 1996: U-Pb single zircon TIMS: Thermal ionisation mass spectrometry).

2.1.5.3 The Asbestos Hills Subgroup

The Asbestos Hills Subgroup conformably overlies the Campbellrand Subgroup (Beukes, 1986). The basal, Kuruman Formation consists of an upward shallowing sequence of micro-banded ironstones with minor phyllites, representing the transition from euxinic basin to shallow water platform facies (Beukes, 1986). The overlying Griquatown Formation consists of clastic textured banded ironstones thought to have been deposited in a shallow epeiric sea (Beukes, 1986). Tuffaceous horizons in the Kuruman and

Table 2.4: The stratigraphy of the Griqualand West Supergroup after Beukes (1986) and Beukes and Smit (1987). See text for source of age data and analytical techniques.

		Formation		Major Lithology	Approximate thickness	Age (Ma)
POSTMASBURG GROUP	Voelwater Subgroup	Mooidraai	Laterally into	Dolomite, chert	250m	
		Hotazel	Beaumont	Banded ironstone		
		Ongeluk		Andesitic lava	900m	2222±13
		Makganyene		Diamictite	50-150m	
GHAAP GROUP	KOGAS SUBGROUP	Nelani		Shale	300m	
		Rooinekke		Banded ironstone		
		Naragas		Quartz wacke, shale	240-600m	
		Kwakwas		Riebeckitic slate		
		Doradale		Banded ironstone		
		Pannetjie		Quartz wacke, shale		
	ASBESTOS HILLS SUBGROUP	Griquatown		Banded ironstone	200-300m	2432±31
		Kuruman	Manganore and Wolhaarkop on Maremane structure	Banded ironstone	150-750m	2465±7
	CAMPBELLRAND SUBGROUP	Gamohaam	Laterally into Naute and Nauga	Limestone, shale	1500-1700m	2521±3
		Kogelbeen		Dolomite, limestone		2552±11
		Klippan		Cherty dolomite		2557±49
		Papkuil		Dolomite		
		Klipfontein-Heuwel		Cherty dolomite		
		Fairfield		Sparry Dolomite		
		Reivilo		Micritic Dolomite		
Monteville		Dolomite, limestone shale				
SCHMIDTSDRIF SUBGROUP		Lokammona		Shale	10-250m	
	Boomplaas		Dolomite, limestone shale			
	Vryburg		Quartzite, shale, lava	2643±2		

Griquatown Formations have been dated at 2465 ± 7 Ma (R.A. Armstrong, U-Pb single zircon SHRIMP *In*: Walraven and Martini, 1995) and 2432 ± 31 (Trendall *et al.* 1990: U-Pb single zircon SHRIMP) respectively.

2.1.5.4 The Koegas Subgroup

The Griquatown Formation grades up into the Koegas Subgroup, thought to have been deposited in a fresh water lake (Beukes, 1986). The Koegas Subgroup comprises mainly clastic sediments viz.: mudstone, siltstone and quartz wacke but also contains minor dolomite, jaspilite and banded ironstone (SACS, 1980; Beukes, 1986).

2.1.5.5. The Makganyene Formation

The Makganyene Formation consists of diamictite, phyllite, dolomite and pyroclastics and reposes unconformably on rocks of the Koegas and Asbestos Hills Formations (Beukes, 1986). The Makganyene Formation is thought to be a glacial to glacio-lacustrine unit (Visser, 1971, Button, 1976), deposited subsequent to uplift and erosion of the older units of the Griqualand West Supergroup (Beukes, 1986). Pyroclastic material present in the Makganyene Formation is probably related to the onset of volcanism that eventually led to extrusion of the Ongeluk Formation lavas (Beukes, 1986), implying a conformable relationship between the Makganyene and Ongeluk Formations.

2.1.5.6 The Ongeluk Formation

The Ongeluk Formation consists of basaltic-andesite and andesitic lava (Cornell *et al.*, 1996) with minor intercalation's of jaspilite and agglomerate (Vajner, 1974; Beukes, 1983). Cornell *et al.* (1996) determined a 2222 ± 13 Ma age (U-Pb whole rock) for the Ongeluk Formation.

2.1.5.7 The Voelwater Subgroup

The Ongeluk Formation is overlain by the Voelwater Subgroup. Published geological maps of the area (SAGS, 1977, 1979, 1995) have shown the outcrop of the Voelwater Subgroup to be geographically restricted to the Black Rock area (Kalahari manganese field), the area to the west of the Maremane structure (Postmasburg area) and a few small exposures in the Korannaberge (Map 1). In the first two of

these areas, the Voelwater Subgroup occupies a stratigraphic position between the Ongeluk Formation lavas and the base of the Olifantshoek Supergroup.

Previous investigations of the Voelwater Subgroup have been concentrated in the Kalahari manganese field, largely as a result of extensive mining and exploration activity. In this area the Voelwater Subgroup has been subdivided into the lower, Hotazel Formation and an upper, Mooidraai Formation. The Hotazel Formation comprises jasper (massive, unstratified, bright red ferruginous chert), jaspilite (banded ironstone comprising jasper bands alternating with hematite rich bands), hematite rich banded ironstones, jacobsite (Mn-rich magnetite) rich banded ironstones and the economically important braunite lutites (finely laminated manganese ore) (Nel *et al.*, 1986; Gutzmer and Beukes, 1995). The Hotazel Formation is interpreted to be chemo-sedimentary in origin (Gutzmer and Beukes, 1995).

The nature of the contact between the banded ironstones of the Hotazel Formation and the underlying Ongeluk Formation is not clear from the published literature. Beukes (1983), Nel *et al.* (1986), and Gutzmer and Beukes (1995) consider the Hotazel Formation to conformably overlie the Ongeluk Formation lavas, as jaspilite and jasper layers, similar to those in the Hotazel Formation, occur in the upper part of the Ongeluk Formation. Jennings (1986), in a description of the geology of the Middelplaats mine (situated 15 Km south of Hotazel), noted that although the contact between the Hotazel Formation and the Ongeluk Formation is sharp, it is erosional and pre-Voelwater Subgroup palaeo-topography can be recognised in the mine area.

The Hotazel Formation is conformably overlain by interbedded dolomite, dolomite breccia and chert of the Mooidraai Formation thought to have been deposited as a prograding platform sequence (Beukes, 1983).

The Beaumont Formation, crops-out along the eastern flanks of the Korannaberge-Langberge, (Map 1) and is interpreted by Beukes (1983) to be a lateral equivalent of the Hotazel and Mooidraai Formations (Beukes, 1983). The Beaumont Formation consists of jasper and jaspilite interbedded with mafic lava, tuff and ferruginous dolomite (Beukes, *op. cit.*).

2.1.5.8 The Wolhaarkop and Manganore Formations

The Wolhaarkop Formation is a unit of chert breccia that grades upwards into undisturbed or partly brecciated and folded banded ironstones of the Manganore Formation (Van Schalkwyk and Beukes,

In detail, the Wolhaarkop Formation consists of unsorted angular fragments of chert in a hematite and manganese bearing siliceous matrix. Quartz or agate filled druses suggest that the breccia originally had an open framework structure (Van Wyk, 1980; Van Schalkwyk and Beukes, 1986).

The Manganore Formation at Sishen mine (Figure 2.1) comprises a basal carbonaceous shale, overlain by interbedded ferruginous chert and shale followed by banded ironstones that contain thickly or thinly bedded (laminated) and massive (weakly laminated) hematite iron ore (Van Schalkwyk and Beukes, 1986). Although complicated by palaeo-topography, bedding in the Manganore Formation at Sishen mine has a general north-south strike and westerly dip (Van Schalkwyk and Beukes, 1986). This is in strong contrast to the underlying Campbellrand Subgroup dolomites that dip at approximately 20° to the north-east.

Visser (1944) interpreted what is now termed the Manganore Formation to be part of the Asbestos Hills Subgroup. Button (1976) and Beukes (1978) considered the Wolhaarkop Breccia to be a superficial chert breccia that developed on an erosion surface and was subsequently covered as a result of the deposition of banded ironstones and iron ore of the Manganore Formation. Button (1976) interpreted the breccia and overlying banded ironstones to be the basal unit of the Postmasburg Group (Table 2.1). Beukes (1978) introduced the name Manganore Formation and suggested that the Manganore Formation is part of the Koegas Subgroup (Table 2.1). More recently, Van Wyk (1980), from observations in the Wolhaarkop area, and Van Schalkwyk and Beukes (1986), working in the Sishen area, correlated the Manganore Formation with the Kuruman and Griquatown Formations of the Asbestos Hills Subgroup (Table 2.1 and 2.4).

The interpretation of the Manganore Formation as an Asbestos Hills Subgroup correlate must take into account: (a) The iron and manganese rich Wolhaarkop Formation breccia that unconformably overlies the Campbellrand Subgroup dolomites. Elsewhere in the Griqualand West basin, the Asbestos Hills Subgroup conformably overlies the Campbellrand Subgroup. (b) The laminated and massive iron ore within, and localised brecciation, of the Manganore Formation.

Van Wyk (1980), Van Schalkwyk and Beukes (1986) and Grobbelaar and Beukes (1986) interpret the Wolhaarkop Formation to be a solution collapse breccia formed by slumping, into sinkholes, of the chert residue following chemical weathering of Campbellrand Subgroup carbonates. In this model, the overlying Manganore Formation is considered to represent the lower part of the Asbestos Hills Subgroup that slumped into the sinkholes. Van Schalkwyk and Beukes (1986) interpret the sinkhole development to

have taken place below the Campbellrand-Asbestos Hills Subgroup contact, during a post-Griqualand West Supergroup (i.e. post-Voelwater Subgroup), pre-Olifantshoek Supergroup period of karstic weathering and erosion. Van Schalkwyk and Beukes (1986) invoke hematization of the Asbestos Hills Subgroup and the Wolhaarkop breccia by supergene solutions, during and immediately after slumping, to explain the genesis of the iron ore deposits in the Mangano Formation and the manganese and iron enrichment of the Wolhaarkop breccia.

2.1.6 The Olifantshoek Supergroup

The Olifantshoek Supergroup (SACS, 1980, 1994) overlies rocks of the Griqualand West Supergroup with angular unconformity (Visser, 1944; Beukes and Smit, 1987). Early workers (e.g. Visser, 1944) sub-divided the lower part of the Olifantshoek Supergroup as shown in Table 2.5.

Unit	Lithology
Upper Matsap Stage	Quartzite, grit, conglomerate, shale.
Middle Matsap Stage	Conglomerate, lava, tuff, quartzite.
Lower Matsap Stage	Quartzite, shale, conglomerate, limestone.

Table 2.5: Lithostratigraphy of the Olifantshoek Supergroup after Visser (1944).

SAGS (1977) and SACS (1980), sub-divided the Olifantshoek Supergroup as shown in Table 2.6. The Lower Matsap Stage of Visser (1944) was divided into the Mapedi and Lucknow Formations, the Middle Matsap Stage was renamed the Hartley Formation. The Upper Matsap Stage was renamed the Volop Group and divided into the Matsap and Brulsand Formations.

Group	Formation	Lithology	Thickness (m)
	Groblershoop	Quartzite, schist, micaceous-quartzite, amphibolite.	>2000
Volop	Brulsand	Quartzite, shale, sub-greywacke.	>4032
	Matsap	Quartzite,sub-greywacke,conglomerate.	
	Hartley	Lava,tuff,quartzite,sub-greywacke, conglomerate.	762
	Lucknow	Quartzite,phyllite, dolomitic limestone.	137-195
	Mapedi	Conglomerate, phyllite, quartzite, lava.	

Table 2.6: Lithostratigraphy of the Olifantshoek Supergroup after SACS (1980).

Although originally considered to be an older stratigraphic unit thrust over the Olifantshoek Supergroup (Vajner, 1974), it has since been recognised that the Groblershoop Formation (Table 2.6) conformably overlies the Volop Group (Botha *et al.*, 1976; Smit, 1977; Stowe, 1986).

A narrow unit of interbedded phyllite and quartzite (overlying the Campbellrand Subgroup dolomites and underlying the Ongeluk Formation lavas) crops out in the footwall of the Blackridge thrust on the western side of the Maremane structure (this unit is indicated as the Mapedi Formation on Map 1). Although originally mapped by Visser (1944) as part of the Lower Matsap Stage (Table 2.5), Button (1976) and SACS (1980) interpreted these clastic sediments to be an unconformity bounded unit of the Griqualand West Supergroup and termed it the Gamagara Formation. Beukes and Smit (1987) presented strong stratigraphic and structural evidence that the Mapedi Formation is an equivalent of the Gamagara Formation that has been duplicated by the Blackridge Thrust. The proposal of Beukes and Smit (1987) is followed here, and as indicated on Map 1, both the “Gamagara Formation” and the Mapedi Formation are referred to as the Mapedi Formation.

Cooper (1978) suggested that the Olifantshoek Supergroup was deposited in a north-south striking “*ensialic rift*” that developed as a result of an “*aborted attempt at continental drift*”. This interpretation was based on observations made in the Magondi belt and the apparent alignment of the Magondi Belt with the Kheis belt (Figure 1.1). Hartnady *et al.* (1985) and Stowe (1986) suggested that the Olifantshoek Supergroup was deposited as a series of overlapping clastic wedges, prograding westwards from the Kaapvaal Craton, but gave no indication of the tectonic setting of the Olifantshoek Supergroup depository.

Jansen (1983) made a detailed study of the sedimentology of the Volop Group along several type-sections. Jansen (*op. cit.*) suggested that the Volop Group represents a fluvial to shallow-marine sequence deposited in a fault-bounded extensional setting.

Cornell (1987) studied the stratigraphy of the Hartley Formation and the mineralogy and petrology of the Hartley Formation lavas. On the basis of this study, Cornell (*op. cit.*) concluded that the Hartley Formation was deposited/extruded in extensional fault-bounded basins, that developed as a result of rifting of the Kaapvaal Craton and that the overlying sediments of the Volop Group and the Groblershoop Formation are a “*miogeosynclinal sequence*” that reflect the development of an approximately north-south trending passive continental margin. No process related studies were made of any of the sedimentary rocks to confirm this conclusion. The geochemistry of the Hartley Formation lavas as

reported by Cornell *et al.* (1998) suggested that they were extruded in a subduction related setting. Cornell *et al.* (1998) nevertheless favoured a rift-related setting, suggesting that the subduction related signature of the Hartley Formation lavas reflects the “*Archaean processes involved in the origin of the Kaapvaal lithosphere or lower crust*”. The only observations noted by Cornell *et al.* (1998) to support a rift related origin were the “*conglomerates of greatly variable thickness*”.

Cheney *et al.* (1990) correlated the Olifantshoek Supergroup with the Waterberg, Soutpansberg and Palapye Groups and considered each group to represent an erosional remnant of a much larger basin that once covered large tracts of the combined Kaapvaal-Zimbabwe Craton.

2.1.6.1 The Mapedi Formation

The Mapedi Formation is the basal unit of the Olifantshoek Supergroup. It comprises a discontinuous basal conglomerate, overlain by several upward coarsening phyllite-quartzite cycles thought to have been deposited in a fluvio-deltaic palaeo-environment (Beukes and Smit, 1987). An amygdaloidal lava unit, with associated tuff and agglomerate, up to 700m thick, was reported to occur near the top of the Mapedi Formation (Beukes and Smit, 1987). Schütte (1993) interpreted this lava horizon to be a thrust emplaced slice of Ongeluk Formation lava.

The basal conglomerate of the Mapedi Formation unconformably overlies rocks of the Griqualand West Supergroup. At the Sishen and Beeshoek mines (Map 1), the conglomerate is comprised of clasts of Manganore Formation banded ironstone and iron ore in a ferruginous matrix and it is mined for its iron ore content (Van Schalkwyk and Beukes, 1986; Grobbelaar and Beukes, 1986).

In the vicinity of Glosam (Map 1), the Mapedi Formation shale overlies a palaeo-karstic erosion surface on the Campbellrand Subgroup dolomites. Crystalline bixbyite manganese ore is developed at the unconformity, in palaeo-topographic lows on the erosion surface. This manganese ore (which was previously exploited at several mines in the Glosam area) has been interpreted as manganiferous vad that accumulated in palaeo-sinkholes on the pre-Mapedi Formation erosional surface and subsequently recrystallised as bixbyite following deposition of the Olifantshoek Supergroup (Grobbelaar and Beukes, 1986).

2.1.6.2 *The Lucknow Formation*

In the area west of Wolhaarkop (Map 1), the Mapedi Formation is conformably overlain by the Lucknow Formation (Beukes and Smit, 1987). The lower part of the Lucknow Formation consists of upward coarsening quartzite-phyllite cycles capped by trough cross-bedded quartzose dolomite units. The upper part of the Lucknow Formation consists of a basal conglomerate overlain by trough cross-bedded quartzites with minor phyllites that were deposited in a braided stream, fluvial environment (Beukes and Smit, 1987). The conglomerate at the base of these fluvial deposits marks an intra-formational unconformity (Beukes and Smit, 1987). In the area north of Wolhaarkop (Map 1), progressively more of the lower part of the Lucknow Formation has been eroded at this unconformity. In the area south-west of Dibeng (based on borehole evidence), the upper part of the Lucknow Formation rests unconformably on the Mapedi Formation (Beukes and Smit, 1987). In the area west of Hotazel (based on borehole evidence), less than 50m of the Mapedi Formation is preserved below the unconformity (Beukes and Smit, 1987).

During the field work for this study, the presence of this major unconformity was confirmed and it was observed that in certain areas the upper part of the Lucknow Formation directly overlies rocks of the Griqualand West Supergroup. As it is considered more appropriate to use an unconformity (marking a major depositional hiatus) as a formation boundary, rather than a conformable contact, the lower part of the Lucknow Formation (i.e. that which conformably overlies the Mapedi Formation of Beukes and Smit, 1987) is here included in the Mapedi Formation (as indicated on Table 2.1). The base of the Lucknow Formation is taken to be the intra-formational unconformity recognised by Beukes and Smit (1987).

2.1.6.3 *The Hartley Formation*

The Hartley Formation (SACS, 1980) consists primarily of basaltic lavas (Smit, 1977; Cornell, 1987) with interbedded tuff, agglomerate and clastic sediments. Rare units of porphyritic (quartz-feldspar-hornblende) andesite are interlayered with the basalts (Cornell *et al.*, 1998). The Hartley Formation crops out along the eastern flanks of the Korannaberge-Langberge and in the vicinity of Boegoeberg dam (Map 1). Smit (1977), working in the Boegoeberg dam area, suggested that the Hartley Formation conformably overlies the Griqualand West Supergroup and that a transitional banded ironstone is developed at the base of the Hartley Formation. SACS (1980), with reference to the Olifantshoek area, noted the presence of a conglomerate (the Neylan bed) at the base of the Hartley Formation and considered the Hartley Formation to unconformably overlie the Lucknow Formation. Work done during this project indicates that the base

of the Hartley Formation is a major unconformity and that the Hartley Formation unconformably overlies older strata of the Olifantshoek and Griqualand West Supergroups.

Smit (1977) and SACS (1980) interpret the contact between the Hartley Formation and the overlying Matsap Formation to be conformable and suggest that the top of the Hartley Formation is marked by the uppermost volcanic horizon.

Crampton (1974), using Rb-Sr whole rock geochronology, obtained a radiometric age of 2070 ± 90 Ma for the Hartley Formation and this date been utilised to define the lower boundary of the Mokolian Erathem (SACS, 1980). The age of the Hartley Formation has recently been more accurately constrained using the Pb-Pb single zircon Kober (1986) evaporation method by Cornell *et al.* (1998), who determined an age of 1928 ± 4 Ma.

2.1.6.4 The Volop Group

The Hartley Formation is conformably overlain by the Volop Group (SACS, 1980). Table 2.7 shows the lithostratigraphy of the Volop Group after SACS (1980). According to these workers, the lower part of the Volop Group (Matsap Formation) consists of brown, purple and grey quartzites with gritty brown sub-greywacke. The overlying Brulsand Formation consists of grey quartzite with minor shale and sub-greywacke. SACS (1980) estimate the thickness of the Volop Group to exceed 4000m.

Formation	Member	Lithology
Brulsand	Vuilnek	White, grey and pink quartzite, phyllite, sub-greywacke.
	Top Dog	White, grey and pink quartzite, phyllite, sub-greywacke
	Verwater	Grey quartzite with hematite nodules
Matsap	Glen Lyon	Grey and brown coarse grained sub-greywacke, conglomerate
	Ellies Rus	Grey or purple quartzite, brown sub-greywacke
	Fuller	Coarse grained brown quartzite and sub-greywacke,conglomerate

Table 2.7: Lithostratigraphy of the Volop Group after SACS (1980).

Jansen (1983) recognised two upward fining sedimentary cycles in the Volop Group, that he interpreted to record an overall marine transgression. Polymodal but unidirectional, south to west directed palaeocurrent directions and preserved sedimentary structures suggest a fluvial braid-stream palaeo-depositional environment for the lower part of the Volop Group (Matsap Formation). Preserved sedimentary structures in the Brulsand Formation indicate a shallow marine palaeo-environment (Jansen, 1983).

2.1.6.5 *The Groblershoop Formation*

Except for the Skurweberge (formed by a resistant unit of quartzite and micaceous quartzite), the Groblershoop Formation (SACS, 1980) is poorly exposed in the region west of the Korannaberger-Langberge (Map 1). Reasonable outcrop is however present in the Orange River valley between Grootdrink and Boegoeberg dam and as such, the majority of the previous work dealing with the Groblershoop Formation has been concentrated in this area.

The Groblershoop Formation comprises quartz-mica pelitic schist, micaceous quartzite and orthoquartzite with minor amounts of amphibolite and amphibolitic-schist (Stowe, 1986; Schlegel, 1988). No consistency has been maintained in published studies of the Groblershoop Formation with regard to its internal stratigraphy (Vajner, 1974; Botha *et al.*, 1976; Smit, 1977; SACS, 1980; Stowe, 1986; Schlegel, 1988).

2.1.7 Stratigraphic units of uncertain correlation in the Kheis belt and the Kaaian Domain

In the south-western part of the Kheis belt and the Kaaian domain, stratotypes thought to be equivalent to the Olifantshoek Supergroup have been strongly overprinted by the extended Namaqua Orogeny (Stowe, 1986). Due to the structural complexity and metamorphic overprint, correlations between stratigraphic units in this area and the Olifantshoek Supergroup are equivocal. These units of uncertain correlation have historically been assigned different stratigraphic nomenclature (viz. the Kaaian Group and the Wilgenhoutsdrif Group).

2.1.7.1 *The Kaaian Group*

The lithostratigraphy of the Kaaian Group, as proposed by SACS (1980), is shown in Table 2.8. Botha *et al.* (1976) and Smit (1977) correlated the Uitdraai Formation, the Sultanaoord Formation and the Dagbreek Formation (SACS, 1980 nomenclature used) with the Top Dog member of the Volop Group.

Formation	Lithology
Uitdraai	Banded or massive grey quartzite, quartz-mica schist
Sultanaoord	White quartzite, subordinate phyllite
Dagbreek	Quartz-mica schist, quartzite, amphibolite

Table 2.8: The lithostratigraphy of the Kaaie Group after SACS (1980).

The Dagbreek Formation and the overlying Sultanaoord Formation (SACS, 1980), are exposed between the Straussburg shear zone and the Brakbos fault (Map 1). Barton and Burger (1983) presented a 1800 Ma maximum age for the Dagbreek Formation based on U-Pb analyses of detrital zircons. This age is deemed to be unreliable as each of the samples analysed comprised a bulk zircon sample and could conceivably represent a mixture of zircons from different age source rocks. R.A. Armstrong (Pers. comm.) dated detrital zircons from the Sultanaoord Formation using the single zircon U-Pb SHRIMP technique. The results of that study indicated a maximum depositional age of 1850 Ma.

The Uitdraai Formation is exposed in a north-west trending zone; bounded by the combined Brakbos fault-Copperton shear zone and the Brulpan fault-Doornberg shear zone; that extends from Groblershoop to south-east of Copperton (where it is covered by the overlying Karoo Supergroup rocks). In the northern part of this zone, the Uitdraai Formation is overlain, along a sheared contact, by the Groblershoop Formation (Moen, 1980). U-Pb single zircon SHRIMP analyses of detrital zircons from the Uitdraai Formation indicate a maximum depositional age of 1850 Ma (Pers. comm. R.A. Armstrong).

2.1.7.2 The Wilgenhoutsdrif Group

Smit (1977) mapped part of the Wilgenhoutsdrif Group and correlated it with the Groblershoop Formation. Moen (1980) remapped the Wilgenhoutsdrif Group and subdivided it into a lower, mainly sedimentary, Zonderhuis Formation and an upper, mainly volcanic, Leerkrans Formation. The Zonderhuis Formation and the Leerkrans Formation are exposed to the west of the Skurweberge, in the vicinity of Grootdrink (Map 1).

The Zonderhuis Formation comprises a basal quartzite unit overlain by dolomite, irregular serpentinite lenses, ferruginous quartzite, quartzite, mafic and pelitic schists and mafic lava (Moen, 1980). To the east of Grootdrink (Map 1), the Zonderhuis Formation has been thrust over schists and micaceous quartzite of the Groblershoop Formation (Moen, 1980; Stowe, 1986). To the south-east of Sultanaoord (Map 1), the

Zonderhuis Formation rests with sheared contact (Moen, 1980) on meta-sediments of the Sultanaoord Formation (Kaaie Group). The stratigraphic relationship between the Zonderhuis Formation, the Kaaie Group and the Olifantshoek Supergroup is not clearly understood.

The Zonderhuis Formation is overlain by sheared and metamorphosed: bimodal (rhyolitic and basaltic) lavas and tuffs, ferruginous chert, quartzite, conglomerate and schist of the Leerkrans Formation (Moen, 1980). Moen (1980) considered the Leerkrans Formation to conformably overlie the Zonderhuis Formation, whereas Stowe (1986) showed that structural elements (folds and foliation) produced during the Kheis orogeny are present in the Zonderhuis Formation but absent in the Leerkrans Formation, indicating an unconformable relationship.

Barton and Burger (1983), using Rb-Sr whole rock geochronology, obtained a radiometric age of 1331 ± 100 Ma for a meta-basaltic lava from the Leerkrans Formation. They obtained similar age dates (1336 and 1287 Ma- no errors given) utilising conventional U-Pb, bulk zircon radiometric dating of two zircon concentrates from a single sample of Leerkrans Formation felsic lava. R.A. Armstrong (Pers. comm.) has recently dated a felsic lava in the Leerkrans Formation (using the more precise, single zircon U-Pb SHRIMP technique) and obtained a crystallisation age of ≈ 1240 Ma.

2.2 Structural studies of the Blackridge thrust system

The Griqualand West Supergroup was subject to east-west orientated compression, producing north-south trending periclinal folds (such as the Ongeluk-Witwater syncline: Map 1), prior to the deposition of the Olifantshoek Supergroup (Visser, 1944; Beukes and Smit, 1987). The cause of this deformation remains unclear.

Studies by Boardman (1941), Visser (1944), Van Wyk (1980) and Beukes and Smit (1987) have shown that eastward vergent folds and thrusts are developed to the east of the Langberge-Korannaberge. These structural elements have been correlated by Beukes and Smit (1987) with the Kheis orogeny of Stowe (1986) and will be further discussed here.

Boardman (1941) and Visser (1944) described a north-south striking, west dipping thrust fault, to the west of the Maremane structure (Map 1), along which rocks of the Griqualand West Supergroup have been juxtaposed over the basal clastic sediments of the Olifantshoek Supergroup. Visser (1944) termed

this thrust fault the Gamagara thrust, but as he considered the Wolhaarkop Formation to be a tectonic breccia, the map pattern of the thrust system was, to a large extent, incorrect.

Van Wyk (1980) interpreted the Wolhaarkop Formation to be a solution collapse breccia, remapped the Gamagara thrust, and termed it the Blackridge thrust. Subsequent workers (e.g. Beukes and Smit, 1987) have utilised the nomenclature of Van Wyk (1980).

Beukes and Smit (1987), using data from exploration diamond drilling and the manganese mines, showed that the Blackridge thrust continues as far north as Black Rock (Map 1), where it branches into an imbricate system. The thrust system cannot be traced any further north than Black Rock due to a lack of exposure and borehole information. The Blackridge thrust has been traced southwards (Map 1) as far as the Duikersdal area (SAGS, 1977). Stowe (1986) suggested that the Blackridge thrust follows an arcuate trace west of Duikersdal, linking up with the ENE-WSW striking, north dipping thrusts recognised by Vajner (1974) in the Boegoeberg dam area.

In general, the Blackridge thrust dips at very gentle angles to the west and is marked by a narrow zone of phyllonite and/or mylonite (Beukes and Smit, 1987). The Griqualand West Supergroup rocks are only weakly deformed in the footwall of the Blackridge thrust (Visser, 1944), which led Beukes and Smit (1987) to suggest that the Blackridge thrust is the sole thrust of the Kheis belt.

Visser (1944) and Jansen (1983) described upright periclinal folds that are developed in the Volop Group rocks that form the Langberge and observed that the folding in the western part of the mountain chain is much more intense than that in the east. Visser (1944) considered these folds to be related to the same phase of deformation that produced the Blackridge thrust.

2.3 The Namaqua Belt

The *Namaqua-Natal Orogen* (equivalent to the Namaqua-Natal Metamorphic Province of Thomas *et al.*, 1994) is a high-grade orogenic belt that extends from northern Namibia to the Indian Ocean (Figure 1.1). The orogen is obscured in the central parts by Phanerozoic cover rocks of the Karoo Supergroup and continuity between the *Namaqua belt* and the *Natal belt* (Figure 1.1) is based on geophysical observations. The age and number of terranes that comprise the Namaqua belt remains unclear, although it is recognised that much of Namaqualand comprises $\approx 1600\text{--}1300$ Ma volcano-sedimentary successions deposited on $\approx 2.0\text{--}1.8$ Ga continental crust (Thomas *et al.*, 1994; Robb *et al.*, 1997). Recent precise

radiometric dating of several units in the western part of the Namaqua belt has identified two main tectono-metamorphic events, each with associated granitoid magmatism. The first event took place between ≈ 1250 and 1150 Ma, the second between ≈ 1065 and 1030 Ma (Robb *et al.*, 1997; Ashwal *et al.*, 1997). Although both events were accompanied by granulite facies metamorphism, peak metamorphic grades were reached during the second event (Robb *et al.*, 1997). Robb *et al.* (1997) term the first event the Kibaran Orogeny and the second event the Namaqua Orogeny.

Available radiometric age-dates for the eastern part of the Namaqua belt are not sufficiently precise to distinguish individual tectono-metamorphic events, although the rocks have clearly undergone polyphase deformation. All of these phases of deformation have been collectively termed the Namaqua Orogeny (Thomas *et al.*, 1994) although some studies suggest that more than one orogenic (collisional) event has occurred in the eastern part of the Namaqua belt (Stowe, 1986; Humphreys *et al.*, 1988; Jackson and Harris, 1997). Available age constraints indicate that deformation, metamorphism and batholith intrusion in the eastern part of the Namaqua belt took place between ≈ 1.20 - 1.05 Ga (Thomas *et al.*, 1994). The term *extended Namaqua Orogeny* is used here to describe the tectono-metamorphic events responsible for the polyphase deformation and metamorphism of the eastern Namaqua belt and the south-western margin of the Kheis belt between ≈ 1.20 and 1.05 Ga.

The eastern part of the Namaqua belt (Map 1) consists of amphibolite, gneiss and meta-sediments of the 1285 ± 14 Ma Areachap Group (Cornell *et al.*, 1990: Pb-Pb single zircon evaporation). The Areachap Group is thought to represent juvenile crust, formed in a magmatic arc or back-arc basin setting above a subduction zone that developed along the south-west margin of the combined Kaapvaal Craton-Kheis belt during the Mid-Proterozoic (Hartnady *et al.*, 1985, Geringer *et al.*, 1986). The Areachap Group was thrust over the Kheis belt during the initial stages of the Namaqua orogeny (Stowe, 1986; Humphreys *et al.*, 1988) and intruded by the ≈ 1200 - 1100 Ma Keimoes Suite (Barton and Burger, 1983: U-Pb whole rock) granitoids. The Keimoes Suite is thought to represent a plutonic core complex that developed in response to collisional tectonics along the south-western margin of the combined Kaapvaal Craton-Kheis belt during the extended Namaqua orogeny (Geringer *et al.*, 1988; Cornell *et al.*, 1990; Thomas *et al.*, 1994).

Late stage oblique-transpression during the extended Namaqua orogeny produced north-west to NNW striking, oblique-dextral sense transcurrent shear zones such as the Straussberg shear zone (Map 1). With subsequent uplift and cooling, whilst still under transpressive stress, north-west to NNW striking, oblique dextral sense, strike slip faults such as the Dagbreek fault (Map 1) developed and caused reactivation of the earlier transcurrent shear zones (Stowe, 1983). The Koras Group (Map 1) sediments and volcanics are

thought to have been deposited in pull-apart basins that developed in response to this late-stage, dextral sense faulting (Hartnady *et al.*, 1985; Thomas *et al.*, 1994).

2.4 Structural and Metamorphic studies of the south-western margin of the Kheis belt, the Kaaiken domain and the eastern part of the Namaqua belt.

Vajner (1974) identified four phases of folding as well as dextral sense, transcurrent shear zones and strike-slip faults in the eastern part of the Namaqua belt, the Kheis belt and the Kaaiken domain. Although Vajner misinterpreted the relative timing of these events, his descriptions of the geometry and style of fabric elements associated with these deformation phases have, to a large extent, been confirmed by more recent workers. Smit (1977) and Botha *et al.* (1977) documented three phases of folding in the Kheis belt, the Kaaiken domain and the Namaqua belt and related all three phases of folding to the Namaqua orogeny. Subsequent workers (e.g. Stowe, 1986) have shown that this interpretation is incorrect.

Coward and Potgieter (1983) described the geology between Prieska and Copperton (Map 1) and recognised two generations of thrust sense shear zones in the Kaaiken Group. The earliest phase of deformation produced eastward vergent (north-west striking), oblique thrust-sense shear zones. These shear zones were subsequently reactivated as north-east vergent, thrust sense shear zones (with sheath folds in high strain zones). Coward and Potgieter (1983) correlated the eastward vergent, oblique thrusting with the Kheis Orogeny, and suggested that “Kheis age” thrust sense shear zones could be traced around the north-western corner of the Marydale basement high. The north-east vergent thrusting was considered by Coward and Potgieter (1983) to be related to the Namaqua orogeny, during which rocks of the Namaqua belt were thrust over the Kheis belt.

More recent workers in the south-western part of the Kheis belt, the Kaaiken domain and the eastern part of the Namaqua belt have related structural elements to either the *Kheis Orogeny* (KD) or the *Namaqua Orogeny* (Stowe, 1983, 1986; Humphreys and Van Bever Donker, 1987; Humphreys *et al.*, 1988). These workers have used different symbols for structural elements and phases of deformation, so in order to rationalise this summary, phases of deformation recognised by previous workers are correlated here with seven phases of deformation: KD and ND₁-ND₆ (Table 2.9) It must be stressed that when referring to phases of deformation (e.g. ND₁) or structural elements such as foliations (e.g. NS₁), folds (e.g. NF₁) or lineations (e.g. NL₁) it is in no way implied that they are related to an individual orogenic event. The development of several generations of structural elements during one progressive deformation is a common feature of fold belts and the individual phases are separated here for descriptive purposes only.

	Kheis Orogeny	Extended Namaqua Orogeny					
This study	KD	ND ₁	ND ₂	ND ₃	ND ₄	ND ₅	ND ₆
Stowe (1983, 1986)	KF1 (NF1a)	KF2 (NF1b)	NF2	NF3	NF4	NNW striking shear-zones and faults	
Humphreys and Van Bever Donker (1987)	FK1	FN1 (FK2)	FN2	FN3	FN4	FN5a	FN5b
Humphreys <i>et al.</i> (1988)	FK1 (FN1a)	FN1b (FK2)	FN2	FN3	FN4	FN5	

Table 2.9: Correlation between the deformation phases recognised by previous workers and those used in this study.

The Kheis orogeny (KD) produced east to south-east vergent thrust sense shear zones (Map 1) and overturned folds in the Groblershoop Formation and Zonderhuis Formation rocks north-west of Boegoeberg dam (Stowe, 1986). Thrust sense shear zones that developed during this deformation are described by Stowe (1986) as having a schistose or phyllonitic fabric. According to Stowe (1986) strain in the Volop Group was mainly accommodated by bedding sub-parallel simple shear along pelitic horizons and a thrust sense shear zone at the base of the Olifantshoek Supergroup. KF folds (KF1 of Stowe, 1986) in the Groblershoop and Zonderhuis Formations are isoclinal, overturned to the east or south-east, have a strong axial planar foliation and sheared-out limbs (Stowe, 1986). Isoclinal KF folds in the Groblershoop and Zonderhuis Formations have characteristic angular hinge zones (Stowe, 1986). KF folds have also been recognised in the Kaaie Group (Stowe, 1986; Humphreys and Van Bever Donker, 1987; Humphreys *et al.* 1988). KD structural elements are present in the Zonderhuis Formation (lower Wilgenhoutsdrif Group) but not the ≈1240 Ma Leerkrans Formation (upper Wilgenhoutsdrif Group). Stowe (1986) suggested that the fold and thrust geometry of the south-western part of the Kheis belt is consistent with that of a thin-skinned fold and thrust belt.

Studies of the Kaaie domain and the eastern part of the Namaqua belt indicate that two main fabric forming tectono-metamorphic events occurred during the extended Namaqua orogeny (Stowe, 1983,1986; Humphreys and Van Bever Donker, 1987; Humphreys *et al.*, 1988), termed here ND₁ and ND₂ followed by two minor, non-pervasive, phases of folding (ND₃ and ND₄). ND₄ was followed by the development of north-west to NNW trending, dextral sense, oblique transcurrent shear zones (ND₅), and late stage oblique-dextral strike slip faults (ND₆).

The oldest phase of deformation, related to the extended Namaqua orogeny, that has been recognised by previous workers in the eastern part of the Namaqua belt and the south-western margin of the Kheis belt, is here termed ND₁. ND₁ was characterised by eastward vergent folding and thrusting. The NF₁ folds recognised by Stowe (1986) and subsequent workers are described as being co-axial but non-coplanar to

the Kheis age KF folds. The NF_1 folds are isoclinal, overturned to the east and have rounded hinge zones with a strong mullion lineation parallel to fold axes. NF_1 folds and thrust sense shear zones are developed in the Kaaian domain, the south-western part of the Kheis belt as well as the ≈ 1240 Ma Leerkrans Formation and the 1285 ± 14 Ma Areachap Group (Stowe, 1983, 1986; Humphreys *et al.*, 1988).

The ND_1 fabric forming event therefore occurred post-1240 Ma. Reactivation of west dipping, KD thrust sense shear zones in the south-western part of the Kheis belt, occurred during the ND_1 deformation (Stowe, 1986). Stowe (1986) and Humphreys *et al.* (1988) argue that the ND_1 deformation was as a result of eastward vergent thrusting, of the Areachap Group volcanic arc, over the combined Kaapvaal Craton-Kheis belt.

KD and ND_1 fabric elements are refolded by north-west to NNW trending NF_2 folds that developed during the ND_2 deformation. In the eastern part of the Namaqua belt, NF_2 folds are tight structures with upright axial planes but they become more open moving eastwards across the Kaaian domain into the Kheis belt (Stowe, 1986). The refolding of KD structures by NF_2 folds can be demonstrated to the north of Groblershoop (Map 1) where KD thrust sense shear zones have been folded by the NF_2 Orange River Synform (Stowe, 1986). Moving south-west into the Namaqua belt, the NF_2 folds become overturned to the south-west and are associated with south-west vergent, thrust sense shear zones (Stowe, 1983).

NF_2 structures in the Namaqua belt and the Kaaian domain are refolded by ENE trending, upright, open NF_3 folds that are confined to discrete zones and rare north-west to NNW trending NF_4 folds with steeply west dipping, to vertical axial planes (Stowe, 1986; Humphreys and Van Bever Donker, 1987).

ND_5 north-west trending, oblique-dextral, transcurrent shear zones (such as the Straussburg shear zone) are interpreted to have formed as a result of oblique transpression at a late stage of the extended Namaqua orogeny (Stowe, 1983; Humphreys and Van Bever Donker, 1987). Subsequent uplift, whilst under continued transpressive stress led to the development of the NNW trending ND_6 faults (e.g. the Brakbos fault and the Doringberg fault), some of which reactivated earlier transcurrent shear zones (Vajner, 1974; Stowe, 1983; Humphreys and Van Bever Donker, 1987).

Metamorphic studies of the Kheis belt (Smit, 1977; Botha *et al.*, 1979; Schlegel, 1986, 1988; Humphreys *et al.*, 1991) have been restricted to the area around Groblershoop and the Kaaian domain, where the Olifantshoek Supergroup and Kaaian Group have been structurally and metamorphically overprinted by the extended Namaqua orogeny and intruded by the Keimoes suite granitoids. In the vicinity of

Boegoeberg dam (Map 1), actinolite-zoisite/clinozoisite-chlorite-plagioclase($An_{0.5}$) retrograde assemblages in the Hartley Formation basalts, are indicative of greenschist facies metamorphism (Smit, 1977; Botha *et al.*, 1979). Sheared mafic sills in the Groblershoop Formation to the north-west of Boegoeberg dam exhibit hornblende-chlorite-plagioclase($An_{0.5}$) assemblages indicative of lower amphibolite facies metamorphism (Botha *et al.*, 1979).

Botha *et al.* (1979) and Schlegel (1988) reported muscovite-almandine \pm quartz \pm plagioclase \pm hornblende assemblages, indicative of upper greenschist facies metamorphism, in meta-pelites of the Groblershoop Formation that were sampled in the vicinity of Groblershoop (Map 1). Schlegel (1988) interpreted almandine-garnet porphyroblast growth to have occurred during both the KF2 (ND_1) and NF2 (ND_2) deformation of Stowe (1983, 1986) but erroneously related the metamorphism to the Kheis orogeny (see Table 2.9). The metamorphism documented by Botha *et al.* (1979) and Schlegel (1988) is best related to the ND_1 and ND_2 phases of the extended Namaqua orogeny.

Schlegel (1988) and Humphreys *et al.* (1991) estimate equilibrium metamorphic conditions of 600-700°C and 8-11Kb for muscovite-hornblende-almandine-plagioclase-quartz and garnet-hornblende-plagioclase-K-feldspar-epidote-quartz assemblages in pelitic schists of the Groblershoop Formation (sampled north-west of Groblershoop). Humphreys *et al.* (1991) suggest that the high pressures indicated by these assemblages preclude the possibility of the Kheis belt being a thin-skinned fold and thrust belt. The samples utilised by Humphreys *et al.* (1991) for geothermobarometry were collected near the boundary of the Kheis belt and the Kaaie Domain. No description of the relationship between the metamorphic minerals and the fabric forming events was given and it is probable that the high pressure metamorphic assemblage of almandine-hornblende-muscovite represents metamorphism related to the Namaqua overprint.

In summary, greenschist facies metamorphism has been described from the Olifantshoek Supergroup in the Boegoeberg dam area. The metamorphic grade increases to upper greenschist/lower amphibolite facies to the north-west and west of Boegoeberg dam. Schlegel (1988) and Humphreys *et al.* (1991) interpret metamorphism to be related to tectono-metamorphic events that pre-date the Namaqua orogeny (i.e. the Kheis orogeny) although the fabric elements described (Schlegel, 1988) are, according to Stowe (1986), related to the extended Namaqua orogeny.

The Kaaie domain is characterised by upper greenschist to lower amphibolite facies metamorphic assemblages (Botha *et al.*, 1979). The eastern part of the Namaqua belt exhibits high grade (upper

amphibolite facies) metamorphic assemblages (Botha *et al.*, 1979; Stowe, 1983). Although a strong foliation developed in the Areachap Group, during both the ND₁ and ND₂ phases of deformation, previous workers have interpreted peak amphibolite facies metamorphism in the Kaaien domain to be syn-ND₂ deformation (Stowe, 1983; Humphreys and Van Bever Donker, 1987; Humphreys *et al.*, 1988).

3. THE GEOLOGY OF THE KORANNABERGE-LANGBERGE

In the sections that follow, the results of mapping in the Korannaberge and Langberge are presented. Although most of the observations were made in the Traverse 1-4 (see maps) and Molopo River areas, isolated localities elsewhere in the mountain chain were also investigated. The positions of these localities are indicated on Map 1 and are referenced in the text using the format: locality 3.1.

The Korannaberge-Langberge are formed mainly of greenschist facies meta-sediments of the Volop Group, in which quartzite is the dominant lithology. Jansen (1983) recognised that the Volop Group rocks are metamorphosed but utilised the sandstone classification scheme of Pettijohn *et al.* (1972) to distinguish between the different types of quartzites. It shall be demonstrated in the following sections that the Volop Group quartzites are often extensively recrystallised, hence it is not possible to identify the primary mineralogy, grain size and morphology. The quartzites of the various members of the Volop Group, the Mapedi Formation and the Lucknow Formation shall be differentiated here on a basis of colour, preserved sedimentary structures and mineralogy.

The approach taken in describing the sedimentology of the Olifantshoek Supergroup is purely descriptive. In the sections that follow, relationships described are based on direct observations during field mapping along selected traverse lines. Palaeocurrent directions referred to are from Jansen (1973) but were confirmed by limited palaeocurrent measurements taken during this study. Detailed facies analysis and palaeocurrent studies were not undertaken and as such the interpretation of depositional palaeoenvironments represents only a broad overview.

3.1 Lithostratigraphy

Table 3.1 shows the lithostratigraphy of the Voelwater Subgroup and the Olifantshoek Supergroup. The thicknesses of lithostratigraphic units were determined from cross-sections produced of the Traverse 2-4 areas. Section lines along which thicknesses were measured are indicated on the maps for Traverse 2-4. Due to incomplete exposure and imbrication of stratigraphy by brittle-ductile thrust sense shear zones it was not possible to determine the thicknesses of lithostratigraphic units in the Traverse 1 area.

3.1.1 The Voelwater Subgroup

All exposures of the Voelwater Subgroup (SACS, 1980), the uppermost unit of the Griqualand West Supergroup, that were studied in the Korannaberge-Langberge area form part of the Beaumont Formation of Beukes (1983). The Voelwater Subgroup was studied at the type locality on farm Voelwater 480 (locality 3.1- situated west of Postmasburg), at the eastern edge of Traverse 3 and in a roadcutting on the

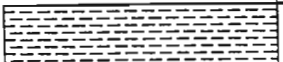








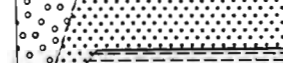
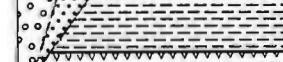


	Main Lithology	Stratigraphic Unit		Maximum thickness (m)
	schist, quartzite	Groblershoop Formation		Unknown
	quartzite	Top Dog member	Brulsand Formation	Unknown
	quartzite	Verwater member		620
	quartzite	Glen Lyon member	Matsap Formation	780
	quartzite, meta-psammite conglomerate	Ellies Rus member		1250
	quartzite, meta-psammite conglomerate	Fuller member		1570
	mafic lava	Hartley Formation		1000
	conglomerate/sed.-breccia			22
	quartzite conglomerate	Lucknow Formation		500
	quartzite, phyllite, dolomite	Mapedi Formation		250
	mafic lava			700
	quartzite, phyllite conglomerate			450
	banded ironstone, chert, dolomite	Voelwater Subgroup		250

Table 3.1: Composite stratigraphic column for the Voelwater Subgroup and Olifantshoek Supergroup rocks that form the Korannaberge and Langberge.

road between Olifantshoek and Sishen (locality 3.2). Outcrops of the Voelwater Subgroup in the Korannaberge were investigated in the Traverse 1 area.

On farm Voelwater 480, the contact with the underlying Ongeluk Formation lavas is not exposed. The Voelwater Subgroup dips west, sub-parallel to the overlying Mapedi Formation (Figure 3.1). The lowermost exposed 50m of the Voelwater Subgroup at this locality comprises interbedded jasper and jaspilite. These ferruginous rocks are overlain by approximately 15m of massive, brown coloured

siliceous chert, which is in turn overlain by approximately 5m of banded ironstone. The banded ironstone consists of <1mm-2cm thick bands of jasper, pink to purple ferruginous chert, or white siliceous chert, alternating with magnetite-hematite rich bands (>80% opaques). The basal conglomerate of the Mapedi Formation rests disconformably on either the banded ironstone or the brown siliceous chert horizon.

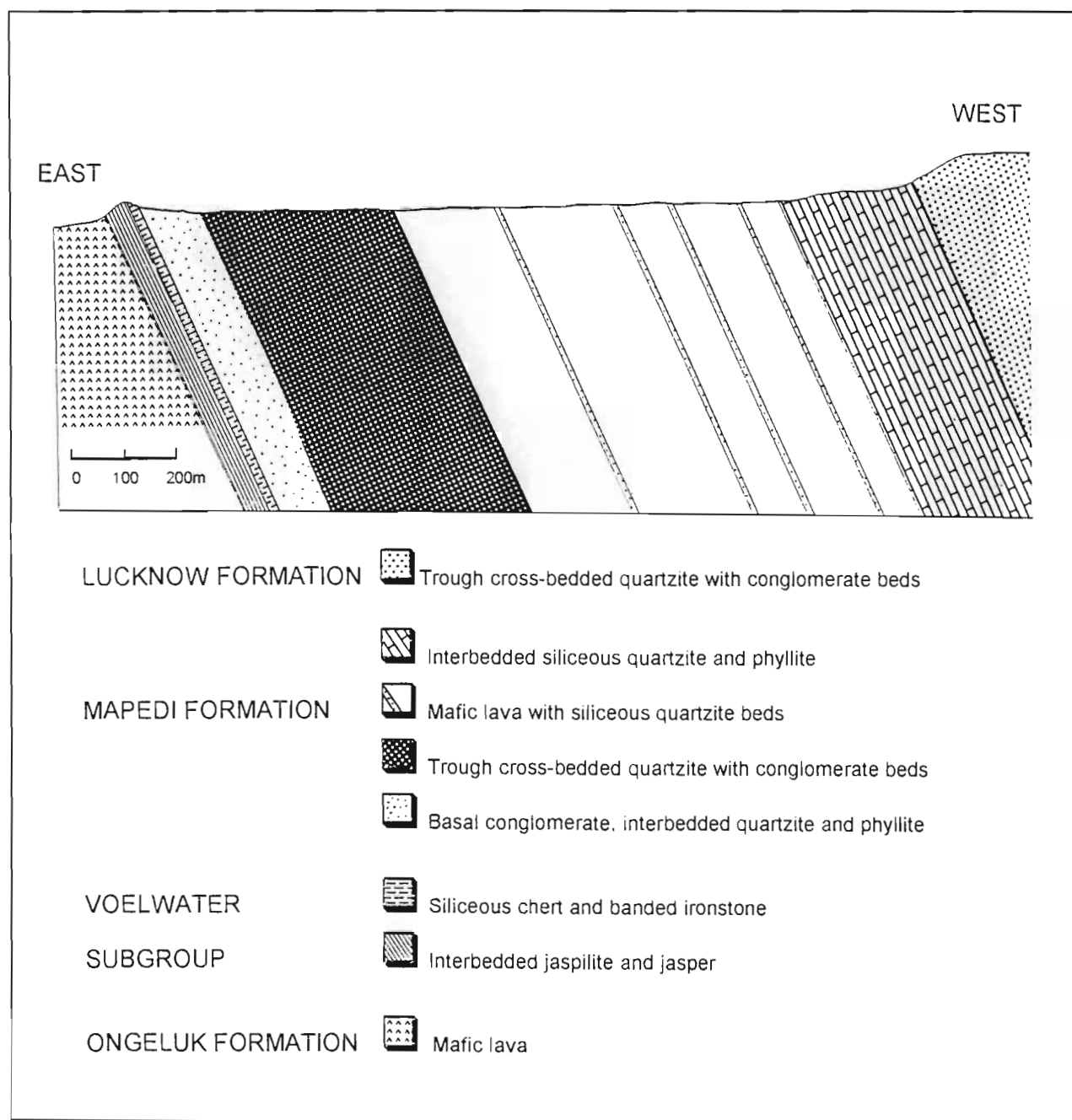


Figure 3.1: Cross section of the Ongeluk Formation, Voelwater Subgroup, Mapedi Formation and Lucknow Formation exposed on farm Voelwater 480.

Exposure of the Voelwater Subgroup in the eastern part of Traverse 3 is extremely poor and only resistant, massive, pink to purple coloured ferruginous chert crops out. The road-cutting at locality 3.2 consists of highly sheared banded ironstone.

In the Traverse 1 area, Voelwater Subgroup rocks are exposed on farms Groenwater 304 and Blaauwkrantz 342. Massive, purple ferruginous chert and banded ironstone are exposed in the core of a breached periclinal anticline on farm Blaauwkrantz 342. The unit is disconformably overlain by quartzites of the Matsap Formation. In places, the banded ironstone is “brecciated” and the chert layers have been broken up to form angular blocks in a matrix of hematite. The “breccia” is interpreted to be an edgewise conglomerate (Beukes, 1978), as in low strain zones (i.e. where the breccia was not strongly deformed during the Kheis orogeny) the “breccia” contains no fractures. Edgewise conglomerates are thought to develop as a result of early silica diagenesis and the development of syneresis (dehydration) cracks in chert layers that are covered by only a narrow veneer (mm-cm scale) of iron rich sediment. The overlying iron rich sediment veneer is removed, and the chert layer broken up, by storm/wave action. Cementation of the chert fragments by Fe-rich sediment leads to the formation of an edgewise conglomerate.

In the eastern part of farm Groenwater 304, Voelwater Subgroup rocks are exposed in the hangingwall of a westward dipping, brittle-ductile, thrust sense shear zone. Numerous, subordinate thrust sense shear zones are developed within the Voelwater Subgroup and as such, its internal stratigraphy remains uncertain. The Voelwater Subgroup at this locality consists of banded ironstone, pink dolomite, ferruginous chert and phyllite. At the isolated outcrop with the 56° foliation reading on farm Groenwater 304, light-red coloured phyllite, overlying banded ironstones, is exposed in an exploration pit. The phyllite contains light green, wedge-shaped chloritoid porphyroblasts.

An inclined borehole drilled by Anglo American Prospecting Services, in the northern part of Groenwater 304 (locality 3.3), showed that interbedded Voelwater Subgroup banded ironstone and phyllite overlies a thick unit (>118m) of lava. In the area between the Korannaberge and Hotazel, exploration drilling indicates that the Voelwater Subgroup is underlain by lava of the Ongeluk Formation (Beukes and Smit, 1987). The borehole information from Groenwater 304 confirms this interpretation.

3.1.2 The Mapedi Formation

The Mapedi Formation was studied on farm Voelwater 480 (locality 3.1). At this locality (Figure 3.1) a basal conglomerate, <2m thick, containing rounded to sub-rounded pebbles of banded ironstone, jasper, jaspilite, ferruginous chert, vein quartz and siliceous chert (i.e. the clasts are largely derived from the underlying Voelwater Subgroup) disconformably overlies the Voelwater Subgroup. The conglomerate is overlain by approximately 450m of clastic sediments, the lower part of which consists of interbedded trough cross-bedded purple quartzite and red iron-rich phyllite. The upper part of the clastic unit consists

of grey to light-brown trough cross-bedded quartzite. Narrow conglomerate layers and single pebble lags typically cap the trough cross-bedded quartzite horizons. This basal clastic unit is interpreted to have been deposited in a fluvial palaeo-environment.

Overlying the clastic sediments is approximately 700m of amygdaloidal mafic lava with narrow (<10m) layers of white to light-green coloured, ripple-marked siliceous quartzite. The lava is overlain by approximately 250m of white, ripple-marked siliceous quartzite, interbedded with grey-green phyllite horizons. Mud drapes overlying ripple-marked quartzite horizons exhibit desiccation cracks, indicating a shallow water palaeo-depositional environment prone to frequent aerial exposure. The overlying Lucknow Formation dips westward, sub-parallel to the Mapedi Formation, but the contact is not exposed.

The upper part of the Mapedi Formation is well exposed on farm Hartley 573 (Traverse 3) where it has a maximum exposed thickness of 590m. At this locality, the Mapedi Formation comprises grey and white highly siliceous quartzite (with asymmetric ripple marks) interbedded with grey-green phyllite. A 60m thick dolomite band, the lower 55m of which consists of poorly stratified dolomite, occurs near the top of the Formation. The upper 5m of the dolomite band consists of oblate dolomite pellitoids, 0.5-2cm in length, in a fine grained quartz-dolomite matrix. The association of the dolomite and the quartzose pellitoidal dolomite is indicative of a high energy, shallow marine palaeo-environment in which the stratified dolomite was eroded to produce the pellitoidal dolomite.

White to light-green siliceous quartzite of the Mapedi Formation crops out in the northern part of farm Drogepoort 345 (Traverse 1). Between this area and Saltrim (Map 1), interbedded quartzite and grey-green phyllite and stratified dolomite of the Mapedi Formation are exposed. In this area the Mapedi Formation is disconformably overlain by the Matsap Formation. A narrow unit of white to light-green, siliceous, Mapedi Formation quartzite occurs in the hangingwall of a thrust on farm Mooihoek 306.

3.1.3 The Lucknow Formation

On farm Voelwater 480 (locality 3.1) the Lucknow Formation consists of grey to white siliceous quartzite interbedded with purple and red-brown quartzite. The quartzites are trough cross-bedded, have narrow conglomerate layers and single pebble lags. The red-brown quartzites are much less siliceous than those of the upper part of the Mapedi Formation and contain up to 10% muscovite and chlorite.

The Lucknow Formation on farm Hartley 573 (Traverse 3) is very similar to that described from farm Voelwater 480. The thickness of the Lucknow Formation on Hartley 573 is approximately 490m. A mafic sill has intruded along the contact between the Mapedi Formation and the Lucknow Formation at this locality. Interbedded grey siliceous quartzite, purple to light-brown quartzite and conglomerate of the Lucknow Formation underlies the Fuller member (Matsap Formation) on farm Eenzaampan 307 (Traverse 1).

Preserved sedimentary structures (dominantly trough cross-bedded units capped by conglomerate layers) and the proportion of immature quartzite in the Lucknow Formation suggests that it was deposited in a fluvial palaeo-environment.

3.1.4 The Hartley Formation

The Hartley Formation (SACS, 1980) is best exposed at the type locality on farm Hartley 573 and in the Olifantshoek allotment area (Traverse 3). A basal clast supported conglomerate (Figure 3.2), approximately 22m thick is developed (the Neylan bed of SACS, 1980) and is well exposed in a road-cutting on the Olifantshoek-Sishen road (locality 3.4). The Neylan bed consists of sub-rounded, poorly sorted clasts of white, grey-green and purple quartzite, jasper, ferruginous chert, banded ironstone and lava in a light-green tuffaceous matrix (Figure 3.3). The clasts vary in size from <1cm to 50cm and, apart from the volcanic material, were derived from the underlying Lucknow Formation, Mapedi Formation and Voelwater Subgroup. The poorly sorted, unstratified nature of the conglomerate and the fine grained, tuffaceous matrix suggests that it formed as a debris flow during the onset of Hartley Formation volcanism.

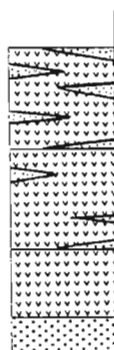
	Thickness	Description
	50	Interbedded basaltic lava (amygdaloidal or pilloidal in places), tuff, welded tuff, red-brown, trough cross-bedded meta-psammite and quartzite.
	150	Basaltic lava (amygdaloidal or pilloidal in places) interbedded with welded tuff, and minor siliceous, ripple marked, green quartzite.
	800	Basaltic lava (amygdaloidal in places) with hyaloclastite flow-top breccias.
	22	Conglomerate (Neylan bed)

Figure 3.2: Composite stratigraphic column for the Hartley Formation in the Traverse 2-3 areas.

On Hartley 573 (Traverse 3), the Neylan bed is overlain by approximately 800m of dark-green, fine grained, massive and amygdaloidal basaltic lavas with light-green hyaloclastite flow-top breccias. Retrograde metamorphism and weathering has largely obliterated the primary mineralogy of the Hartley Formation lavas. The freshest, least altered lava sample was obtained from a quarry on the western side of the Olifantshoek allotment area (Traverse 3). In this sample euhedral plagioclase laths up to 0.6mm in length are randomly orientated in a groundmass of small ($< 0.2\text{mm}$) plagioclase crystals, chlorite, epidote and magnetite (Figure 3.4).

On Hartley 573 and the eastern side of the Olifantshoek allotment area, the lavas are overlain by 200m of interbedded amygdaloidal lava, pillow lava, hyaloclastite, welded tuff and grey-green phyllites (probably tuff horizons). Narrow layers ($< 2\text{m}$) of green siliceous quartzite occur in the lower 150m of this unit. The upper part of the unit is characterised by intercalations of red-brown trough-cross bedded quartzite and meta-psammite. The Hartley Formation grades up into the red-brown quartzites of the Matsap Formation.

The upper contact of the Hartley Formation is taken here to be the top of the last volcanic horizon, as suggested by SACS (1980).

Isolated exposures of the Hartley Formation occur on farms Pudahush 533 and Watermeyer 576, along the eastern edge of Traverse 2. At these localities interbedded amygdaloidal lava, welded tuff (Figure 3.5), siliceous green quartzite and red-brown quartzite are exposed and are equivalent to the upper part of the Hartley Formation on farm Hartley 573.

The narrow unit of Mapedi Formation quartzite on farm Mooihoek 306 (Traverse 1) is overlain by massive and amygdaloidal mafic lavas, with tuff layers, that are here correlated with the Hartley Formation. At the contact between these lavas and the underlying Mapedi Formation is a sedimentary breccia comprising large angular blocks of Mapedi Formation quartzite in a matrix of brown quartzite (Figure 3.6). This sedimentary breccia is interpreted to be a talus slope deposit that developed as a result of mass-wasting prior to extrusion of the lavas. The breccia is a lateral equivalent of the Neylan bed conglomerate.

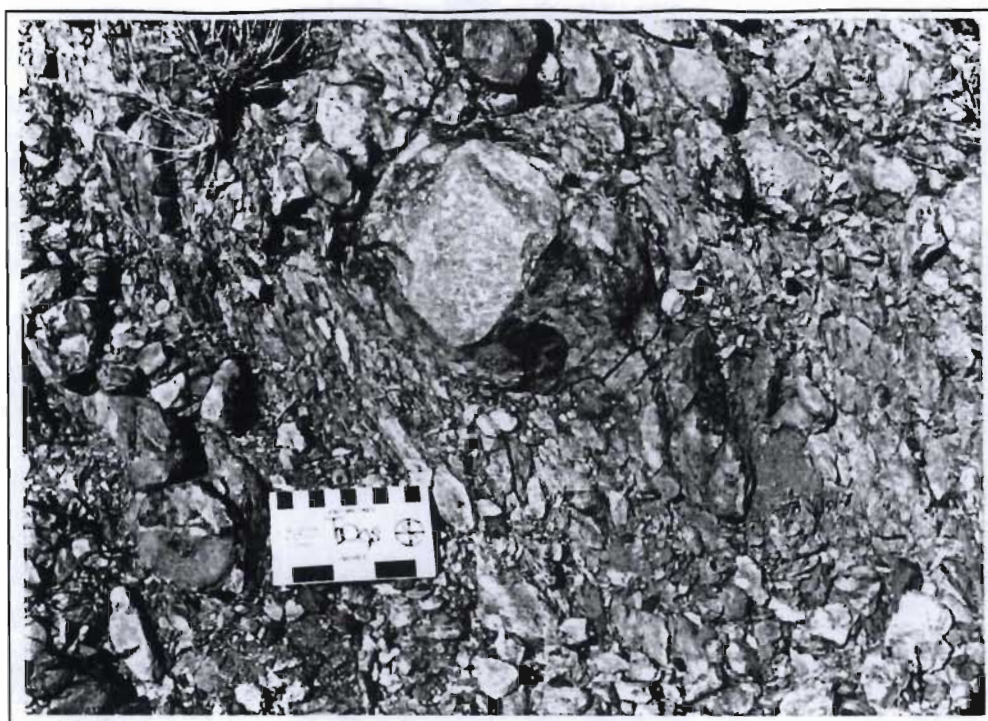


Figure 3.3: The Neylan bed conglomerate, situated at the base of the Hartley Formation. locality 3.4- Map 1.

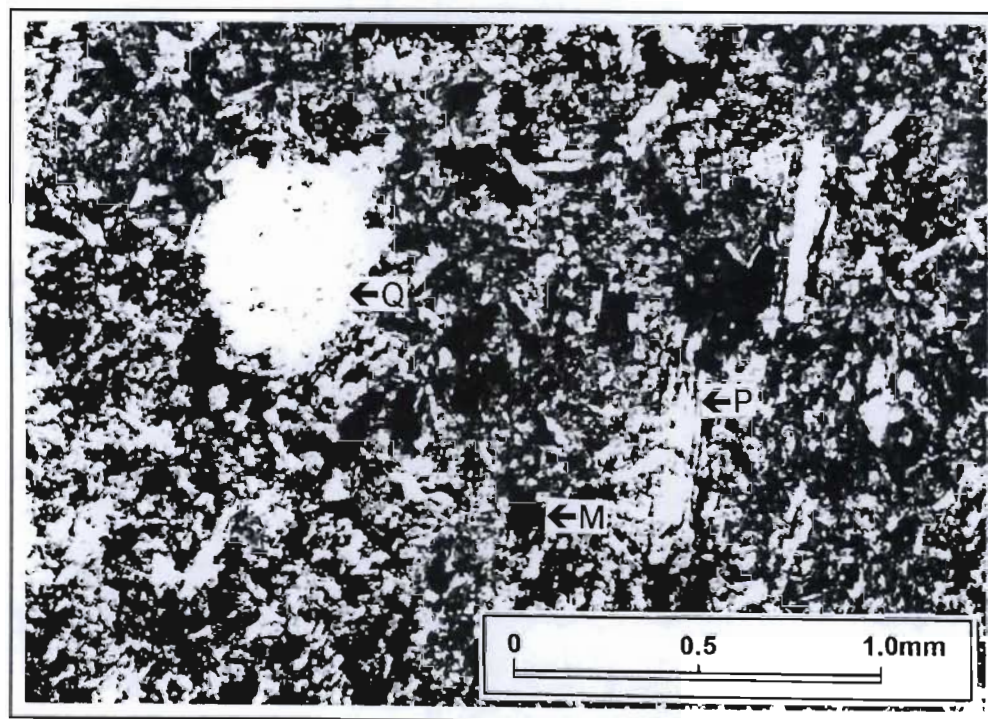


Figure 3.4: Photomicrograph of a sample of Hartley Formation lava exposed in a quarry on the western part of the Olfantshoek allotment area (Traverse 3). P=plagioclase, M=magnetite, Q=quartz filled amygdale. Cross-polarised transmitted light.

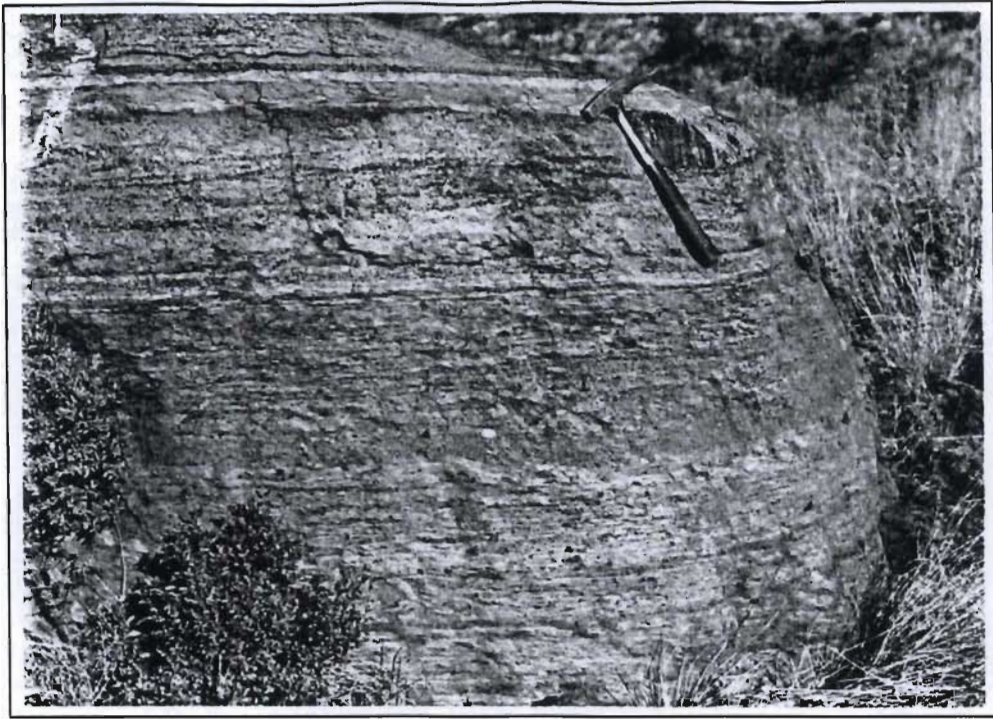


Figure 3.5: Welded tuff (a preserved ignimbrite deposit) in the Hartley Formation on farm Pudahush 533- Traverse 2.



Figure 3.6: The sedimentary breccia developed at the base of the Hartley Formation on farm Mooihoek 306 (Traverse 1). The clast assemblage is dominated by clasts of white to light-green siliceous quartzite of the Mapedi Formation. Rare clasts of Voelwater Subgroup jasper are also present (see immediately below compass).

3.1.5 The Matsap Formation

The Matsap Formation has been subdivided by SACS (1980) into three members viz.: the Fuller, Ellies Rus and Glen Lyon members (Table 3.1). The stratigraphy and lithology of each of these members shall be described below.

3.1.5.1 *The Fuller member*

As described in section 3.1.4, the Fuller member conformably overlies the Hartley Formation in the Traverse 2 and 3 areas. Only the upper part of the Fuller member is exposed in the eastern part of the Traverse 4 area.

In the Traverse 1 area, the Hartley Formation on farms Mooihoek 306 and Blaauwkrantz 342 is overlain by the Fuller member, the contact is not exposed however. The Fuller member disconformably overlies the Mapedi Formation on the western side of Groenwater 304 and the Lucknow Formation on farm Eenzaampan 307. In the central part of farm Blaauwkrantz 342 and the central and eastern parts of Groenwater 304, the Fuller member disconformably overlies the Voelwater Subgroup (Figure 3.7). At the two localities where the contact was observed (the Fuller member-Lucknow Formation contact on Eenzaampan 307 and the Fuller member-Voelwater Subgroup contact in the north-eastern part of Groenwater 304) a small pebble conglomerate between 2 and 5m in thickness is developed. This is overlain by trough cross-bedded purple to brown quartzite. 10 to 20m above the Fuller member-Lucknow Formation contact on farm Eenzaampan 307 and the Fuller member-Hartley Formation contact on farm Mooihoek 306, the trough cross-bedded quartzite is overlain by a clast supported conglomerate up to 16m thick that has narrow intercalations of trough cross-bedded quartzite. The conglomerate contains sub-rounded clasts, up to 60cm in length, of jasper, ferruginous chert, white to light-green coloured siliceous quartzite and banded ironstone.

Apart from the large-pebble to boulder conglomerate observed near the base of the unit in the Traverse 1 area, the Fuller member mapped in the areas covered by Traverses 1-4 is very similar. The dominant lithology in all of these areas is red-brown to light-brown, trough cross-bedded quartzite. Subordinate red-brown meta-psammite and poorly exposed red phyllite horizons occur interbedded with the quartzite. Conglomerate layers up to 40 cm in thickness are common (Figure 3.8) and contain rounded to sub-rounded clasts up to 15cm in diameter.



Figure 3.7: A sedimentary contact between the basal conglomerate of the Fuller member and ferruginous chert of the Voelwater Subgroup (farm Groenwater 304- Traverse 1).

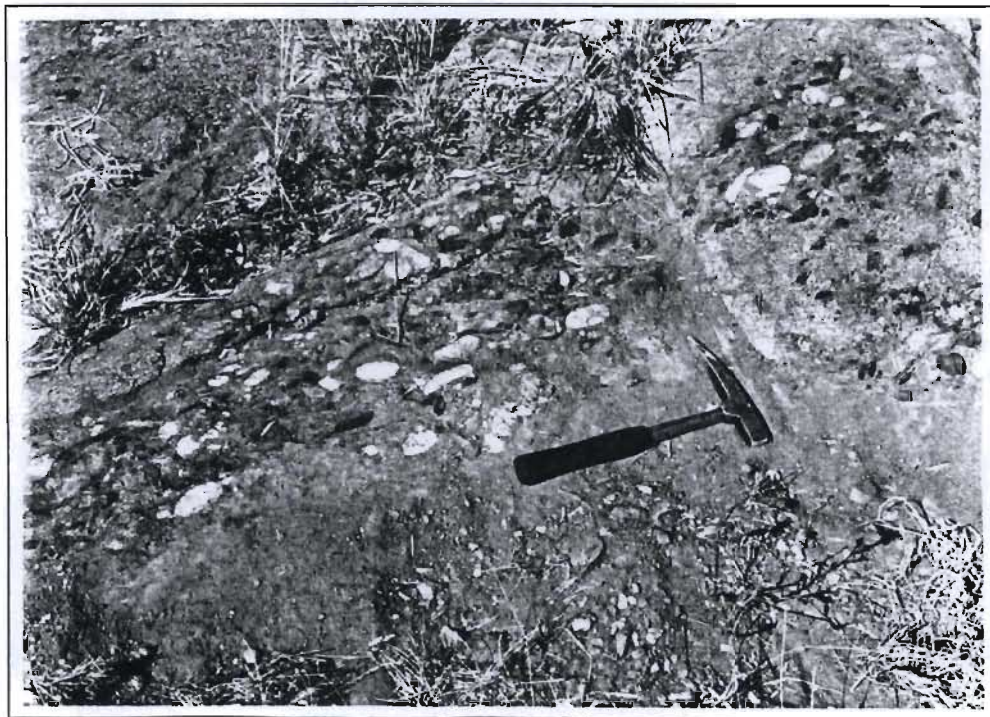


Figure 3.8: Polymict conglomerate band in the Fuller member (farm Drogepoort 345-Traverse 1). The clast assemblage comprises jasper, ferruginous chert, siliceous chert, banded ironstone, vein quartz and siliceous white quartzite and was probably derived from the underlying Mapedi Formation, Lucknow Formation and Voelwater Subgroup.

Single pebble lags, capping trough cross-bedded horizons, are commonly developed, as are lenses of poorly stratified quartzitic grit-stone up to several metres thick. Planar-bedded horizons up to 1.5m thick consisting of alternating quartz and heavy mineral layers were observed at several localities in the Fuller member (Figure 3.9). Planar-bedded heavy mineral layers such as these are indicative of upper flow regime conditions.

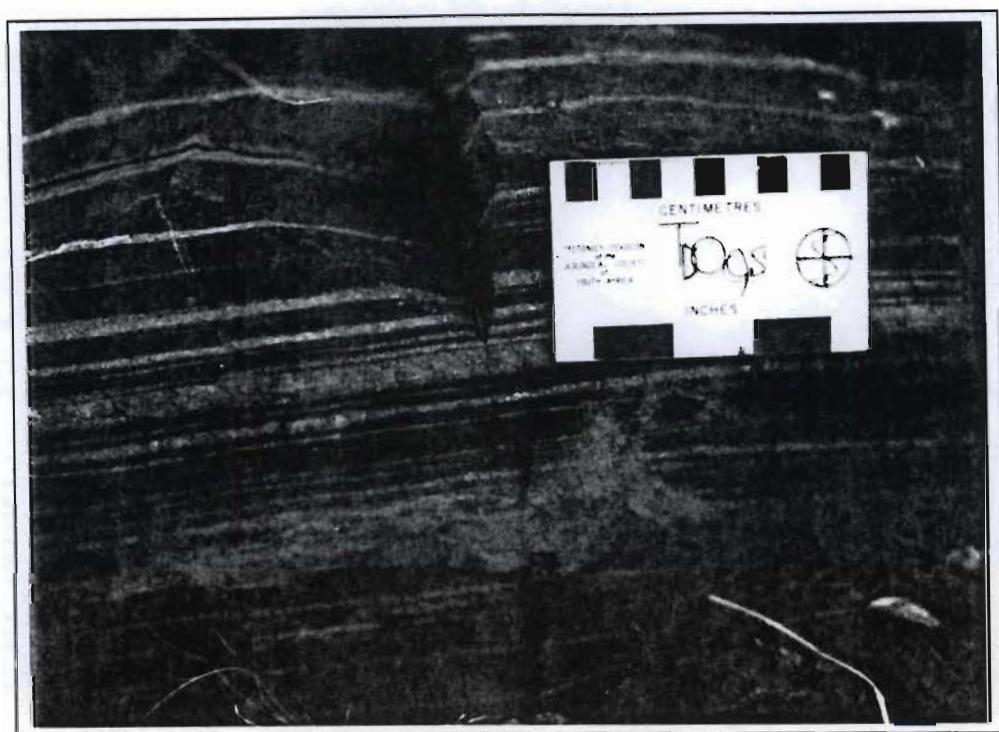


Figure 3.9: Planar bedded heavy mineral layers in the Fuller member (farm Watermeyer 576- Traverse 2). The dark bands are comprised of rounded opaque heavy minerals and zircon grains up to 0.4mm in diameter. The lighter bands consist of quartzite.

The sedimentary structures observed in the Fuller member quartzite, the polymodal south to south-west, unidirectional palaeocurrent (Jansen, 1983: confirmed during this study), the high proportion of conglomerate layers and grit bands as well as the planar-bedded heavy mineral horizons indicate a proximal, high energy, braided stream fluvial palaeo-environment for the deposition of the Fuller member.

The complete Fuller member succession is not exposed in the Traverse 2-4 areas. An estimate of the total thickness was obtained immediately to the north of Traverse 3 (Map 1), where the Fuller member is estimated to be 1570m in thickness.

3.1.5.2 *The Ellies Rus member*

The basal unit of the Ellies Rus member is a prominent, 30m thick, light-brown, trough cross-bedded siliceous quartzite horizon. This marker bed is overlain by interbedded light-purple quartzite and quartzitic grit-stone which grades up into light-brown quartzite overlain by grey siliceous quartzite with purple to light-brown meta-psammite intercalations.

Trough cross-bedding is the dominant preserved sedimentary structure (Figure 3.10) although planar cross-bedded units were also observed. Narrow conglomerate layers and polymict grit bands are common in the lower part of the Ellies Rus member. The clast assemblage of these conglomerate and grit horizons comprises banded ironstone, jasper, ferruginous and siliceous chert, vein quartz and quartzite.

Preserved sedimentary structures and the polymodal, unidirectional, south to west directed palaeocurrent (Jansen, 1983) in the Ellies Rus member indicate a fluvial palaeo-environment, similar to that of the Fuller member. The smaller proportion of conglomerate layers and the lack of upper flow regime indicators suggests that the Ellies Rus member represents a more distal facies relative to the Fuller member.

The complete Ellies Rus member succession is only exposed in the Traverses 2 and 4 areas. The unit is estimated to be 1250m thick in the Traverse 2 area.

3.1.5.3 *The Glen Lyon member*

The Glen Lyon member comprises purple, grey and brown quartzite in which planar cross-bedding, trough cross-bedding and asymmetric ripple-marks are the dominant sedimentary structures. Although some pebbly quartzite and quartzitic gritstone horizons occur, no conglomerate bands were observed. Narrow (<1m), strongly foliated, grey-green phyllite horizons are interbedded with the quartzites but are rarely exposed. Palaeocurrent indicators in the Glen Lyon member indicate a polymodal, unidirectional south-west to north-east palaeocurrent (Jansen, 1983) and the unit is interpreted to represent a distal facies fluvial deposit. The thickness of the Glen Lyon Member in the Traverse 2 area is approximately 780m. In the Traverse 3 area it is approximately 700m.

3.1.6 The Brulsand Formation

SACS (1980) divide the Brulsand Formation into the Verwater, Top Dog and Vuilnek members. On published geological maps (SAGS, 1977, 1979) of the Korannaberge and the Langberge, the Brulsand Formation is subdivided into the Verwater and Top Dog members, and this approach is followed here.

3.1.6.1 *The Verwater member*

The base of the Verwater member is marked by a prominent, grey coloured, ripple-marked siliceous quartzite horizon approximately 30m in thickness. It is overlain by interbedded gritty, light-brown trough cross-bedded quartzite and meta-psammite interbedded with ripple-marked, siliceous grey quartzite. The ripple-marked quartzite horizons have mud drapes that show desiccation cracks indicating shallow water deposition (Figure 3.11). Herring-bone cross-bedding was observed on farm Gamayana 532 (Traverse 2) and palaeocurrent indicators imply polymodal, bi-directional flow conditions (Jansen, 1983). This suggests that the Verwater member was deposited in a shallow marine, intertidal palaeo-environment. The Verwater member is approximately 500m thick in the Traverse 3 area and 620m thick in the Traverse 2 area.

Figure 3.12 shows a photomicrograph of a weakly deformed quartzite sample from the Verwater member in which the original sedimentary grains can be recognised. This is rarely observed in thin sections of the Volop Group and is included here for comparative purposes (c.f. Figures 3.32 and 3.35).

3.1.6.2 *The Top Dog member*

The Top Dog member comprises three (in the Traverse 3 area) or four (in the Traverse 2 area) resistant quartzite units separated by wide tracts of Kalahari sand in which no exposure was observed. The contact between the Top Dog member and the underlying Verwater member is marked by a prominent, siliceous, ripple-marked, grey quartzite horizon. The lower part of the Top Dog member consists of interbedded siliceous grey-quartzite and light-brown quartzite. Ripple marks and planar cross-bedding are the dominant sedimentary structures.

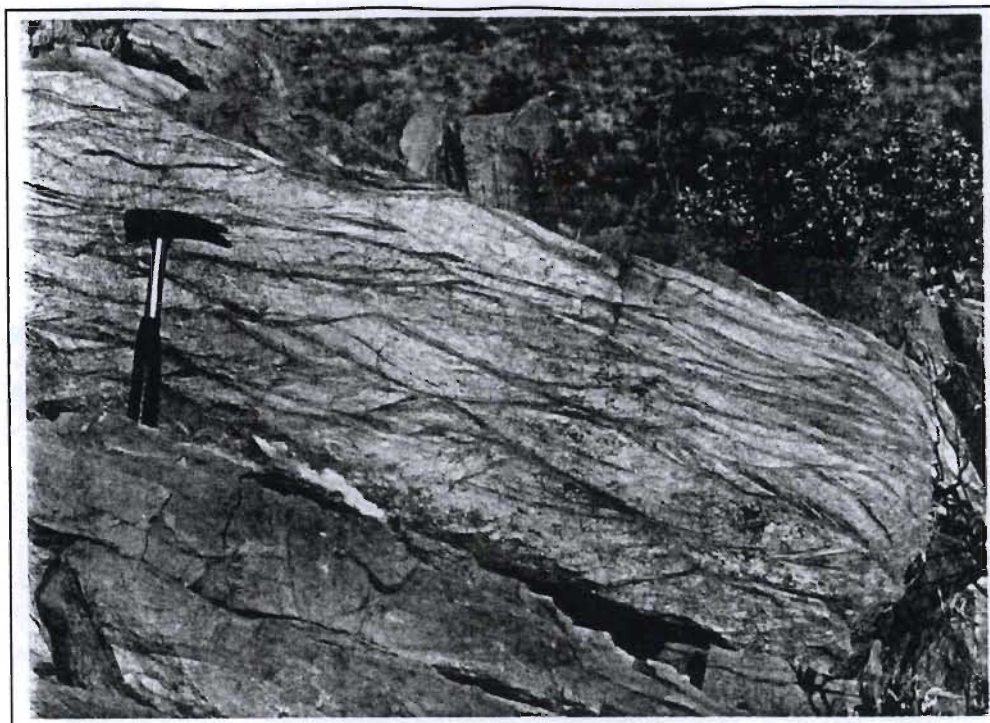


Figure 3.10: Trough cross-bedded quartzite in the Ellies Rus member (farm Watermeyer 576- Traverse 2).

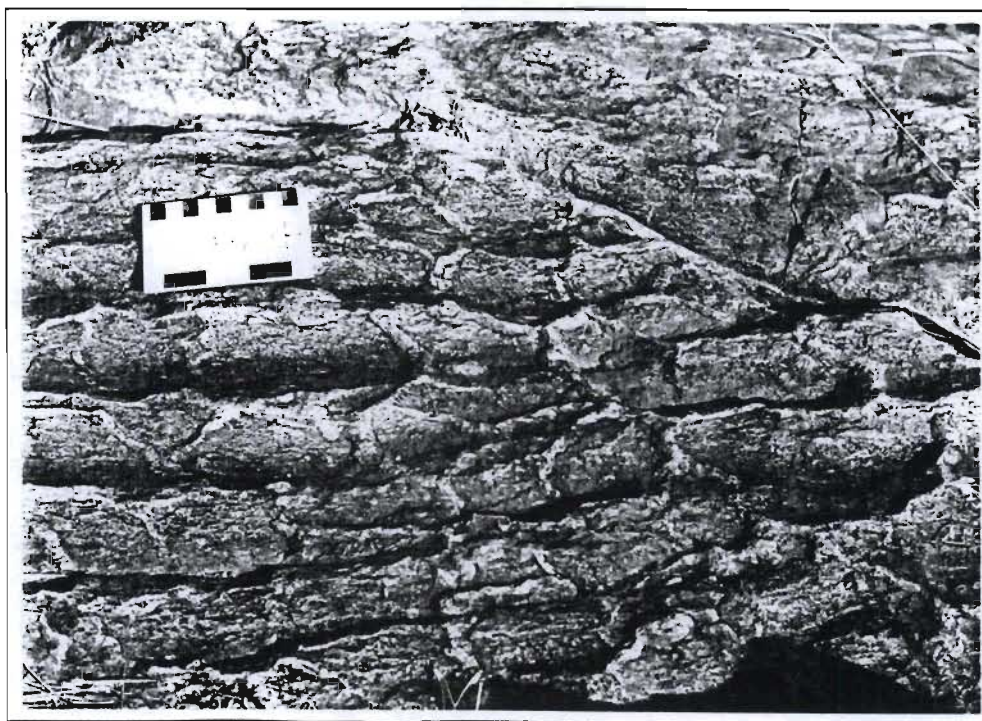


Figure 3.11: Desiccation cracks developed in a mud drape on a ripple-marked quartzite horizon of the Verwater member (farm Inglesby 580- Traverse 2).

The second resistant quartzite band (forming the synclinal closure on the boundary between Lukin 581 and Coombs 587- Traverse 2) comprises a lower, grey-green coloured, siliceous quartzite unit (Figure 3.13), that contains planar bedded heavy mineral layers indicative of upper flow regime conditions. Overlying the grey-green quartzite is a grey siliceous quartzite horizon which is in turn overlain by a light-brown, trough cross-bedded quartzite unit. The third resistant quartzite band (exposed in the central part of Smithers 528 and Coombs 587) comprises brown quartzite with scattered, subrounded pebbles of quartzite up to 12 cm in length, overlain by siliceous, grey coloured, ripple-marked quartzite.

The fourth resistant quartzite unit, well exposed on the western side of Traverses 2 and 3, consists of grey to grey-green, planar cross-bedded and ripple marked siliceous quartzite interbedded with light brown, more argillaceous quartzite. Narrow planar bedded heavy mineral bands, similar to those developed in the second resistant quartzite band, are developed in the siliceous quartzite.

The highly siliceous nature of most of the Top Dog member quartzites, the indications of upper flow regime conditions and the stratigraphic position overlying the intertidal Verwater member sediments suggests that the Top Dog member was deposited in a high energy, shallow marine palaeo-environment.

The upper contact of the Top Dog member is not exposed on the western side of the Korannaberge-Langberge mountain chain. In the area where the Top Dog member is best exposed (Traverses 2 and 3) exposure is discontinuous. No reliable estimate of the thickness of the Top Dog Member can be given.

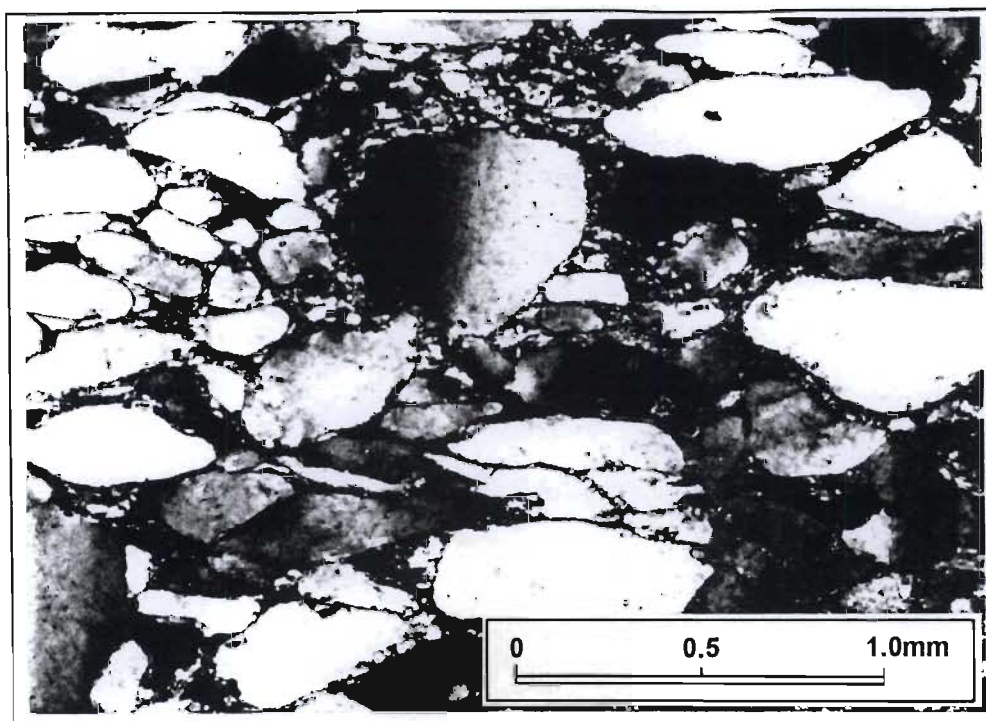


Figure 3.12: Photomicrograph of a sample of Verwater member quartzite from farm Schaapkloof 584 (Traverse 3). Note the sub-rounded grains. The quartz grains exhibit weak undulose extinction and minor recrystallisation along grain boundaries. The phyllosilicates in the matrix are muscovite and chlorite. Transmitted cross-polarised light.

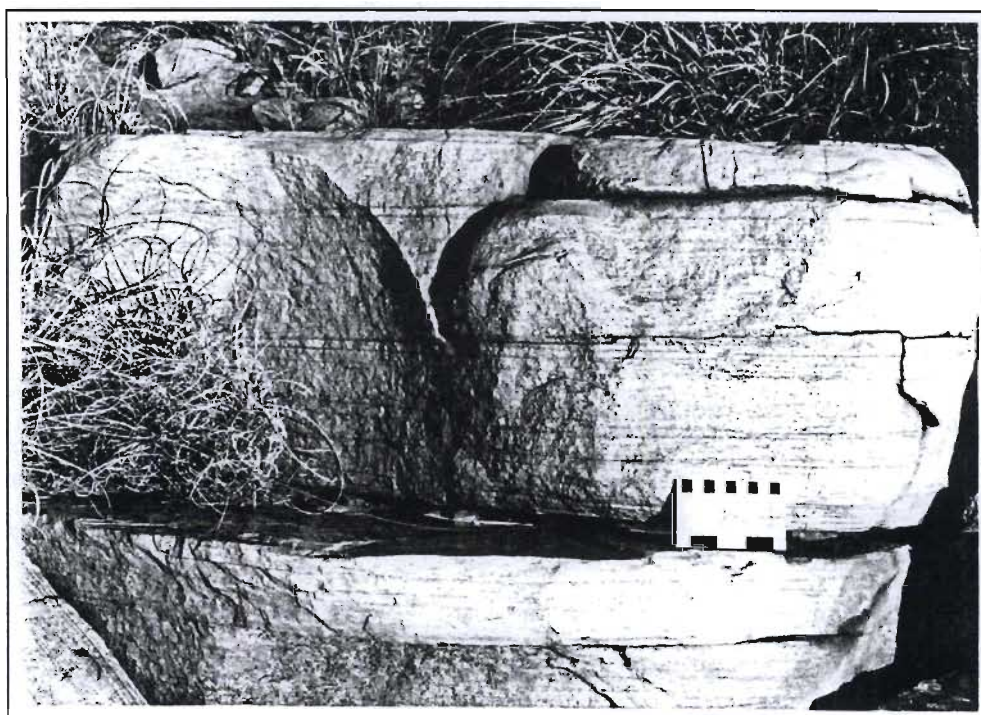


Figure 3.13: Mature quartzite with low angle cross-bedding. Top Dog member (farm Lukin 581- Traverse 2).

3.1.7 Mafic sills.

Mafic sills in the Olifantshoek Supergroup were observed in Traverse areas 1-4. These sills vary in thickness from a few metres to 350m and only the larger sills are indicated on the maps for Traverses 1-4. Exposure of these mafic intrusions is extremely poor but the thicker sills form low angle, grass covered slopes and can easily be traced out on aerial photographs. The mafic intrusions are generally parallel to bedding (e.g. near the boundary of Blaauwkrantz 342 and Mooihoek 306- Traverse 1), but in a quarry on the northern part of farm 573 (Traverse 4- near the 69° foliation reading) narrow (< 3m) mafic dykes cross-cut bedding and may represent feeder dykes to a 40m thick bedding parallel sill exposed at the same locality.

The primary mineralogy of the mafic sills is difficult to ascertain in most samples due to shearing, retrograde metamorphism and alteration. Two samples from the Traverse 2 area are only slightly altered and are described below.

Sample PS0715 was obtained from a 250m thick sill exposed in the northern part of farm Watermeyer 576. Sample PS0716 was taken from the isolated outcrop situated in the centre of farm Pudukhush 533. The appearance of the mafic intrusions at both localities is very similar. Scattered euhedral plagioclase megacrysts up to 2.5 cm in length and aggregates of subhedral magnetite crystals give the rock a speckled appearance (Figure 3.14). In thin section these plagioclase megacrysts and magnetite aggregates are set in a groundmass of plagioclase, clinopyroxene and orthopyroxene grains 0.5-2mm in length (Figure 3.15). Both samples contain a minor amount of biotite, typically rimming the magnetite crystals. Modal analyses of these samples, based on 600 point counts per sample are shown in Table 3.2. Samples PS0715 and PS0716 have a similar composition and according to the classification scheme of Streckeisen (1976) are gabbronorites.

	PS0715	PS0716
Plagioclase	66%	62.9%
Orthopyroxene	18.7%	19.8%
Clinopyroxene	13.8%	11.8%
Magnetite	1%	4%
Biotite	0.5%	1.5%

Table 3.2: Modal analyses of samples PS0715 and PS0716.

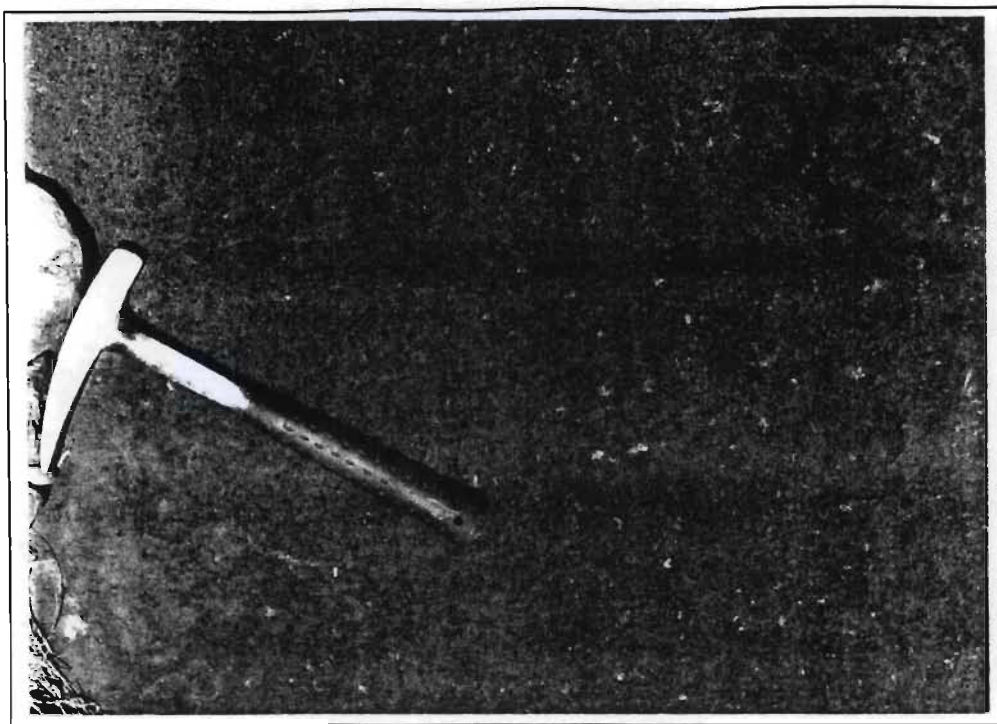


Figure 3.14: An unfoliated core-stone from the gabbro-norite sill exposed on farm Watermeyer 576.

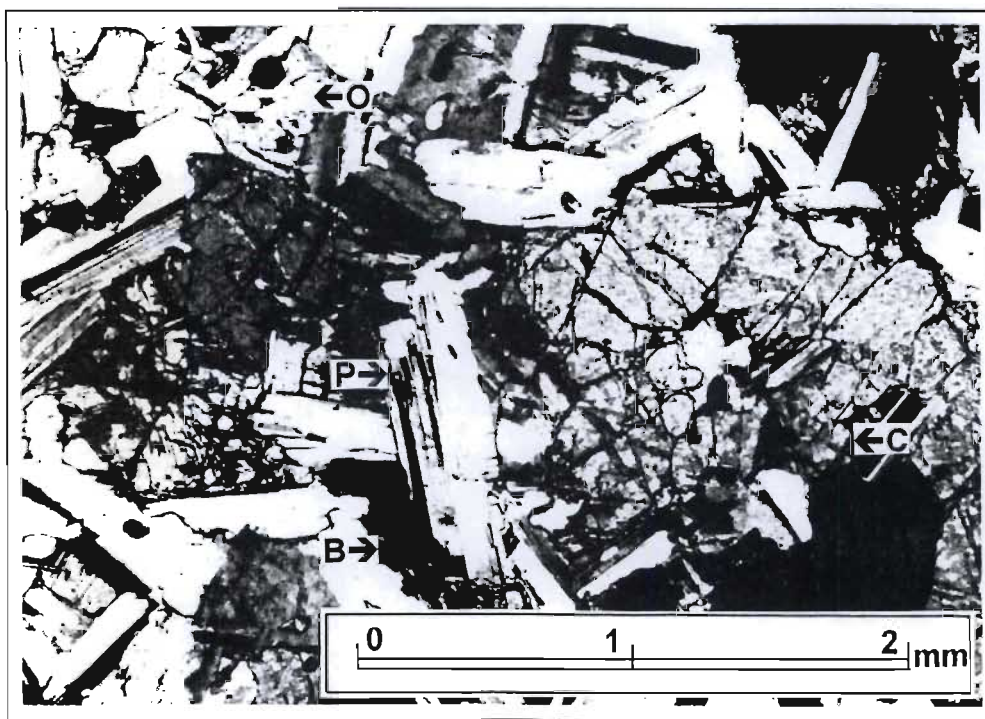


Figure 3.15: Photomicrograph of the groundmass of sample PS0716. P=plagioclase, C=Clinopyroxene, O=orthopyroxene, B=biotite rimming magnetite.

3.2 Structural geology

The Voelwater Subgroup and the overlying rocks of the Olifantshoek Supergroup, that form the Korannaberge-Langberge mountain chain, have been folded and thrust eastwards over the Kaapvaal Craton during the Kheis orogeny. In this section, the geometry and style of structural elements observed in the Traverse 1-4 areas and the Molopo River area (Map 1) are described. The microfabrics that are associated with each of the structural elements that developed during the Kheis orogeny are documented.

The orientation of planar and linear structural elements observed in, and in the vicinity of, magnetic horizons (e.g. the Voelwater Subgroup) were measured using a sun-compass. A commercial nautical almanac was used to calculate the suns' azimuth for each observation time.

The equal area stereographic projections were plotted using the *Rockware Utilities*™ STEREO program. This program was used to calculate and plot best-fit great circles (π -circles) and to contour stereographic projections where necessary.

3.2.1 Fold geometry

Folds with north-south to north-east - south-west trending fold axes are developed in the rocks of the Voelwater Subgroup and Olifantshoek Supergroup that form the Korannaberge-Langberge. Four orders of folding were observed, but at all scales it is bedding that is deformed and they are related to a single deformation event.

1st order folds:

These are large scale, open to close, gently southward plunging folds that have only been recognised north-west of Olifantshoek near the junction of the Korannaberge and the Langberge (Map 1). Two 1st order folds are exposed in this area forming a syncline-anticline pair with fold wavelengths in the order of 10 km. The axial planes of the 1st order folds are subvertical. The closure of the 1st order syncline, defined by the trace of a resistant quartzite horizon in the Top Dog member, is exposed in the north-western part of farm Lukin 581 (Traverse 2). In the northern part of the Korannaberge (including the Traverse 1 area) and the southern part of the Langberge (including the Traverse 4 area), 1st order folds are not developed.

2nd order folds:

The map trace of the closures of some of the 2nd order folds are discernible on Map 1. 2nd order folds are developed in both the axial region, and on the limbs, of the 1st order folds. 2nd order folds have wavelengths of between 1.5 and 4 km. Good examples of 2nd order folds are developed at the following localities:

- The anticline-syncline pair on the western side of Drogepoort 345 (Traverse 1).
- The anticline defined by the trace of the Ellies Rus member-Glen Lyon member contact on farm Gamayana 532 (Traverse 2).
- The anticline-syncline pair on the western part of the Olifantshoek allotment area (Traverse 3)
- The syncline defined by the trace of the Glen Lyon member-Verwater member contact near the boundary of farms 267 and 268 (Traverse 4).

3rd order folds:

3rd order folds are developed throughout the study area, they are small scale folds with wavelengths less than 500m. Good examples of 3rd order folds are exposed on the western side of the Olifantshoek allotment area (Traverse 3) in the vicinity of contact between the Glen Lyon member and the Verwater member.

4th order folds:

Small scale 4th order folds with wavelengths varying from 5m to a few cm are developed in some of the more incompetent horizons (such as the phyllite layers) or where there is a large competency contrast in a thinly bedded unit (typically in narrow interbedded layers of quartzite and phyllite).

Figure 3.16 shows the orientation of bedding surfaces and 3rd order fold axes measured in the Traverse 2 area. The π -axis, defining the mean fold axis, plunges 10° in direction 186° , parallel to the directly measured 3rd order fold axes. Bedding measurements from the Traverse 3 area (Figure 3.17) define a π -axis that plunges 12° in direction 186° , parallel to the directly measured 3rd order fold axes. Figure 3.18 shows 3rd order folds observed in the Ellies Rus member on farm Puduhush 353 (Traverse 2). These folds are situated on the eastern limb of a 1st order syncline (Map 1) and have S-fold geometry. Figure 3.19 shows the axial region of a 3rd order fold exposed on farm Gamayana 532 (Traverse 2), closer to the core of the 1st order syncline. In the areas where 1st order folds are developed (Traverse 2 and 3), 2nd and 3rd order folds are open on the limbs of the 1st order folds but are tighter in the core of the 1st order folds.

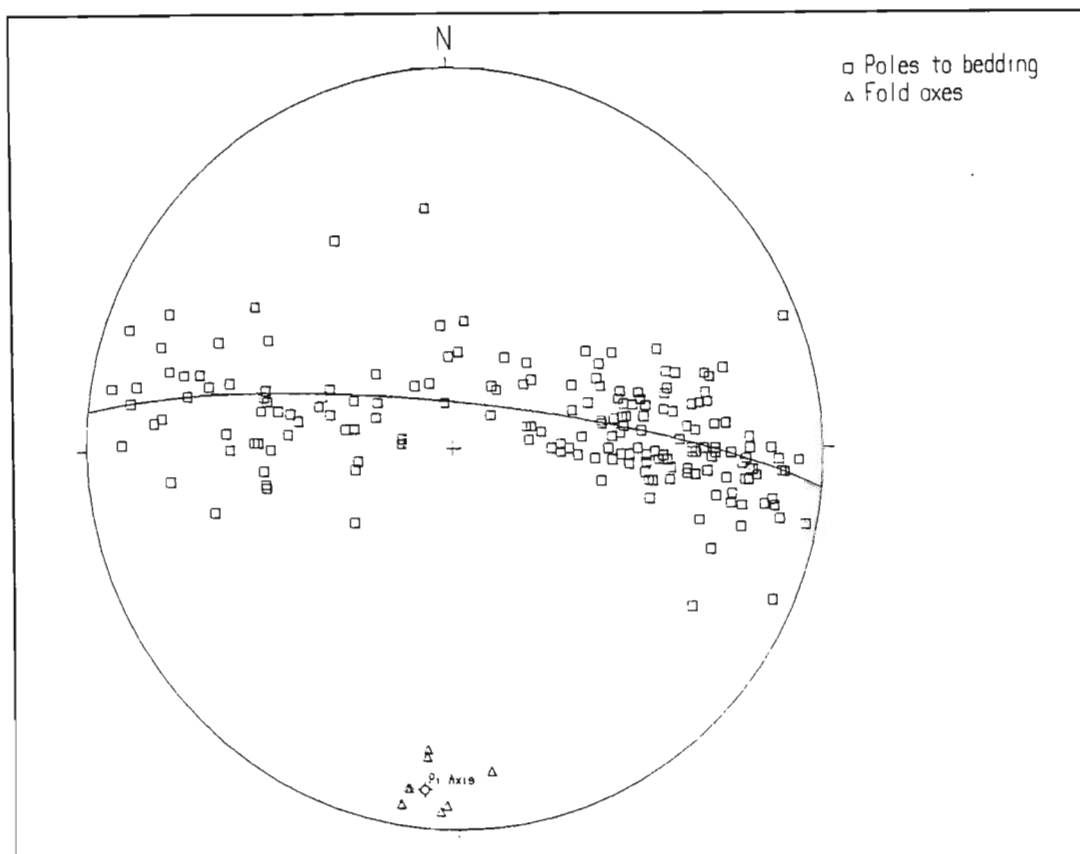


Figure 3.16: Equal area, stereographic projection (π -diagram) of bedding plane ($n=182$) and fold axes ($n=7$) orientations in the Traverse 2 area.

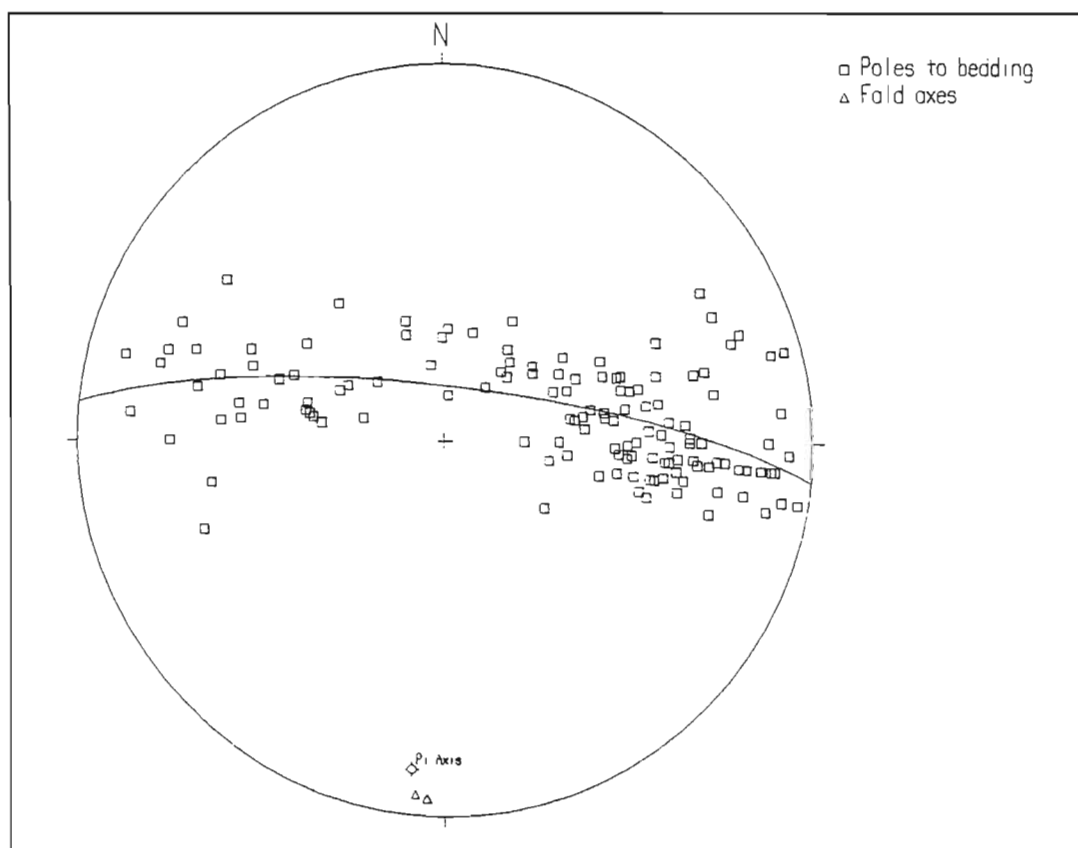


Figure 3.17: Equal area, stereographic projection (π -diagram) of bedding plane ($n=133$) and fold axes ($n=2$) orientations in the Traverse 3 area.

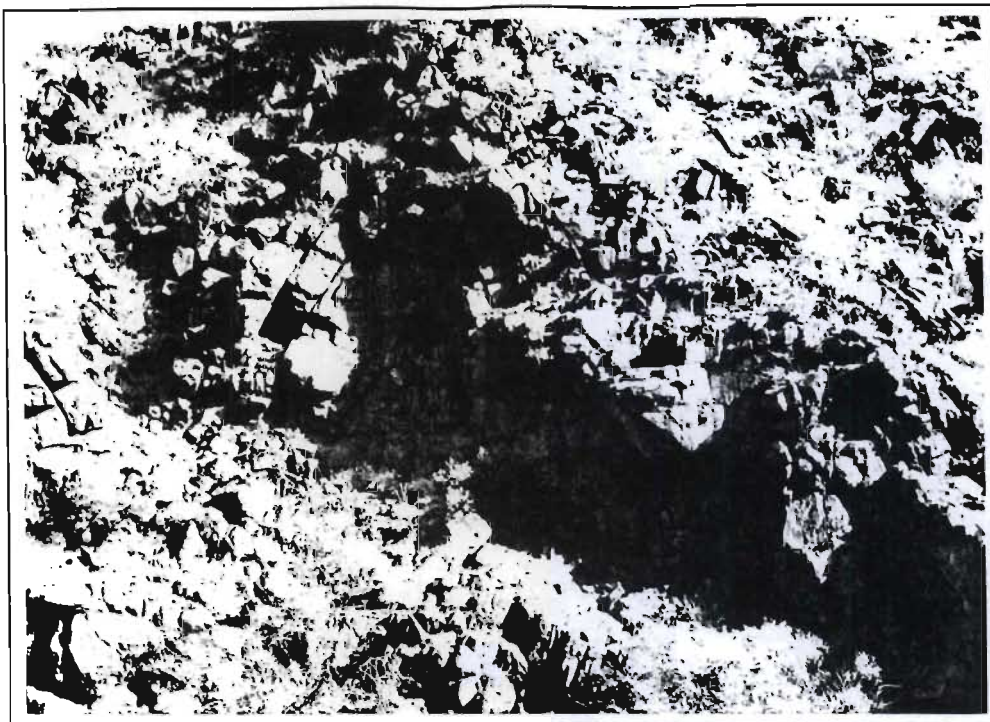


Figure 3.18: 3rd order folds in the Ellies Rus member (Traverse 2). The field of view of the photograph is approximately 50×75m. East is to the left of the photograph.



Figure 3.19: Shallow southward plunging 3rd order fold in the Glen Lyon member (Traverse 2). East is to the right of the photograph.

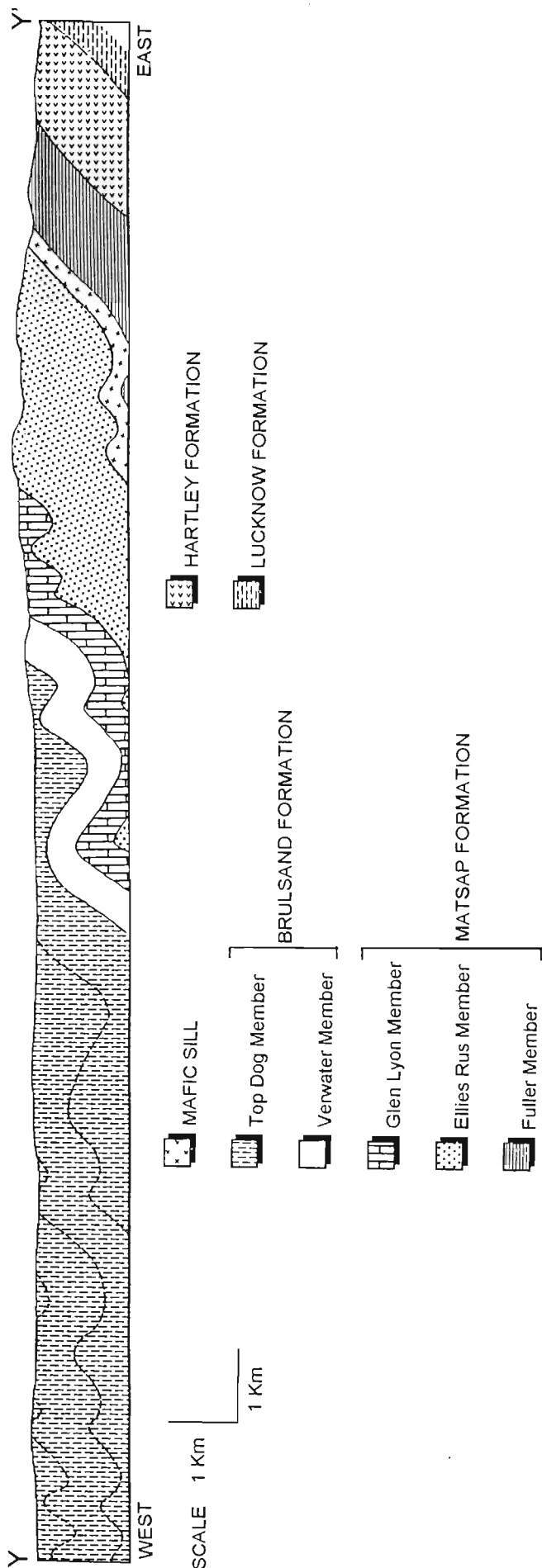
This trend is also illustrated by the map trace of the bedding-parallel form lines on the maps for Traverses 2 and 3.

Figure 3.20 shows a cross-section of the Traverse 2 area, constructed parallel to the direction of tectonic transport. Figure 3.21 shows a similarly constructed cross-section for the Traverse 3 area. On both cross-sections it can be seen that the fold axial planes are upright to steeply east dipping.

2nd order folds in the Traverse 4 area are periclinal and plunge at shallow angles to the NNE and SSW. Apart from this difference, the overall fold geometry observed in the Traverse 4 area is very similar to that observed in the Traverse 2 and 3 areas. Figure 3.22 is a stereographic projection of bedding measurements made in the Traverse 4 area. The periclinal nature of the folds is illustrated by the bedding planes that dip to both the north-east and south-west. A π -circle and π -axis have not been plotted as a π -circle cannot accurately constrain the mean fold axes using bedding orientations measured on periclinal folds. The computed π -axis for the Traverse 4 bedding data plunges 8° in direction 020° . The plunge of this π -axis is meaningless, but the plunge direction (020°) is a good estimate of the trend of the periclinal folds in the Traverse 4 area (020 - 200°).

2nd order folds in the Traverse 1 area show similar geometry to those observed in the Traverse 4 area, except in the immediate hanging- and foot-wall of brittle ductile thrust sense shear zones. A breached periclinal anticline formed by rocks of the Voelwater Subgroup and the disconformably overlying Fuller member is exposed on farms Groenwater 304 and Blaauwkrantz 342. The orientations of bedding measurements made in the Traverse 1 area are shown in Figure 3.23. The gently north and south dipping bedding readings are indicative of the gentle plunges ($<20^\circ$) of the folds in this area. The computed π -axis trends 185° , indicating a mean fold axis trend of 005 - 185° . The cross-section of the Traverse 1 area (Figure 3.24) illustrates that except in the hanging- and foot-wall of the brittle-ductile shear zones, the folds are open to close, upright structures.

Figure 3.20: Geological cross-section from Y to Y' of Traverse 2. The horizontal and vertical scales are equal.



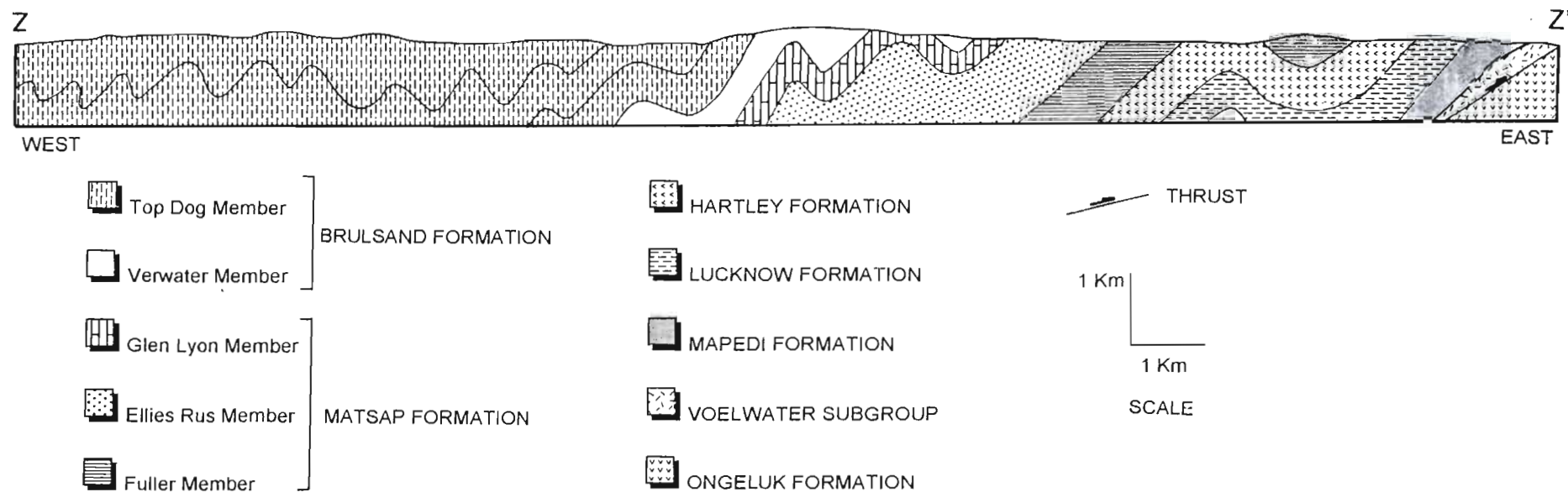


Figure 3.21: Geological cross section from Z to Z' of Traverse 3. The horizontal and vertical scales are equal.

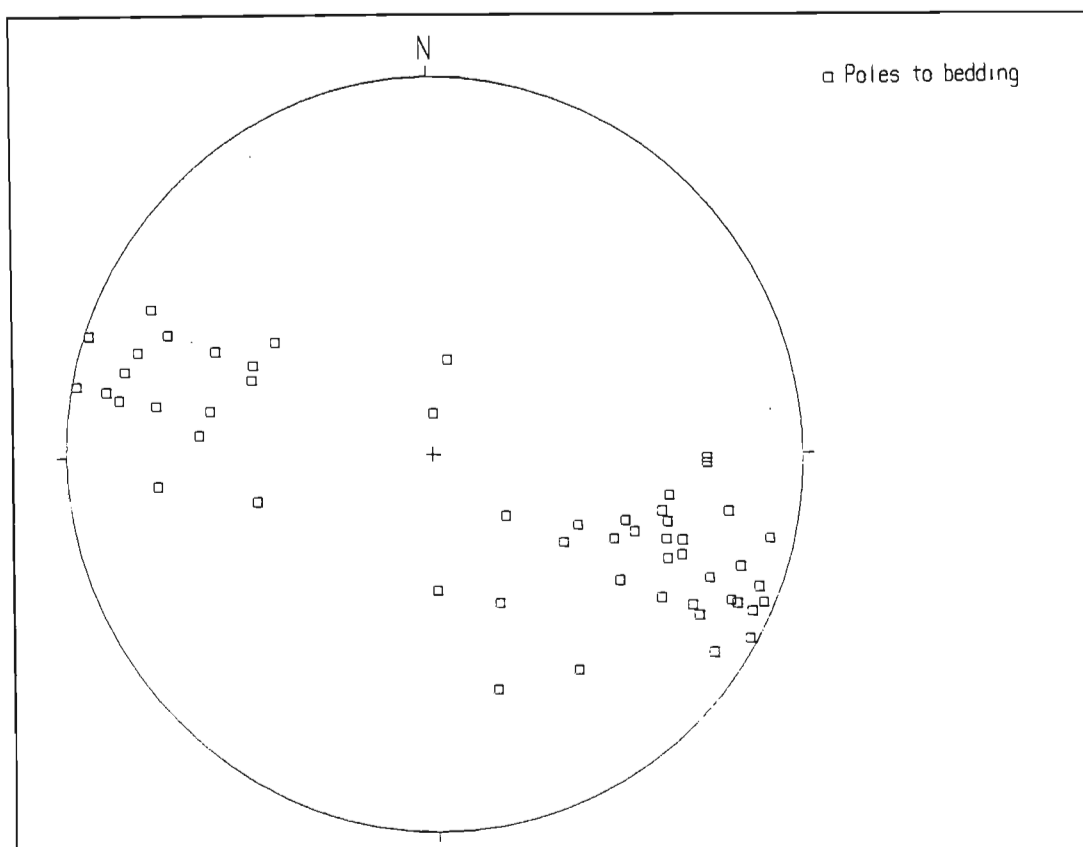


Figure 3.22: Equal area, stereographic projection (π -diagram) of bedding plane ($n=52$) orientations for the Traverse 4 area.

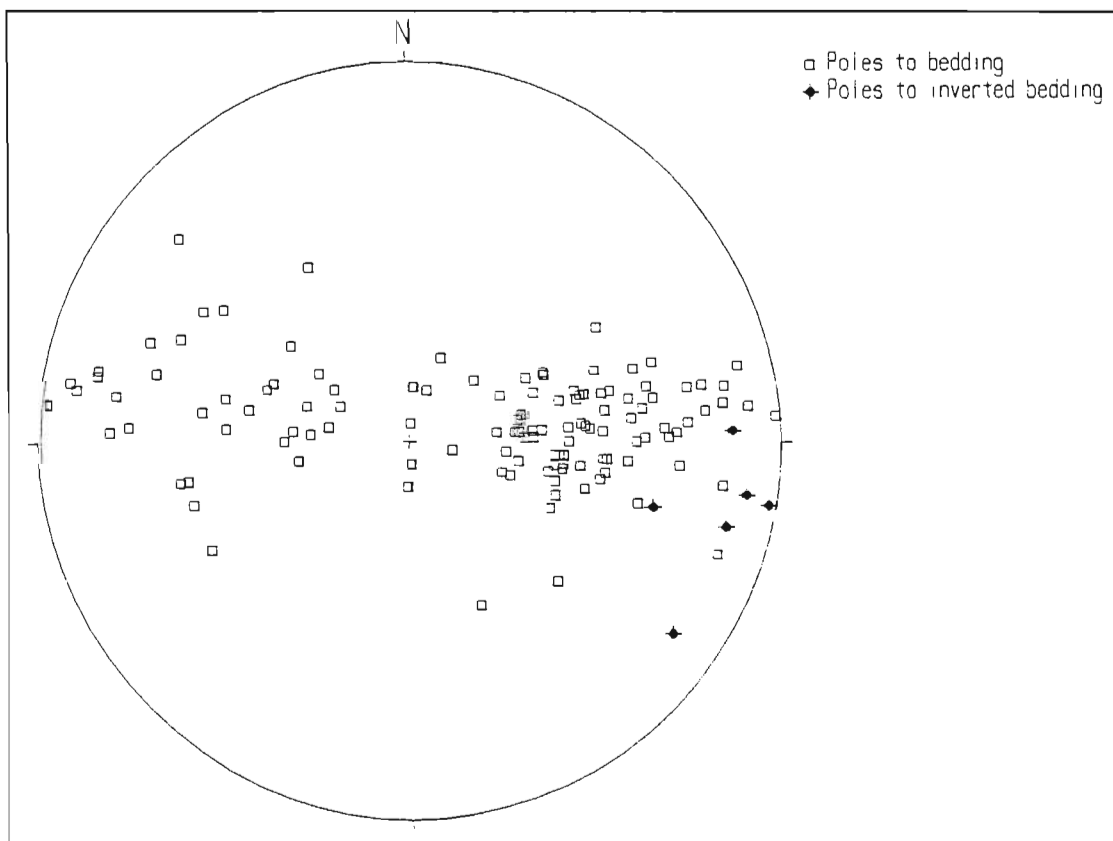
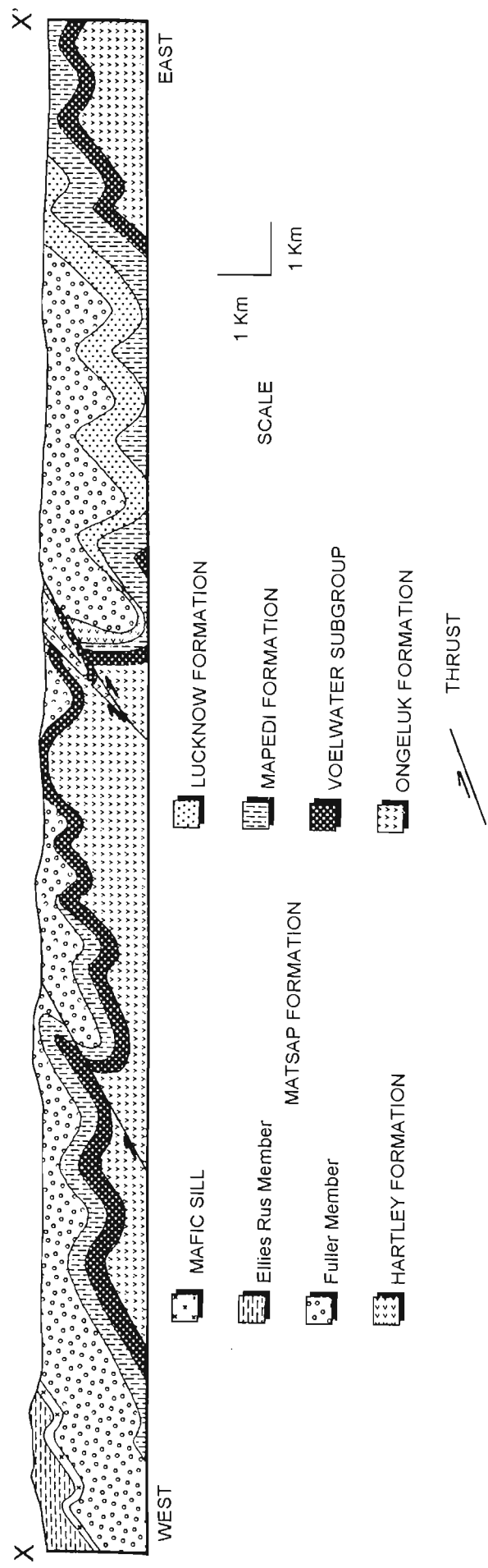


Figure 3.23: Equal area, stereographic projection (π -diagram) of bedding plane ($n=125$) orientations for the Traverse 1 area.

Figure 3.24: Geological cross section from X to X' of the Traverse 1 area. Horizontal and vertical scales are equal.



3.2.2 Fold cleavage and foliations

An axial planar cleavage and bedding sub-parallel shear zones developed during the folding. Figure 3.25 is a sketch illustrating the geometry of the bedding parallel shear zones and the axial planar cleavage developed in a 3rd order anticline shown in Figure 3.18. Bedding-parallel shear zones in this example are situated along narrow, highly sheared meta-psammite horizons that are interbedded with the quartzite. Mineral elongation lineations in the shear zones, defined by elongate aggregates of quartz and mica, plunge down the dip of the foliation perpendicular to the fold axis. S-C fabrics (Berthe *et al.*, 1979) are well developed in the shear zones on the limbs of the fold and indicate opposing senses of movement. This is consistent with the shear zones having developed during folding by flexural slip.

Figure 3.26 illustrates the micro-fabric development in a meta-psammite sample from a flexural-slip, bedding-parallel shear zone in the Glen Lyon member on farm Gamayana 532 (Traverse 2). The foliation is defined by muscovite and elongate, partially recrystallised quartz ribbons. This highly sheared, recrystallised meta-psammite can be classified as a phyllonite (Roering *et al.*, 1989).

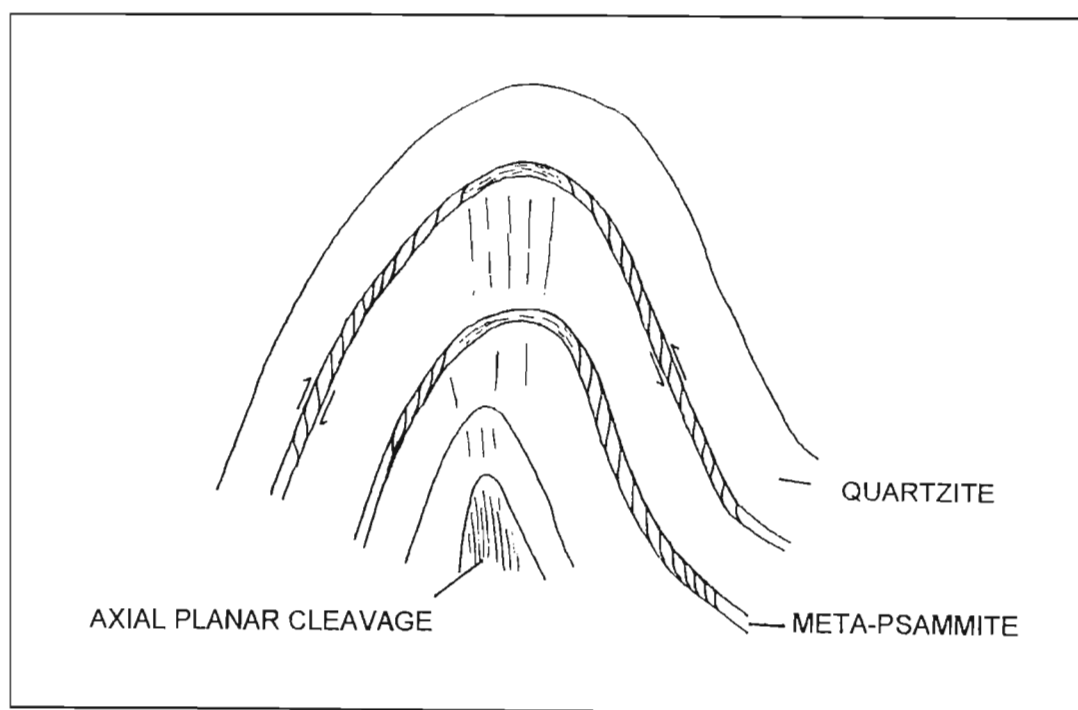


Figure 3.25: Flexural-slip shear zone geometry in a 3rd order fold.

The axial planar cleavage observed in the axial region of the 3rd order fold illustrated in Figure 3.25 is also developed in the axial regions of 1st and 2nd order folds in the Traverse 1-4 areas (Figure 3.27).

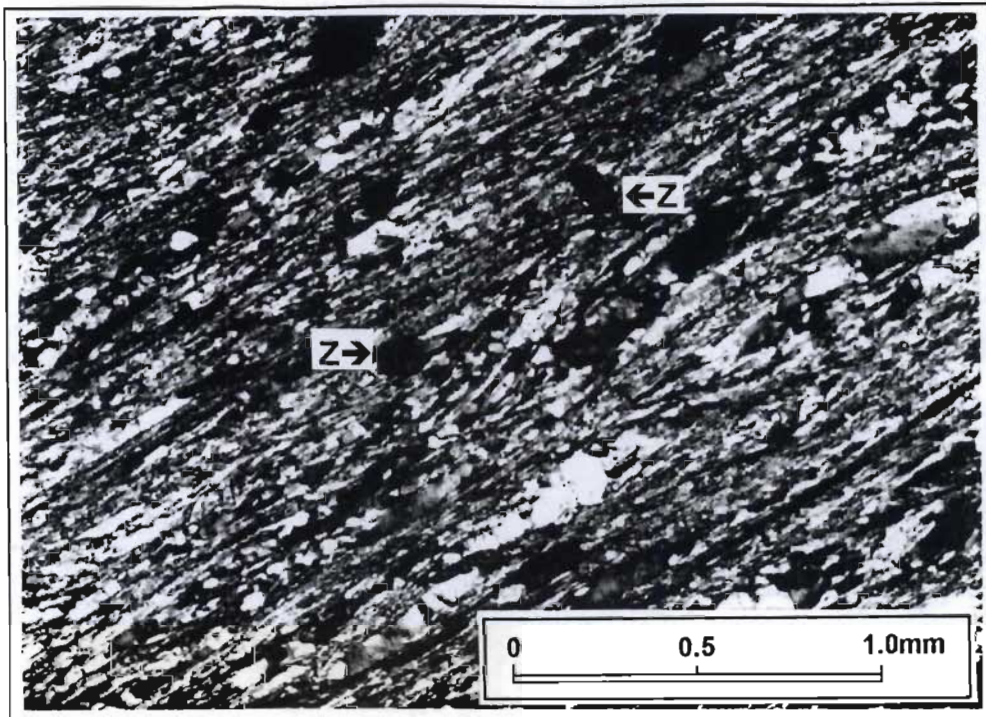


Figure 3.26: Phyllonite developed along a bedding parallel, flexural-slip shear zone. The sub-rounded minerals (with pressure shadows) labelled “Z” are detrital zircons. Transmitted cross-polarised light.

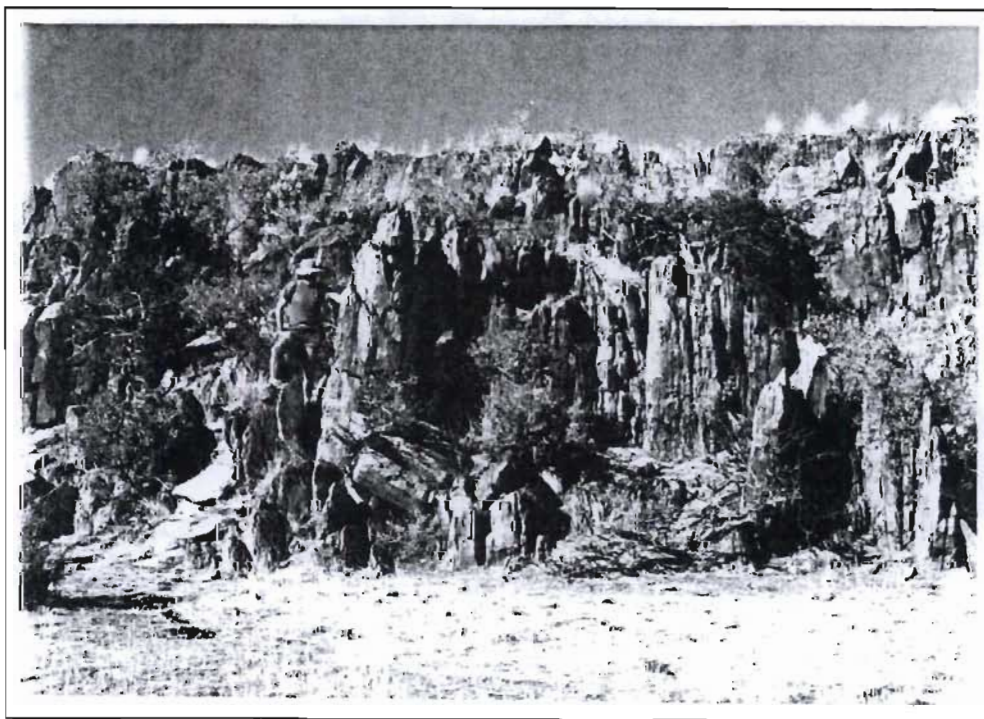


Figure 3.27: Axial planar cleavage developed in the axial region of a 2nd order fold. Top Dog member (farm Mutsistan 523- Traverse 2).

The orientations of axial planar cleavage planes measured in the Traverse 1 area are shown in Figure 3.28, those for Traverse 2 are shown in Figure 3.29 and those for Traverses 3 and 4 in Figures 3.30 and 3.31 respectively. In all of these areas the axial planar cleavage strikes parallel to the trend of the fold axes and is subvertical.

Figure 3.32 shows the microfabric developed in a Fuller member quartzite with a strongly developed axial planar cleavage. This rock was sampled in the hinge zone of a 3rd order fold on farm Drogepoort 345 (Traverse 1). The cleavage is defined by thin layers of muscovite and chlorite that anastomose around flattened and partially recrystallised quartz grains that exhibit strong undulose extinction.

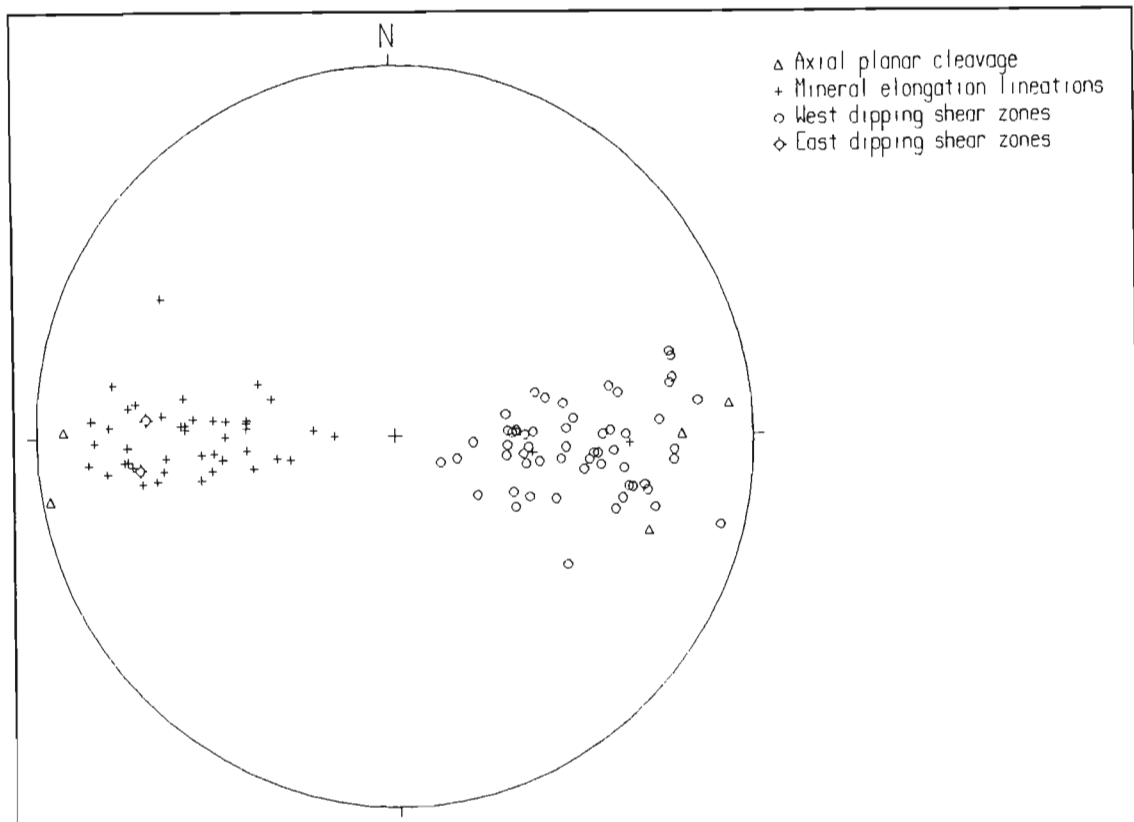


Figure 3.28: Equal area, stereographic projection (π -diagram) of the orientations of planar and linear fabric elements measured in the Traverse 1 area. (Axial planar cleavage: $n=5$; West dipping shear zones: $n=56$; East dipping shear zones: $n=2$; Mineral elongation lineations: $n=41$).

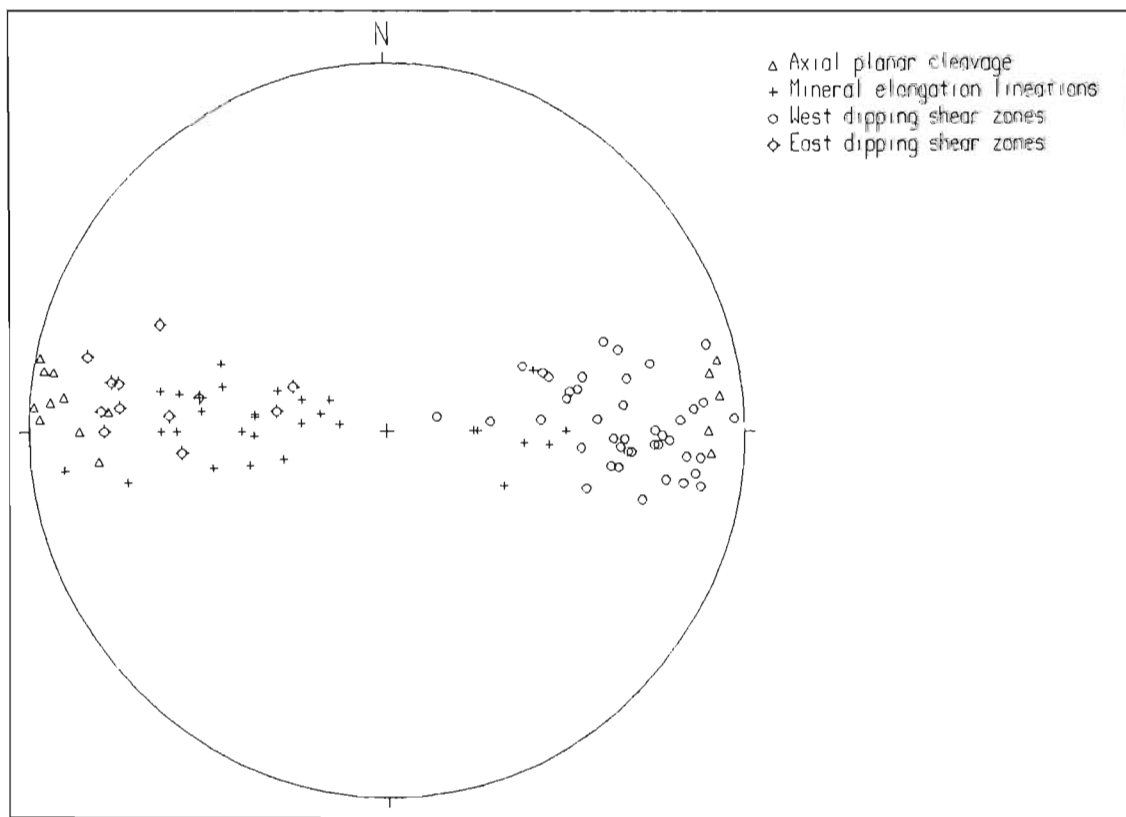


Figure 3.29: Equal area, stereographic projection (π -diagram) of the orientations of planar and linear fabric elements measured in the Traverse 2 area (Axial planar cleavage: $n=15$; West dipping shear zones: $n=42$; East dipping shear zones: $n=12$; Mineral elongation lineations: $n=29$).

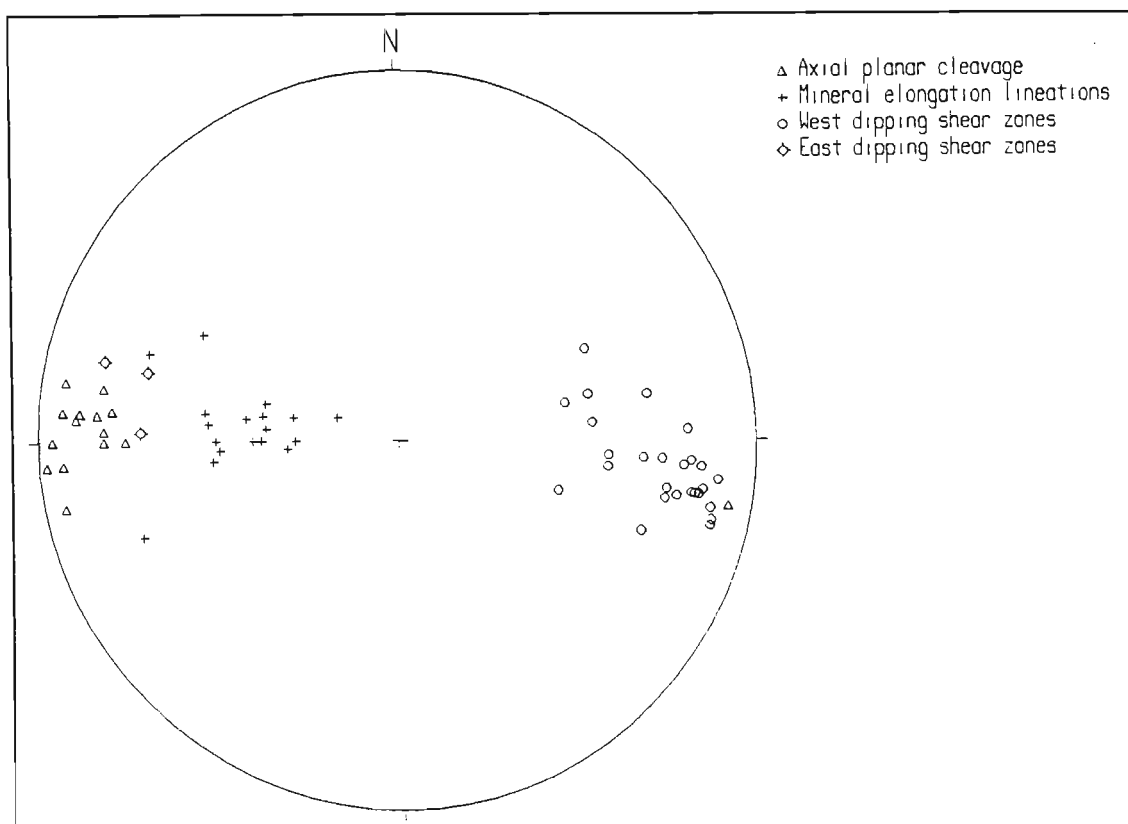


Figure 3.30: Equal area, stereographic projection (π -diagram) of the orientations of planar and linear fabric elements measured in the Traverse 3 area (Axial planar cleavage: $n=15$; West dipping shear zones: $n=26$; East dipping shear zones: $n=3$; Mineral elongation lineations: $n=18$).

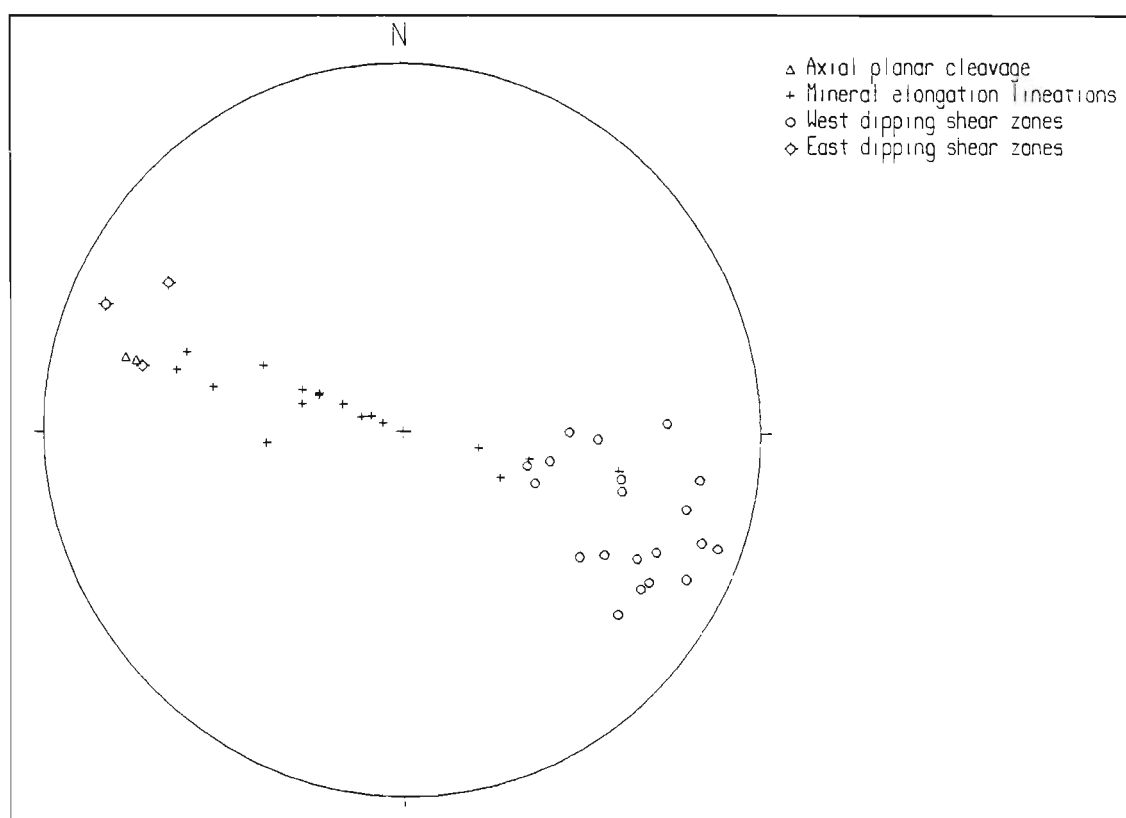


Figure 3.31: Equal area, stereographic projection (π -diagram) of the orientations of planar and linear fabric elements measured in the Traverse 4 area (Axial planar cleavage: $n=2$; West dipping shear zones: $n=20$; East dipping shear zones: $n=3$; Mineral elongation lineations: $n=17$).

3.2.3 Thrust sense shear zones

At locality 3.2, a road cutting on the Olifantshoek-Sishen road, banded ironstones of the Voelwater Subgroup overlie the Ongeluk Formation along a highly sheared contact. The banded ironstones have a strong west dipping, bedding sub-parallel foliation with an associated down-dip mineral elongation lineation. Small scale isoclinal folds, overturned to the east, are developed in discrete zones in the banded ironstone. Fold asymmetry and S-C fabrics indicate a west over east, thrust sense of movement. This thrust sense shear zone is indicated on Map 1 and Figure 3.21.

The contact between the Neylan bed (Hartley Formation) and the Lucknow Formation is exposed in a road-cutting at locality 3.4, immediately to the west of locality 3.2. Bedding sub-parallel shear zones are developed in narrow meta-psammite layers that are interbedded with the Lucknow Formation quartzite. The Neylan bed conglomerate has a strong foliation that dips steeply west, sub-parallel to the contact with the underlying Lucknow Formation. The foliation is heterogeneous and anastomoses around pods of weakly deformed conglomerate (see Figure 3.3: section 3.1.4). In high strain zones, lava clasts, and to a lesser extent the quartzite, jasper, ferruginous chert, jaspilite and banded ironstone clasts, are elongated parallel to a down-dip mineral elongation lineation defined by rod-shaped aggregates of quartz and mica. S-C fabrics in high strain zones indicate west over east thrust sense of movement. The shear zone has preferentially developed at the disconformity between the Lucknow and Hartley Formations.

Within the Matsap and Brulsand Formations along Traverses 2-4, west dipping thrust sense shear zones are developed (Figure 3.33). The shear zones are confined to the meta-psammite and argillaceous quartzite units and are typically <1m in width. No large scale duplication of stratigraphy could be recognised and the shear zones do not form mappable lineaments. Fabric development in these shear zones is very similar to that observed in the bedding sub-parallel shear zones related to the flexural-slip folding. Thus, except where the thrust sense shear zones cut eastward dipping bedding (Figure 3.34) it is very difficult to distinguish between the two structures. As the lineations in the two types of shear zones are parallel, they have been interpreted to have formed during the same progressive deformation event. The foliation and lineation data from the two types of shear zones are undifferentiated on Figures 3.28-3.31.

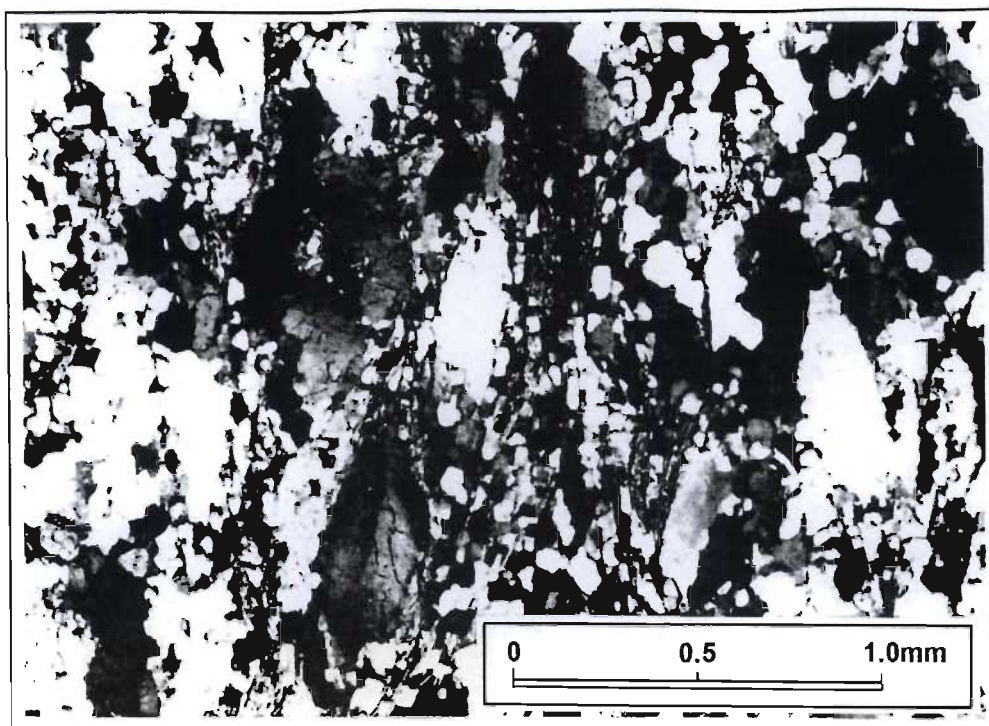


Figure 3.32: Photomicrograph of a sample of Fuller member quartzite with a well developed axial planar cleavage.



Figure 3.33: A westward dipping, bedding sub-parallel shear zone, developed in an argillaceous horizon bounded by siliceous quartzite. S-C fabrics indicate west over east thrust sense of movement. East is to the right of the photograph. Ellies Rus member, farm Gamayana 532- Traverse 2.

Figure 3.35 shows microfabric development in a sample of Ellies Rus member quartzite taken from an eastward vergent thrust sense shear zone that cuts across an east dipping fold limb. The foliation is defined by elongated quartz grains and thin layers of muscovite. Partial recrystallisation of the quartz grains has occurred. In hand specimen, greater than 50% of the rock is composed of visible fragments. This rock can therefore be classified as a protomylonite (Roering *et al.*, 1989).

The fold and thrust geometry of the Traverse 1 area is shown in Figure 3.24. Major duplication of stratigraphy has occurred along thrust sense shear zones in this area and these structures constitute mappable lineaments. Folds in the immediate hangingwall and footwall of the major thrust sense shear zones are overturned to the east.

Figure 3.28 shows the orientation of structural elements measured in the Traverse 1 area. Shear zones dip predominantly to the west, but a few east dipping, flexural-slip shear zones were observed. Mineral elongation lineations plunge predominantly to the west down the dip of the shear zone foliation.

Figure 3.36 shows highly sheared, Fuller member quartzite situated in the thrust sense shear zone exposed on the western part of farm Groenwater 304. The rock has a very glassy, fine grained appearance in hand-specimen (<50% visible fragments). In thin section (Figure 3.37) it can be seen that the rock is intensively recrystallised and can be classified as a mylonite (Roering *et al.*, 1989). Although not shown in Figure 3.37, the mylonite also contains small (<0.4mm) epidote porphyroblasts that form part of the prograde metamorphic assemblage (quartz-muscovite-epidote).

The fabric elements observed in the thrust sense shear zones (mylonite or protomylonite) are characteristic of ductile deformation. Disruption and displacement of stratigraphy (i.e. brittle deformation) has however occurred along these thrust sense shear zones. A dislocation plane is exposed on the northern part of farm Windhoek 301 (near the 47° foliation reading). At this locality, two different quartzite horizons of the Fuller member, with different bedding attitudes, are juxtaposed along a 20cm wide zone of foliated quartz veining. Quartz shear fibres (Ramsay and Huber, 1987) in the veins plunge westward, parallel to the mineral elongation lineations in the hangingwall and footwall rocks. The thrust sense shear zones that are responsible for the disruption and displacement of stratigraphy can thus be regarded as brittle-ductile in nature (Ramsay and Huber, 1987).

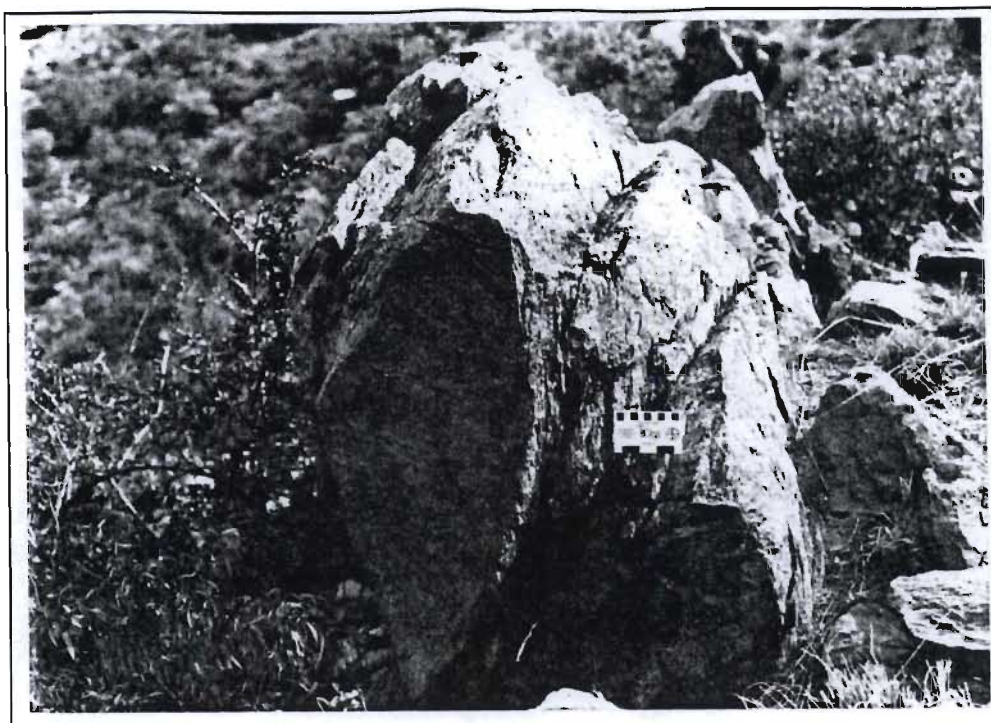


Figure 3.34: A west dipping thrust sense shear zone cutting across an east dipping fold limb. A bedding plane (solid line labelled S_0) and cross-bedding (dashed line) are marked on the rock. East is to the right of the photograph as indicated. Ellies Rus member quartzite, farm Watermeyer 576- Traverse 2.

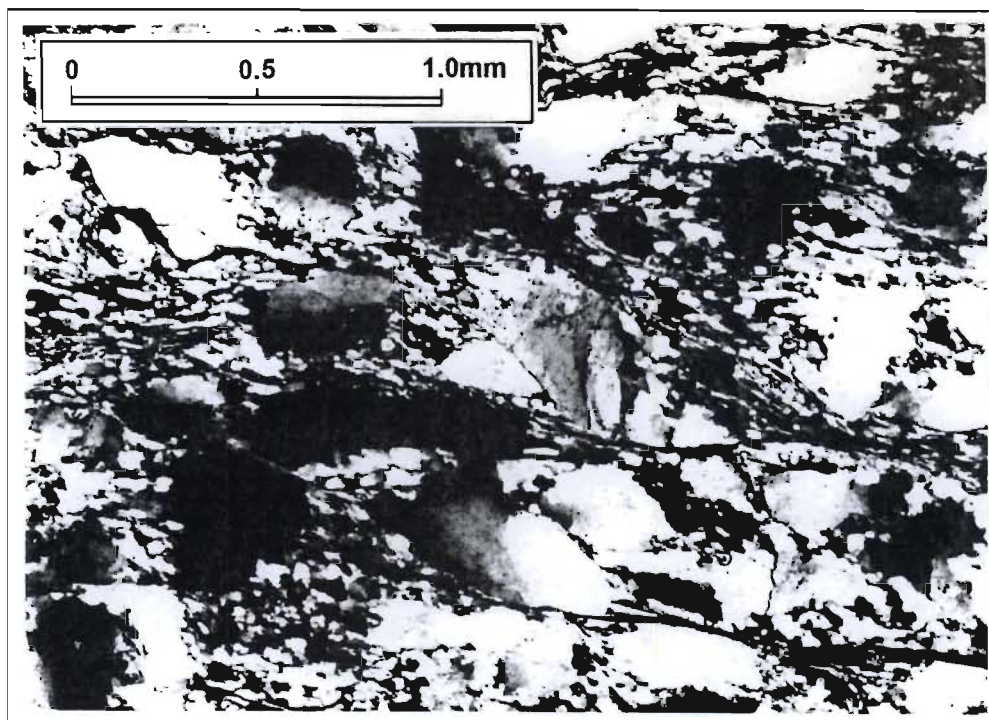


Figure 3.35: Protomylonite developed in a west dipping, thrust sense shear zone. Transmitted cross-polarised light.

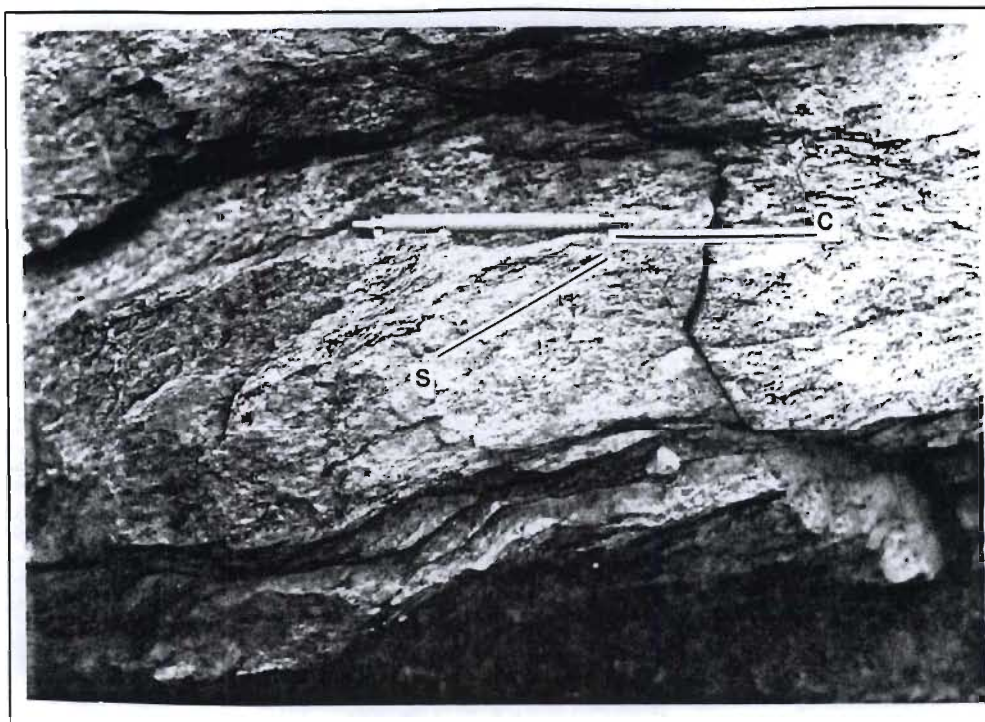


Figure 3.36: Mylonitised Fuller member quartzite. East is to the right of the photograph. S-C fabrics indicate a west over east, thrust sense of movement. (s= shear fabric, c= cutting fabric)

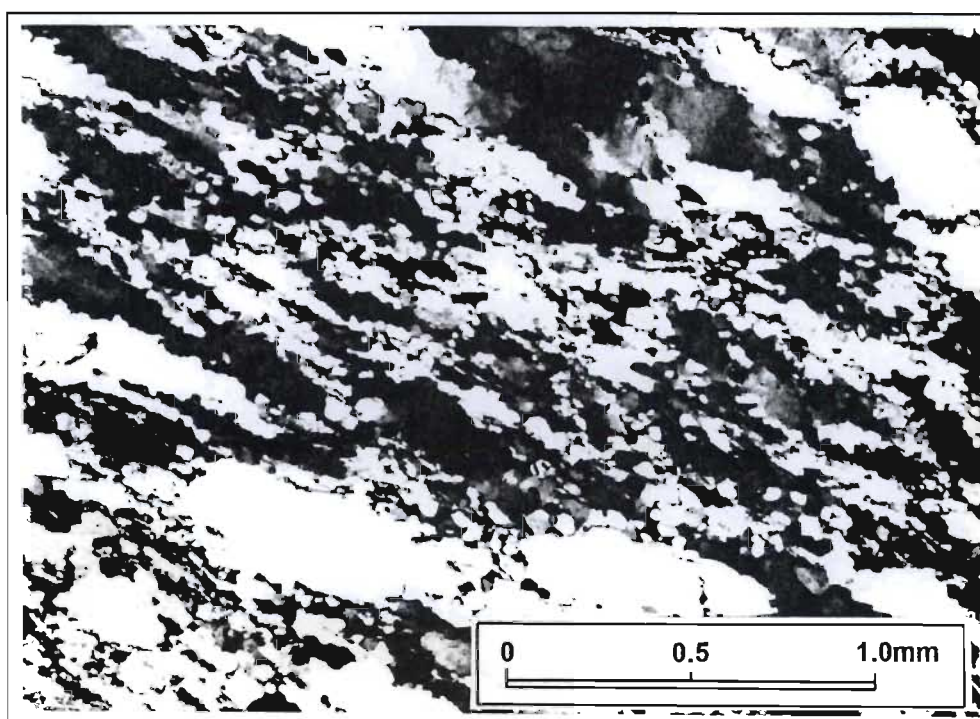


Figure 3.37: Photomicrograph of the mylonite shown in Figure 3.34. Transmitted cross-polarised light.

In the immediate hangingwall of the thrust sense shear zone situated on the eastern part of farm Groenwater 304 (near the 56° foliation reading), the Voelwater Subgroup banded ironstones and phyllites are intensely sheared. Chloritoid porphyroblasts in the phyllite layers have pressure shadows and are part of the prograde metamorphic assemblage. The foliation in the banded ironstones is defined by thin layers of specularite studded with small (<1mm) bright red crystalline hematite and brown-yellow piemontite (manganese epidote) porphyroblasts (confirmed with XRD). Antitaxial quartz-specularite extensional veins (Ramsay, 1980) up to 2cm wide are developed perpendicular to the foliation. The azimuth of the fibres in these veins (268°) is parallel to that of the mineral elongation lineations in the banded ironstones. The antitaxial veins thus developed during the thrusting event.

The brittle-ductile thrust sense shear zones observed in the Korannaberge can only be traced a few kilometres north and south of the Traverse 1 area before disappearing beneath the Kalahari sand cover. The northern extension of these thrust sense shear zones is uncertain. In the south, the shear zones are interpreted to link up with the thrust sense shear zone observed at locality 3.2 (Map 1).

3.2.4 The Molopo River area

Isolated exposures of quartzite in the Molopo River valley (Map 1) have been mapped as part of the Lucknow, Matsap and Brulsand Formations by SAGS (1984). In the west, interbedded purple and grey-green quartzite and pebbly quartzite are exposed. Planar cross-bedding and planar bedded heavy mineral layers occur in the quartzite. To the east, light brown trough cross-bedded quartzite is interbedded with grey siliceous quartzite. Based on similarities between these quartzites and the Verwater and Top Dog members observed in the Traverse 1-4 areas, it is tempting to correlate the outcrops with the Brulsand Formation. The Molopo River outcrops are however situated along strike of the Groblershoop Formation quartzites that form the Skurweberge (Map 1). The significance of this is examined in Chapter 8. The quartzites exposed in the Molopo River valley are considered here to be part of the Olifantshoek Supergroup but of uncertain stratigraphic correlation.

Figure 3.38 shows the orientation of bedding and axial planar cleavage measurements made on an anticline in the western part of the Molopo River area (locality 3.6). Bedding on the western limb dips approximately 10° shallower than bedding on the eastern limb. The π -axis, defining the fold axis, plunges 4° in direction 182°. The axial plane (defined by the mean orientation of the axial planar cleavage) is plotted and passes through the π -axis as expected. The dip of the axial surface is 60° in direction 270°. The fold is thus inclined to the east and indicative of an eastward vergence.

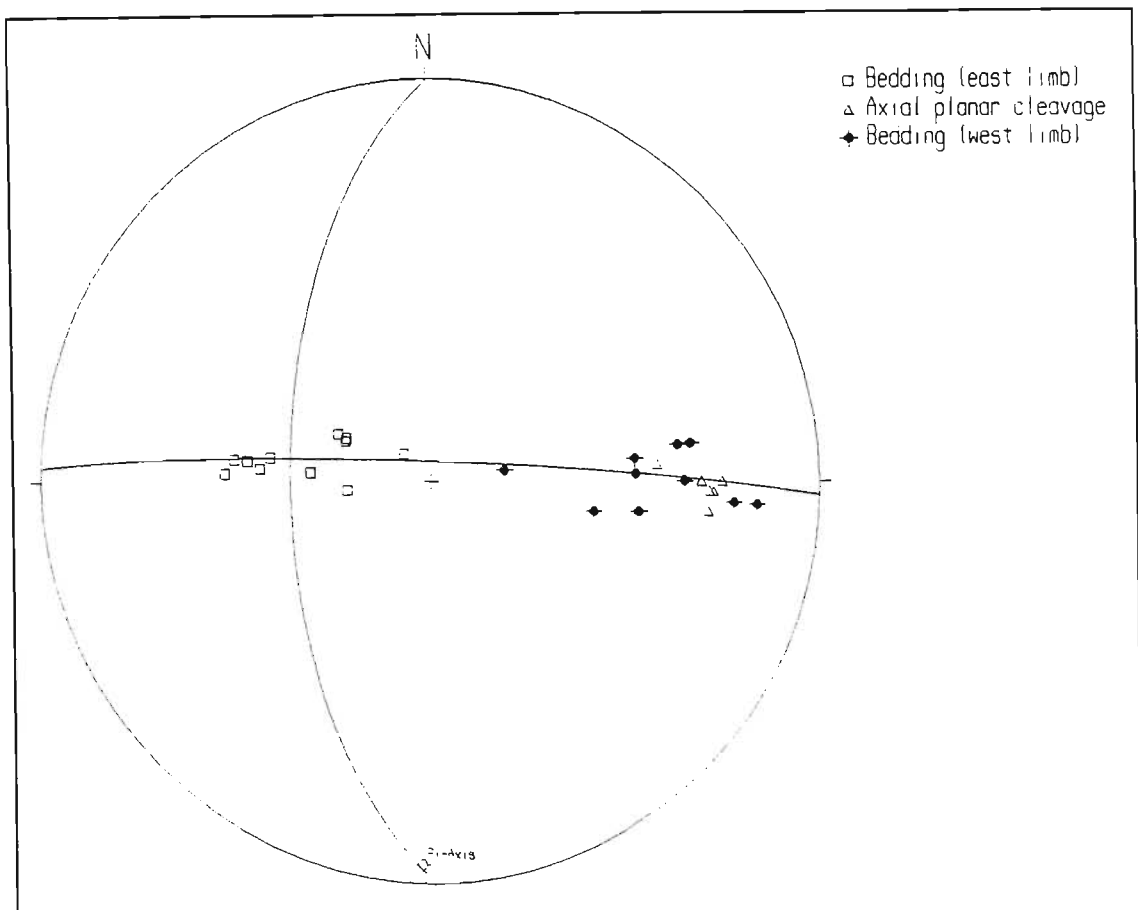


Figure 3.38: Equal area, stereographic projection (π -diagram) of the orientations of bedding ($n=21$) and axial planar cleavage ($n=6$) measured on the anticline at locality 3.6.

The axial planar cleavage does not dip consistently west in the Molopo River area. In the quartzites to the east of locality 3.6, the cleavage dips steeply about the vertical to both the east and west (Figure 3.39). Thrust sense shear zones, dipping at moderate angles to the west and cutting across bedding were observed in the Molopo River area. Mineral elongation lineations plunge to the west in the dip direction (Figure 3.39), perpendicular to the axial surface of the anticline described at locality 3.6 .

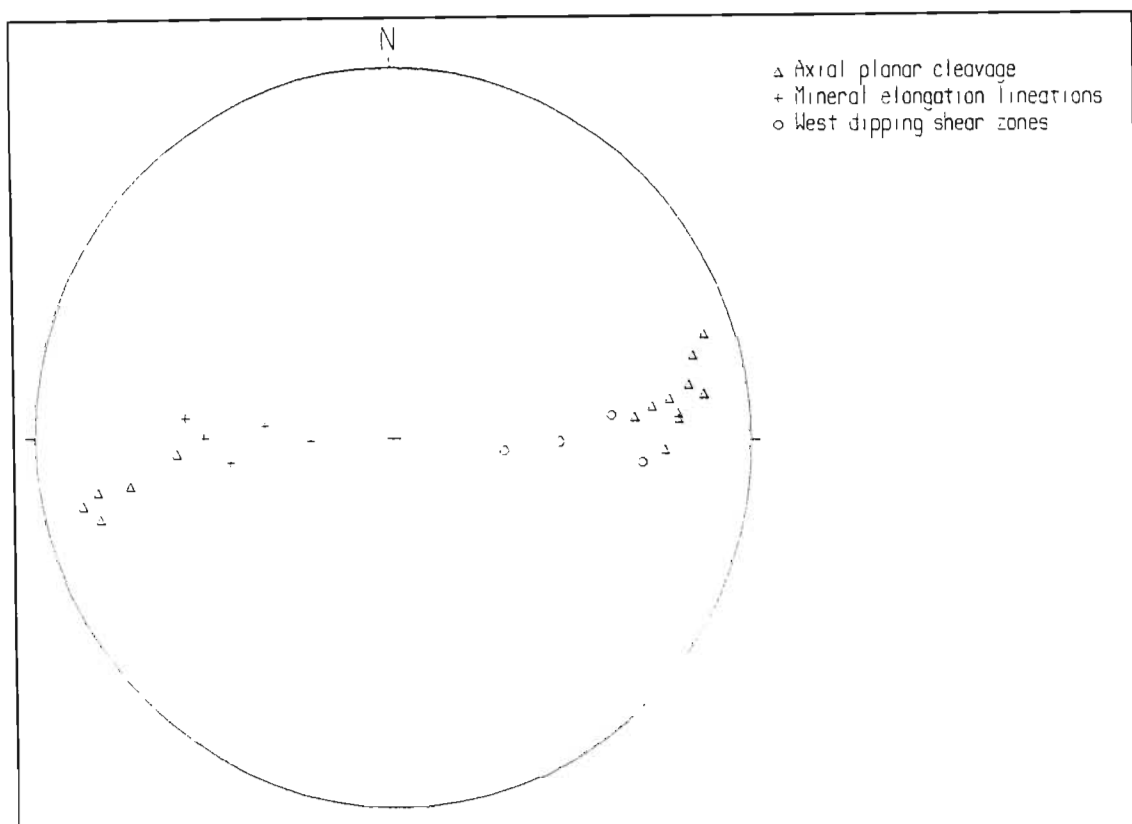


Figure 3.39: Equal area, stereographic projection (π -diagram) of planar and linear fabric elements measured east of locality 3.6 in the Molopo River area (Axial planar cleavage: $n=14$; Mineral elongation lineations: $n=5$; West dipping shear zones: $n=4$).

3.3 Summary

3.3.1 Stratigraphy and depositional environment

In the area immediately west of the Maremane structure (Map 1) the Mapedi Formation (Olifantshoek Supergroup) overlies the Ongeluk Formation and the Ghaap Group (Griqualand West Supergroup) with *angular unconformity* (Beukes and Smit, 1987). The unconformity at the base of the Lucknow Formation truncates the map pattern of the Ongeluk-Witwater syncline (Van Wyk, 1980; Beukes and Smit, 1987). The preserved eastern limb of a periclinal anticline (the western limb has been truncated at the Mapedi Formation unconformity) forms the eastern part of the Maremane structure. Deformation of the Griqualand West Supergroup to produce these large scale, approximately north-south trending, periclinal folds must have occurred prior to deposition of the Mapedi Formation.

The Voelwater Subgroup as well as the Wolhaarkop and Manganore Formations are only developed immediately below the basal unconformity of the Olifantshoek Supergroup on the western edge of the preserved Griqualand West Basin.

The Mapedi Formation (Figure 3.40) *disconformably* overlies the Voelwater Subgroup in the areas mapped during this study. The basal conglomerate of the Mapedi Formation is overlain by a succession of clastic sediments comprising immature purple quartzites interbedded with narrow conglomerate and phyllite horizons that grade up into white siliceous quartzites. Based on detailed facies-analysis in the Sishen area, Van Schalkwyk and Beukes (1986) interpret this basal clastic unit to have been deposited in a fluvio-deltaic palaeo-environment.

In the area west of Postmasburg (Map 1), the siliceous quartzites are conformably overlain by approximately 700m of mafic lava. The lavas are conformably overlain by interbedded siliceous quartzites and grey-green phyllites deposited in a shallow water environment prone to periods of aerial exposure and resultant desiccation crack formation (probably deposited in a shallow marine intertidal environment). In the Traverse 3 area only the upper part of the Mapedi Formation is exposed. In this area, the interbedded siliceous quartzites and grey-green phyllites are overlain by dolomite and pelitoidal dolomite deposited in a high energy, shallow marine palaeo-environment.








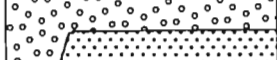




The lithostratigraphy of the Mapedi Formation thus records an initial fall in alluvial base level, accompanied by mafic volcanism, followed by a marine transgression.

The Mapedi Formation shallow marine sediments are disconformably overlain by fluvio-clastic sediments of the Lucknow Formation, indicating that a second fall in alluvial base level occurred. A debris flow diamictite (the Neylan bed) or sedimentary breccia, situated at the base of the Hartley Formation (carrying clasts of the underlying Voelwater Subgroup, Mapedi Formation and Lucknow Formation) indicates that renewed relative uplift occurred prior to (and during?) extrusion of the Hartley Formation lavas. Observations in the Korannaberge indicate that the Hartley Formation volcanism was localised.

Where developed, the Hartley Formation is conformably overlain by the Volop Group. The Fuller member was deposited in a high energy fluvial palaeo-environment. The overlying Ellies Rus and Glen Lyon members, and the lower part of the Verwater member, represent progressively lower energy, more distal fluvial deposits. The upper part of the Verwater member was deposited in an intertidal palaeo-environment. The Verwater member is overlain by the high energy shallow marine sediments of the Top Dog member. The Groblershoop Formation pelitic schists conformably overlie the Brulsand Formation (Botha *et al.*, 1976; Stowe, 1986) and probably represent deeper water pelitic marine sediments. The lithostratigraphy of the Volop Group and the Groblershoop Formation thus records an overall marine transgression.

The clasts in the conglomerate layers in the lower part of the Volop Group were largely derived from the underlying rocks of the Voelwater Subgroup and Lucknow and Mapedi Formations. Palaeocurrent analysis of the Volop Group by Jansen (1983) indicates that sediment transport in the Fuller member and the Ellies Rus member was predominantly from the north to the south, parallel to the present strike of the Olifantshoek Supergroup. Sediment transport in the overlying Glen Lyon member and Brulsand Formation was dominantly from the east towards the west (Jansen, *op. cit.*).

Figure 3.40: Composite stratigraphic column of the Voelwater Subgroup and the Olifantshoek Supergroup for the Korannaberge-Langberge area. Note that the thickness of units indicated in the hatched column is not to scale. Palaeo-depositional environment is based upon: Mapedi Formation (Beukes and Smit, 1987; this study); Lucknow Formation (this study), Hartley Formation (this study), Matsap Formation (Jansen, 1983; this study), Brulsand Formation (Jansen, 1983; this study), Groblershoop Formation (this study).

	Main Lithology	Stratigraphic Unit		Maximum thickness (m)	Palaeo-depositional environment
	schist, quartzite	Groblershoop Formation		Unknown	Marine
	quartzite	Top Dog member	Brulsand Formation	Unknown	High energy shallow marine
	quartzite	Verwater member		620	Fluvial to intertidal
	quartzite	Glen Lyon member	Matsap Formation	780	Low energy fluvial (distal)
	quartzite, meta-psammite conglomerate	Ellies Rus member		1250	Fluvial
	quartzite, meta-psammite conglomerate	Fuller member		1570	High energy fluvial (proximal)
	mafic lava	Hartley Formation		1000	Volcanic
	conglomerate/sed.-breccia			22	Debris flow/talus slope
	quartzite conglomerate	Lucknow Formation		500	Fluvial
	quartzite, phyllite, dolomite	Mapedi Formation		250	Intertidal to shallow marine
	mafic lava			700	Volcanic.
	quartzite, phyllite conglomerate			450	Fluvio-deltaic
	banded ironstone, chert, dolomite	Voelwater Subgroup		250	Unknown

3.3.2 The Kheis orogeny

As noted above, the Griqualand West Supergroup was deformed to produce large scale, north-south trending periclinal folds (such as the Ongeluk-Witwater syncline), prior to deposition of the Olifantshoek Supergroup. Based on the map pattern (Map 1), this early deformation occurred subsequent to the extrusion of the Ongeluk Formation lavas. No structural elements that pre-date the Kheis orogeny were observed in the Voelwater Subgroup, suggesting that the Voelwater Subgroup was deposited subsequent to the early deformation that produced the north-south trending periclinal folds.

During this study, folds and eastward vergent thrusts have been observed in rocks of the Voelwater Subgroup and the Olifantshoek Supergroup. These structures, as well as the Blackridge thrust; that caused duplication of both the Olifantshoek and Griqualand West Supergroups (Beukes and Smit, 1987); developed during the Kheis orogeny. Folding was by flexural-slip as indicated by the geometry of bedding parallel shear zones on fold limbs. Folding gave way to the development of eastward vergent brittle-ductile thrust sense shear zones that, in the Korannaberge, caused duplication of the Olifantshoek Supergroup and the Voelwater Subgroup. On Map 1 this system of shear zones is indicated as the Korannaberg thrust and has been traced south to Olifantshoek (locality 3.2). The Korannaberg thrust is interpreted to be the northward continuation of a thrust mapped in the Lucas Dam area (locality 3.5) by SAGS (1977) and to link at depth with the Blackridge thrust. The surface link between the Korannaberg and Blackridge thrusts occurs to the south of Wolhaarkop (SAGS, 1977; Van Wyk, 1980).

As indicated by the map for Traverse 1, the gabbro-norite sills that have intruded the Olifantshoek Supergroup were deformed during the Kheis orogeny.

Prograde mineral assemblages of quartz-muscovite-chlorite \pm epidote in the Volop Group quartzites and quartz-muscovite \pm chloritoid in phyllites of the Voelwater Subgroup are indicative of greenschist facies metamorphic conditions.

4. THE GEOLOGY OF THE BOEGOEBERG DAM AREA

The results of mapping in the Boegoeberg dam and surrounding area (Map 1, Map 2) are presented in the following sections. The majority of observations were made in the area mapped as Map 2. Localities within this area are indicated on Map 2 and referenced in the text using the format: L1, D1 or P1 (note that these are not grid-references). The positions of localities outside the area covered by Map 2 are indicated on Map 1 and are referenced using the format: locality 4.1.

The Map 2 area, or parts thereof, has previously been mapped by Vajner (1974), Smit (1977), Altermann and Halbich (1990, 1991) and the South African Geological Survey (SAGS, 1995). All of these published maps are inconsistent in terms of the stratigraphic units recognised in the area and the position of major structural features. In section 4.1, stratigraphic units recognised in the Boegoeberg dam area are described and, where possible, correlated with units recognised in the Langberge-Korannaberge area. In section 4.2 the structural geology of the Boegoeberg dam area is described. The lithostratigraphy and structural geology of the Boegoeberg dam area are summarised in section 4.3.

4.1 *Lithostratigraphy*

Figure 4.1 summarises the lithostratigraphy of the Boegoeberg Dam area as determined during this study. Thicknesses of stratigraphic units were determined from accurate cross sections (except where otherwise stated).

4.1.1 The Zeekoebaart Formation

Vajner (1974) and Altermann and Halbich (1990, 1991) interpreted both the interbedded lavas and sediments in the central part of the Map 2 area (the Waterval member of Vajner, 1974), and the lavas in the south-western part (the Blinkfontein volcanic member of Vajner, 1974) as being rocks of the Zeekoebaart Formation. Smit (1977) correlated the Waterval member of Vajner (1974) with the Hartley Formation of the Olifantshoek Supergroup. This correlation was confirmed during the present study and will be further discussed in section 4.1.3.

A sequence of mafic volcanic rocks exposed in the southern parts of farm Zeekoebaart 9 and the Boegoeberg water reserve underlie the Mapedi Formation and are interpreted to be part of the Zeekoebaart Formation. This interpretation is based on both outcrop continuity and lithological

similarities between these rocks and the main outcrop of the Zeekoebaart Formation volcanics in the south (Map 1). The Zeekoebaart Formation in this area is very poorly exposed and the rocks that do crop out are strongly foliated. The base of the Zeekoebaart Formation is not exposed in the Map 2 area. The Zeekoebaart Formation consists, for the most part, of dull green coloured amygdaloidal mafic lavas. Subordinate layers of highly sheared agglomerate with clasts of quartzite and schist were observed at a few localities. No indications of primary layering were observed in the Map 2 area.

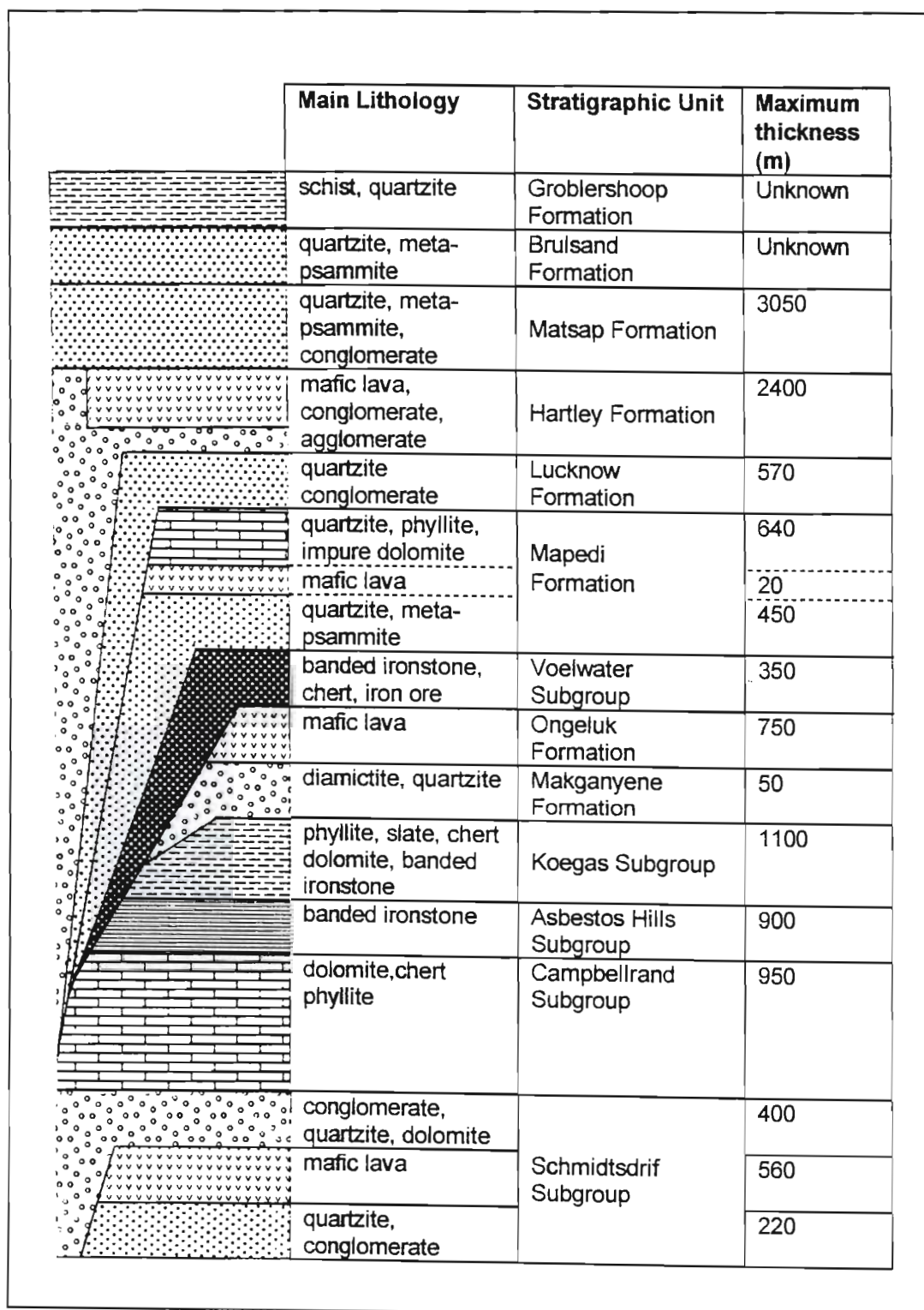


Figure 4.1: Summary stratigraphic column of the Boegoeberg Dam area.

4.1.2 The Griqualand West Supergroup

Much of the inconsistency in the literature has been caused by authors correlating rocks exposed in the central part of the Map 2 area with units of either the Olifantshoek Supergroup (Smit, 1977; SAGS, 1995) or the Griqualand West Supergroup (Vajner, 1974; Smit, 1977; Altermann and Halbich, 1990, 1991). The rocks in this area are highly strained and stratigraphic duplication has occurred along thrust sense shear zones. The lower part of the Griqualand West Supergroup was studied on farm Geelbeksdam (locality 4.1- south of Westerberg) in order to document the stratigraphy of the Griqualand West Supergroup where it is well exposed and only weakly deformed.

A detailed study of the mineralogy and sedimentology of the Griqualand West Supergroup in the study area is beyond the scope of this thesis. The approach taken in describing the Griqualand West Supergroup was to document characteristic features that can be used to identify the various units in the field and, in particular, features that can be used to distinguish them from similar rock types that form part of the Olifantshoek Supergroup.

4.1.2.1 The Schmidtsdrif Subgroup

The Schmidtsdrif Subgroup, the basal unit of the Griqualand West Supergroup, is not exposed in the Map 2 area. On farm Geelbeksdam (Figure 4.2), lavas of the Zeekoebaart Formation are overlain by 220m of eastward dipping, trough cross-bedded, light-brown to grey coloured quartzite of the Schmidtsdrif Subgroup (Figure 4.3). In the lower 50m of this unit, conglomerate bands up to 20cm thick are developed and contain clasts of vein quartz and lava, the contact itself is not exposed. The quartzite is conformably overlain by approximately 560m of dark green coloured, mafic lava. Several flows, bounded by flow-top breccias 0.5 -3m in thickness, can be recognised (Figure 4.3). Near the base of each flow, the lava is porphyritic and contains euhedral plagioclase phenocrysts up to 3cm in length. In discrete zones, the lath-like phenocrysts are aligned parallel to flow banding which dips east, sub-parallel to the over- and underlying sediments. Moving upwards through each flow, the proportion of phenocrysts in the lava steadily decreases and they eventually disappear. Featureless equigranular lava, followed by amygdaloidal lava dominate the middle to upper part of each flow.

The lavas are overlain by a narrow band (<2m) of gritty, brown coloured, trough cross-bedded quartzite that is in turn overlain by 350m of grey to white coloured, siliceous ripple-marked quartzite and brown weakly stratified, but otherwise featureless, dolomite that are interbedded on 5-20m scale.

Figure 4.2: Geological map of farm Geelbeksdam and the surrounding area. Modified after Vajner (1974).

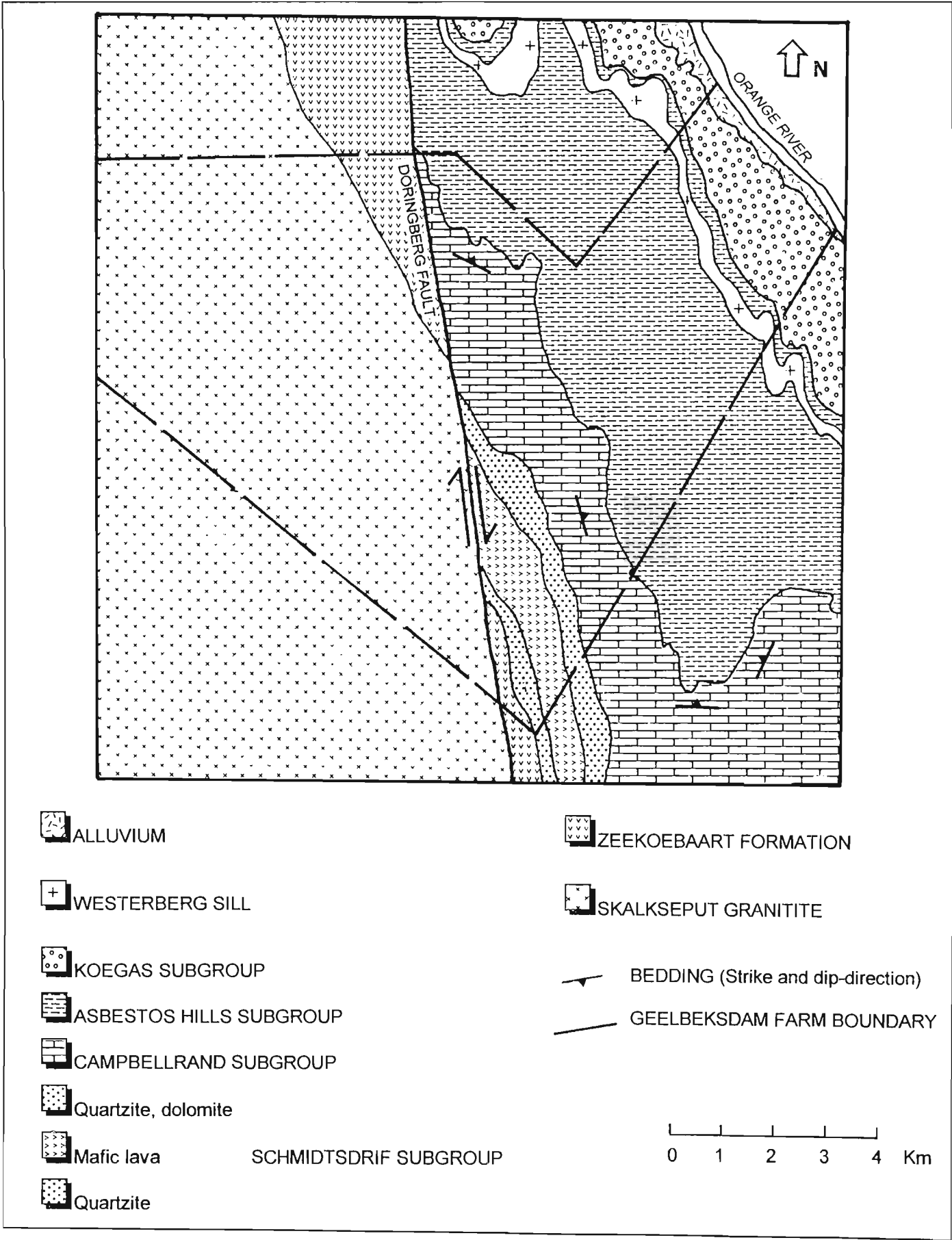
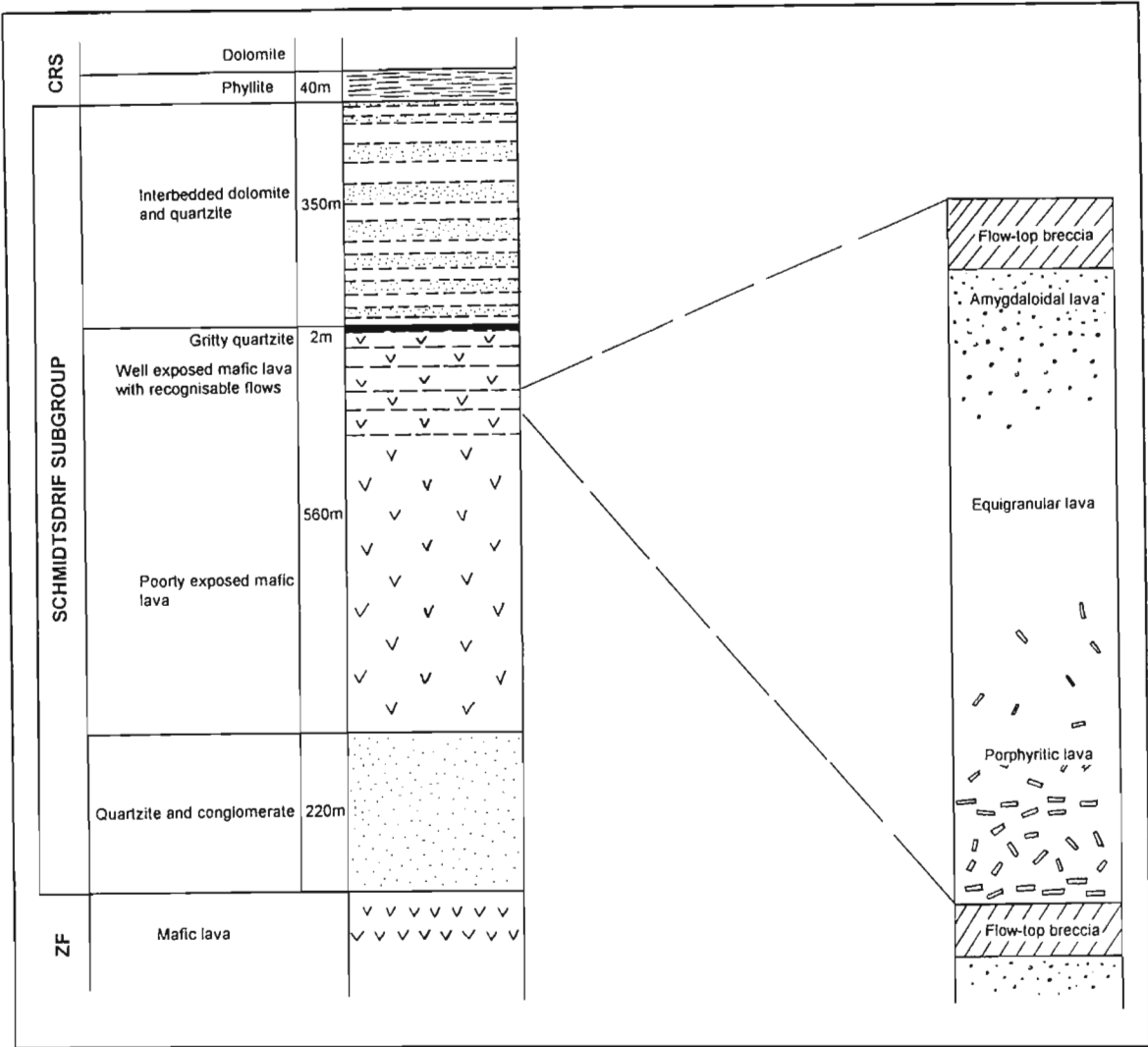


Figure 4.3: Field log of the stratigraphy of the Schmidtsdrif Subgroup on Geelbeksdam. The insert shows the textural variations within an individual lava flow in the Schmidtsdrif Subgroup. ZF= Zeekoebaart Formation. CRS= Campbellrand Subgroup.



On farm Witvlei (locality 4.2), 5 km south of Geelbeksdam, a 25m thick conglomerate unit unconformably overlies lavas of the Zeekoebaart Formation. The conglomerate band is overlain by interbedded quartzite and dolomite, identical to the upper unit of the Schmidtsdrif Subgroup exposed on farm Geelbeksdam (Figure 4.3). The conglomerate thus occupies the same stratigraphic position as the gritty, brown quartzite on farm Geelbeksdam. The conglomerate consists of poorly sorted, rounded to sub-rounded clasts of lava and quartzite in a gritty, brown matrix. The clasts vary in size from small pebbles a few cm in width to large boulders up to 0.5m across. Within the conglomerate, lenses of trough cross-bedded, gritty brown quartzite up to 10m in width and 1.5m in thickness are developed. Bedding in these lenses dips eastward, parallel to that in the overlying interbedded quartzites and dolomites. The conglomerate exposed at this locality was termed the Witvlei conglomerate by Vajner (1974) who considered it to be the uppermost unit of the Zeekoebaart Formation. On the basis of stratigraphic position it is interpreted here to be part of the Schmidtsdrif Subgroup and a lateral equivalent of the gritty

brown quartzite exposed on farm Geelbeksdam. The porphyritic lavas and the lower quartzite of the Schmidtsdrif Subgroup (Figure 4.3) have been eroded at this locality, such that the conglomerate rests unconformably on the Zeekoebaart Formation.

On farm Geelbeksdam the interbedded quartzites and dolomites, that overlie the gritty brown quartzite, are overlain by 40m of red phyllite with narrow dolomite and chert bands (Figure 4.3). The Schmidtsdrif Subgroup grades upwards through this zone into the brown dolomites, with narrow chert bands, of the Campbellrand Subgroup.

The Griqualand West Supergroup in the Geelbeksdam area has been deformed by north-south trending folds, such as the syncline south-east of the farm (Figure 4.2). The NNW trending Doringberg fault has juxtaposed the Zeekoebaart Formation and the Schmidtsdrif Subgroup against the Skalkseput granite.

4.1.2.2 The Campbellrand Subgroup

Within the Map 2 area, the Campbellrand Subgroup consists of grey dolomites that weather to a brown or grey-green colour. The dolomites have numerous, finely banded, grey siliceous chert layers, typically 2-25cm in thickness. Some thicker chert bands up to 2m thick were observed. Minor, red or purple coloured ferruginous chert bands occur within the dolomites. Columnar and domical stromatolites were observed in certain dolomite horizons. Where the contact is exposed (e.g. the south-western part of farm 314-adjacent to the Orange river), a narrow band (<20m) of red phyllite is developed between the Campbellrand Subgroup and banded ironstones of the Asbestos Hills Subgroup. This phyllite contains round ferruginous concretions up to 8cm in diameter. Due to structural repetition and the lack of reliable marker beds, no indication of the thickness of the Campbellrand Subgroup was possible in the Map 2 area. On farm Geelbeksdam, the unit is 950m thick.

4.1.2.3 The Asbestos Hills Subgroup

The Asbestos Hills Subgroup is exposed in the southern, central part of the Map 2 area. The basal 40-60m of the Asbestos Hills Subgroup consists of banded ironstones comprising hematite-magnetite rich layers interbedded with white siliceous and purple ferruginous chert layers on a 5-10mm scale. The iron rich layers are dark brown to black in colour. The remainder of the Asbestos Hills Subgroup comprises brown-yellow weathering banded ironstones. These banded ironstones consist of narrow bands, 1mm to 2cm in thickness, of dark-brown to black iron rich layers alternating with brown siliceous chert or light-brown to

yellow-brown siltstone layers. The siltstone layers comprise phyllosilicates and siderite, the iron-rich layers are comprised predominantly euhedral recrystallised magnetite grains.

Bedding parallel, blue-grey coloured, crocidolite asbestos seams are common throughout the Asbestos Hills Subgroup in the Map 2 area but are particularly well developed in the lower part of the unit, in and immediately above the dark weathering hematite rich banded ironstones. In places the asbestos has been partially or completely replaced by silica to form tigers-eye.

Due to structural complexity, no estimate of the thickness of the Asbestos Hills Subgroup could be made in the Map 2 area. Vajner (1974) reported well constrained thicknesses (from exploration drilling), ranging between 650-900m, for the Asbestos Hills Subgroup in the Westerberg area.

4.1.2.4 The Koegas Subgroup

The Koegas Subgroup is exposed in the south-eastern portion of the Map 2 area. As it is poorly exposed and intensely foliated by Kheis age, thrust sense shear zones, no conclusions could be made regarding its thickness or internal stratigraphy. The Koegas Subgroup within the Map 2 area consists of intercalated red or green phyllite, slate and meta-psammite with minor banded ironstone, dolomite and chert. Vajner (1974) estimated a maximum thickness of 1100m for the Koegas Subgroup in the Westerberg area.

4.1.2.5 The Makganyene Formation

The Makganyene Formation is not developed in the Map 2 area, but is exposed immediately to the south at locality 4.3. The Makganyene Formation is less than 50m thick in this area, too narrow to indicate on Map 1. It is underlain by the Koegas Subgroup and overlain by the Ongeluk Formation. The Makganyene Formation at this locality comprises a poorly sorted, weakly stratified diamictite with lenses of light grey-green, pebbly quartzite. The diamictite is matrix supported and contains angular to subrounded clasts, ranging in size from 5mm to 1m, of chert, banded ironstone, jasper, dolomite and quartzite in a green-grey matrix. In thin section it was observed that the matrix is comprised of fine quartz grains, calcite and phyllosilicates, minor amounts of ore minerals and detrital zircons occur.

Neither the upper, nor lower contacts of the Makganyene Formation are exposed in this area. Bedding in the Makganyene Formation at locality 4.3 strikes approximately north-south and dips steeply east, sub-parallel to that in the underlying Koegas Subgroup and the overlying Ongeluk Formation.

4.1.2.6 The Ongeluk Formation

The Ongeluk Formation is not exposed in the Map 2 area, but is exposed to the east of locality 4.3. At this locality, the Ongeluk Formation consists of dull green coloured, brown weathering mafic lavas. The lavas are commonly amygdaloidal and hyaloclastite flow top breccias were observed in places. A layer of banded ironstone, comprising alternating bands of bright red jasper and magnetite, outcrops near the base of the Ongeluk Formation. The complete Ongeluk Formation is not exposed in the Boegoeberg dam area. An exposed thickness of 750m is estimated for the Ongeluk Formation in the area immediately south of Map 2.

Immediately north of locality 4.3, north-south striking, steeply east dipping rocks of the Ongeluk Formation, Makganyene Formation and Koegas Subgroup are overlain with angular unconformity by the basal conglomerate of the Lucknow Formation. The Lucknow Formation strikes ENE-WSW at this locality and dips north at 40°.

4.1.2.7 The Voelwater Subgroup

The Voelwater Subgroup has not been recognised in the Boegoeberg dam area prior to this investigation. As a result of structural repetition by thrusting, rocks of the Voelwater Subgroup outcrop in four north-east to east striking linear zones (Map 2). For descriptive purposes, these zones shall be referred to as Zones 1 to 4. Zone 1 corresponds to the most northerly linear zone, Zone 4 to the most southerly zone. The correlation of the rocks in these four zones with the Voelwater Subgroup is based upon:

- (a) Lithological similarities between these rocks and the Voelwater Subgroup rocks observed in the Korannaberge-Langberge area.
- (b) Differences between these rocks and the Griqualand West Supergroup strata in both the Map 2 and Geelbeksdam areas.
- (c) The regional map pattern of the Voelwater Subgroup.
- (d) Structural geology.

(a) and (b) are dealt with in the paragraphs that follow, (c) and (d) in section 4.2. Contacts between the Voelwater Subgroup and the underlying strata are typically sheared, at no locality could a sedimentary contact be demonstrated.

The Voelwater Subgroup in Zones 1 and 2 has been interpreted by previous workers to be either part of the Asbestos Hills Subgroup (Vajner, 1974; Altermann and Halbach, 1990, 1991; SAGS, 1995) or the basal unit of the Hartley Formation (Smit, 1977). It shall be shown in section 4.1.3.3 that the Hartley Formation disconformably overlies the Voelwater Subgroup in the Map 2 area, hence the interpretation of Smit (1977) is incorrect. The Voelwater Subgroup in Zone 1 consists of banded ironstone comprising hematite rich layers interbedded on a 2mm to 4cm scale with siliceous and/or ferruginous chert (Figure 4.4). These banded ironstones are identical in both appearance and composition to the Voelwater Subgroup banded ironstones observed on the eastern flanks of the Korannaberg-Langberge mountain chain. The resistant nature and high hematite content of the Voelwater Subgroup in this and the other zones has resulted in it forming purple to black coloured, sparsely vegetated, positive topographic features. These are very distinct in appearance when compared to the outcrops of all other stratigraphic units in the study area (including the Asbestos Hills Subgroup banded ironstones).

The majority of the Voelwater Subgroup rocks in Zone 2 comprise hematite-rich banded ironstones. At the western edge of Zone 2, a discontinuous lens of banded brown siliceous chert, approximately 12m in thickness occurs at the base of the Voelwater Subgroup. In the vicinity of locality L1 (farm Bovenzeekoebaart 313), layers of finely laminated hematite iron ore occur interbedded with banded ironstone.



Figure 4.4: Voelwater Subgroup banded ironstone comprising alternating hematite rich and siliceous chert layers. (Farm 312- Map 2).

The Voelwater Subgroup in Zone 3 occurs as discontinuous lenses overlying dolomites of the Campbellrand Subgroup. These lenses are disconformably overlain by the Mapedi Formation. Figure 4.5 shows a sketch of the lens exposed at locality L2 (farm Bovenzeekoebaart 313). The lens comprises banded brown siliceous chert (similar to that in Zone 2), purple ferruginous chert and banded ironstone consisting of interbedded hematite and ferruginous/siliceous chert layers. The banded ironstones contain layers, up to a metre in thickness, of finely laminated hematite iron ore (Figure 4.6). At locality L3 (farm 312) laminated hematite iron ore occurs in layers up to 5m in thickness.

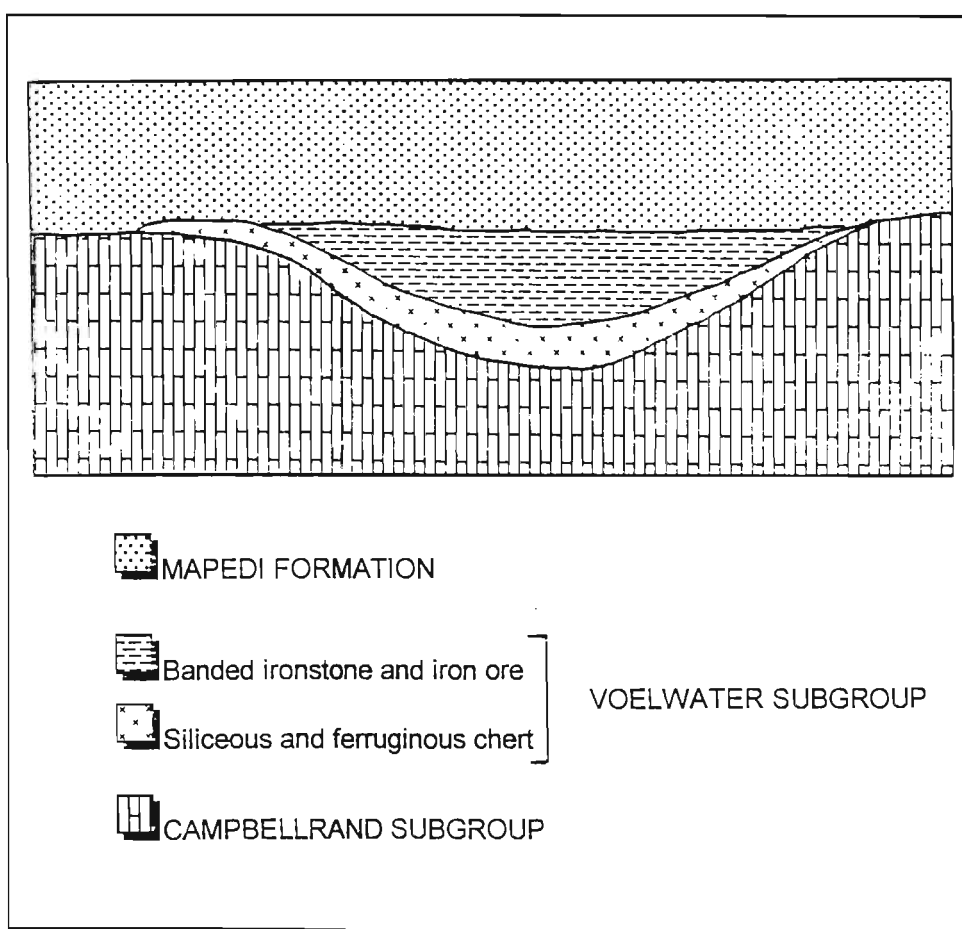


Figure 4.5: Cross-section of the lens of Voelwater Subgroup rocks exposed at locality L2 (farm Bovenzeekoebaart 313).

Near the common boundary of farms 314, 315 and 311 (locality L4), Voelwater Subgroup rocks are disconformably overlain by the Lucknow Formation (Figure 4.7). The banded ironstones at this locality were previously interpreted to be part of the Asbestos Hills Subgroup (Vajner, 1974; SAGS, 1995) but are lithologically distinct from the yellow-brown coloured Asbestos Hills Subgroup banded ironstones exposed to the west. The Voelwater Subgroup banded ironstones at this locality comprise interbedded hematite and ferruginous/siliceous chert layers. Both the Voelwater Subgroup and the overlying Lucknow

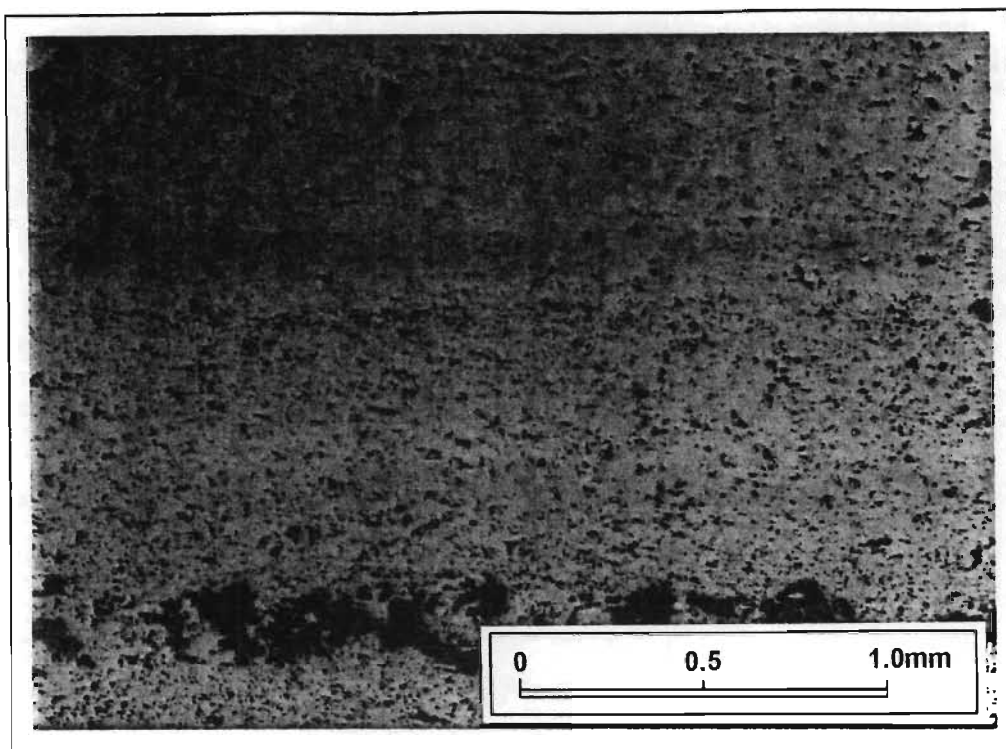


Figure 4.6: Photomicrograph of finely laminated iron ore from the Voelwater Subgroup. The primary layering is defined by a subtle change in the hematite grain size and by layers of gangue minerals. Plane-polarised reflected light.



Figure 4.7: Lucknow Formation quartzite overlying banded ironstones of the Voelwater Subgroup. View is southwards from locality L4.

Formation have a north-south strike in contrast to the east-west strike of the Asbestos Hills Subgroup exposed immediately to the west.

The southern-most linear zone of Voelwater Subgroup rocks, Zone 4, crops out on farms 315 and 311. The rocks in this zone were previously interpreted by Vajner (1974) as being part of the Koegas Subgroup but of uncertain stratigraphic correlation, as they are lithologically distinct from the Koegas Subgroup rocks exposed to the south. The rocks in Zone 4 were mapped by the SAGS (1995) as being part of the Asbestos Hills Subgroup. Based on similarities between the rocks exposed in Zone 4 and those in Zones 1-3 the hematite rich rocks in this area are correlated with the Voelwater Subgroup. The Voelwater Subgroup in Zone 4 consists of hematite-chert banded ironstones. Edgewise conglomerates identical to those developed in the Voelwater Subgroup in the Korannaberge were observed at locality L5.

Banded ironstones of the Voelwater Subgroup are exposed on the western boundary of the Map 2 area on farm Zeekoebar 9 (locality P3). These banded ironstones were formerly mapped as Campbellrand Subgroup by Vajner (1974) and SAGS (1995). At this locality, the Voelwater Subgroup has been thrust over the Mapedi and Zeekoebaart Formations. The banded ironstones of the Voelwater Subgroup are disconformably overlain by the Matsap Formation (section 4.1.3). The map pattern of the Voelwater Subgroup continues westward, parallel to the overlying Matsap and Brulsand Formations that form the Eselberge mountains (Map 1).

4.1.3 The Olifantshoek Supergroup

The map pattern of the Olifantshoek Supergroup follows an arcuate trace from the Traverse 4 area (Map 1), where it has a general NNE strike and westerly dip, to the Boegoeberg dam area where the strike varies between north-east and east and the dip direction between north-west and north. The trace of the Blackridge thrust, as determined during this study, passes through the central and southern parts of the Map 2 area. Thus the Olifantshoek Supergroup strata exposed in both the hangingwall and footwall of the Blackridge thrust converge in the Map 2 area (Map 1).

4.1.3.1 The Mapedi Formation

As outlined in chapters 2 and 3, the stratigraphic unit termed the Mapedi Formation is taken here to also include the lower part of the Lucknow Formation of SACS (1980) and Beukes and Smit (1987). The contact between the Mapedi Formation and the Lucknow Formation, as defined here, is marked by a

disconformity separating fluvial to shallow marine sediments (quartzite, phyllite, dolomite) and mafic lava (Mapedi Formation and the lower part of the Lucknow Formation of SACS, 1980) from fluvial quartzites and conglomerates (the upper part of the Lucknow Formation of SACS, 1980).

The Mapedi Formation in the study area comprises quartzite, phyllite, dolomite and lava. The confusion regarding the stratigraphic correlation of this unit has largely arisen due to workers interpreting the dolomites to be part of the Campbellrand Subgroup and the quartzites and phyllites as part of the Schmidtsdrif Subgroup (Vajner, 1974; Smit, 1977; Altermann and Halbach, 1990, 1991). Botha *et al.* (1976) noted that the clastic sediments and carbonates that outcrop in the vicinity of Boegoeberg dam are not “typical” of the Griqualand West Supergroup and suggested that these rocks might be an equivalent of the Olifantshoek Supergroup. On the most recently published map (SAGS, 1995) outcrops of these clastics and carbonates are interpreted to be either Schmidtsdrif Subgroup, Campbellrand Subgroup or Lucknow Formation.

Within the Map 2 area, the Mapedi Formation is generally strongly foliated, forms tight overturned folds and contains numerous, small scale thrust sense shear zones. As a result of this the internal stratigraphy of the Mapedi Formation could not be determined at any one locality. To resolve this problem, use was made of several prominent marker beds in the Mapedi Formation to compile a generalised stratigraphic profile, based on observations made at several different localities in the study area.

The basal contact of the Mapedi Formation was not observed in the Map 2 area. The lower part of the Mapedi Formation is best exposed in the southern part of the Boegoeberg Water Reserve, where it unconformably overlies dolomites of the Campbellrand Subgroup. The lower 450m of the Mapedi Formation consists of red-brown phyllites interbedded with light-brown to grey coloured trough cross-bedded siliceous quartzite and red-brown meta-psammite. This unit is interpreted to have been deposited in a fluvial palaeo-environment, similar to that of the lower part of the Mapedi Formation in the Korannaberge-Langberge area.

The clastic sediments of the lower part of the Mapedi Formation are conformably overlain by a unit of amygdaloidal mafic lava, the thickness of which varies between 6 and 20m. The primary igneous minerals in the lava have largely been altered by retrograde metamorphism. The lava consists predominantly of chlorite, epidote and magnetite. Relict, highly saussurised plagioclase crystals, less than 0.5mm in length, are visible in less foliated samples. Calcite and quartz fills preserved amygdaloids.

The lava horizon is overlain by approximately 20m of white siliceous quartzite (The basal unit of the Lucknow Formation of SACS, 1980: included in the Mapedi Formation here). This quartzite horizon weathers positively to form a prominent white ridge that can be traced easily on aerial photographs. On farm Bovenzeekoebaart 313 and Zeekoebar 9, the white quartzite marker is overlain by interbedded brown to white coloured, ripple-marked quartzite and grey-green coloured phyllites. The ripple-marked quartzite horizons commonly have narrow (<2cm) black to grey coloured mud drapes on bedding surfaces. These mud drapes have desiccation cracks indicating a shallow water depositional palaeo-environment. Narrow layers of rip-up mud clasts occur in the quartzite horizons.

The interbedded quartzites and phyllites are overlain by gritty, cross-bedded impure dolomites (Figure 4.8) that contain layers and lenses of cross-bedded calcareous quartzite (These calcareous rocks were also included in the Lucknow Formation of SACS (1980) but are included in the Mapedi Formation here). These features can be used to distinguish the Mapedi Formation dolomites from the interbedded dolomites and chert of the of the Griqualand West Supergroup in the study area. In thin section, the carbonates consist mainly of dolomite, but also contain poorly sorted, angular to subrounded grains of quartz, alkali feldspar, plagioclase and lithic chert. A small amount of muscovite and chlorite occurs in the matrix. The calcareous quartzite layers are composed of the same minerals, but contain a significantly lower proportion of dolomite. The quartzitic dolomites are typical shallow marine, near-shore sediments. The maximum thickness of the upper part of the Mapedi Formation in the Boegoeberg dam area (taken from the top of the mafic lava horizon to the disconformity at the base of the Hartley Formation) is 610m.

The Mapedi Formation in the Boegoeberg dam area thus records an overall transition from a fluvial to a shallow marine palaeo-depositional environment. This succession would be expected as a result of a marine transgression.

4.1.3.2 The Lucknow Formation

The Lucknow Formation is only exposed in the south-eastern part of the Map 2 area. A few kilometres south of the Map 2 area (locality 4.3- Map 1), the Lucknow Formation overlies rocks of the Koegas Subgroup, Makganyene Formation and Ongeluk Formation with angular unconformity. At this locality, a conglomerate band is developed at the base of the Lucknow Formation. The conglomerate is clast supported and consists of sub-rounded clasts of banded ironstone, vein quartz, ferruginous chert and quartzite in a gritty, quartz and hematite rich matrix. The conglomerate is overlain by interbedded purple and light-brown quartzite with narrow meta-psammite intercalations.

The basal contact of the Lucknow Formation is only exposed at locality L4 (farm 311) in the Map 2 area, where the Lucknow Formation disconformably overlies banded ironstones of the Voelwater Subgroup (see Figure 4.7). The basal unit of the Lucknow Formation at this locality is a light brown, pebbly quartzite that contains scattered pebbles and narrow conglomerate bands of ferruginous chert, vein quartz, siliceous chert, banded ironstone and quartzite. The pebbly quartzite is overlain by a monotonous sequence of interbedded light-brown and purple trough cross-bedded quartzites with minor meta-psammite horizons. Narrow (<20cm) conglomerate bands typically cap trough cross-bedded quartzite horizons.

The Lucknow Formation exposed in the Boegoeberg dam area is very similar to that in the Korannaberge-Langberge area and is interpreted to have been deposited in a fluvial palaeo-environment. The Lucknow Formation has a maximum exposed thickness of 570m in the Map 2 area, but the upper contact is not exposed and the unit may have been significantly thicker.

4.1.3.3 The Hartley Formation

The Hartley Formation crops out in the central part of the Map 2 area where it has been duplicated by a thrust sense shear zone. The maximum width of outcrop occurs along the Orange River.

The basal contact of the Hartley Formation, like most of the contacts in the Map 2 area, is usually sheared. An exception is at locality L1, situated in the northern part of farm Bovenzeekoebaart 313, where a disconformable relationship between the Hartley Formation and the underlying Voelwater Subgroup can be recognised. A narrow (<1m thick) conglomerate (consisting of small, sub-rounded to angular pebbles of ferruginous chert, banded ironstone and laminated hematite iron ore in a fine grained quartz-hematite matrix) is developed at the base of the Hartley Formation. The clasts in the conglomerate have all been derived from the underlying Voelwater Subgroup. The conglomerate is discontinuous and in places the Voelwater Subgroup is overlain by an agglomerate consisting of angular fragments of the Voelwater Subgroup in a “matrix” of very fine grained, bright green lava (Figure 4.9). Pillow structures can be recognised in the lava indicating sub-aqueous extrusion. These relationships suggest that after deposition of the basal conglomerate, angular fragments of the Voelwater Subgroup were ripped up by extruding lava to produce the agglomerate. The Hartley Formation thus disconformably overlies the Voelwater Subgroup at this locality.

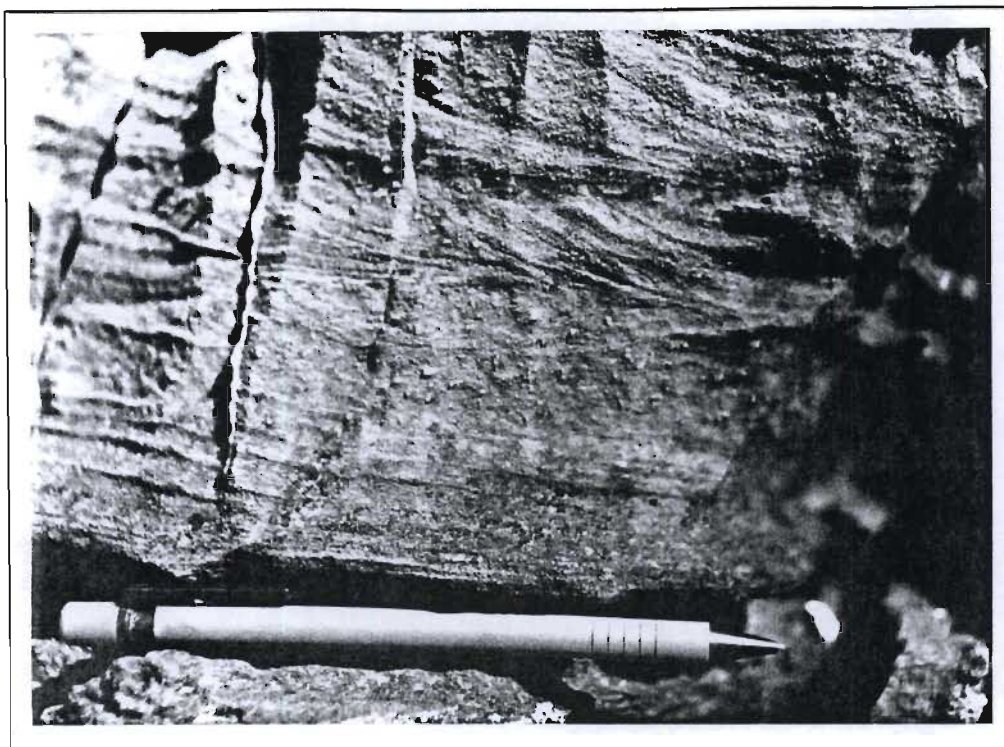


Figure 4.8: Cross-bedded impure dolomite of the Mapedi Formation (Farm Zeekoebar 9- Map 2).



Figure 4.9: Agglomerate developed at the base of the Hartley Formation. Locality L1- Farm Bovenzeekoebaart 313.

Moving west of locality L1, the Hartley Formation overlies first dolomites of the Campbellrand Subgroup and then the Mapedi Formation. Although the contact is not exposed at locality L6, the rocks on either side have a strong north-dipping foliation. It is suggested therefore that the thrust sense shear zone mapped between the Campbellrand Subgroup and the Mapedi Formation south-east of L6 follows the contact between the Hartley and Mapedi Formation west of L6 (i.e. the disconformity has been utilised as a zone of preferential shearing).

The basal conglomerate or agglomerate of the Hartley Formation is overlain by andesitic lava with subordinate tuff, quartzite, welded tuff, agglomerate and meta-psammite. The lavas are dominantly equigranular or amygdaloidal. Where deformation is not intense, hyaloclastite flow contacts and flow-top breccias can be seen to bound individual lava flows. These flow boundary rocks are bright green in colour and contrast strongly with the dark, green crystalline lavas in the body of individual flows.

Pillow lavas are common feature, particularly in the lower parts of the Hartley Formation and exhibit the bright green colour characteristic of the rapidly cooled parts of the Hartley Formation volcanics (Figure 4.10). Rare porphyritic lava horizons are developed, containing scattered euhedral plagioclase phenocrysts up to 1cm in length.

The igneous mineralogy of the Hartley Formation lavas has been largely altered by the retrograde metamorphism associated with the Kheis orogeny. In thin section the lava consists almost exclusively of chlorite, epidote, and magnetite. Plagioclase phenocrysts in the porphyritic lava flows are completely saussurised. Quartz and calcite occurs in most samples, typically in relict amygdales.

Volcanic components dominate the lower 1540m (thickness measured in the vicinity of the Orange River) of the Hartley Formation, where only a few narrow (<2m) grey-green coloured, ripple-marked siliceous quartzite horizons are developed. The upper 860m consists of light-brown meta-psammite, trough cross-bedded quartzite and conglomerate interbedded with lava and tuff. The proportion of volcanic material decreases towards the top of the unit and the uppermost volcanic horizon marks the top of the Hartley Formation. The conglomerate bands in the Hartley Formation are very distinctive and comprise sub-rounded clasts of ferruginous chert, white to grey-green siliceous quartzite, banded ironstone and siliceous chert in a black ferruginous matrix. Clast size varies from <1cm to 60cm and the conglomerates are poorly sorted and unstratified. These ferruginous conglomerate layers are best developed in the 200m below the contact between the Hartley Formation and the Matsap Formation, where they attain thicknesses of 60m and are interbedded with quartzite, meta-psammite and subordinate volcanic horizons.

The conglomerate bands are not restricted to the Hartley Formation, but also occur in the lower part of the overlying Matsap Formation. The contact between the Hartley Formation and the Matsap Formation is transitional and conformable.

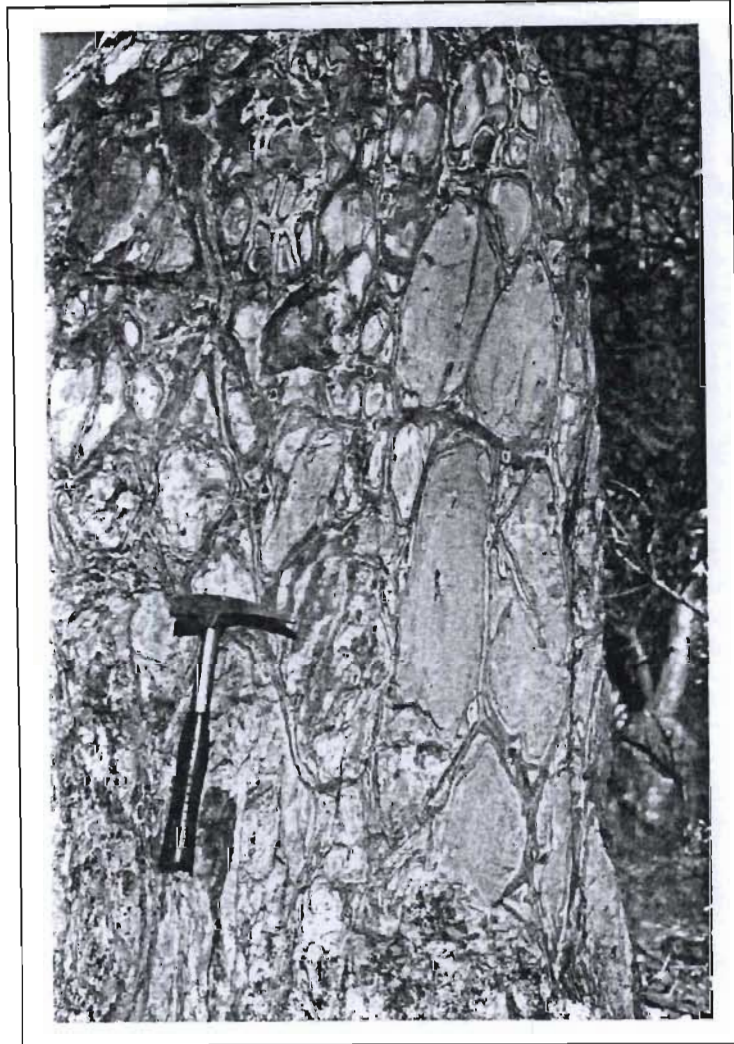


Figure 4.10: Pillow lava in the Hartley Formation. Farm Zeekoebaart 306. This outcrop is only weakly foliated, but the pillows have been elongated parallel to a north-west plunging mineral elongation lineation (approximately parallel to the handle of the hammer).

4.1.3.4 The Matsap Formation

Both the Fuller and Ellies Rus members of the Matsap Formation are exposed in the Map 2 area. A resistant light-brown quartzite horizon, similar to that developed at the contact between the Fuller and Ellies Rus members in the Korannaberge-Langberge area, forms prominent cliffs in the extreme northern part of the study area. This horizon is overlain by purple quartzite that is indistinguishable from that of the Fuller member. In the eastern part of the study area, where outcrop of the Matsap Formation is very poor it was impossible to distinguish between the Fuller and the Ellies Rus members. These two members

are not differentiated on Map 2 and shall be collectively referred to as the Matsap Formation in the description that follows.

The lower part of the Matsap Formation consists of interbedded conglomerate, light-brown quartzite and meta-psammite. In the central part of farm Zeekoebaart 306 it conformably overlies the Hartley Formation as described above. On the western part of farm Zeekoebar 9 (Locality P3), the Matsap Formation disconformably overlies the Voelwater Subgroup. A basal conglomerate approximately 30m thick is developed, this conglomerate is unstratified, poorly sorted and comprises rounded to sub-rounded clasts, up to 30cm in size, of banded ironstone, chert and quartzite in a quartz-hematite matrix. The conglomerate grades up into interbedded quartzites and meta-psammite.

The Matsap Formation consists, for the most part, of purple to light-brown, trough cross-bedded quartzite. Trough cross-bedded units are frequently capped with narrow conglomerate layers. Narrow planar bedded, heavy mineral layers are developed in the lower part of the Formation. Red-brown to purple phyllite horizons (<30cm in thickness) are developed, but are only exposed in excavations along the western bank of the Orange River in the Boegoeberg Water Reserve.

The significant amount of conglomerate, occurring as both lenses and layers, interbedded with trough cross-bedded quartzite and meta-psammite at the base of the Matsap Formation indicates that these sediments were deposited in a high energy fluvial palaeo-environment. The amount of coarse grained clastic material decreases moving upwards through the Matsap Formation. The complete Matsap Formation is not exposed in the Map 2 area. Based on measurements made by Vajner (1974) along the Orange River, the Matsap Formation is approximately 3050m in thickness.

4.1.4 Mafic intrusions

Two generations of mafic intrusions were observed in the Boegoeberg dam area. The distinction between the two generations is based on structural evidence and will be further discussed in section 4.2. The earlier generation is represented by the Westerberg sill which crops out in the southern part of farm 314. The Westerberg sill at this locality could not be sampled as it is strongly foliated and weathered. Vajner (1974), obtained fresh material from boreholes drilled in the Westerberg area and described it as a diabase (South African term for a coarse grained, weakly metamorphosed dolerite >2000 Ma). The Westerberg sill is 150-200m thick and occupies a consistent stratigraphic position near the top of the Asbestos Hills Subgroup (Vajner, 1974).

Mafic sills in the Hartley and Matsap Formations were observed in the Map 2 area. Only one of these sills, developed in the Matsap Formation, is indicated on Map 2 (farm 308). Several sills intrude the Hartley Formation, but their outcrop is discontinuous and their boundaries could not be accurately delineated.

Good exposure of mafic sills in the Hartley Formation was observed on farm Zeekoebaart 306 (locality L7) and in the Boegoeberg Water Reserve (locality L8). At both of these localities, the sills comprise both fine ($< 0.5\text{cm}$ grain size) and coarse ($0.5\text{-}2\text{cm}$) grained material. The sills have weathered to form rounded boulders with a red-brown pitted appearance. The pitted appearance is a result of the weathering of dark green, largely altered pyroxene phenocrysts.

At both localities, the mafic intrusions have undergone retrograde metamorphism. The primary igneous mineralogy is thus difficult to ascertain. Narrow, thrust sense shear zones cut through the sills. Within, and adjacent to these shear zones the mafic intrusions are highly altered and consist almost exclusively of quartz, chlorite, epidote and actinolite. Highly saussiterised plagioclase laths can be recognised, as can relict pyroxene crystals, largely altered to epidote and chlorite. Only one sample was obtained (locality L8) where the primary mineralogy and textures were sufficiently well preserved in order to determine the modal composition of the original igneous rock. In this sample (PS0791), clinopyroxene and orthopyroxene crystals up to 3mm in length occur in a groundmass comprising saussiterised plagioclase laths and graphic textured quartz-alkali feldspar intergrowths (Figure 4.11).

Table 4.1 shows the modal composition of sample PS0791 as determined from 800 point counts. According to the classification scheme of Streckeisen (1976) this rock could be classified as either a gabbro norite or a diorite. Plagioclase composition is used to distinguish between these two rock types. As the plagioclase laths in this sample are almost completely saussiterised, this was not possible. The large proportion of pyroxene, and particularly the high orthopyroxene content, suggests that the rock is a gabbro norite.

An attempt was made to date the gabbro norite sill exposed at locality L8 using the U-Pb SHRIMP method. Analysis of the small yield of zircons separated from a 24kg sample of the gabbro norite indicated that they had undergone severe radiogenic Pb-loss and it was not possible to determine a crystallisation age (Armstrong, 1997a).

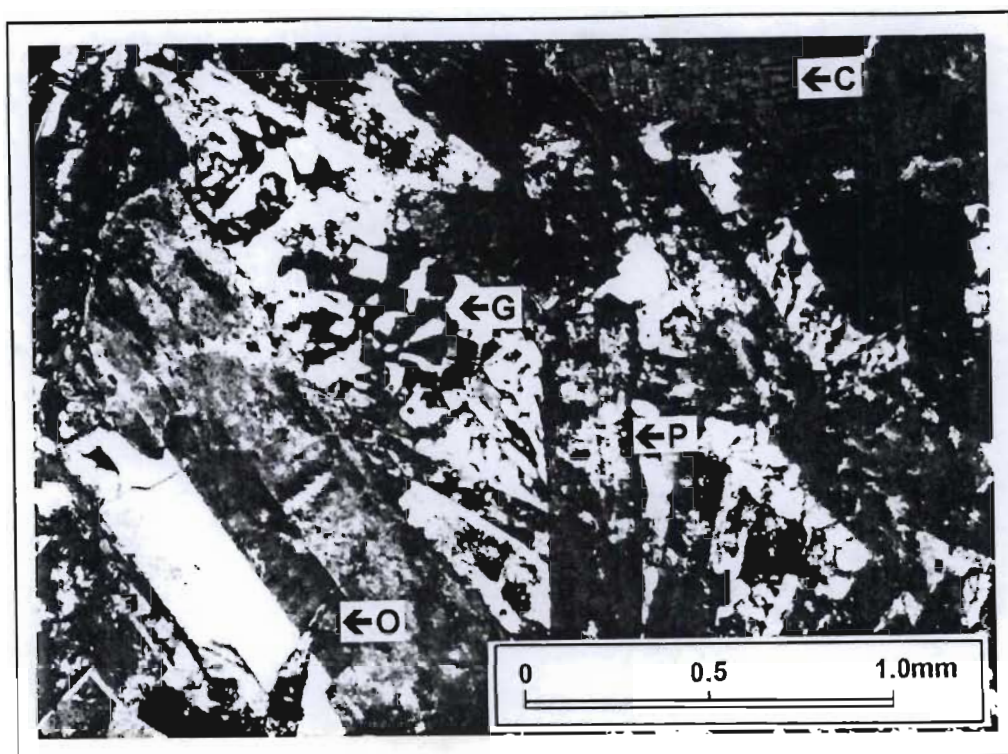


Figure 4.11: Photomicrograph of sample PS0791. Transmitted cross-polarised light. C=Clinopyroxene, O=Orthopyroxene, P=Saussiterised plagioclase, G=Graphic quartz-feldspar intergrowth.

Plagioclase	44.00%
Clinopyroxene	17.38%
Orthopyroxene	17.25%
Quartz	10.01%
Alkali feldspar	9.63%
Magnetite	1.75%

Table 4.1: Modal analysis of sample PS0791 from locality L8 (Boegoeberg Water Reserve).

4.2 Structural geology

All stratigraphic units in the Boegoeberg dam area have undergone polyphase deformation. The structural elements observed can be related to pre-Olifantshoek Supergroup folding of the Griqualand West Supergroup, the Kheis orogeny or the extended Namaqua orogeny. In the sections that follow, the style, orientation and relative timing of structural features observed in the Boegoeberg dam area are described. Particular attention is paid to the Voelwater Subgroup in an effort to confirm the observation made in the

Korannaberge-Langberge that the Voelwater Subgroup was not deformed prior to deposition of the Olifantshoek Supergroup.

4.2.1 Pre-Olifantshoek Supergroup deformation

As noted in Chapters 2 and 3, the Griqualand West Supergroup was deformed prior to a period of erosion and subsequent deposition of the Olifantshoek Supergroup. The map patterns of large scale, north-south trending, upright periclinal folds produced during this phase of deformation are visible on Map 1. Note that the folds are much tighter in the western part of the preserved Griqualand West basin (Westerberg area) than in the eastern parts (Campbell area).

Throughout most of the Map 2 area, the original traces of these early folds have been severely disrupted by folds and thrust sense shear zones related to the Kheis Orogeny. An exception to this is the approximately north-south trending synclinal closure defined by form lines in the Asbestos Hills Subgroup at locality D1 (farm 314).

The bedding orientations in the Griqualand West Supergroup, plotted on Map 2, show a complex pattern, often inconsistent with the form lines and bedding measurements defining the “Kheis age” folds in the overlying Olifantshoek Supergroup rocks. A stereographic projection of Griqualand West Supergroup bedding planes (excluding the Voelwater Subgroup) measured in the Map 2 area (Figure 4.12) serves to illustrate this complex pattern. As the Griqualand West Supergroup has been extensively deformed during the Kheis orogeny, the use of a π -girdle and π -axis to define the mean fold axis would be incorrect and they have not been plotted. Nevertheless, the π -maxima (contour highs) define a weak east-west striking, south dipping π -girdle related to the early north-south trending folding.

Small scale folds, that developed during this deformation, were observed in discrete zones within both the Campbellrand and Asbestos Hills Subgroups (Figure 4.13). The orientation of fold axes, measured on these small scale folds, define a weak north-south trend consistent with that of the larger structures (Figure 4.14). Most of the fold axes orientations shown in Figure 4.14 were measured in Kheis orogeny low-strain zones within the Campbellrand Subgroup and the stereonet reflects this bias. The anomalous north-west plunging fold axes were measured in Kheis orogeny high strain zones, where small scale pre-Olifantshoek Supergroup folds have been rotated into parallelism with the Kheis movement direction.

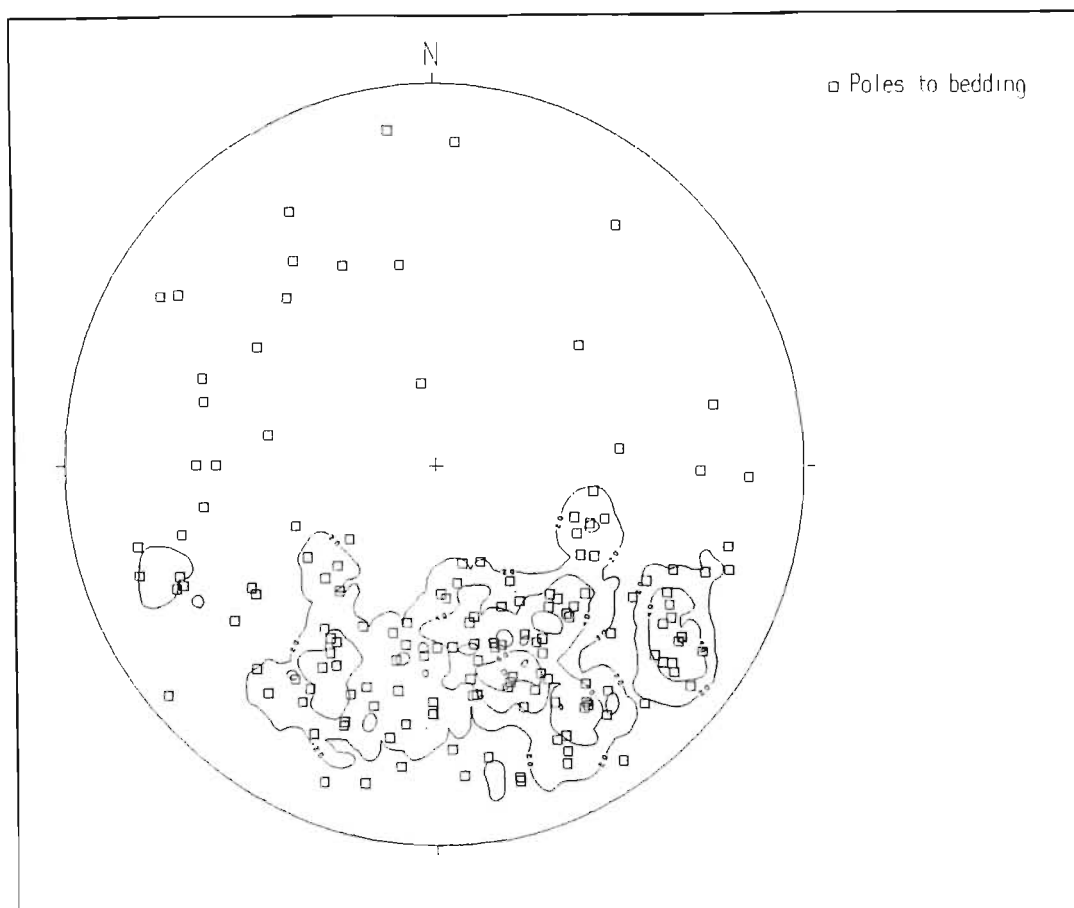


Figure 4.12: Equal area, stereographic projection (π -diagram) of bedding plane orientations ($n=153$) of the Griqualand West Supergroup measured in the Map 2 area.

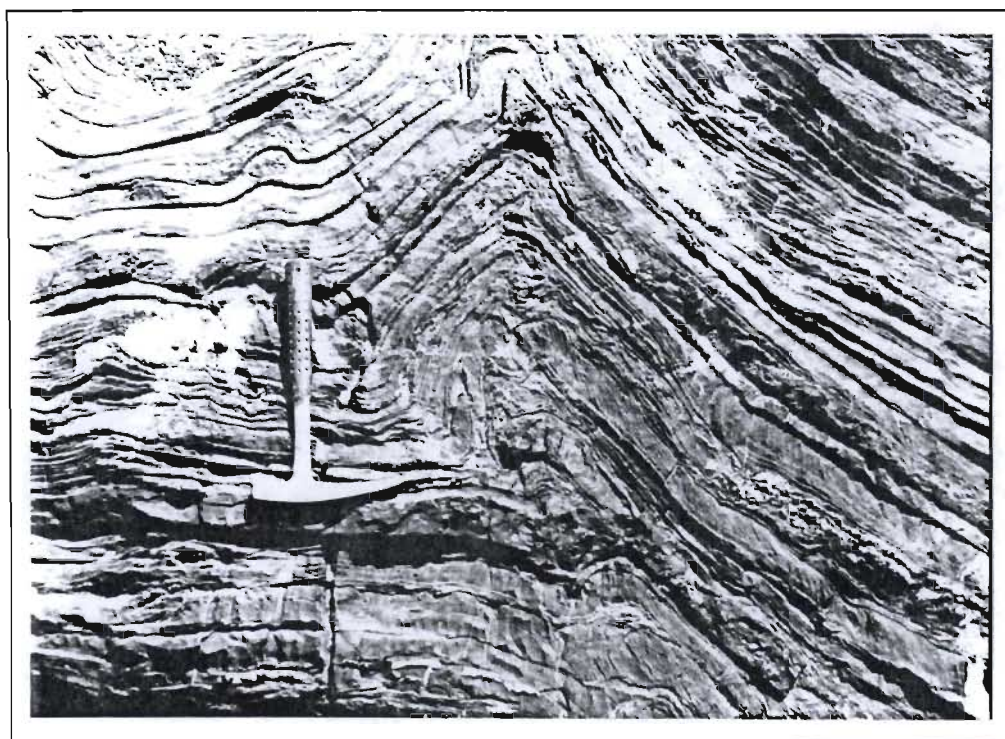


Figure 4.13: Small scale fold in Campbellrand Subgroup dolomite. Note the small shear zone dislocating the chert band in the core of the fold.

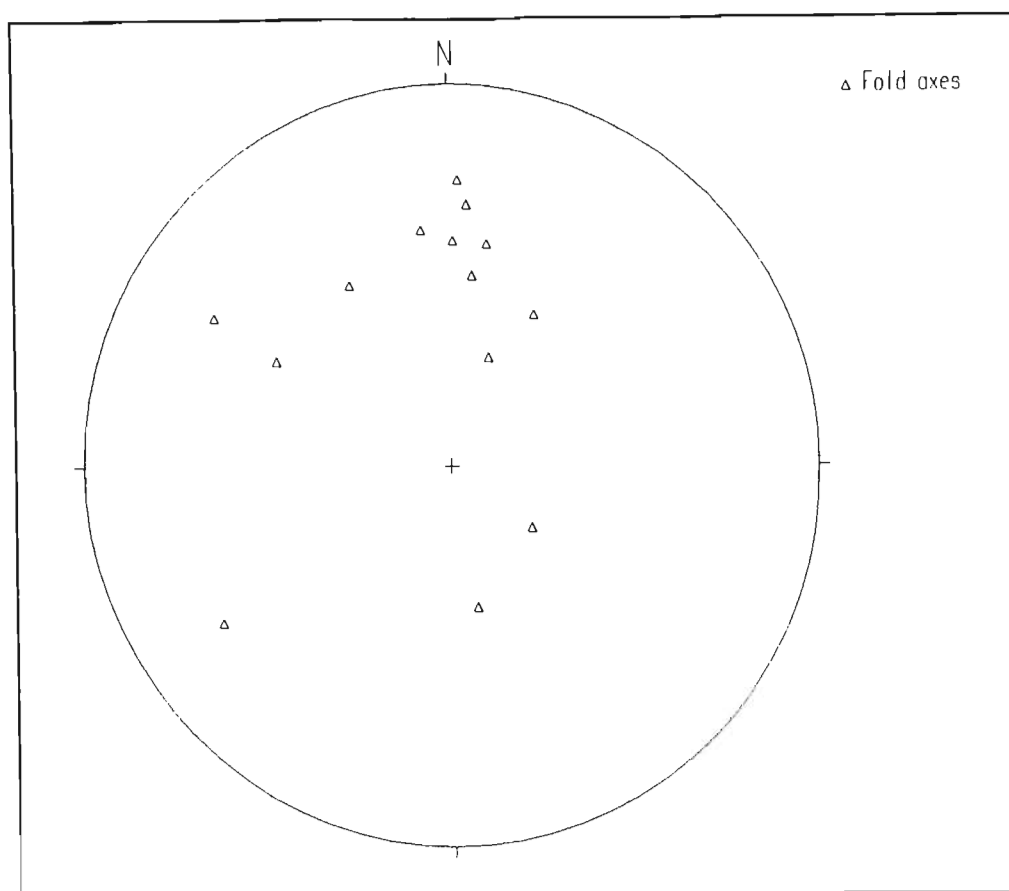


Figure 4.14: Equal area stereographic projection of small scale, pre-Olifantshoek Supergroup fold axes orientations (n=14) measured in the Map 2 area.

Boudinage, related to this early folding event, was observed in discrete zones within the Campbellrand Subgroup, especially where there is a well developed, finely laminated, compositional banding. Crocidolite asbestos occurs in bedding-parallel seams in the Asbestos Hills Subgroup. The asbestos fibres in these seams are orientated parallel to the principle extension direction within the fold axial surface (Figure 4.15). Along the limbs of some folds, the asbestos fibres are sigmoidal indicating progressive fibre growth during bedding sub-parallel movement.

The Koegas Subgroup rocks in the southern part of the study area are poorly exposed and have been intensely sheared during the Kheis orogeny. Based on the map pattern of the Griqualand West Supergroup in the Westerberg area and observations made at locality 4.3 (Map 1), the Koegas Subgroup, Ongeluk and Makganyene Formations were folded during the pre-Olifantshoek Supergroup deformation. Vajner (1974) noted that the Westerberg sill was also deformed during this event (see Figure 4.2).

No evidence was observed in the Voelwater Subgroup for pre-Olifantshoek Supergroup deformation. Form lines and bedding in the Voelwater Subgroup (Map 2) exhibit a simple trend parallel to the overlying rocks of the Olifantshoek Supergroup. No asbestos is developed in the Voelwater Subgroup

banded ironstones (c.f. the Asbestos Hills Subgroup). Throughout the Map 2 area and along the southern part of the Eselberge, the Voelwater Subgroup has a north-east to east strike and a north-west to north dip, parallel to the *disconformably* overlying strata of the Olifantshoek Supergroup (Map 1). In contrast, the pre-Voelwater Subgroup strata of the Griqualand West Supergroup are overlain with *angular unconformity* by the Olifantshoek Supergroup. A good example of this is at locality 4.3 (immediately south of the Map 2 area) where the basal Lucknow Formation conglomerate truncates the map pattern of a north-south trending syncline.

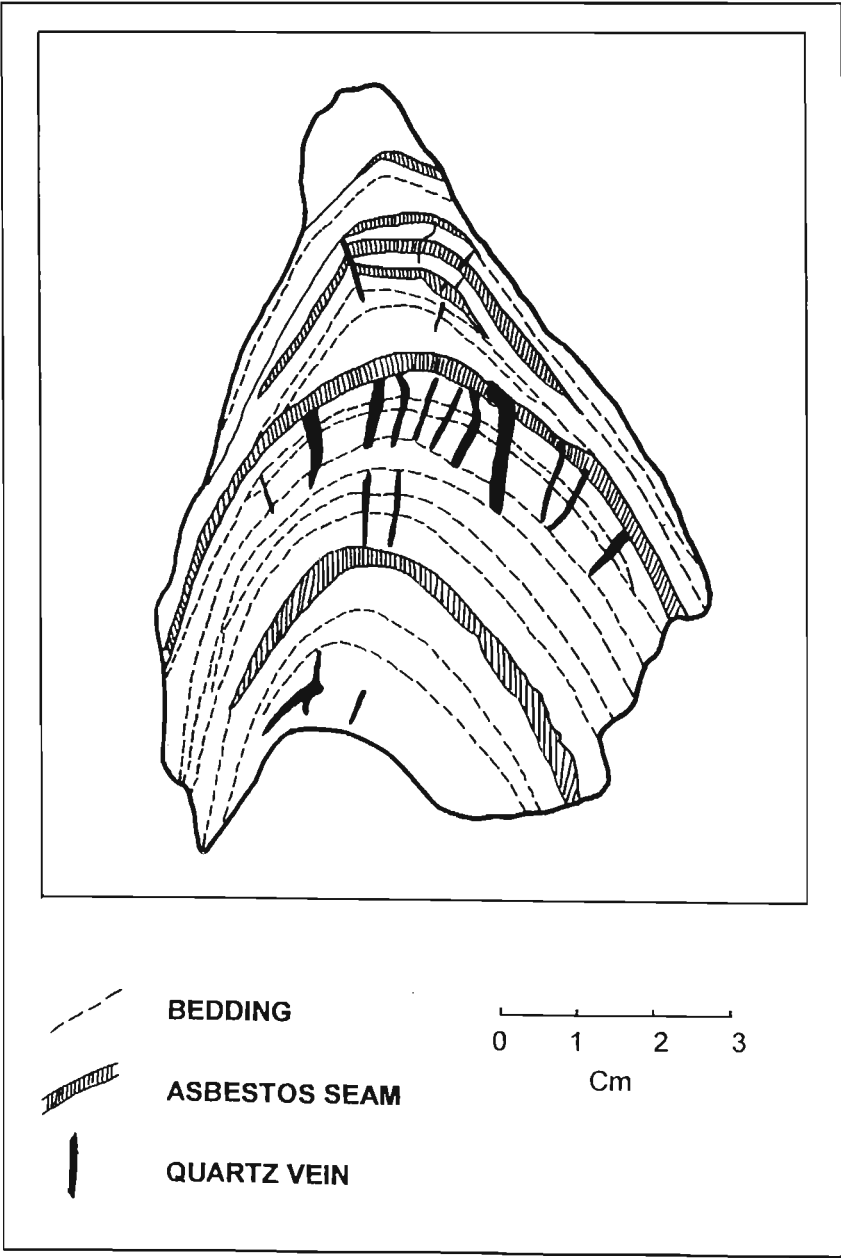


Figure 4.15: Tracing of a polished slab of Asbestos Hills Subgroup banded ironstone cut perpendicular to the fold axial plane. Extension parallel to the fold axial surface is indicated by the growth direction of the asbestos fibres.

As outlined in chapter 2, SACS (1980), Nel *et al.* (1986) and Gutzmer and Beukes (1995) interpret the Voelwater Subgroup to conformably overlie the Ongeluk Formation. The Voelwater Subgroup has

therefore been included as the uppermost unit of the Griqualand West Supergroup (SACS, 1980; Beukes and Smit, 1987).

In the Boegoeberg dam area, all observed contacts between the Voelwater Subgroup and the underlying Griqualand West Supergroup were highly sheared. No outcrop was observed where an angular unconformity between these units could be unequivocally demonstrated. However, all observations made in the Korannaberge-Langberge mountain chain and the Boegoeberg dam area indicate that the pre-Olifantshoek Supergroup folds developed as a result of an east-west orientated compressional event that occurred prior to deposition of the Voelwater Subgroup. Folds are periclinal, trend north-south and have upright axial planes. Small scale folds and boudinage, preferentially developed in zones of high competency contrast, indicate that bedding parallel shearing played an important role in the development of the folds.

4.2.2 The Kheis Orogeny

Craton-vergent folding, thrusting and bedding sub-parallel simple shear occurred during the Kheis orogeny. Each of these structural elements shall be described separately below, but it must be stressed that they formed during one progressive deformation.

4.2.2.1 *Folding*

The closures of folds that developed during the Kheis orogeny are well defined by form lines and lithological contacts in the Olifantshoek Supergroup (e.g. in the Mapedi Formation on farm Bovenzeekoebaart 313). Deformation of the Griqualand West Supergroup has mainly occurred by shearing along the contacts with the overlying Olifantshoek Supergroup, shearing and rotation of bedding in the vicinity of major thrust sense shear zones and by bedding sub-parallel simple shear in the Asbestos Hills and Koegas Subgroups .

Although locally complicated by discrete zones of Namaqua folding and faulting, the Kheis belt shows an overall change in structural trend from north-east/south-west in the north-eastern part of the Map 2 area to east-west in the central and western parts of the Map 2 area (see also Map 1). The orientation of periclinal Kheis fold axes mirror this change in structural trend and show a range in orientations from north-east/south-west to east-west (Figure 4.16). In contrast to the upright Kheis folds in the Langberge (Traverses 2-4), folds in the Boegoeberg dam area are mainly overturned to the south-east and have

steeply north-west to north dipping axial planes. The orientations of axial planar cleavage planes measured in the Map 2 area are shown in Figure 4.16. The cleavage dips steeply in a direction that ranges between north-west and north. The axial planar cleavage and the shear zone foliation are sub-parallel and unless a small scale fold is developed it is hard to differentiate between the two fabric elements. The shear zone foliation and axial planar cleavage measurements are undifferentiated on Map 2.

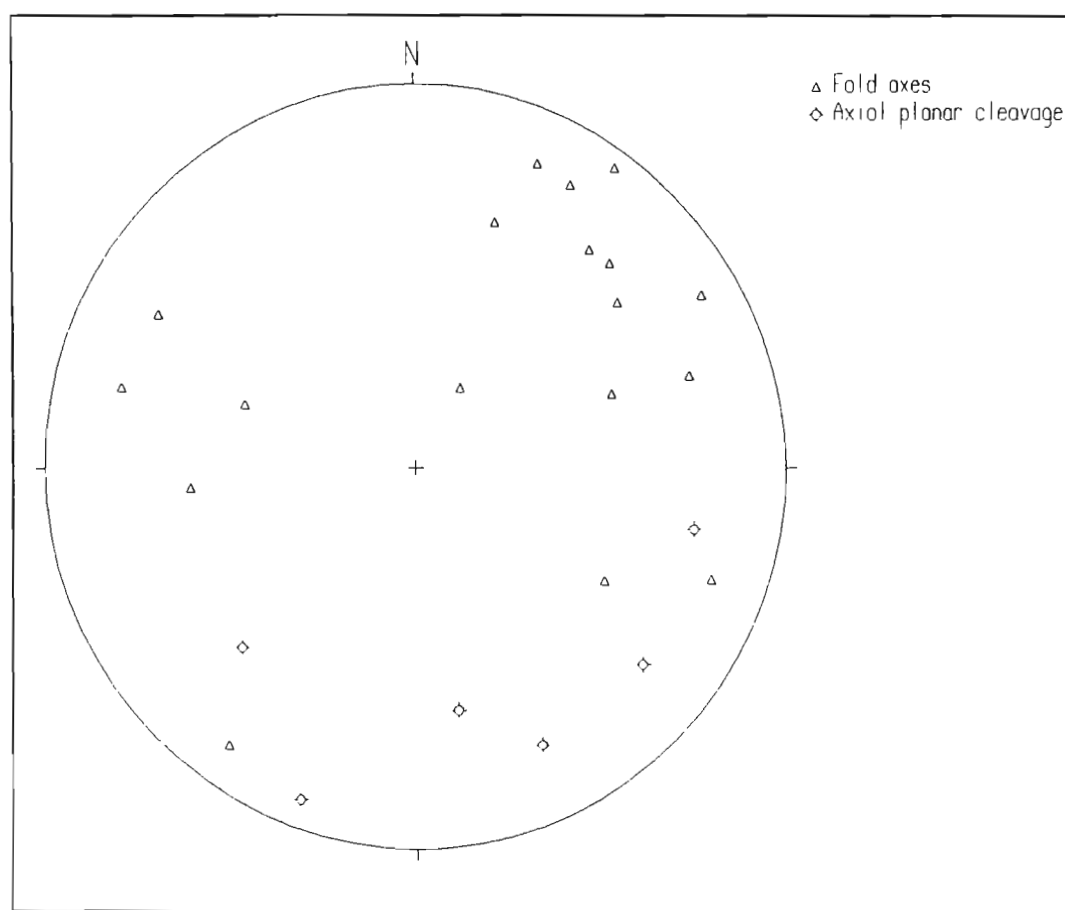


Figure 4.16: Equal area, stereographic projection of fold axes (n=17) and axial planar cleavage (n=6) that developed in rocks of the Olifantshoek Supergroup during the Kheis orogeny (Map 2 area).

Bedding orientation measurements for the Olifantshoek Supergroup define a disperse, single π -maxima, characteristic of overturned folds (Figure 4.17). Poles to bedding for the Voelwater Subgroup define a similarly orientated cluster in the south-east quadrant (Figure 4.18). Figures 4.19 and 4.20 are cross-sections of the Map 2 area drawn approximately parallel to the movement direction. Both sections illustrate the overturned nature of the Kheis folds.

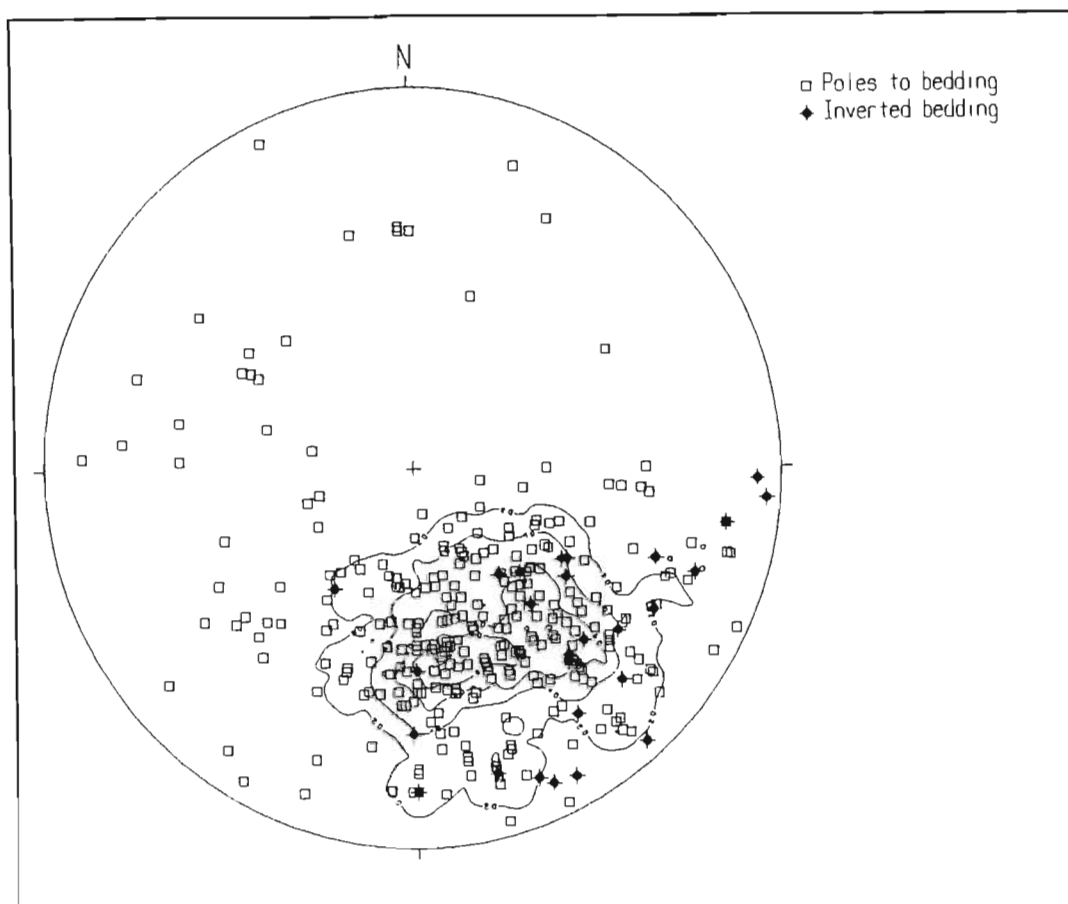


Figure 4.17: Equal area, stereographic projection of Olifantshoek Supergroup bedding planes (n=307) measured in the Map 2 area.

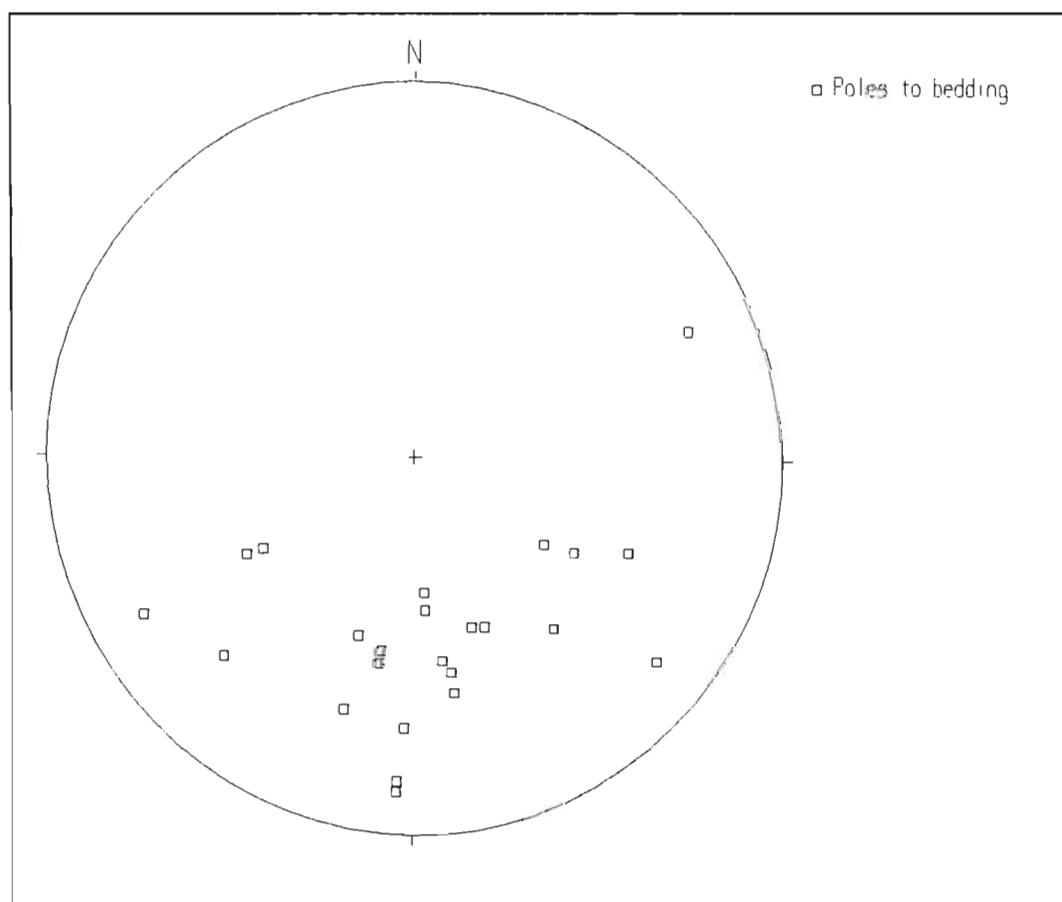


Figure 4.18: Equal area projection of Voelwater Subgroup bedding planes (n=24) measured in the Map 2 area.

Figure 4.19: Cross-section from A-C for the Map 2 area. Horizontal and vertical scales are equal.

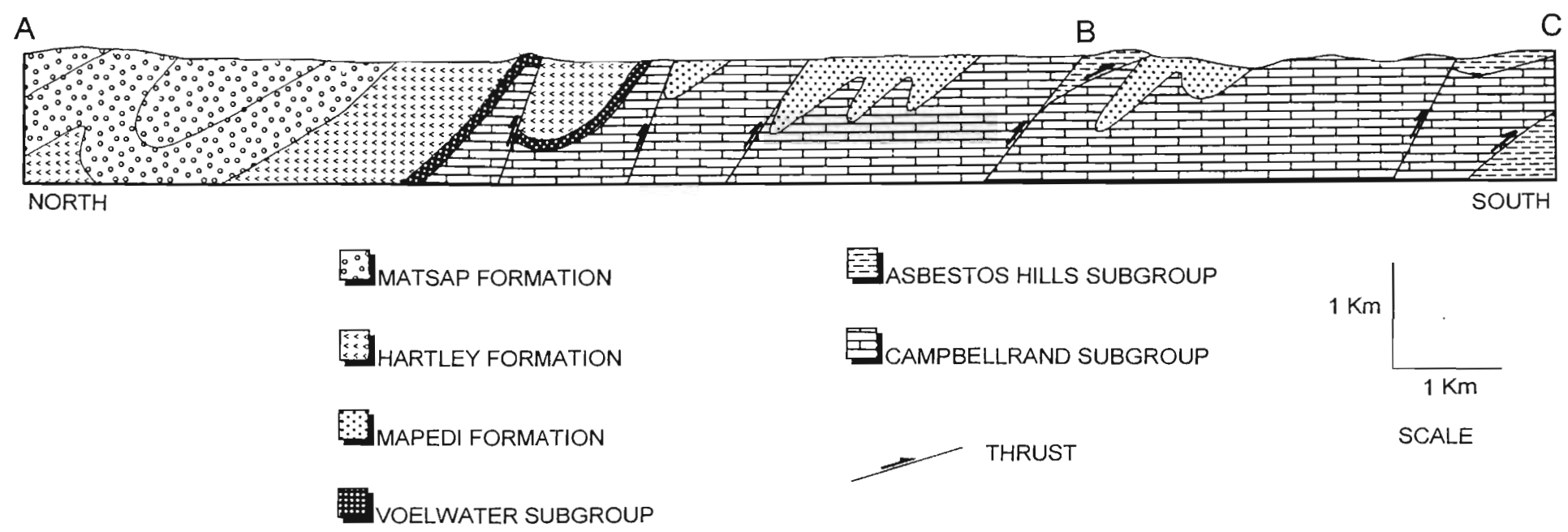
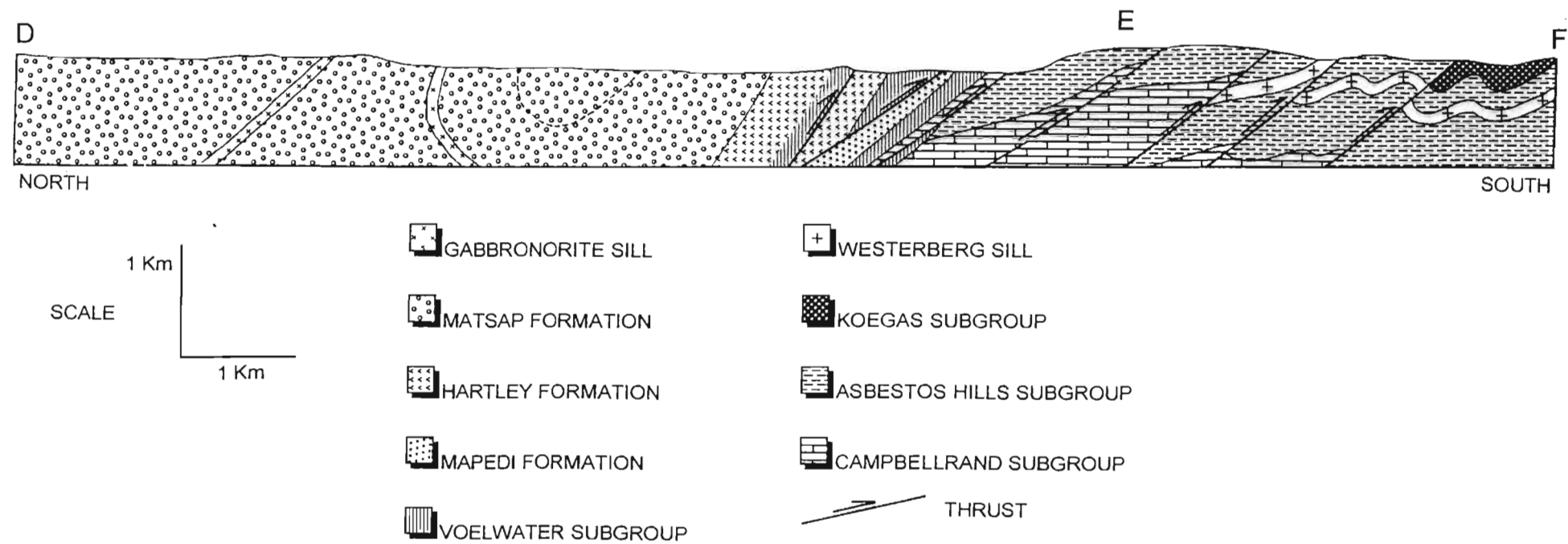


Figure 4.20: Cross-section from D-F for the Map 2 area. Horizontal and vertical scales are equal.



4.2.2.2 Bedding sub-parallel simple shear

Bedding sub-parallel, thrust sense shear zones are developed in most stratigraphic units in the study area. These shear zones are preferentially developed in incompetent horizons and are characterised by an intense planar fabric (foliation) and a well developed mineral elongation lineation.

Foliation measurements made in bedding sub-parallel shear zones are plotted in Figure 4.21. The bedding sub-parallel shear zones are parallel to major brittle ductile thrusts (section 4.2.2.3) and the orientation measurements are not differentiated in this stereographic projection or on Map 2. The foliation planes show a range in strike from north-east to east and dip northwards at moderate to steep angles. This range in strike is due to the arcuate structural trend of the Kheis belt in the Map 2 area.

Figure 4.22 shows the orientations of all mineral elongation lineations that were measured in the Map 2 area. Although there is a variation in trend from north to west, the mean lineation trend is north-west (307°). Movement on Kheis age bedding sub-parallel shear zones and thrusts in the Boegoeberg dam area was thus oblique with a small dextral component.

In the Matsap Formation, bedding sub-parallel shear zones are preferentially developed in meta-psammite, phyllite and conglomerate bands. In high strain zones, the quartzites themselves are foliated. The foliation in the phyllite horizons is defined by muscovite with subordinate chlorite and fine grained, elongate quartz grains. These rocks can be classified as phyllonites. The foliation in the quartzite and meta-psammite horizons is defined by layers of phyllosilicates (muscovite and chlorite) that wrap around partially to completely recrystallised quartz grains (Figure 4.23). In all shear zones developed in the quartzite and meta-psammite, greater than 50% of the rock comprises visible fragments. These rocks can therefore be classified as proto-mylonites (Roering *et al.*, 1989). The matrix of the strained conglomerate layers is often mylonitic (highly recrystallised and composed of <50% visible fragments), but as the clasts themselves constitute visible fragments the strained conglomerates should be classified as a proto-mylonites.

Mineral elongation and stretching lineations in bedding parallel shear zones in the Matsap Formation are defined by elongate quartz grains, rod shaped aggregates of quartz and phyllosilicates or by strongly elongated clasts in the conglomerate layers. The mineral elongation lineations plunge obliquely down the plane of the shear zone foliation to the north-west (Figure 4.24). Kinematic indicators such as S-C fabrics,

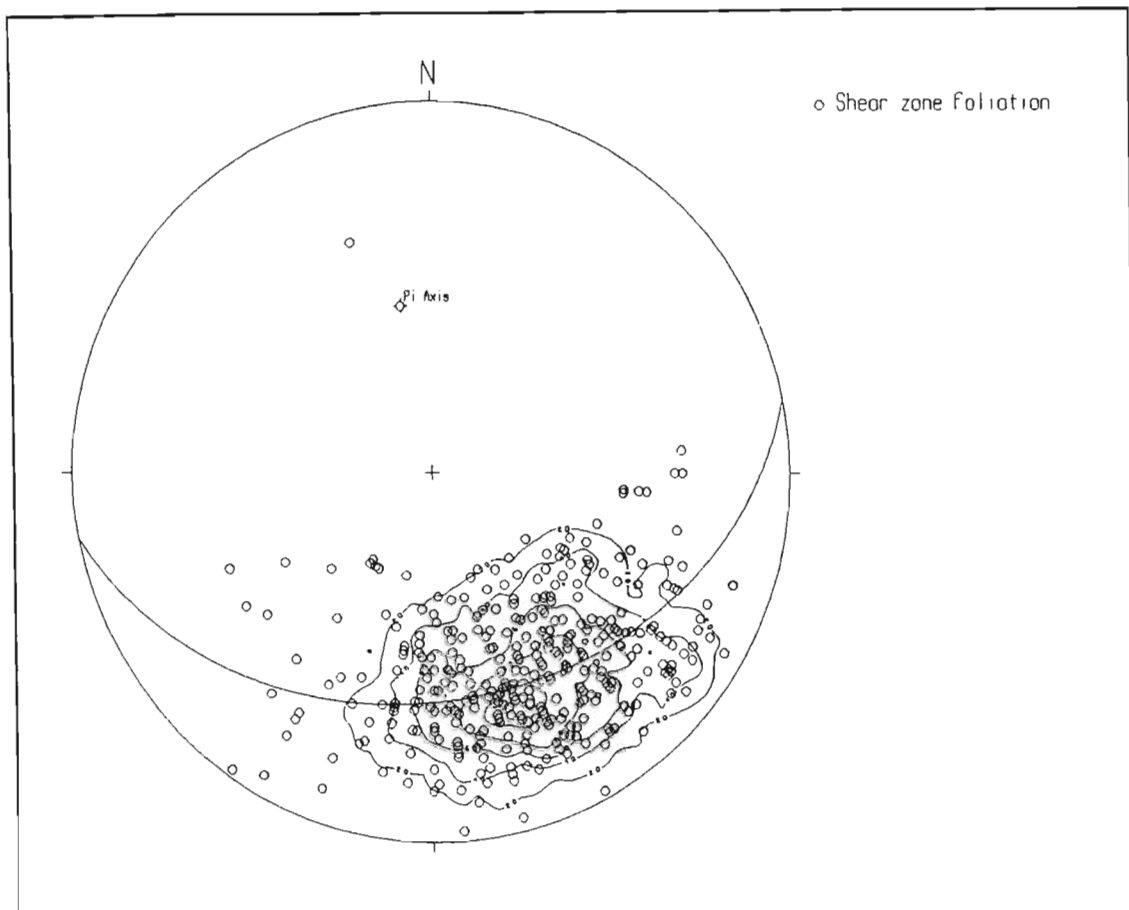


Figure 4.21: Equal area stereographic projection (π -diagram) of foliation planes ($n=325$) from bedding sub-parallel shear zones and brittle-ductile thrust sense shear zones that developed during the Kheis orogeny. Map 2 area.

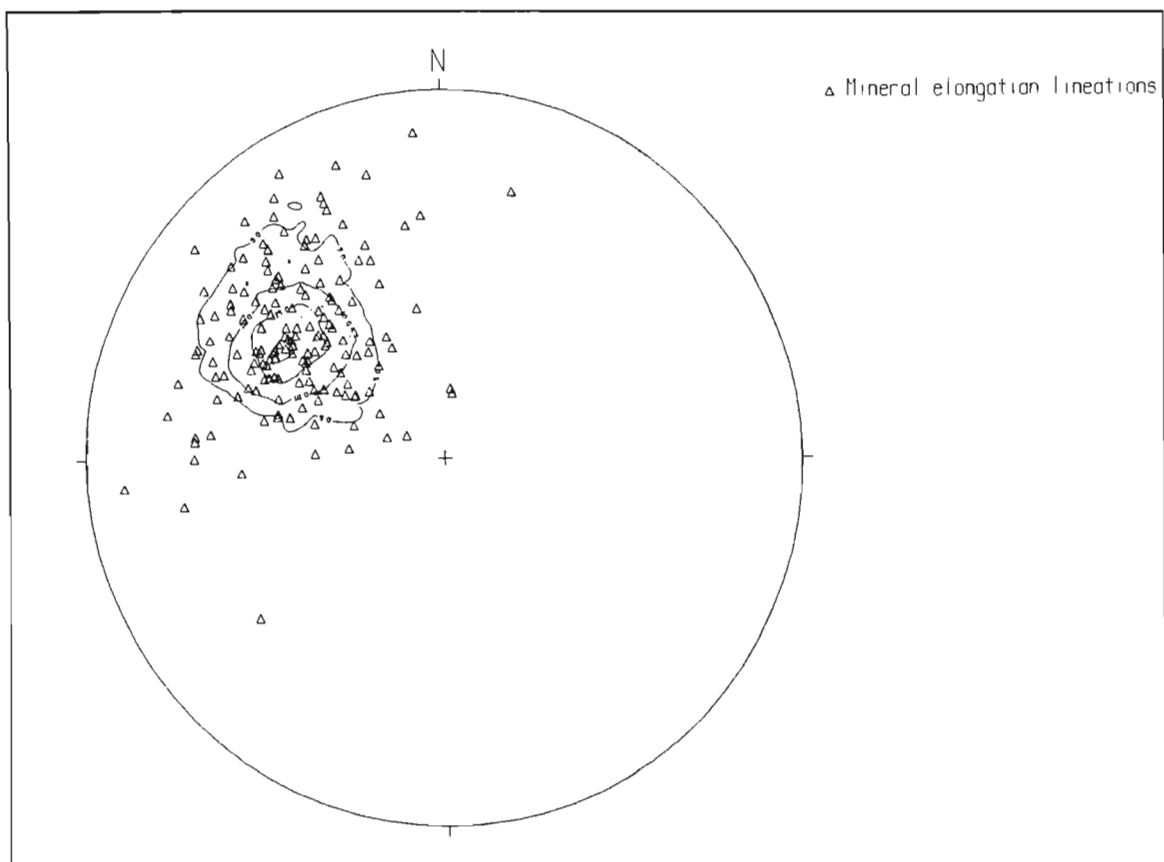


Figure 4.22: Equal area stereographic projection of mineral elongation and stretching lineations ($n=155$) that formed during the Kheis orogeny in the Map 2 area.

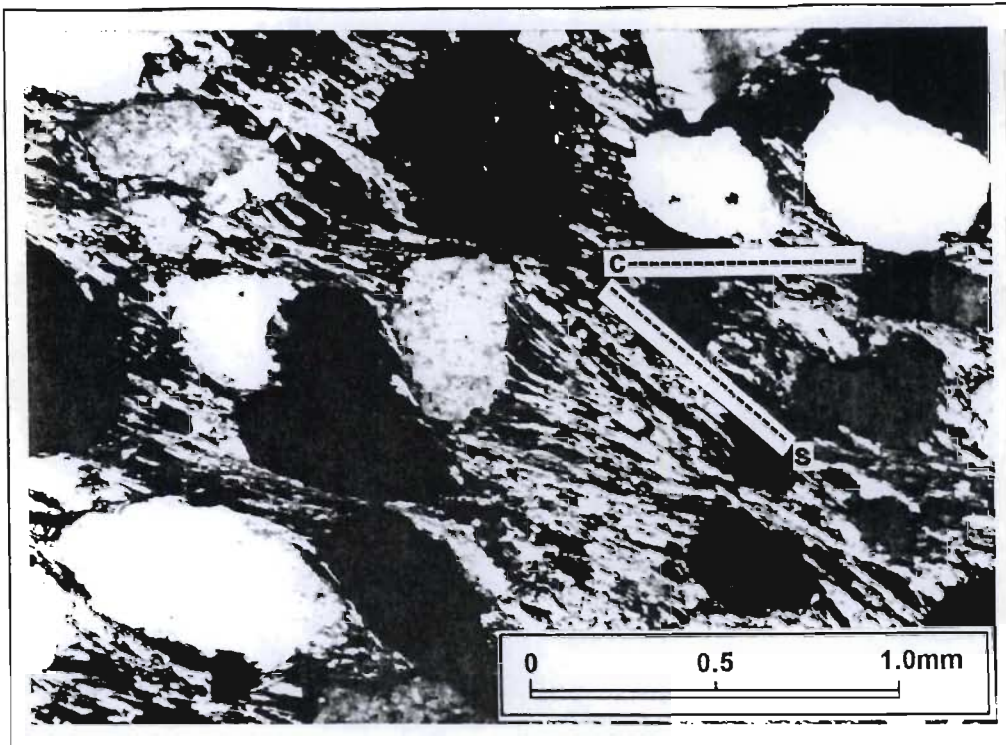


Figure 4.23: Photomicrograph of a Matsap Formation meta-psammite (proto-mylonite) from a bedding sub-parallel thrust sense shear zone. The “s” and “c” planes are indicated. Transmitted, cross-polarised light.

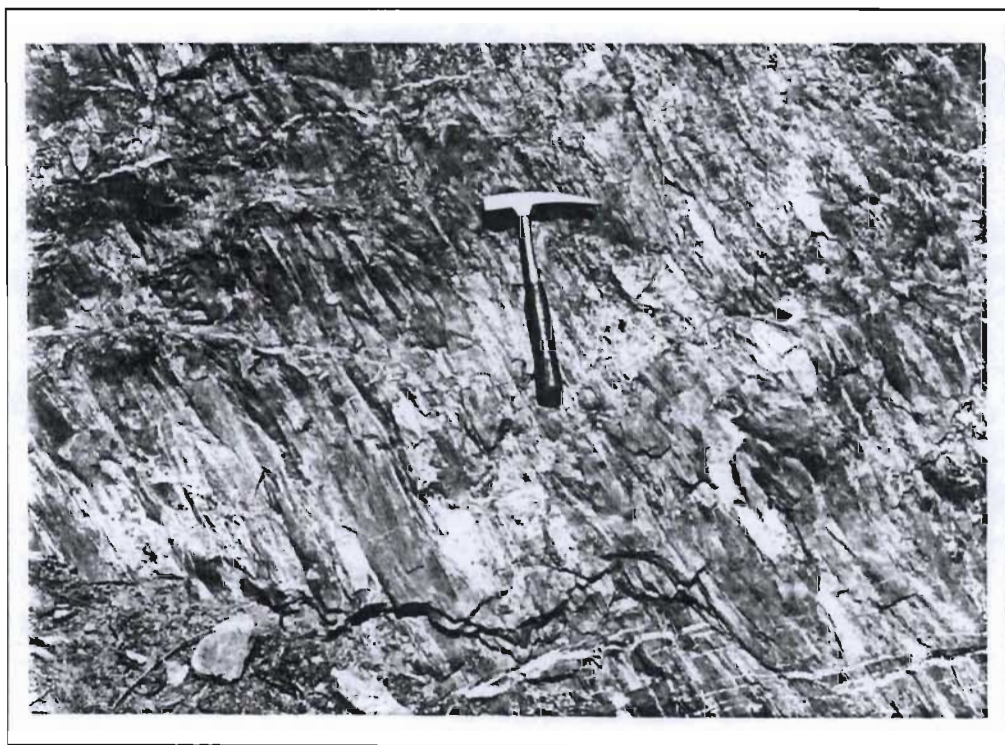


Figure 4.24: A highly strained conglomerate layer in the Matsap Formation. A stretching lineation defined by the long axes of elongated pebbles plunges obliquely down the plane of the foliation. Farm Zeekoebaart 306.

both on outcrop and in thin section (Figure 4.23), in association with the mineral elongation lineations, imply a north-west over south-east oblique-dextral thrust sense of movement.

Oblique thrust sense shear zones, parallel to both bedding and the primary igneous layering are well developed in the Hartley Formation. Shear zones are preferentially developed in conglomerate and meta-psammite layers, but can also be recognised in many of the lava horizons. Figure 4.25 shows the microfabrics developed in a highly sheared Hartley Formation meta-psammite. The foliation is defined by muscovite and elongated, partially to completely recrystallised, quartz grains. This rock is not a phyllonite as the quartz grains are visible in hand specimen. Less than 50% of the rock comprises visible fragments and the rock is thus classified as a mylonite (Roering *et al.*, 1989).

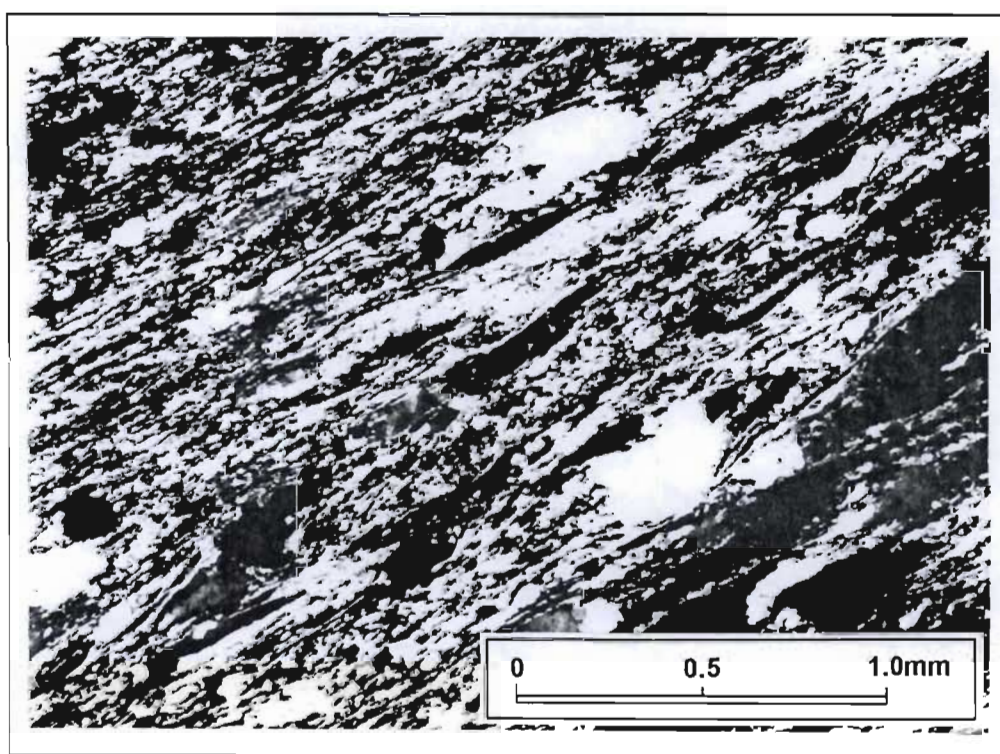


Figure 4.25: Photomicrograph of a mylonite from the Hartley Formation. Transmitted cross-polarised light.

Thrust sense shear zones, sub-parallel to the igneous layering are preferentially developed in the dark green coloured Hartley Formation lava flows. Quartz-calcite filled amygdales are often elongated, defining a stretching lineation that plunges obliquely down the plane of the foliation to the north-west. Phacoids (elongate low strain pods) are a prominent feature in the strained Hartley Formation lavas, the long axes of these phacoids plunge to the north-west, parallel to the stretching lineations defined by the strained amygdales. The bright green coloured hyaloclastite flow top breccias, volcanic agglomerates and pillow lava horizons are significantly more competent than the dark green lava horizons and are only weakly foliated.

In thin section, the foliation in the strained lavas is defined by narrow layers of chlorite that anastomose around less strained zones of epidote, saussiterised plagioclase, quartz, calcite and ore minerals. In extremely highly sheared lava, the rock is composed almost completely of chlorite with only minor epidote, quartz, calcite and ore minerals.

The gabbro-norite sills in the Olifantshoek Supergroup were weakly deformed by oblique thrust sense shear zones during the Kheis orogeny. Deformation in the gabbro-norite sills occurred along discrete, narrow (<1m) shear zones. Neither stretching lineations nor unequivocal kinematic indicators were observed in the foliated zones. Orientated hand samples were taken to investigate the nature of the shear zones. In thin section the foliation in these samples is defined by layers of chlorite±actinolite and aligned saussiterised plagioclase laths. S-C fabrics in the phyllosilicate layers are consistent with a north-west over south-east thrust sense of movement.

Bedding sub-parallel thrust sense shear zones in the Voelwater Subgroup banded ironstones are well developed throughout the study area. Small scale folds, overturned to the south-east, often with “sheared out” limbs, are developed in discrete chert-rich horizons (Figure 4.26). Deformation in the more hematite-rich banded ironstones has been accommodated by intense shearing parallel to the compositional banding. The foliation in the hematite layers is defined by specularite (flaky hematite with a metallic lustre) studded with bright red hematite and yellow-brown piemontite (manganese epidote) porphyroblasts (Figure 4.27). A weak north-west plunging mineral elongation lineation, defined by the preferred orientation of specularite grains is developed in the Voelwater Subgroup.

During the Kheis orogeny, strain in the Mapedi Formation was mainly accommodated by the formation of tight overturned folds and movement along narrow thrust sense shear zones that can be parallel or discordant to bedding. The foliation in the phyllite and meta-psammite horizons is identical to that developed in similar lithologies in the Matsap Formation. All observed outcrops of the mafic lava are strongly foliated. Strained amygdales in the foliated lava define a north-west plunging elongation lineation.

The Campbellrand Subgroup dolomites and cherts are very competent and only exhibit a strong foliation in the immediate hanging-wall and foot-wall of major brittle-ductile thrust sense shear zones. No evidence for bedding sub-parallel simple-shear zones was observed in this stratigraphic unit.

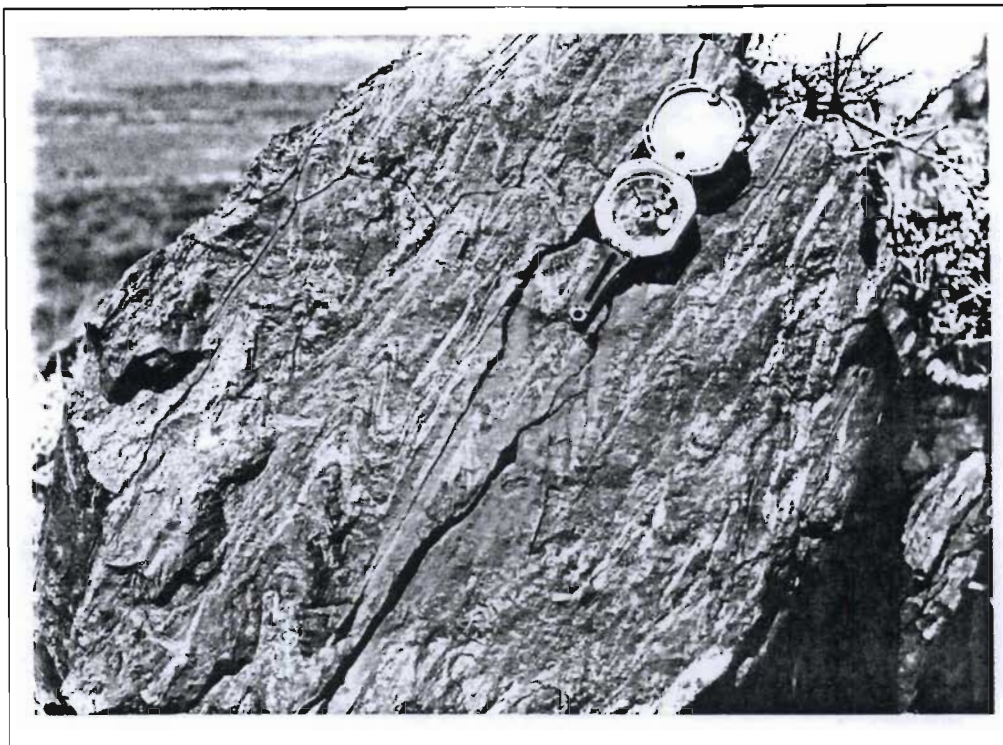


Figure 4.26: Tight overturned folds in a bedding sub-parallel thrust sense shear zone developed in Voelwater Subgroup banded ironstones. The compositional banding dips north-west. Farm Zeekoebaart 306.

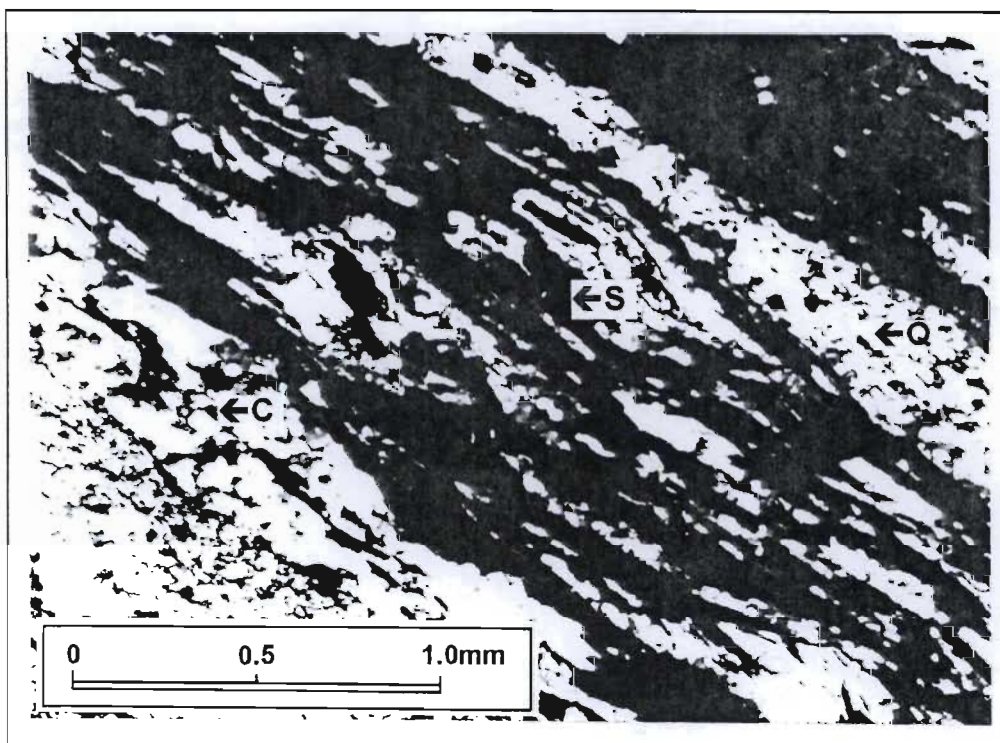


Figure 4.27: Photomicrograph of a sample of strongly foliated Voelwater Subgroup banded ironstone (Farm Zeekoebaart 306). S=Specularite, C=Crystalline hematite, Q=Quartz. Transmitted cross-polarised light.

Bedding sub-parallel, thrust sense shear zones are particularly well developed in the Asbestos Hills Subgroup where the attitude of bedding (after the pre-Olifantshoek Supergroup folding), was such that it was easily exploited by simple shear during the Kheis orogeny (i.e. bedding was sub-parallel to the trend of the Kheis belt). Good examples of bedding sub-parallel shear zones in the Asbestos Hills Subgroup are exposed at locality D3 (farm Bovenzeekoebaart 313). At this locality bedding is disrupted in discrete, strongly foliated zones in which S-C fabrics indicate a north-west over south-east thrust sense of movement (Figure 4.28).

Syn-tectonic veining is developed within the bedding sub-parallel thrust sense shear zones, particularly in the Matsap Formation, Hartley Formation and Voelwater Subgroup. In the Matsap and Hartley Formations, quartz veins up to 60cm thick occur parallel to the foliation in high strain zones. On the bounding surfaces of the veins, quartz shear-fibres are developed (Ramsay and Huber, 1987). The quartz fibres plunge to the north-west, parallel to the mineral elongation lineations in the wall rocks.

At locality P1 (farm Zeekoebaart 306), closely spaced quartz-siderite veins are developed in highly sheared meta-psammite and lava of the Hartley Formation. The quartz-siderite veins are parallel to the foliation, and quartz shear-fibres are parallel to the lineations, in the wall rocks. This indicates that the quartz-siderite veins formed during the Kheis orogeny. Both the veins and the host rocks exhibit malachite staining, indicative of copper mineralisation. The malachite staining is as a result of weathering of narrow stringers of chalcocite, bornite, covellite and dendritic native copper that occur within the quartz-siderite veins (Figure 4.29). Similar veining is developed in a conglomerate layer in the Matsap Formation at locality P2 (farm 307). The copper bearing veins were mined on a small scale at both P1 and P2 in the early 1900's.

Bedding sub-parallel, thrust sense shear zones in the Voelwater Subgroup are often characterised by fibrous antitaxial (Ramsay, 1980) quartz-specularite veins (Figure 4.30, 4.31). Quartz fibres within the veins plunge to the north-west, parallel to the Kheis mineral elongation lineations. The veins that are at an oblique angle to bedding have curved quartz fibres, indicating that they developed at an early stage in the deformation and were rotated with subsequent bedding sub-parallel simple shear.



Figure 4.28: A bedding sub-parallel shear zone in banded ironstone of the Asbestos Hills Subgroup. S-C fabrics indicate a north-west over south-east thrust sense of movement. South-east is to the right of the photograph.

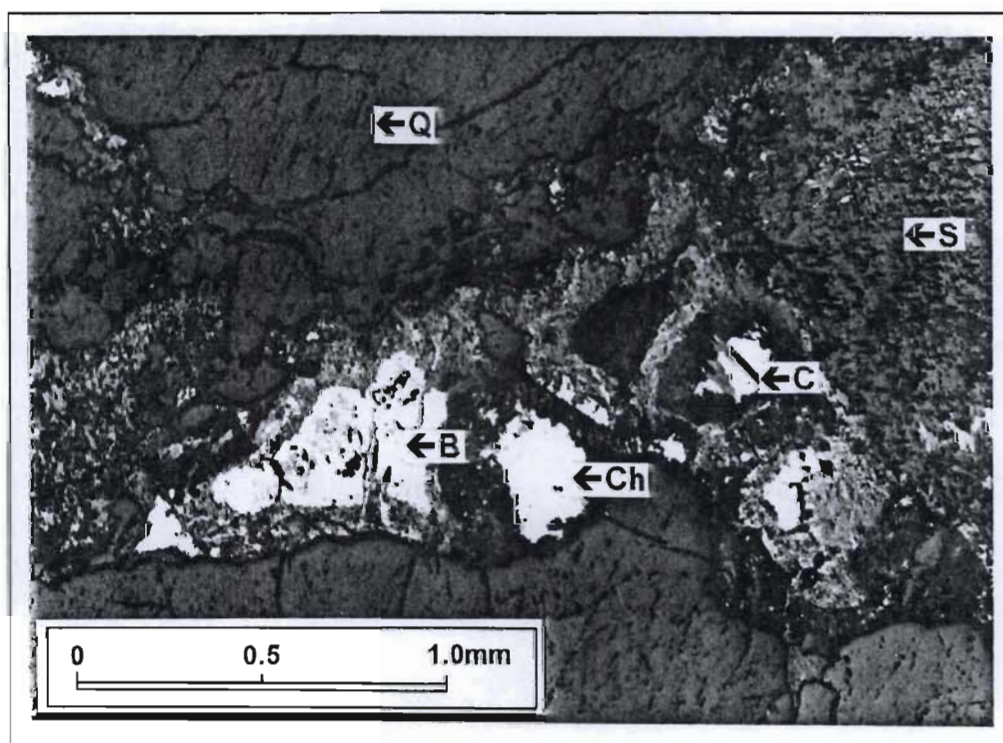


Figure 4.29: Photomicrograph of Cu-mineralised veining developed at locality P1 (farm Zeekoebaart 306). Reflected plane-polarised light. Ch=Chalcocite, B=Bornite, C=Covellite Q=Quartz, S=Siderite.



Figure 4.30: Extensional quartz-specularite veins in banded chert of the Voelwater Subgroup. Viewed in cross-section. South is to the right of the photograph. Locality: Farm 312.



Figure 4.31: Plan view of the extensional veins illustrated in Figure 4.28. Quartz fibres have grown parallel to the extension direction.

4.2.2.3 Brittle-ductile, thrust sense shear zones.

The Blackridge thrust follows an arcuate trace from the area north of Duikersdal (Map 1) to the Boegoeberg dam area where it branches into a complex imbricate system (Map 2). The fabric elements developed in the shear zones that comprise this imbricate system are ductile in nature. Older strata have been juxtaposed over younger strata along these shear zones indicating that dislocation (i.e. brittle deformation) has occurred (Figure 4.32). These features can therefore be classified as brittle-ductile, thrust sense shear zones and (c.f. the bedding sub-parallel shear zones) form mappable lineaments. It is important to note that the bedding sub-parallel shear zones and the brittle-ductile thrust sense shear zones are both a response to the same deformation event and can be considered to be part of the same system.

The brittle-ductile thrust sense shear zones strike between north-east and east and dip northwards. Mineral elongation lineations plunge obliquely down the plane of the foliation to the north-west. The fabric elements developed in these brittle-ductile shear zones are, for the most part, identical to those developed in the bedding parallel shear zones and the descriptions will not be repeated here. Deformation of the rocks in the hanging- and foot-wall of the brittle-ductile shear zones is more intense however and competent lithologies such as quartzite are mylonitised (see Figure 4.34). Features, not observed in the bedding sub-parallel shear zones, that have developed as a result of the high strain in these brittle-ductile thrust shear zones, are described below.

At locality D4 (farm Bovenzeekoebaart 313), interbedded narrow layers of quartzite (<10cm thick) and phyllite (<1m thick) of the Mapedi Formation have been highly strained in the footwall of a major thrust sense shear zone. The quartzite bands have been intensely folded on a 10-50cm scale. A north-west plunging mineral elongation lineation is developed at this locality. In low strain zones, the fold axes trend perpendicular to the elongation lineation and plunge gently (<10°) to both the north-east and the south-west. In high strain zones the fold axes plunge approximately 60° to the north-east and south-west and trend at an oblique angle to the mineral elongation lineation. When cut perpendicular to the fold axial plane these steeply plunging folds have eye-shaped closures similar to those of sheath folds. These are not true sheath folds as the limbs have not been rotated into parallelism with the mineral elongation lineation. “Sheath-like” folds such as these are thought to represent an incipient stage of sheath fold development (Quinquis *et al.*, 1978). At locality D10 (farm 312) sheath folds (Quinquis *et al.*, 1978) are developed in banded ironstones of the Voelwater Subgroup in the hanging- and foot-wall of a brittle-ductile shear zone (Figure 4.33). At this locality fold axes plunge steeply to the north, parallel to the mineral elongation lineation.

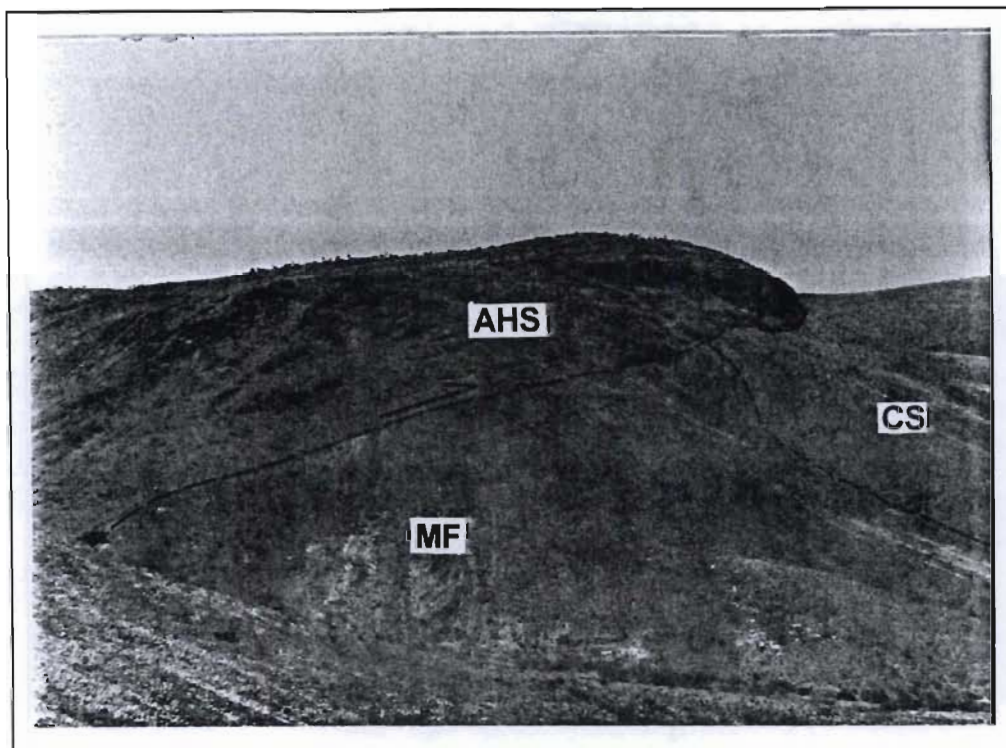


Figure 4.32: View (looking south-east from locality D3- farm Bovenzeekoebaart 313) of the brittle-ductile thrust sense shear zone along which the Asbestos Hills Subgroup (AHS) has been thrust over the Mapedi Formation (MF) and the Campbellrand Subgroup (CS).

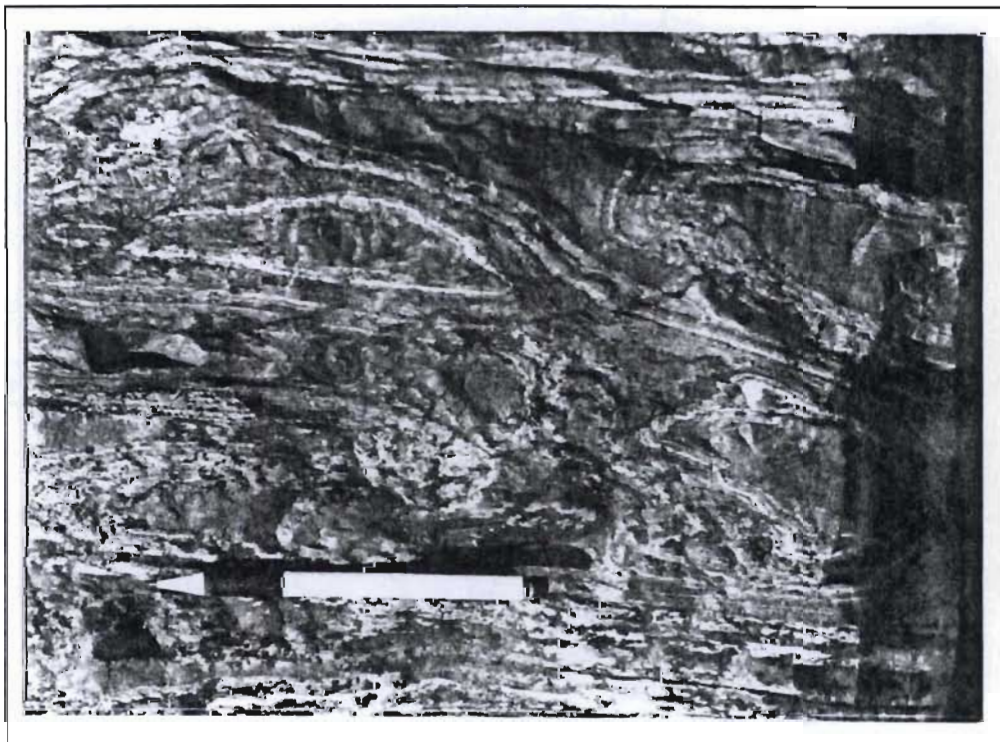


Figure 4.33: Sheath folds developed in banded ironstones of the Voelwater Subgroup. Locality D10- farm 312.

At locality P3 (farm Zeekoebar 9), lenses of braunite (manganese ore) occur in the footwall of a brittle-ductile, thrust sense shear zone that has juxtaposed banded ironstones of the Voelwater Subgroup over dolomites and phyllites of the Mapedi Formation. The braunite occurs in high strain zones in the Mapedi Formation and was mined on a small scale at the beginning of the century. It is suggested that this braunite deposit was formed by hydrothermal fluids preferentially channelled along the high strain zones in the Mapedi Formation during the Kheis orogeny. The source of the manganese was probably the overlying Voelwater Subgroup banded ironstones.

4.2.3 The extended Namaqua orogeny

The Griqualand West and Olifantshoek Supergroups in the western and central parts of the Map 2 area were weakly deformed during the extended Namaqua Orogeny. Namaqua age structural elements in the Map 2 area can be related to gentle NNW trending folding in discrete zones followed by dextral sense, strike-slip movement on the Doringberg fault (Map 1).

4.2.3.1 NNW trending folds

Small scale (0.2 - 2.5m wavelength), NNW trending, open, upright Namaqua folds are developed in discrete zones in the Map 2 area. These folds deform both bedding and the Kheis foliation (Figure 4.34). A crenulation cleavage, axial planar to the folds is developed in strongly foliated and incompetent lithologies.

Figure 4.35 shows the orientation of small scale NNW plunging Namaqua fold axes measured in the Map 2 area. The mean trend of the Namaqua fold axes is 342°. The variation in plunge of the fold axes from 20 to 70° is a result of the variation in dip, of both bedding and foliation, due to the original fold and thrust geometry of the Kheis belt in the Map 2 area. The axial planar cleavage dips steeply about the vertical to both the north-east and south-west (Figure 4.35).

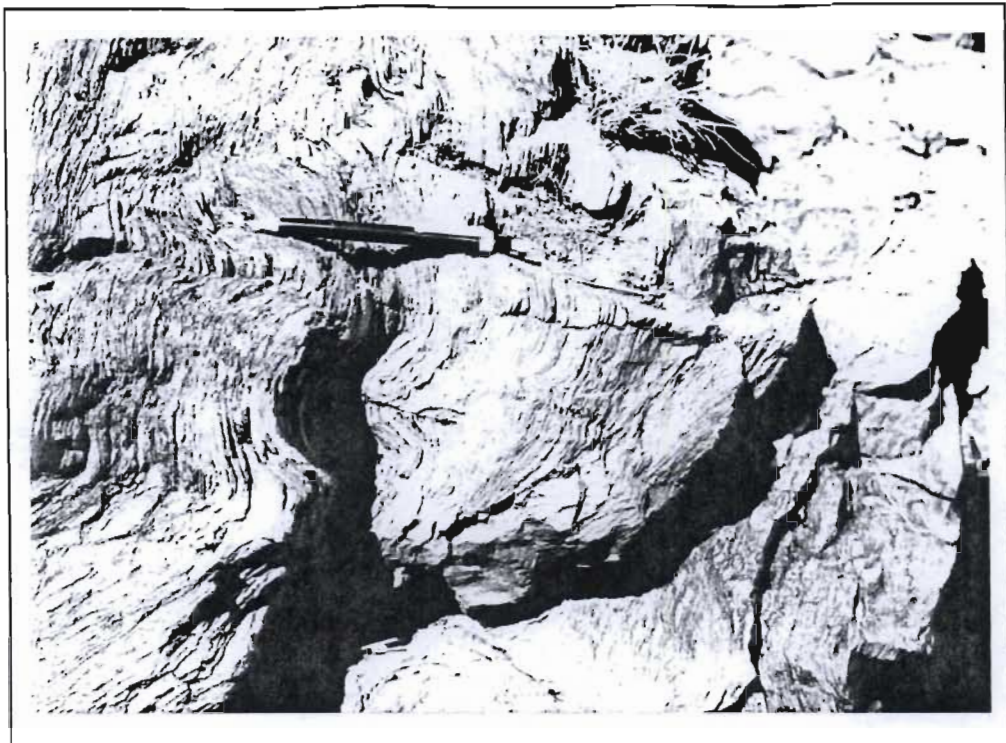


Figure 4.34: Small scale NNW plunging Namaqua folds developed in mylonitised Mapedi Formation quartzite (north is to the left of the photograph). A sub-vertical cleavage, axial planar to the small scale folds, crenulates the mylonitic foliation. Farm Bovenzeekoebaart 313- located in the brittle-ductile thrust sense shear zone north of locality D5.

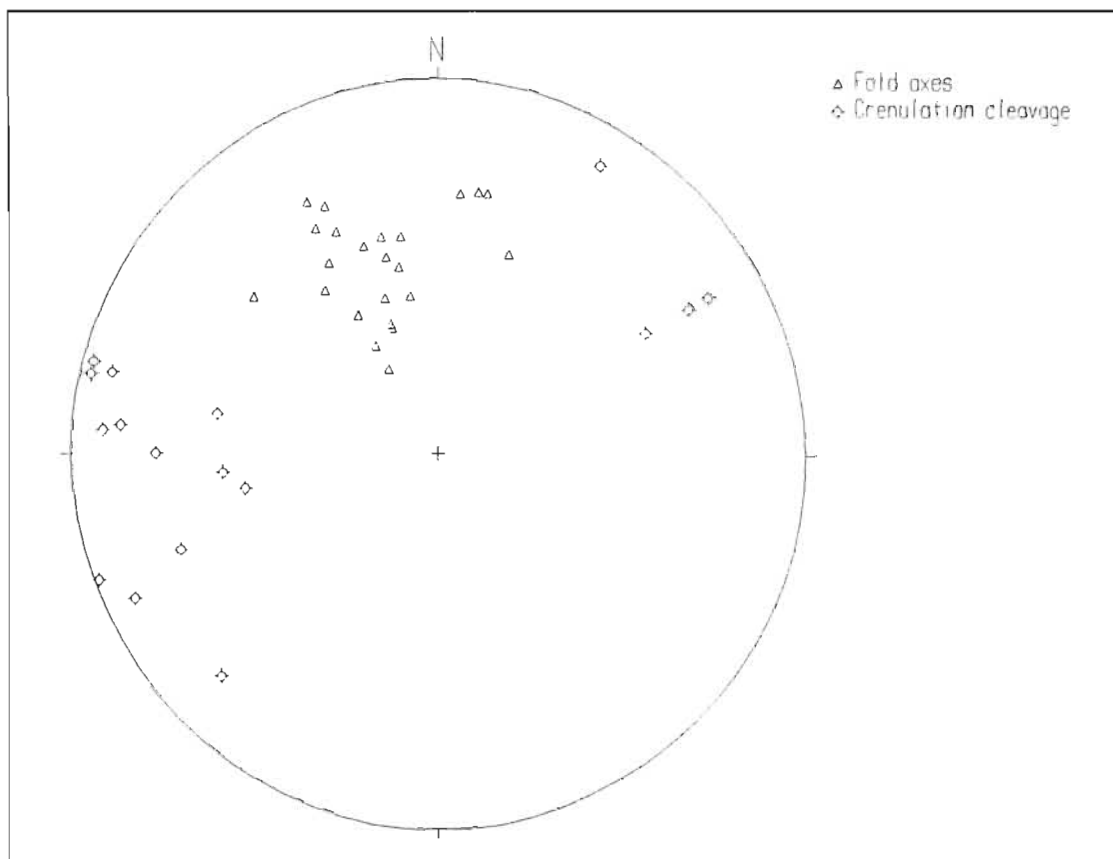


Figure 4.35: Equal area, stereographic projection (π -diagram) of Namaqua fold axes ($n=23$) and cleavage ($n=16$) orientations for the Map 2 area

4.2.3.2 *The Doringberg fault*

The Doringberg fault has an arcuate trend and is exposed for a strike length of approximately 125km. Its southern continuation is obscured by rocks of the Phanerozoic Karoo Supergroup (Map 1). The Doringberg fault strikes north-west in the area west of Prieska but swings to have a NNW strike in the Westerberg area. The fault zone is exposed in a road-cutting immediately south-west of Westerberg (locality 4.4). At this locality, the mafic lava unit of the Schmidtsdrif Subgroup has been juxtaposed against banded ironstones of the Asbestos Hills Subgroup. The banded ironstones on the eastern side of the fault are brecciated in discrete zones. The breccia zones are bounded by slickensided fault planes that dip steeply to the west. Slickenlines on these fault planes plunge at $<10^\circ$ to the SSE indicating strike-slip movement on the fault. The Schmidtsdrif Subgroup lavas on the western side of the Doringberg fault are strongly fractured and poorly exposed.

Due to the brittle nature of the deformation, no kinematic indicators are developed within the fault zone. Based on the displacement of the Schmidtsdrif Subgroup (situated on the western side of the fault at locality 4.4 and the eastern side of the fault on farm Geelbeksdam- locality 4.1) an apparent dextral displacement of 7.5 km has occurred on this fault.

The Doringberg fault splays into two branches immediately south of the Map 2 area (Map 1). The northern parts of these two branches are exposed in the Map 2 area. The western branch has a NNW strike, parallel to the main fault in the south and is exposed at locality D6 (farm Bovenzeekoebaart 313). Quartzites of the Mapedi Formation are brecciated at this locality (Figure 4.36). The breccia zone is 1.5m wide and is bounded by slickensided fault planes (Figure 4.37). Slickenlines on these fault planes plunge very gently to the south. At locality D7 (farm Bovenzeekoebaart 313) the western branch of the Doringberg fault has displaced a thrust contact between the Campbellrand and Asbestos Hills Subgroups (Figure 4.38). Based on separation of the thrust contact, and rotation of bedding and foliation either side of the fault (Map 2), 500m of apparent dextral sense, strike-slip displacement has occurred.

The western branch swings into parallelism with, and has probably re-activated, a Kheis age brittle-ductile thrust sense shear zone to the north-west of locality D6. The fault zone is poorly exposed in this area and no observations could be made regarding the movement kinematics. No indications of brecciation were observed west of locality D8 and the fault is interpreted to terminate in this area.

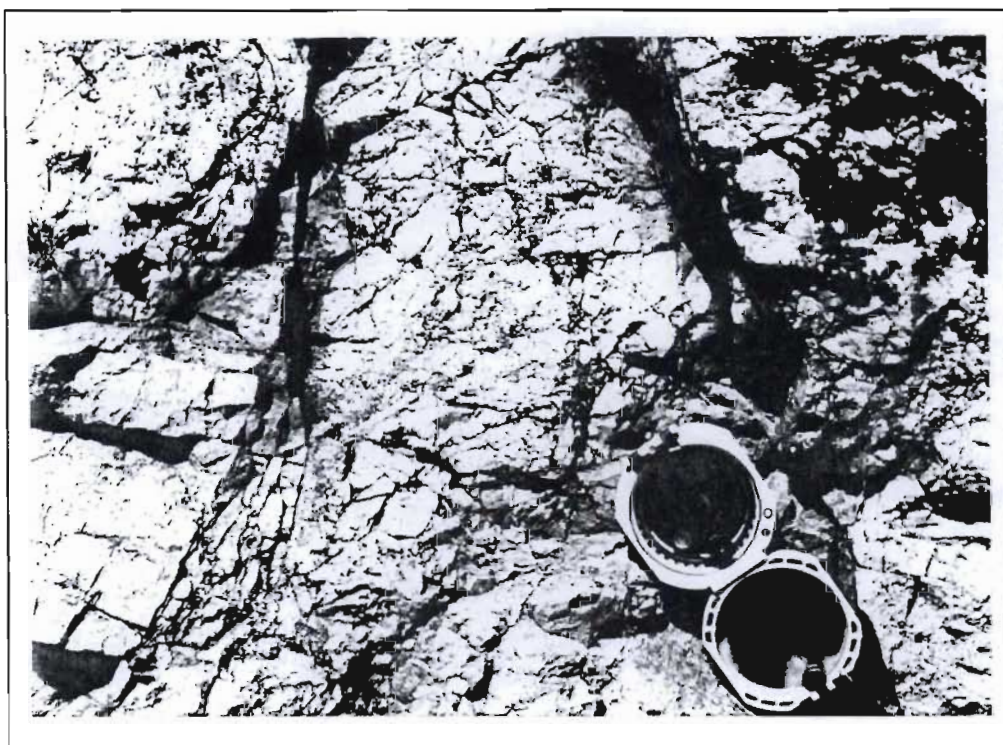


Figure 4.36: Fault breccia developed in Mapedi Formation quartzite along the western branch of the Doringberg fault. Locality D6-farm Bovenzeekoebaart 313.



Figure 4.37: Slickensided fault plane bounding the breccia shown in Figure 4.36. Note the gentle plunge of the slickenlines.

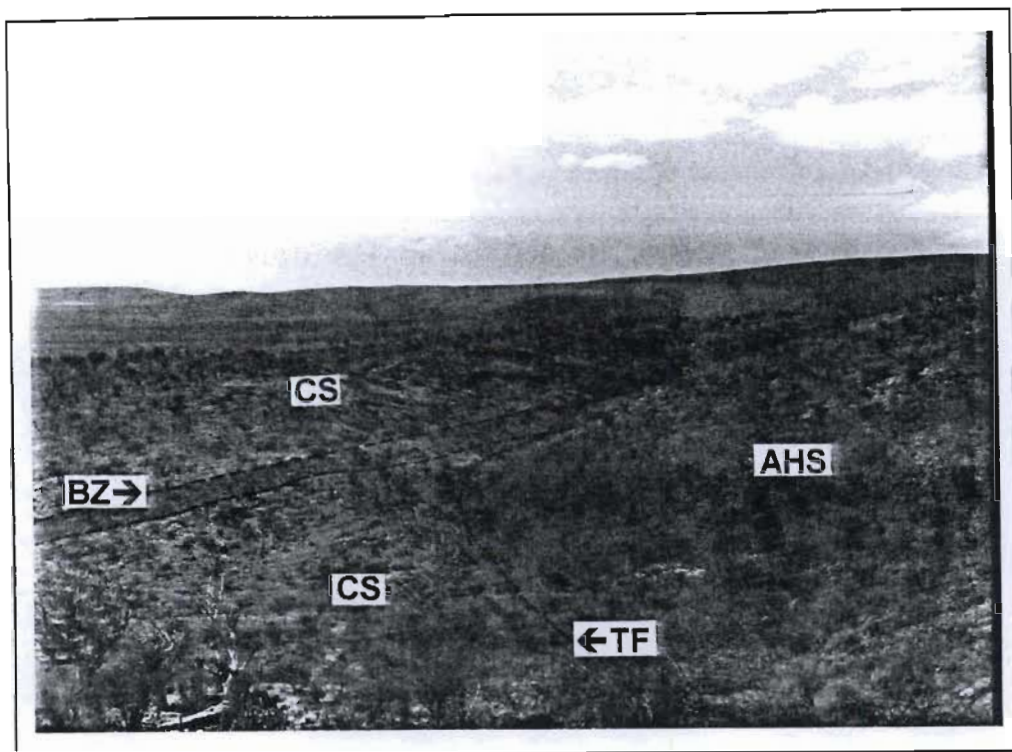


Figure 4.38: The western branch of the Doringberg fault at locality D7 (farm Bovenzeekoebaart 313). North is to the left of the photograph. The fault breccia zone (BZ) truncates a brittle-ductile thrust sense shear zone (TF), formed during the Kheis orogeny that has thrust dolomites of the Campbellrand Subgroup (CS) over banded ironstones of the Asbestos Hills Subgroup (AHS).

The eastern branch of the Doringberg fault forms a prominent lineament on aerial photographs but the fault zone is only exposed at locality D9 (farm 315) where an isolated outcrop of Lucknow Formation quartzite occurs. The quartzite on the eastern side of this outcrop is brecciated, but no slickensided fault planes are exposed. This small outcrop is interpreted to be an erosional relic of part of the Lucknow Formation that was displaced, with 1.7 km of apparent dextral translation, from the main outcrop of Lucknow Formation to the south-east (Map 1, Map 2).

Although stratigraphic displacement indicates 1.7 km of apparent dextral strike-slip translation on the eastern branch of the Doringberg fault, its anomalous north-east strike (c.f. the NNW strike of the main Doringberg fault and the western branch) suggests that movement on the fault had a significant oblique component. The 1.7 km of apparent dextral movement therefore represents the minimum displacement. On aerial photographs, it can be observed that the eastern branch follows an arcuate trace north of locality D9 and eventually merges with a brittle-ductile, thrust sense shear zone that formed during Kheis orogenesis.

4.3 Summary

4.3.1 Stratigraphy and depositional environment

Figure 4.39 summarises the stratigraphy of the Griqualand West and Olifantshoek Supergroups for the Boegoeberg dam area.

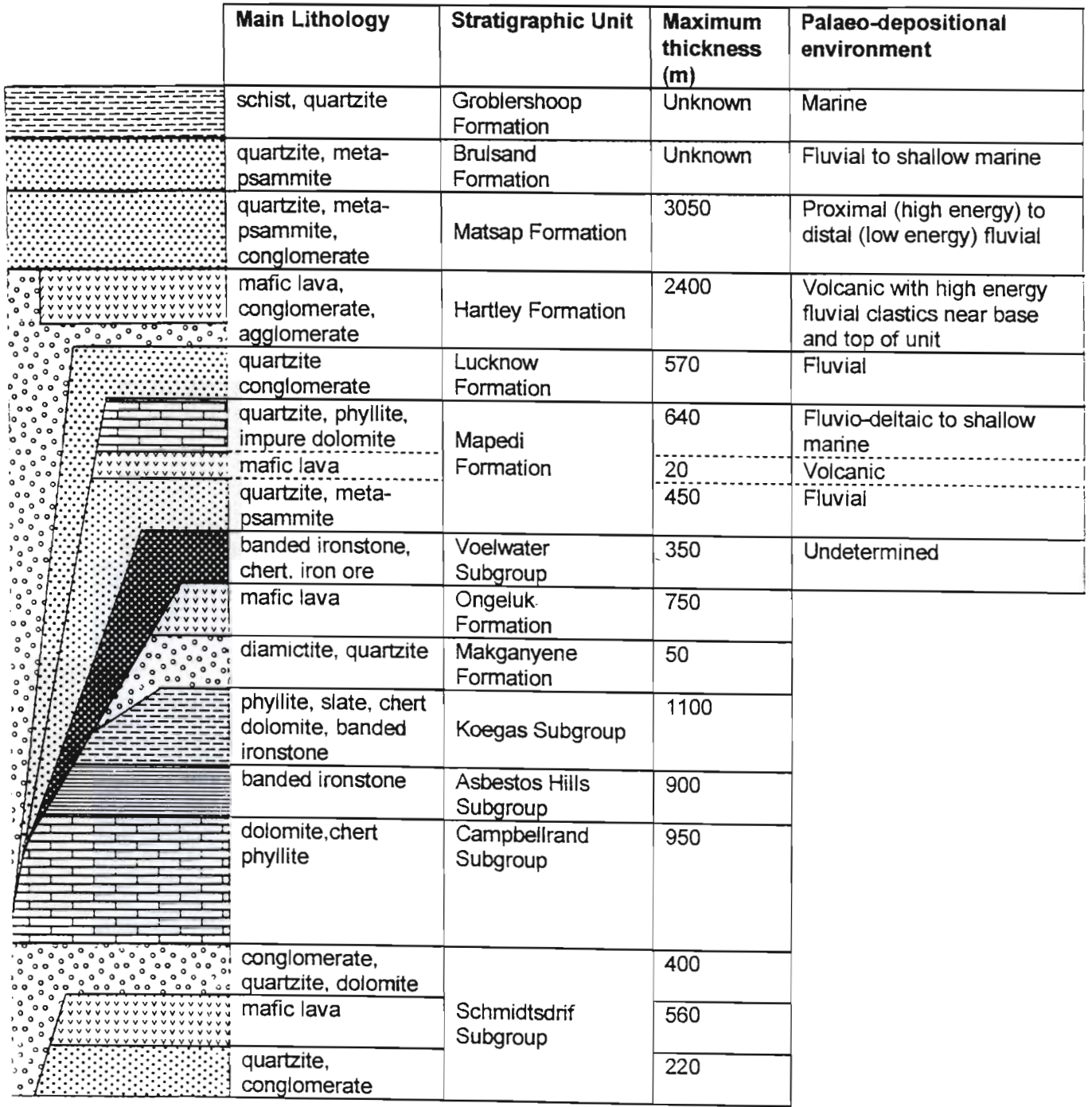
A mafic lava unit and a disconformably overlying conglomerate, that were interpreted by Vajner (1974) to be part of the Zeekoebaart Formation, are interpreted to be part of the Schmidtsdrif Subgroup. In certain areas, the lower part of the Schmidtsdrif Subgroup has been removed at the above mentioned disconformity such that the conglomerate rests on mafic lavas of the Zeekoebaart Formation.

The Schmidtsdrif Subgroup is transitionally and conformably overlain by the Campbellrand Subgroup dolomites and cherts which are in turn conformably overlain by banded ironstones of the Asbestos Hills Subgroup. The dominantly clastic Koegas Subgroup was not studied in any depth during this study. Previous work suggests that it conformably overlies the Asbestos Hills Subgroup (Vajner, 1974; Beukes, 1986). Immediately south of the Map 2 area, the Koegas Subgroup is overlain by the Makganyene Formation. The contact between these two units was not observed. In the Griquatown area (Map 1), the Makganyene Formation disconformably overlies the Koegas Subgroup, further west it rests disconformably on rocks of the Asbestos Hills Subgroup (Beukes, 1986). The Makganyene Formation is overlain by the Ongeluk Formation lavas immediately south of the Map 2 area.

A unit comprising siliceous and ferruginous chert and hematite rich banded ironstones has been described from the Boegoeberg dam area. Previous workers have correlated this unit with the Asbestos Hills Subgroup, the Koegas Subgroup or the Hartley Formation. Based on similarities between this unit and the Voelwater Subgroup observed in the Korannaberge-Langberge, this unit is interpreted to be part of the Voelwater Subgroup.

Deformation of the Griqualand West Supergroup occurred prior to deposition of the Voelwater Subgroup indicating an unconformable relationship between the two units. This is contrary to the widely accepted opinion that the Voelwater Subgroup conformably overlies the Ongeluk Formation (SACS, 1980; Nel *et al.*, 1986; Gutzmer and Beukes, 1995).

Figure 4.39: Lithostratigraphic column of the Griqualand West and Olifantshoek Supergroups in the Boegoeberg dam area. The disconformity at the base of the Makganyene Formation and the thickness of the Koegas Subgroup are based on observations by Beukes (1986) and Vajner (1974). The thickness of units in the hatched column is not to scale.



In the Boegoeberg dam area, the Olifantshoek Supergroup overlies the Griqualand West Supergroup (excluding the Voelwater Subgroup) with angular unconformity. The Olifantshoek Supergroup disconformably overlies the Voelwater Subgroup.

The lower part of the Mapedi Formation consists of interbedded trough cross-bedded quartzite and meta-psammite that were deposited in a fluvial palaeo-environment. This unit is conformably overlain by a highly altered mafic lava horizon that attains a maximum thickness of 20m. The mafic lava horizon is overlain by interbedded siliceous quartzites and phyllites that grade upwards into interbedded cross-bedded dolomites and quartzites that were deposited in a shallow marine palaeo-environment. The Mapedi Formation thus records a transition from a fluvial to shallow marine palaeo-depositional environment (i.e. a marine transgression).

The Lucknow Formation is only exposed in the south-eastern part of the Map 2 area where it occurs in the footwall of the Blackridge thrust system. Immediately south of the Map 2 area, a conglomerate unit developed at the base of the Lucknow Formation overlies the Koegas Subgroup, Makganyene and Ongeluk Formations with angular unconformity. In the Map 2 area, the lateral equivalent of this basal conglomerate, a pebbly quartzite unit with numerous narrow conglomerate bands, disconformably overlies the Voelwater Subgroup. The basal pebbly quartzite of the Lucknow Formation is overlain by trough cross-bedded quartzite (with narrow conglomerate bands) that was deposited in a fluvial palaeo-environment.

These observations differ from those made in the Traverse 3 and Voelwater area (locality 3.1- Map 1) where the Lucknow Formation disconformably overlies the Mapedi Formation. Stratigraphic studies by Beukes and Smit (1987) and mapping by SAGS (1977) indicate significant thinning of the Mapedi Formation below the disconformity at the base of the Lucknow Formation (in the area south of Locality 3.1). Approximately 20 Km south of Wolhaarkop (Map 1), the Mapedi Formation is not developed in the footwall of the Blackridge thrust and here the Lucknow Formation directly overlies rocks of the Griqualand West Supergroup (Map 1). The major disconformity at the base of the Lucknow Formation records a rapid fall in alluvial base levels after deposition of the shallow marine Mapedi Formation sediments.

In the Map 2 area, the Hartley Formation overlies the Campbellrand Subgroup with angular unconformity or the Voelwater Subgroup and Mapedi Formation with disconformity. The basal unit of the Hartley Formation in the Boegoeberg dam area is either a small pebble conglomerate or a volcanic agglomerate

that is correlated with the Neylan bed of SACS (1980). The basal unit of the Hartley Formation thus records a renewed rapid fall in alluvial base level accompanied by mafic volcanism. Pillow lava horizons in the Hartley Formation are common, indicating sub-aqueous extrusion. The amount of clastic material interbedded with the lavas increases towards the top of the unit. The upper part of the Hartley Formation consists mainly of clastic sediments with a significant proportion of thick, poorly sorted, conglomerate horizons. The contact between the Hartley Formation and the Matsap Formation is transitional and conformable. The thick conglomerate layers are also developed in the lower part of the Matsap Formation.

The thick conglomerate layers in the Matsap Formation are confined to the lower 100m where they are interbedded with trough cross-bedded quartzite and meta-psammite. The bulk of the Matsap Formation consists of red-brown, purple or light-brown coloured, trough cross-bedded quartzites with narrow conglomerate bands. The proportion of coarse grained clastic material and upper flow-regime indicators decrease moving upwards. The Matsap Formation is overlain by siliceous quartzites of the Brulsand Formation and meta-pelites of the Groblershoop Formation (Stowe, 1986).

The Olifantshoek Supergroup was intruded by gabbro-norite sills of similar composition to those observed in the Langberge-Korannaberge area. The sills post-date the Olifantshoek Supergroup, but pre-date the Kheis orogeny. The relative age of the gabbro-norite sills in the Korannaberg-Langberge area can be bracketed in the same interval. The sills are interpreted to be part of the same igneous suite.

4.3.2 Structural geology

4.3.2.1 Pre-Voelwater Subgroup Folding

Prior to deposition of the Voelwater Subgroup, the Griqualand West Supergroup was deformed to produce north-south trending periclinal folds. The folds are upright open structures in the eastern part of the preserved Griqualand West basin but become progressively tighter moving towards the west. Folding was accompanied by bedding parallel simple shear, which resulted in the development of discrete zones of small scale folds and boudinage in the Griqualand West Supergroup. Crocidolite asbestos fibre-growth occurred in the Asbestos Hills Subgroup during this deformation.

4.3.2.2 *The Kheis orogeny*

The Kheis orogeny occurred subsequent to deposition of the Voelwater Subgroup, the Olifantshoek Supergroup and intrusion of the gabbro-norite sills. The Kheis age Blackridge thrust follows an arcuate trace from the Duikersdal area to the Boegoeberg dam area where it branches to form a complex imbricate system. Within this imbricate system, rocks of the Olifantshoek Supergroup, Voelwater Subgroup and the Griqualand West Supergroup are structurally interleaved. Juxtaposition of older stratigraphic units over younger stratigraphic units occurred along steeply north to north-west dipping, brittle-ductile, thrust sense shear zones. Mineral elongation lineations in these shear zones plunge obliquely down the plane of the foliation to the north-west implying south-east vergent, oblique thrust sense of movement.

The steep dip of the Blackridge thrust system in the Boegoeberg dam area is in contrast to the shallow dips of the Blackridge thrust reported from the Sishen, Wolhaarkop and Black Rock areas (Van Wyk, 1980; Beukes and Smit, 1987). With the exception of overturned folding and bedding sub-parallel shear in its immediate footwall (in the area south-east of Boegoeberg dam), no Kheis age structural elements can be recognised south-east of the Blackridge thrust system.

The trend of fold axes in the Voelwater Subgroup and the Olifantshoek Supergroup mirror the trend of the brittle-ductile, thrust sense shear zones. The folds are overturned to the south and their relationship to the thrust sense shear zones indicates that they formed during the same progressive deformation. Sheath-like folds and sheath folds occur in high strain zones associated with the brittle-ductile thrust sense shear zones.

4.3.2.3 *The extended Namaqua orogeny*

Structural elements produced during the Pre-Voelwater folding and the Kheis orogeny were deformed during the extended Namaqua orogeny. Gentle folding about NNW trending fold axes was followed by dextral sense, strike-slip movement on the Doringberg fault.

5. THE GEOLOGY OF THE MARYDALE BASEMENT HIGH

The term Marydale basement high is an informal name used to describe the Archaean granite-greenstone terrain situated between the Doornberg shear zone and the Doringberg fault (Map 1). The Marydale basement high comprises the Marydale Group greenstones, the Draghoender granite and the Skalkseput granite (Vajner, 1974; SACS, 1980). The rocks of the Marydale basement high and the Zeekoebaart Formation were investigated on a regional scale in order to determine the relative ages of the various rock types and to ascertain whether the basement rocks were deformed during Kheis and extended Namaqua orogenesis. The Zeekoebaart Formation was studied in an effort to resolve its uncertain internal stratigraphy. Localities described are indicated on Map 1 and are referenced in the text using the format: locality 5.1.

An attempt was made to date the Draghoender granite, the Skalkseput granite and the Zeekoebaart Formation. Zircons were separated from samples of these units at the CSIR (Council for Scientific and Industrial Research (Pretoria) and analysed at the Australian National University (Canberra) by Dr R.A. Armstrong using the SHRIMP ion microprobe. The data were reduced as described by Compston *et al* (1992).

5.1 Lithology, relative ages and geochronology

5.1.1 The Marydale Group

Xenoliths of amphibolite and serpentinite, ranging in size from metre-scale pods to rafts, several hundred metres long, occur in the Draghoender granite and are exposed in road cuttings south-east of Marydale (locality 5.1). These xenoliths are highly sheared and intruded by numerous granitoid veins. Vajner (1974) correlated the mafic xenoliths in the Draghoender granite with the Marydale Group. Although it is probable that these mafic xenoliths are Archaean greenstone material, any correlation with the Marydale Group is highly speculative.

Rocks tentatively correlated with the Marydale Group (Vajner, 1974) form a prominent NNW striking ridge called Swartkop (locality 5.2). Swartkop ridge comprises dolomite, banded ironstone, chlorite schist, serpentinite and amphibolite. Both bedding and the schistosity strike NNW and dip steeply to the west. These rocks are identical to those described from the Modderfontein Formation of the Marydale Group (SACS, 1980; Scott, 1987) and are therefore correlated with that unit.

Although the contact between the Draghoender granite and the Modderfontein Formation is not exposed at Swartkop ridge, numerous granitic veins cross-cut bedding in the meta-sediments. This suggests that the Draghoender granite is younger than the Marydale Group.

5.1.2 The Draghoender granite.

The granitoid rocks of the Marydale basement high form a typical, deeply weathered, granitoid terrain consisting of widely spaced, low, rounded outcrops surrounded by windblown sand, and alluvium. The Draghoender granite is a biotite-rich porphyritic granite containing pink alkali feldspar phenocrysts 1-5cm in length. Along the Doornberg shear zone the Draghoender granite has a strong foliation defined by layers of biotite and alignment of the feldspar phenocrysts.

The Draghoender granite was sampled at locality 5.1 for the purpose of radiometric dating. The zircons from the Draghoender granite are typically subhedral and dark-brown to pink in colour. Most grains consist of a rounded central core surrounded by a zoned rim but some structureless (no obvious core/rim relationship) zircons are present. The cores are generally clearer and less coloured than the rims indicating higher U and Th contents in the rims (Armstrong, 1997a).

A combined total of 13 analyses of zircon cores, rims and structureless zircons were performed. The U-Th-Pb results for the Draghoender granite are presented in Table 5.1 and plotted on a conventional U-Pb Wetherill concordia diagram in Figure 5.1. From this plot it can be seen that there is some scatter of the data indicating a complex age pattern. Most of the analyses plot as a slightly discordant group from which a $^{207}\text{Pb}/^{206}\text{Pb}$ age of 2853 ± 4 Ma is calculated. This age is interpreted to represent the crystallisation age of the Draghoender granite. Most of the core/rim structures reflect different crystallisation conditions in the magma with time. The older ages determined on grain 1 and grain 4 (Table 5.1) indicate an inherited component in the granite. The presence of these xenocrystic zircons indicates a basement or protolith which is at least 3125 Ma old.

5.1.3 The Skalkseput granite

The Skalkseput granite is a leucocratic biotite-muscovite granite. In places the granite is porphyritic and it contains light-grey, K-feldspar phenocrysts up to 2cm in length. Even when it is strongly foliated it can be distinguished from the Draghoender granite by the light colour and low biotite content. No exposure was found where the relative ages of the Skalkseput granite and the Draghoender granite could be

Table 5.1: U-Th-Pb data from ion microprobe analyses of zircons from the Draghoender granite, the Skalkseput granite and the Zeekoebaart Formation. Uncertainties given at the one sigma level (Analyses performed by R.A. Armstrong).

Grain.spot	U/ppm	Th/ppm	Th/U	Pb*/ppm	204/206	% 1206	206/238	±	207/235	±	207/206	±	Ages (in Ma)				% CONC
													206/238	207/235	207/206	±	
Draghoender Granite																	
1.1	85	50	0.58	62	0.000010	0.01	0.6030	0.0143	20.057	0.504	0.2412	0.0014	3042	3094	3128	10	97
1.2	240	128	0.53	178	0.000068	0.09	0.6259	0.0135	20.742	0.462	0.2404	0.0008	3133	3127	3122	5	100
2.1	163	122	0.74	100	0.000350	0.47	0.5064	0.0129	14.179	0.397	0.2031	0.0018	2641	2762	2851	14	93
2.2	487	53	0.11	244	0.000166	0.22	0.4703	0.0100	13.386	0.294	0.2064	0.0007	2485	2707	2878	6	86
3.1	51	40	0.79	33	0.001302	1.74	0.5352	0.0166	14.796	0.735	0.2005	0.0071	2764	2802	2830	59	98
3.2	351	46	0.13	190	0.000488	0.65	0.5036	0.0106	14.177	0.309	0.2042	0.0008	2629	2762	2860	6	92
4.1	25	13	0.51	17	0.000013	0.02	0.5731	0.0181	18.276	0.619	0.2313	0.0021	2920	3004	3061	14	95
5.1	247	41	0.17	140	0.000444	0.59	0.5269	0.0115	15.130	0.344	0.2083	0.0008	2728	2824	2892	6	94
6.1	44	50	1.14	28	0.000046	0.06	0.4766	0.0148	13.496	0.457	0.2054	0.0021	2512	2715	2869	17	88
7.1	38	49	1.29	26	0.000024	0.03	0.5143	0.0188	14.561	0.561	0.2053	0.0017	2675	2787	2869	14	93
8.1	338	41	0.12	188	0.000042	0.06	0.5225	0.0113	14.716	0.334	0.2043	0.0009	2710	2797	2861	7	95
9.1	945	563	0.60	601	0.000006	0.01	0.5416	0.0112	15.161	0.318	0.2030	0.0003	2790	2825	2851	2	98
10.1	41	64	1.55	30	0.000077	0.10	0.5261	0.0141	14.812	0.424	0.2042	0.0015	2725	2803	2860	12	95
Skalkseput Granite																	
1.1	1489	73	0.05	304	0.003139	4.17	0.1774	0.0041	3.088	0.116	0.1262	0.0034	1053	1430	2046	49	52
1.2	102	62	0.60	70	0.000034	0.05	0.5760	0.0148	16.931	0.458	0.2132	0.0012	2932	2931	2930	9	100
2.1	1211	226	0.19	318	0.002581	3.43	0.2324	0.006	5.602	0.162	0.1748	0.0018	1347	1916	2604	17	52
2.2	24	7	0.31	15	0.000249	0.32	0.5517	0.0211	17.341	0.743	0.2280	0.0034	2832	2954	3038	24	93
3.1	61	31	0.51	40	0.000010	0.01	0.5664	0.0147	16.735	0.478	0.2143	0.0020	2893	2920	2938	15	99
4.1	45	23	0.52	33	0.000087	0.11	0.6099	0.0177	20.073	0.630	0.2387	0.0021	3070	3095	3111	14	99

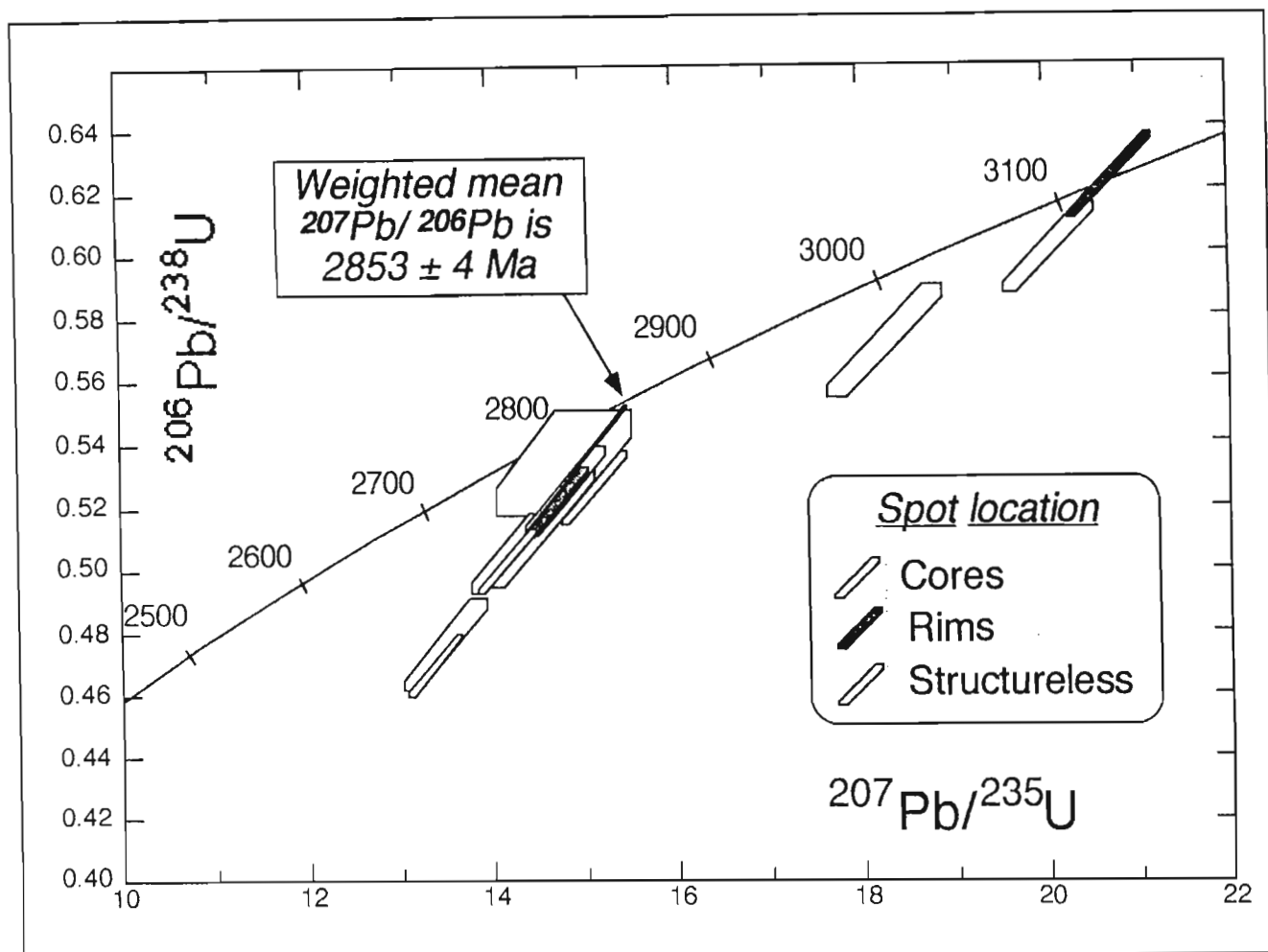


Figure 5.1: U-Pb concordia diagram of SHRIMP analyses of zircons from the Draghoender granite (Analyses performed by R.A. Armstrong).

unequivocally demonstrated. Numerous veins of leucocratic granite and pegmatite that are present in the Draghoender granite may be related to the Skalkseput granite.

Vajner (1974) described a granite-pebble conglomerate (the Skalkseput conglomerate) developed at the contact between the Zeekoebaart Formation and the underlying Skalkseput granite. Vajner (1974) thus considered the Zeekoebaart Formation to unconformably overlie the Skalkseput granite. The contact between the Skalkseput granite and the Zeekoebaart Formation is exposed at locality 5.4, situated on farm Skalkseput (the type locality for both the Skalkseput granite and the Skalkseput conglomerate: Vajner, 1974; SACS, 1980). At this locality it can be convincingly demonstrated that the Skalkseput granite is intrusive into the Zeekoebaart Formation. The contact follows an irregular trace and narrow slivers of the Zeekoebaart Formation lavas are surrounded by tongues of the Skalkseput granite (Figure 5.2). The contact itself is abrupt and marked by a narrow (<20cm) transitional zone of coarse grained, pegmatitic material (Figure 5.3) consisting of large alkali feldspar and quartz megacrysts in a fine grained,

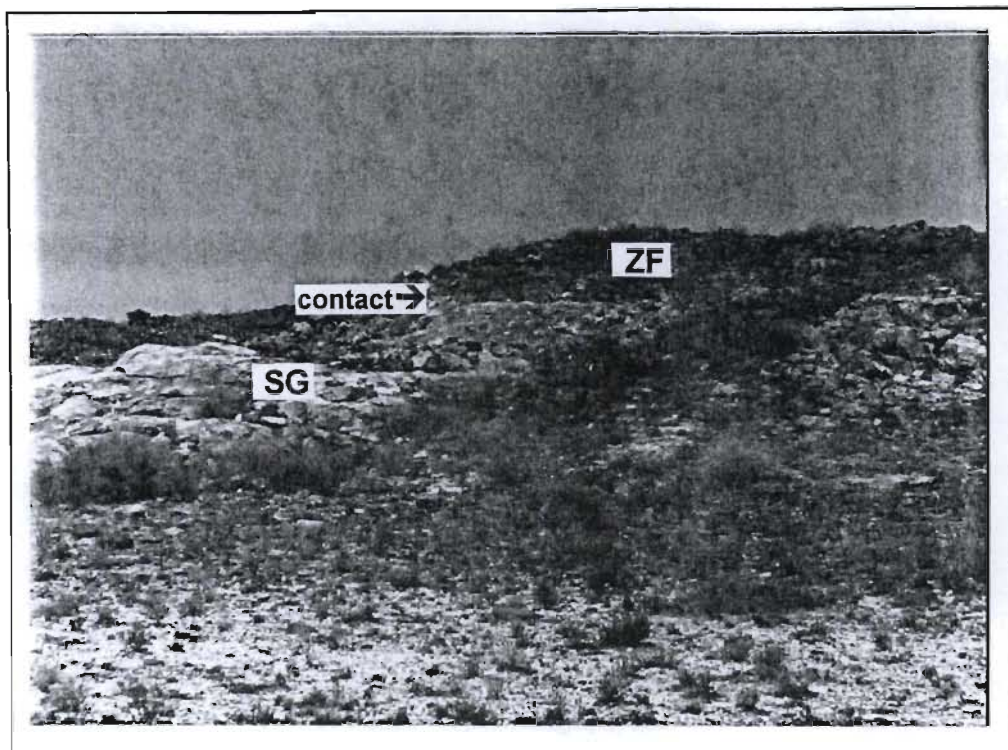


Figure 5.2: The contact between the Zeekoebaart Formation (ZF) and the Skalkseput granite (SG). Locality 5.4.

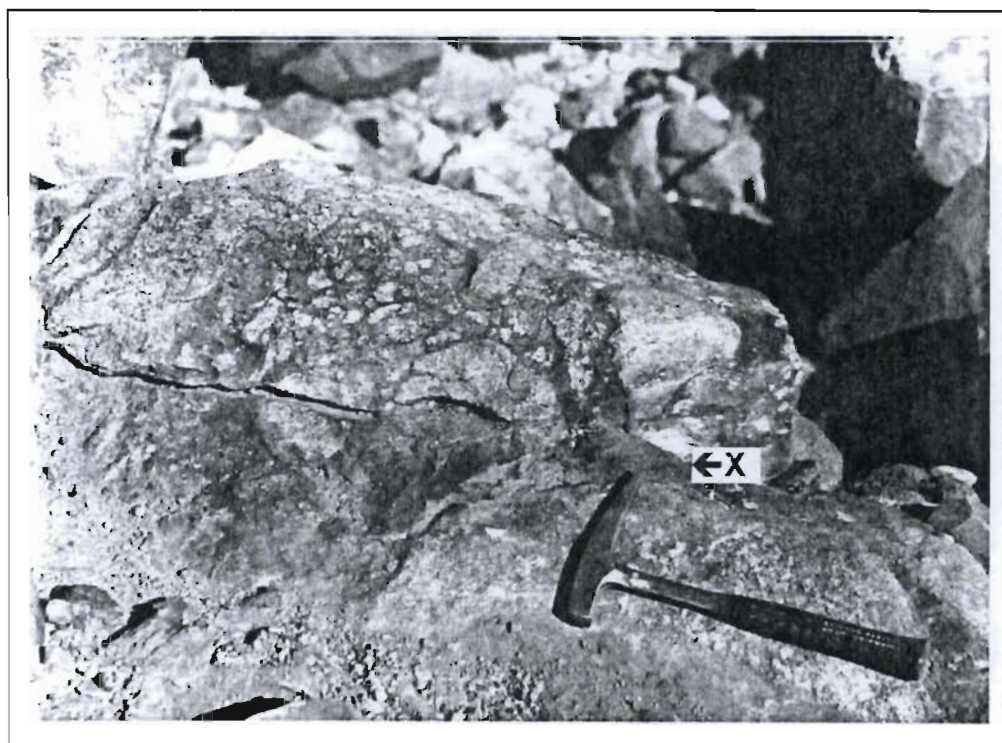


Figure 5.3: The coarse grained pegmatoidal rock developed at the contact between the Skalkseput granite and the Zeekoebaart Formation. Note the lava xenolith (X) within the granite.

light green coloured, quartz-feldspar-chlorite groundmass. Xenoliths of Zeekoebaart Formation lava were observed in, and immediately below this narrow transitional zone.

The Skalkseput granite was sampled at locality 5.4 for radiometric dating. The zircons from the Skalkseput granite exhibit complex core/rim structures similar to those from the Draghoender granite. The zircons are dark coloured, semi-opaque and show signs of substantial alteration. The central core areas are relatively clear, but the rims are highly metamict and difficult to analyse due to their high U concentrations and consequent radiation damage (Armstrong, 1997a). After six analyses were completed on these zircons it became obvious that due to the heterogeneous zircon population and the highly altered nature of the rims, the establishment of a concordant and meaningful crystallisation age was unlikely. The four analyses of cores show a spread in $^{207}\text{Pb}/^{206}\text{Pb}$ ages from 3111 to approximately 2930 Ma (Figure 5.4, Table 5.1). The maximum age is similar to that for the xenocrystic zircons in the Draghoender granite. Two analyses of cores overlap concordantly on the U-Pb concordia diagram (Figure 5.4), the $^{207}\text{Pb}/^{206}\text{Pb}$ ages for these two zircon cores are 2930 ± 9 and 2938 ± 15 Ma (Table 5.2) but without acceptable data from the zircon rims it is not possible to determine the significance of these ages. The two analyses of zircon rims are extremely discordant (with U concentration as high as 1489 p.p.m.) and indicate a complex Pb loss history (Armstrong, 1997a).

The poor results from this sample of Skalkseput granite contrast with results obtained by R.A. Armstrong (Pers. comm.) who analysed zircons from the Skalkseput granite sampled at locality 5.5. U-Pb single zircon SHRIMP dating of this sample yielded a concordant $^{207}\text{Pb}/^{206}\text{Pb}$ age of 2718 ± 8 Ma.

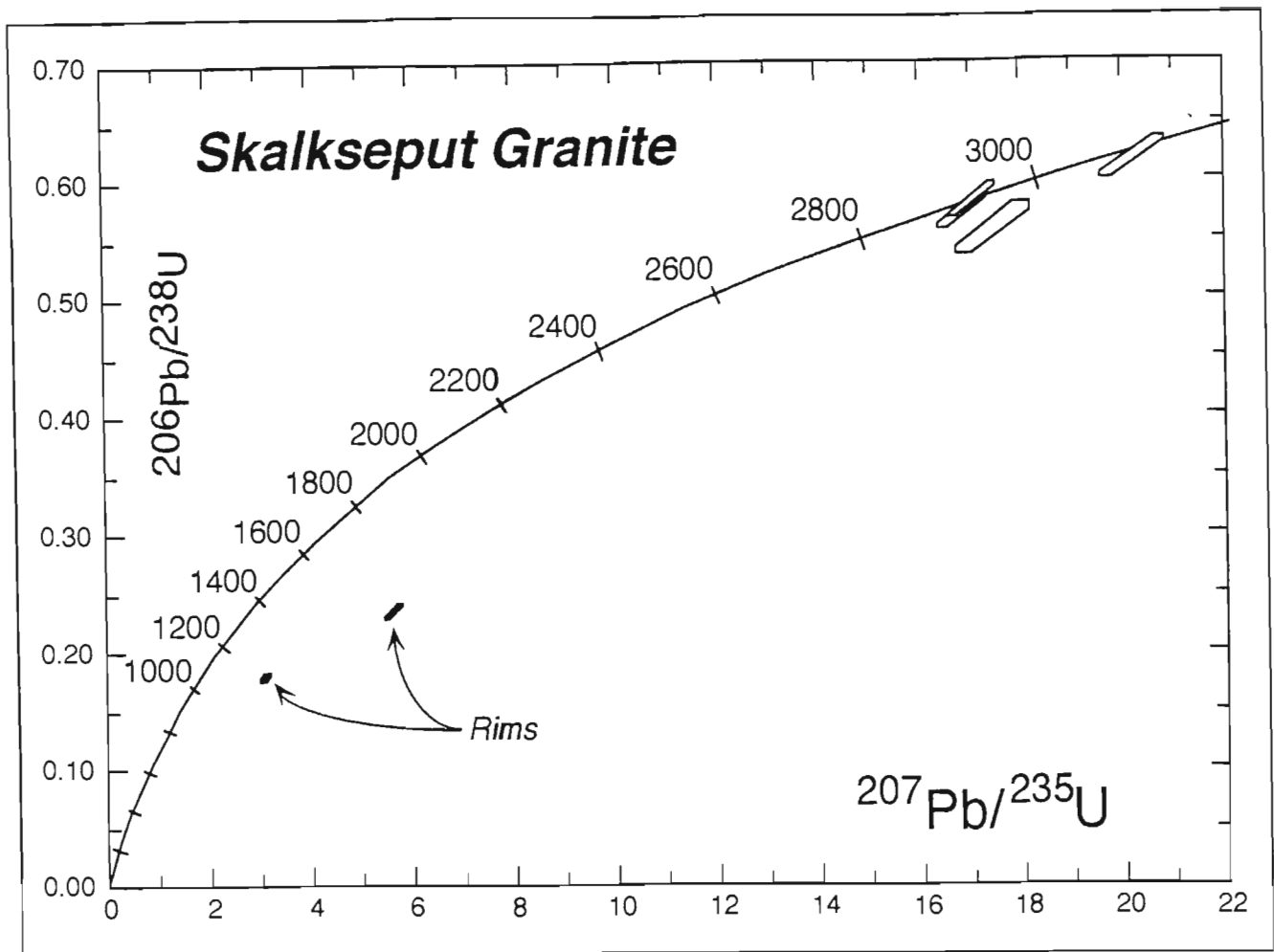


Figure 5.4: U-Pb concordia diagram of SHRIMP analyses of zircons from the Skalkseput granite (Analyses by R.A. Armstrong).

5.1.4 The Zeekoebaart Formation

Vajner (1974) subdivided the Zeekoebaart Formation as shown in Table 5.2. In Chapter 4 the Waterval member was correlated with the Hartley Formation, as suggested by Smit (1977). The Skalkseput “conglomerate” is a pegmatitic contact rock developed at the contact between the Skalkseput granite and the Zeekoebaart Formation. The Witvlei conglomerate member has been shown in this study (Chapter 4) to be part of the Schmidtsdrif Subgroup. The remaining two subdivisions of the Zeekoebaart Formation, as suggested by Vajner (1974), are the Geelbeksdam porphyry and the Blinkfontein volcanic members.

Vajner (1974) described the Geelbeksdam porphyry member as a rhyodacitic quartz porphyry and, based on work by Rogers and Du Toit (1908), suggested that it occurs at the base of the Zeekoebaart Formation. The Geelbeksdam porphyry member was only described from one outcrop situated on the eastern side of the Doringberg fault (Vajner, 1974). No evidence for a quartz porphyry was found during the present study, although some highly altered granitic rock is exposed at locality 5.6 and 5.7. These rocks are

Member		Thickness (m)	
Witvlei conglomerate		<100	
Blinkfontein volcanic		600-900	
Waterval	Skalkseput conglomerate	400-700	0-2m
Geelbeksdam porphyry		<50	

Table 5.2: Stratigraphic subdivisions of the Zeekoebaart Formation (after Vajner, 1974).

interpreted to be Skalkseput granite that has been altered in the Doringberg fault zone. The porphyry described by Rogers and Du Toit (1908) occurs in the Schmidtsdrif Subgroup and not the Zeekoebaart Formation.

The Blinkfontein volcanic member is the only unit described by Vajner (1974) that is considered to be part of the Zeekoebaart Formation. The Zeekoebaart Formation is strongly foliated and outcrops very poorly in the northern and the western sectors of its map pattern. Good exposure is located in the south-east (in the vicinity of locality 5.4), adjacent to the Orange River, where the rocks are only weakly deformed. The Zeekoebaart Formation comprises a fairly monotonous sequence of highly altered, fine grained mafic lava. The lavas commonly exhibit amygdales and pipe-amygdales filled with quartz, chlorite, calcite and pyrite. Flow banding and hyaloclastite flow top breccias define a weak primary layering that is difficult to measure. The Zeekoebaart Formation in the vicinity of locality 5.4 dips at moderate angles to the east.

In thin section the Zeekoebaart Formation lavas are characterised by retrograde metamorphic assemblages typical of greenschist facies metamorphism. The lavas are extensively altered to chlorite, epidote and actinolite but in the weakly deformed lavas in the south-east, partly altered relict pyroxene and plagioclase phenocrysts were observed. The groundmass comprises saussiterised plagioclase laths, quartz, chlorite, epidote, actinolite and ore minerals. In the highly sheared lavas in the north and to the west no original igneous textures or minerals could be recognised in thin section. Highly sheared agglomerate layers were observed in the Zeekoebaart Formation in the Map 2 area and at locality 5.9. The agglomerate comprises quartzite, slate, phyllite and lava clasts in a green, tuffaceous matrix.

The contact zone between the Zeekoebaart Formation and the Draghoender granite is highly sheared, and the relative ages of these two units could not be determined using field relationships. An attempt was made to date the Zeekoebaart Formation using the SHRIMP ion microprobe. Mafic lavas such as the

Zeekoebaart Formation typically contain very few primary igneous zircons so a composite 60kg sample, comprising 5 individual samples from several adjacent flows, was taken at locality 5.4. A substantial number of zircons were separated from this sample but it was clear that they represented a highly heterogeneous population. The following zircon types were recognised: clear, euhedral prismatic grains; clear and faceted round grains; small, variably coloured, euhedral and subhedral zircons with well developed compositional zoning; rounded resorbed, anhedral grains (Armstrong, 1997a).

A total of 9 analyses were carried out on the SHRIMP. The U-Pb-Th data are presented in Table 5.1 and plotted on a U-Pb Wetherill concordia diagram in Figure 5.5. All the data spread along the concordia as a poorly-constrained discordia trend between approximately 1300 and 0 Ma. It would appear from these results that all the zircons have undergone unusually severe radiogenic Pb-loss, both recently and at some intermediate stage/s. As these rocks have only undergone greenschist facies metamorphism it is difficult to explain why such extreme Pb-loss has occurred. Although the zircon population is heterogeneous at least some of the zircons exhibit features of primary magmatic zircons. If the zircons were metamorphic in origin, then one would expect them to define the age of metamorphism rather than show such a spread in ages. The extreme Pb-loss is not easily attributed to radiation damage in the zircon grains as the observed U and/or Th concentrations are generally moderate to low.

It is worth noting, however that U-Pb SHRIMP analysis of zircons from a basic lava in the Marydale Group produced very similar and confusing results (Pers. comm. R.A. Armstrong).

5.2 Structural geology

The basement rocks and the Zeekoebaart Formation in the northern and western parts of the Marydale basement high are highly deformed and poorly exposed. A Kheis age, brittle-ductile thrust sense shear zone (forming part of the Blackridge thrust system) mapped in the Map 2 area can be traced westward into the Zeekoebaart Formation and the Skalkseput granite. The map trace of this thrust sense shear zone is indicated on Map 1. The shear zone is marked by a prominent but discontinuous vein-quartz ridge. The Zeekoebaart Formation lavas are very strongly foliated in both the footwall and hangingwall of the vein-quartz ridge. The quartz vein dips steeply to the north-west, parallel to the foliation in the wall-rock. The Skalkseput granite has been mylonitised in the shear zone, mineral elongation lineations, defined by strained quartz grains in the mylonite plunge steeply to the north-west. S-C fabrics indicate north-west over south-east thrust sense of movement. The thrust sense shear zone can be traced as far as the exposure of Marydale Group greenstones that form Swartkop ridge (Map 1).

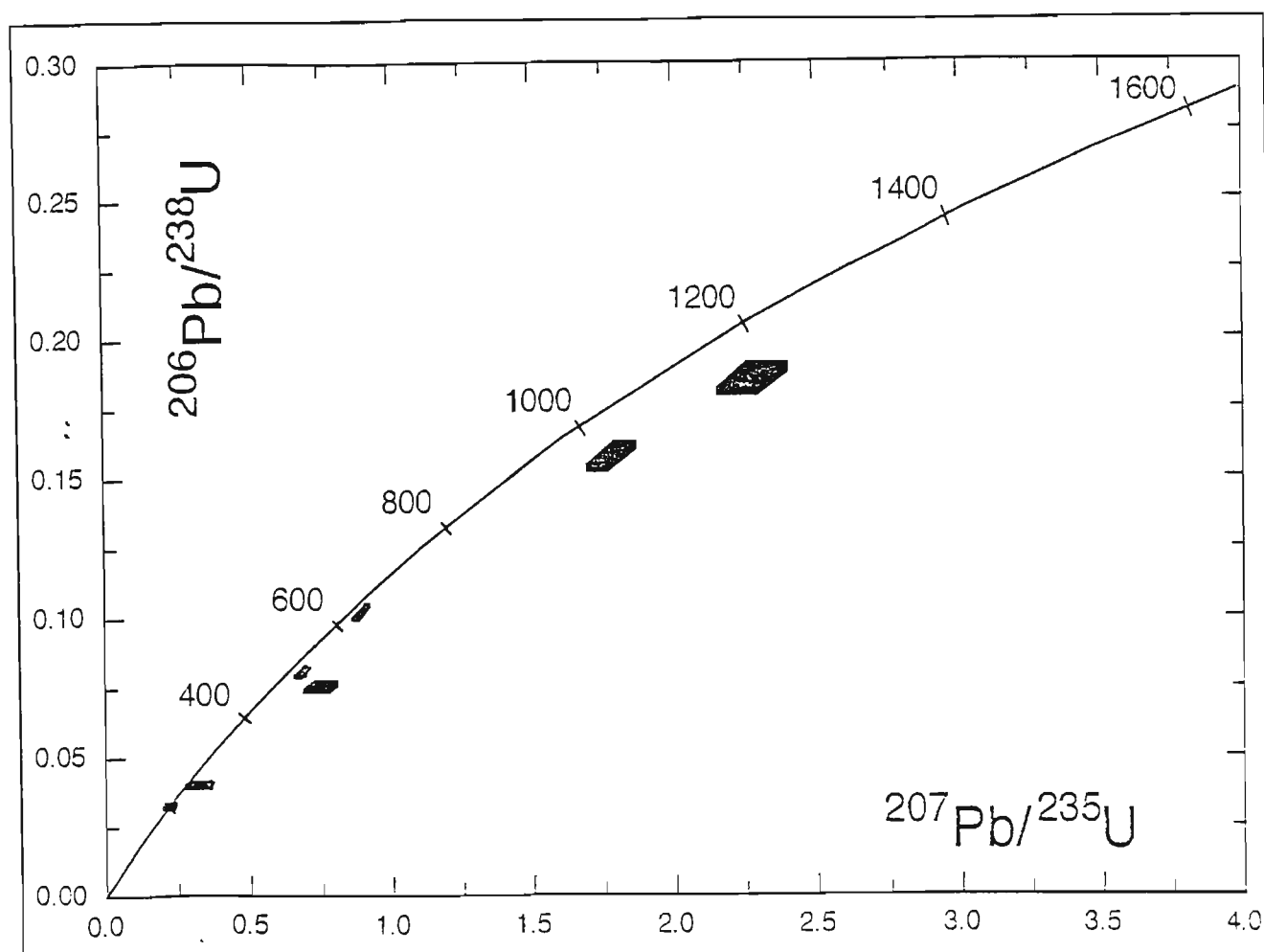


Figure 5.5: U-Pb concordia diagram of SHRIMP analyses of zircons from the Zeekoebaart Formation. (Analyses by R.A. Armstrong).

All outcrops of the Zeekoebaart Formation along the southern margin of the Eselberge (Map 1) have a strong north-west dipping foliation and associated down-dip mineral elongation lineation that formed during the Kheis orogeny.

Foliation data from the Marydale basement high show a bimodal distribution (Map 1). Along the northern margin the foliation dips north-west and is related to the Kheis orogeny. Along the western margin of the Marydale basement high (Map 1), a strong NNW striking foliation is developed in the Draghoender granite. Mineral elongation lineations, defined by rod shaped aggregates of quartz and mica, plunge steeply down the dip of the foliation to the WSW. Leucocratic granite veins define folds, the axes of which plunge to the WSW, parallel to the mineral elongation lineation. S-C fabrics indicate an ENE vergent, thrust sense of movement. This NNW structural trend dominates the western edge of the Marydale basement high in the footwall of the Doornberg shear zone.

Coward and Potgieter (1983) suggested that this change in trend of structural elements was as a result of the Kheis belt “wrapping around” the north-west margin of the Marydale basement high. The ENE vergent thrust sense shear zones developed along the western edge of the Marydale basement high cannot be of the same generation as the south-east vergent, Kheis age thrust sense shear zones. The mineral elongation lineations in both sets of shear zones plunge steeply down the dip of the foliation indicating dip-slip movement. If the two sets of shear zones were both formed during the same compressional event, one would expect movement on the NNW trending shear zones to have a significant oblique-sinistral component. The NNW trending shear zones are thus interpreted to be related to a different event. The NNW trending shear zones are parallel to the structural trend of the Namaqua belt.

The zone of ENE vergent shear zones appears to be restricted to the western edge of the Marydale basement high. At locality 5.9, an agglomerate in the Zeekoebaart Formation has a typical Kheis age foliation, clasts are “stretched-out” in the plane of the foliation defining an elongation lineation. Both the foliation and the elongation lineation are deformed by open, upright folds, the axes of which trend 340° and plunge $4-10^{\circ}$. A steeply east dipping crenulation cleavage is developed in the hinge region of the NNW trending folds. These folds are interpreted to be an equivalent of the Namaqua age, NNW trending folds observed in the Map 2 area.

5.3 Summary

The rocks exposed at Swartkop ridge, east of Marydale, are correlated with the Modderfontein Formation of the Marydale Group. Bedding in the meta-sediments at Swartkop ridge is cross-cut by granitic veins probably related to the intrusion of the Draghoender granite.

The age of the Draghoender granite as determined during this study is 2853 ± 4 Ma (U-Pb single zircon SHRIMP). Published radiometric ages for the Marydale Group range between 2915 (+120, -130) Ma and 3010 (+206, -300) Ma. All available evidence indicates that the Draghoender granite is younger than the Marydale Group.

The relative ages of the Draghoender granite and the Zeekoebaart Formation could not be resolved in the field. Attempts to accurately date the Zeekoebaart Formation were inconclusive. The Zeekoebaart Formation is intruded by the Skalkseput granite. An attempt to date the Skalkseput granite at the type locality (where the intrusive relationship with the Zeekoebaart Formation can be demonstrated) was unsuccessful. A sample of the Skalkseput granite from a different locality has been dated at 2718 ± 8 Ma

(U-Pb single zircon SHRIMP: Pers. comm. R.A. Armstrong). Assuming that the Skalkseput granite comprises only one generation of granitoid intrusives, the Zeekoebaart Formation is older than 2718 ± 8 Ma.

South-east vergent, Kheis age, thrust sense shear zones are developed in the Zeekoebaart Formation and the basement granitoids in the northern parts of the Marydale basement high. Shear zones along the western edge of the Marydale basement high have a NNW trend, parallel to the structural trend of the Namaqua belt, and dip steeply to the west. Kinematic indicators in these shear zones imply an ENE vergent thrust sense of movement. No unequivocal cross-cutting relationships were observed between the south-east vergent and the ENE vergent thrust sense shear zones, yet their geometry cannot be explained in terms of a single deformation event. It is suggested that the ENE vergent shear zones are related to the extended Namaqua orogeny and truncate the structural trend of the Kheis belt.

The ENE vergent shear zones are only developed along the western margin of the Marydale basement high, where the basement rocks and Zeekoebaart Formation are overlain by meta-sediments of the Kaaien Group. In Chapter 6, the structural geology of the Kaaien Group will be examined in an effort to further constrain both shear zone geometry, and timing, in this area.

6. THE STRUCTURAL GEOLOGY OF THE SOUTHERN PART OF THE KAAIEN DOMAIN

The Kaaïen domain (see Figure 1.1) is a linear “belt” of rocks thought to be stratigraphic equivalents of the Olifantshoek Supergroup and the Spioenkop Formation (a unit of uncertain stratigraphic correlation) that were highly deformed during the extended Namaqua orogeny and have a NNW structural trend, parallel to that of the Namaqua belt.

The western margin of the Kaaïen domain is marked by the combined Straussburg-Copperton shear zone (Map 1). The eastern margin of the Kaaïen domain is marked, in part, by the Doornberg shear zone, the Brulpan fault and the Brakbos fault. The eastern boundary of the Kaaïen domain in the “gap” between the Brulpan fault and the Brakbos fault is indicated as a dotted line on Figure 1.2 (a copy is located in the front map pocket), west of this line the Kaaïen Group rocks have a dominant NNW structural trend. This study concentrated on the Uitdraai Formation (Kaaïen Group) and Spioenkop Formation rocks, exposed between the Doornberg shear zone and the Copperton shear zone, that form the Kaaïen hills (Map 1).

The stratigraphic correlation of the dominantly meta-sedimentary Kaaïen Group is uncertain, yet most previous workers have suggested that it represents an Olifantshoek Supergroup correlate; deformed during the Kheis orogeny; that has been structurally and metamorphically overprinted by the extended Namaqua orogeny (Botha *et al.*, 1976; Tankard *et al.*, 1982; Coward and Potgieter, 1983; Stowe, 1986; Humphreys *et al.*, 1988). The predominantly meta-sedimentary Spioenkop Formation is considered by most workers (SACS, 1980; Cornell *et al.*, 1986; Stowe, 1986, Humphreys *et al.*, 1988) to be part of the Marydale Group (i.e. Archaean “greenstone” rocks) even though it is separated from the main outcrop of Marydale Group rocks and comprises very dissimilar lithotypes. Scott (1987) considered the Spioenkop Formation to be part of the Kaaïen Group.

The Kaaïen domain was studied in three areas. The Blaauwputs area (locality 6.4), the Marydale area (locality 6.1) and the Prieska Poort area (localities 6.2 and 6.3). The principle aims of this investigation were:

- (a) To determine whether the Kaaïen Group and the Spioenkop Formation were deformed during the Kheis orogeny.
- (b) To document the structural elements that developed, during the extended Namaqua orogeny, in the southern part of the Kaaïen domain and relate them to tectono-metamorphic events recognised by previous workers in the northern part of the Kaaïen domain and the Namaqua belt.

- (c) To constrain the relative timing of the north-east (Kheis age) and NNW trending shear zones observed in the rocks of the Marydale basement high.
- (d) To confirm the correlation between the Kaaie Group and the Olifantshoek Supergroup.
- (e) What suggestions can be made as regards the age and stratigraphic correlation of the Spioenkop Formation?

6.1 The Marydale area

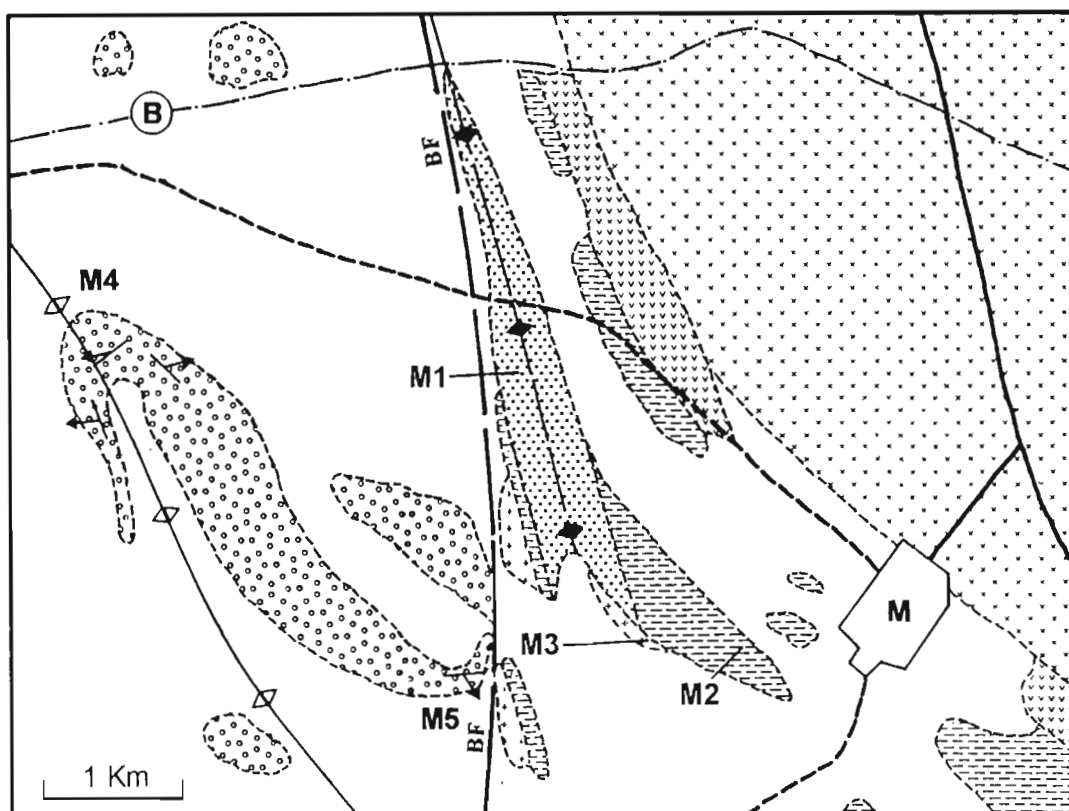
6.1.1 Lithology







The town of Marydale lies near the contact between the Kaaie Domain and the Marydale basement high (Map 1, Figure 6.1). As outlined in Chapter 5, the Draghoender granite is strongly foliated in the contact zone. Within the area indicated on Figure 6.1, exposure of the Draghoender granite is extremely poor. Rocks of the Spioenkop Formation are exposed immediately to the west of the contact.




Immediately west of the Draghoender granite is an amphibolite unit that has a strongly developed, west dipping foliation. Smit (1977) correlated this amphibolite unit with the Hartley Formation of the Olifantshoek Supergroup, but no direct evidence for a volcanic protolith or sedimentary intercalations (that characterise the Hartley Formation in the Boegoeberg dam area), were observed during this study.


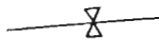

To the west of the amphibolite, the Spioenkop Formation can be subdivided into two units (here termed units MQ and Q) on the basis of lithology. Unit MQ comprises micaceous brown quartzite and quartz-mica schist with brown quartzite intercalations. Unit Q comprises siliceous white quartzite with narrow micaceous quartzite intercalations. Sedimentary structures, with the exception of planar bedded heavy mineral layers, are not preserved in either of the two units. No conglomerate or pebbly horizons were observed. Units Q and MQ contain amphibolite horizons, up to 40m in thickness, that are sub-parallel to the lithological layering. Xenoliths of quartzite, observed in the amphibolite at locality M1 (Figure 6.1), suggest that the amphibolite layers are metamorphosed mafic intrusions. The amphibolite layers in the Marydale area consist of hornblende with subordinate quartz, plagioclase, alkali feldspar and ore minerals.

Immediately to the east of the Brulpan fault, a grey biotite-hornblende tonalite is exposed. This tonalite was considered by Vajner (1974) to be part of the Draghoender granite. It is entirely different in both appearance and composition to the Draghoender granite and is interpreted here to be a younger intrusion.



-  TONALITE
 -  UITDRAAI FORMATION
 -  UNIT MQ
 -  UNIT Q
 -  AMPHIBOLITE
 -  DRAGHOENDER GRANITE-GNEISS
- SPIOENKOP FORMATION

-  RAILWAY
-  GRAVEL ROAD
-  TAR ROAD
- B= BRULPAN SIDING
- M=MARYDALE

-  BRULPAN FAULT
-  F₃ FOLD AXIS
-  F₂ FOLD AXIS

S₂ FABRIC ELEMENTS:



-  LINE: STRIKE OF FOLIATION
-  ARROW: PLUNGE OF L₂ LINEATION

Figure 6.1: Geological map of the Marydale area.

Pegmatite veins from the tonalite intrude the Spioenkop Formation implying that the tonalite post-dates the Spioenkop Formation (Figure 6.2).

The Brulpan fault is not exposed in the Marydale area, but the lineament defining its trace can be observed on aerial photographs. Quartzites of the Uitdraai Formation are exposed to the west of the Brulpan fault. The Uitdraai Formation in this area comprises brown to grey coloured quartzite. No sedimentary structures, with the exception of planar bedded heavy mineral layers, are preserved.

6.1.2 Structural geology

Structural elements related to three phases of deformation have been recognised in the Marydale area. The earliest phase of deformation (D_1) resulted in the production of F_1 isoclinal folds with sharp hinges. An S_1 foliation, defined by the preferred orientation of muscovite, is developed axial planar to the F_1 folds in the micaceous quartzites and the quartz-mica schists but not the siliceous quartzite horizons. As a result of the strong overprint during the D_2 deformation, F_1 isoclinal folds are rarely observed in the Marydale area and only at outcrop scale. Due to the isoclinal nature of the F_1 folds, the S_1 foliation is generally sub-parallel to bedding, except at rare F_1 closures.

F_1 folds are refolded by folds associated with a D_2 deformation (Figure 6.3). The D_2 deformation in the Marydale area was heterogeneous and a distinction can be made between high- and low-strain zones in which the orientations of F_2 fold axes differ.

6.1.2.1 Low strain zones

The outcrop of unit Q, forming a prominent NNW trending ridge, can be classified as a D_2 low strain zone. The bedding sub-parallel S_1 foliation is not developed in the siliceous quartzites, but is developed in the micaceous quartzite intercalations. Bedding and the S_1 foliation have been folded by a large scale NNW-SSE trending F_2 anticline (Figure 6.1). The F_2 anticline is tight and overturned to the east. Figure 6.4 shows the orientation of bedding planes and the S_1 foliation measured along the ridge formed by unit Q. Great circles representing the foliation and bedding attitudes intersect in the north-west and south-east quadrants. These intersections (β -axes) plunge to the NNW and the SSE at angles between 5 and 40° and give an indication of the periclinal nature of the F_2 anticline. In the field it was observed that the fold axis of the F_2 anticline is undulatory, plunging NNW in some areas and SSE in others.

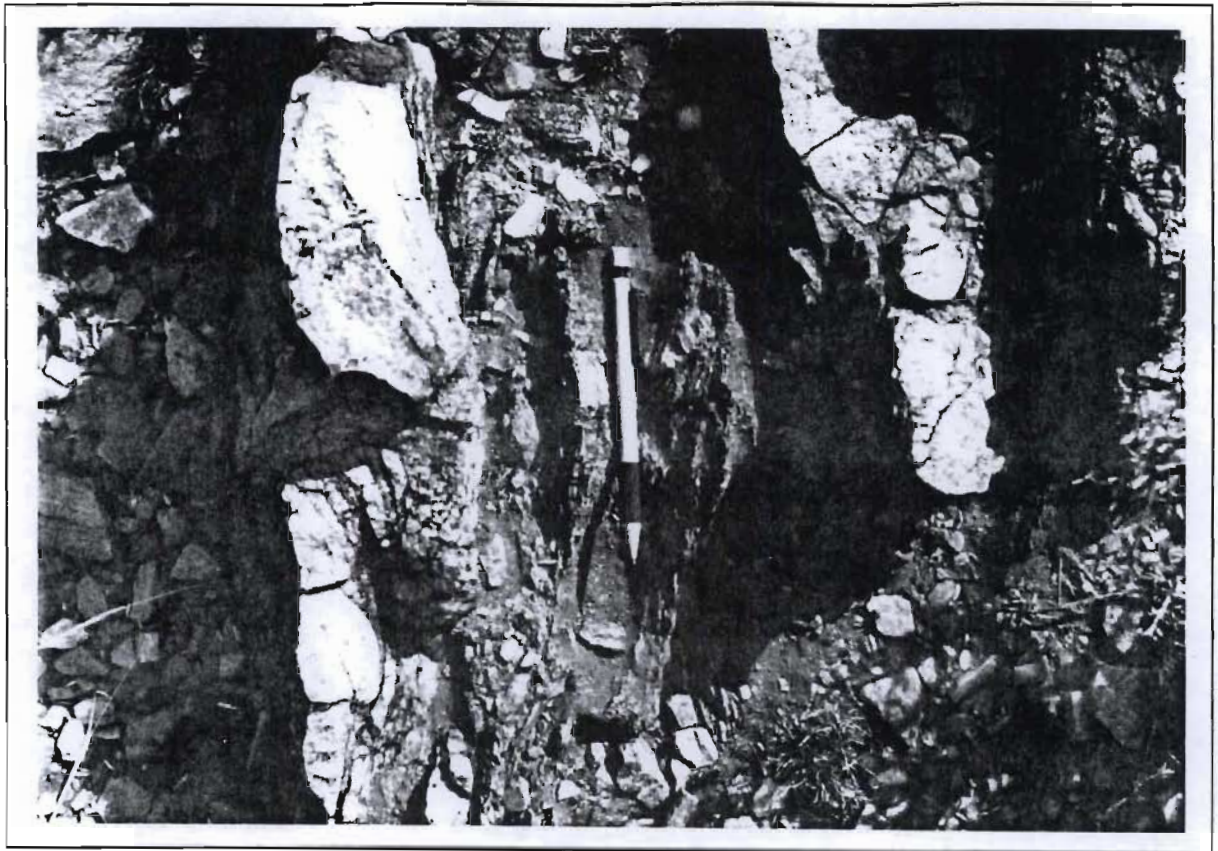


Figure 6.2: A weakly foliated pegmatite vein cutting across strongly foliated quartzite and micaceous quartzite of the Spioenkop Formation. The vein passes under the pencil. (Locality M3- Figure 6.1).



Figure 6.3: Small scale F_1 folds with angular hinge zones that are refolded by a steeply plunging F_2 fold. Locality M2- Figure 6.1.

Centimetre scale, cusplate-lobate folds producing fold mullion structures (Wilson, 1953) are developed at the contacts between siliceous quartzite horizons and the narrow micaceous quartzite intercalations. The lineation defined by the axes of these folds (L_2 mullion lineation) plunges at varying angles to the NNW and SSE (Figure 6.5), parallel to the periclinal F_2 fold axis. A weakly developed L_2 mineral elongation lineation, defined by strained quartz grains, plunges down the dip of the bedding planes to the WSW, perpendicular to the fold mullions and the F_2 fold axis (Figure 6.5).

In thin section (Figure 6.6), it can be observed that the siliceous quartzite from this low strain zone is extensively recrystallised and comprises quartz containing stubby muscovite laths. The muscovite laths in this zone show no strong preferred orientation.

6.1.2.2 High strain zones

In the Marydale area, the majority of the strain during the D_2 deformation has been accommodated in the more incompetent micaceous quartzites and quartz-mica schists of unit MQ. All outcrops of unit MQ studied in the Marydale area can be classified as high-strain zones. As in the low-strain zones, bedding and the S_1 foliation have been folded by F_2 folds. Numerous, small-scale F_2 folds with cm-m scale wavelengths are developed in the high strain zones. A strong WSW dipping S_2 foliation is developed in discrete zones at locality M2. The foliation in the quartz-mica schists is defined by layers of muscovite with a preferred orientation. In the highly sheared micaceous quartzite horizons, the S_2 foliation is defined by layers of muscovite and tabular quartz grains (Figure 6.7). The tabular quartz grains consist of partially or completely annealed aggregates of very small quartz grains. This rock is interpreted to be an annealed mylonite. The S_2 foliation at locality M2 strikes NNW and dips steeply to the WSW (Figure 6.8). Mineral elongation lineations in these shear zones (defined by rod shaped aggregates of quartz and mica) plunge down the dip of the foliation to the WSW (Figure 6.8), parallel to the L_2 elongation lineations in unit Q (i.e. parallel to those in low-strain zones). S-C fabrics within the D_2 shear zones at locality M2 indicate an eastward vergent, thrust sense of movement.

Figure 6.9 shows the attitude of bedding and the bedding sub-parallel S_1 foliation measured in unit MQ at locality M2. The single cluster of β -axes approximates the mean attitude of the F_2 fold axes in this high-strain zone. In contrast to the F_2 fold axes in unit Q that plunge at between 5 and 40° to the NNW and SSE, the F_2 fold axes in unit MQ plunge at steep angles to the WSW. The mean orientation of the F_2 fold axes, as indicated on Figure 6.9, is parallel to the small scale F_2 fold axes and the L_2 mullion lineations

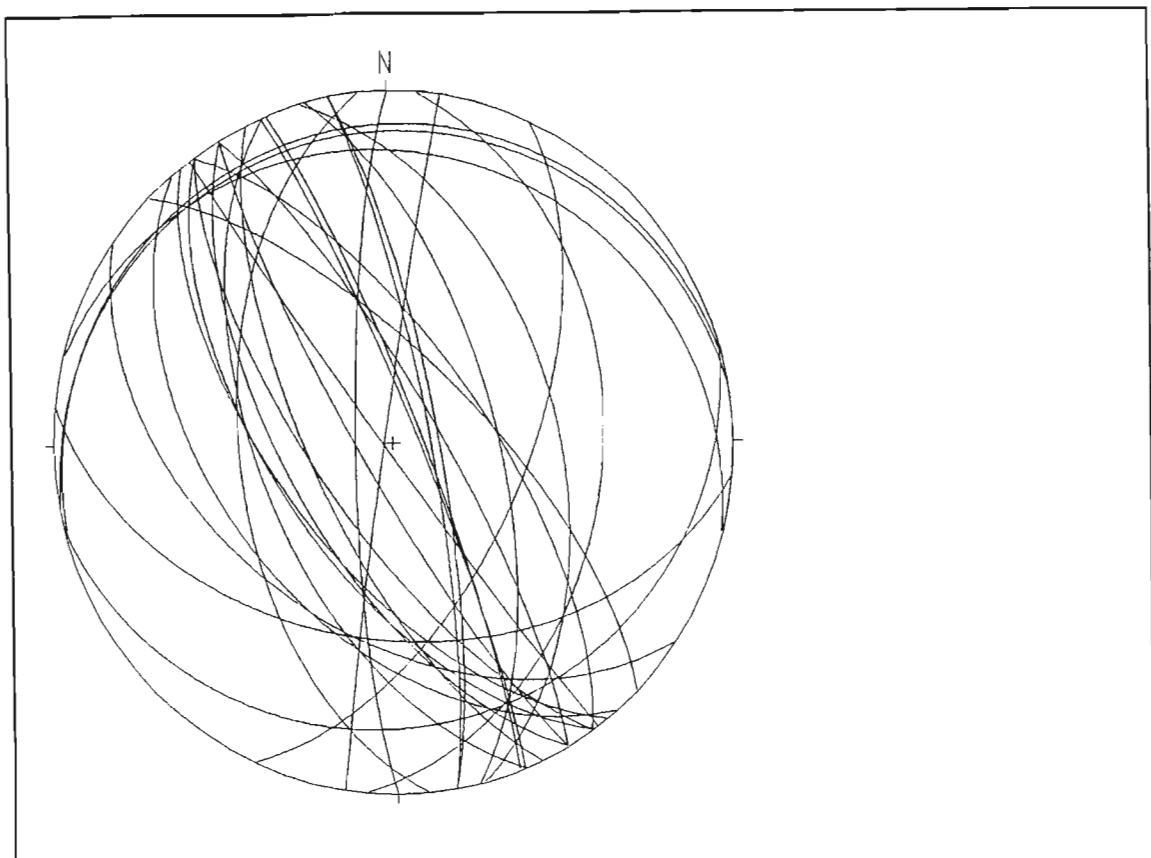


Figure 6.4: Equal area stereographic projection (β -diagram) of the orientations of bedding and S_1 foliation ($n=29$) measured in the D_2 low strain zone formed by unit Q.

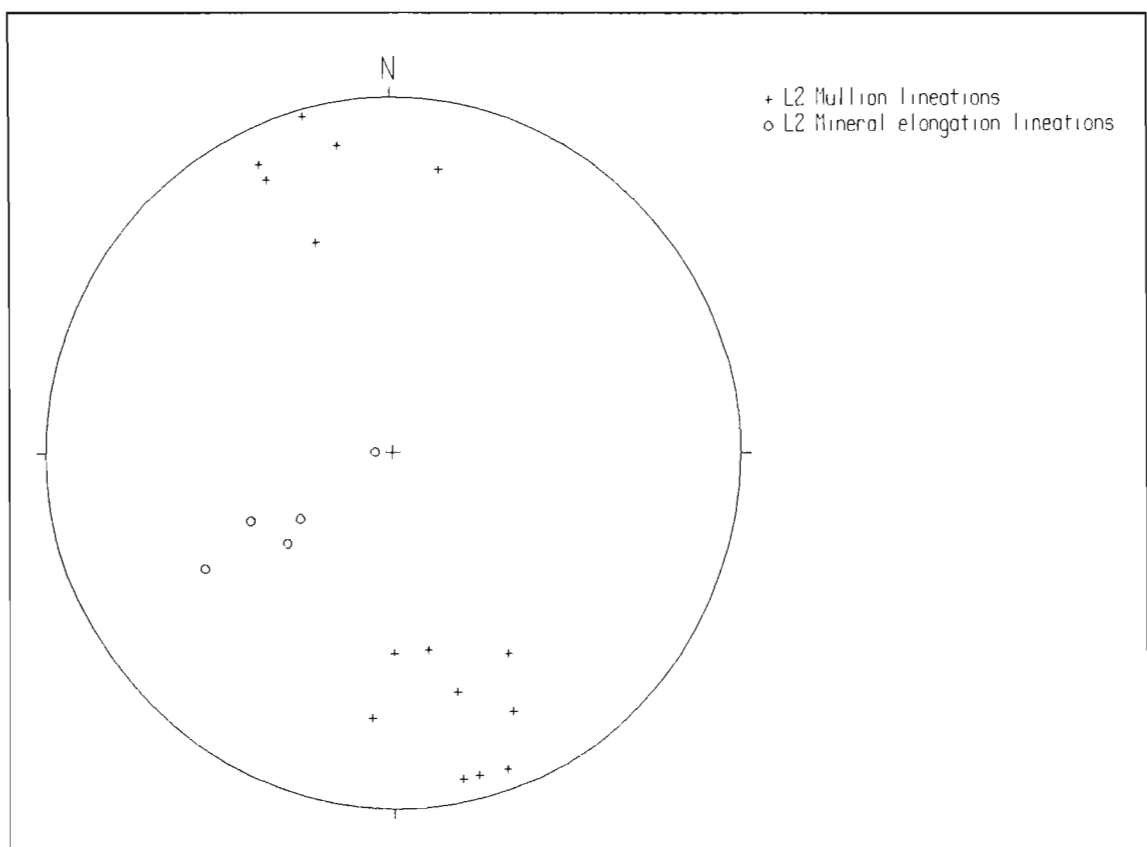


Figure 6.5: Equal area, stereographic projection of L_2 lineations (mullions: $n=15$; elongation: $n=5$) from the low strain zone formed by unit Q.

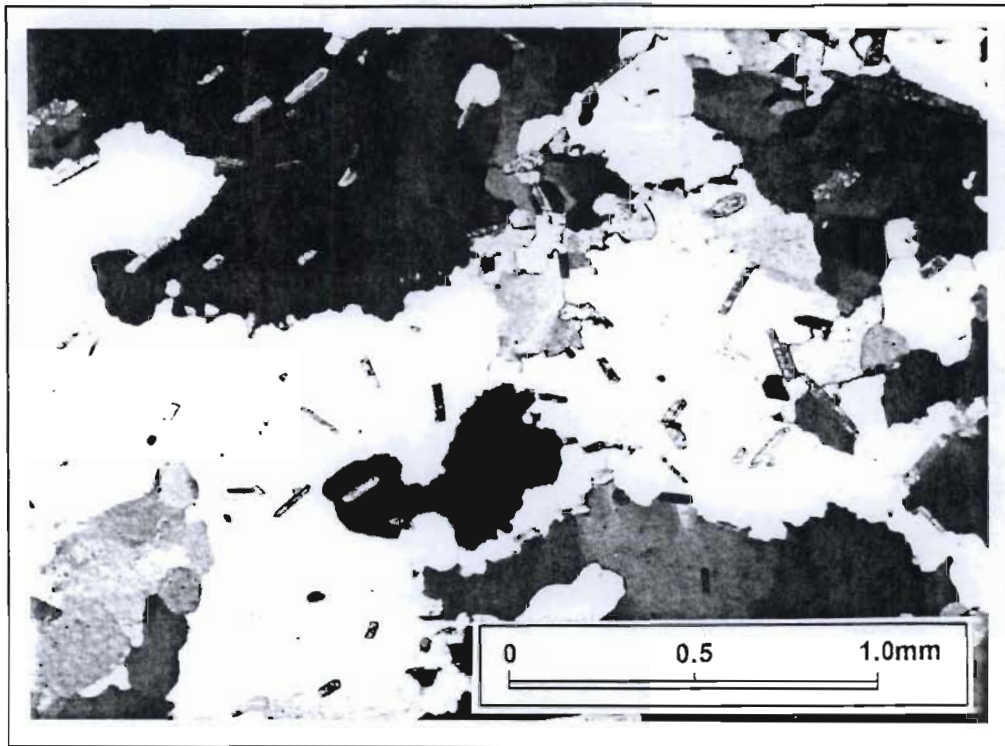


Figure 6.6: Photomicrograph of a sample of siliceous quartzite from unit Q (low strain zone). Note the lack of foliation. Cross-polarised, transmitted light.

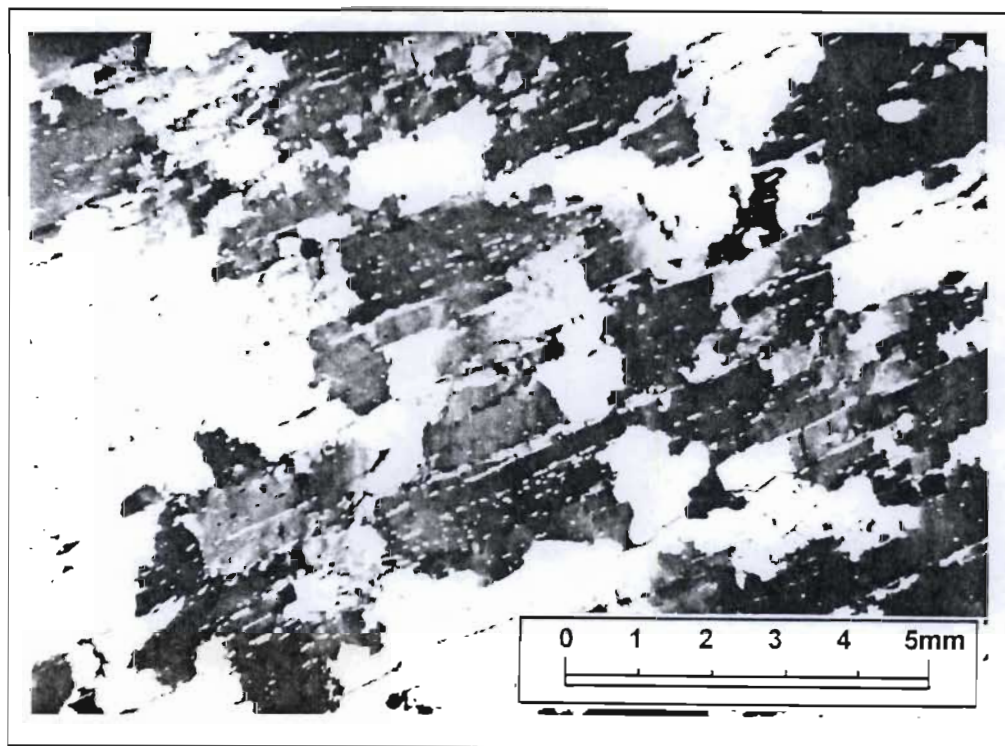


Figure 6.7: Photomicrograph of an annealed mylonite developed in a micaceous quartzite horizon at locality M2 (Unit MQ- high strain zone). Cross-polarised, transmitted light.

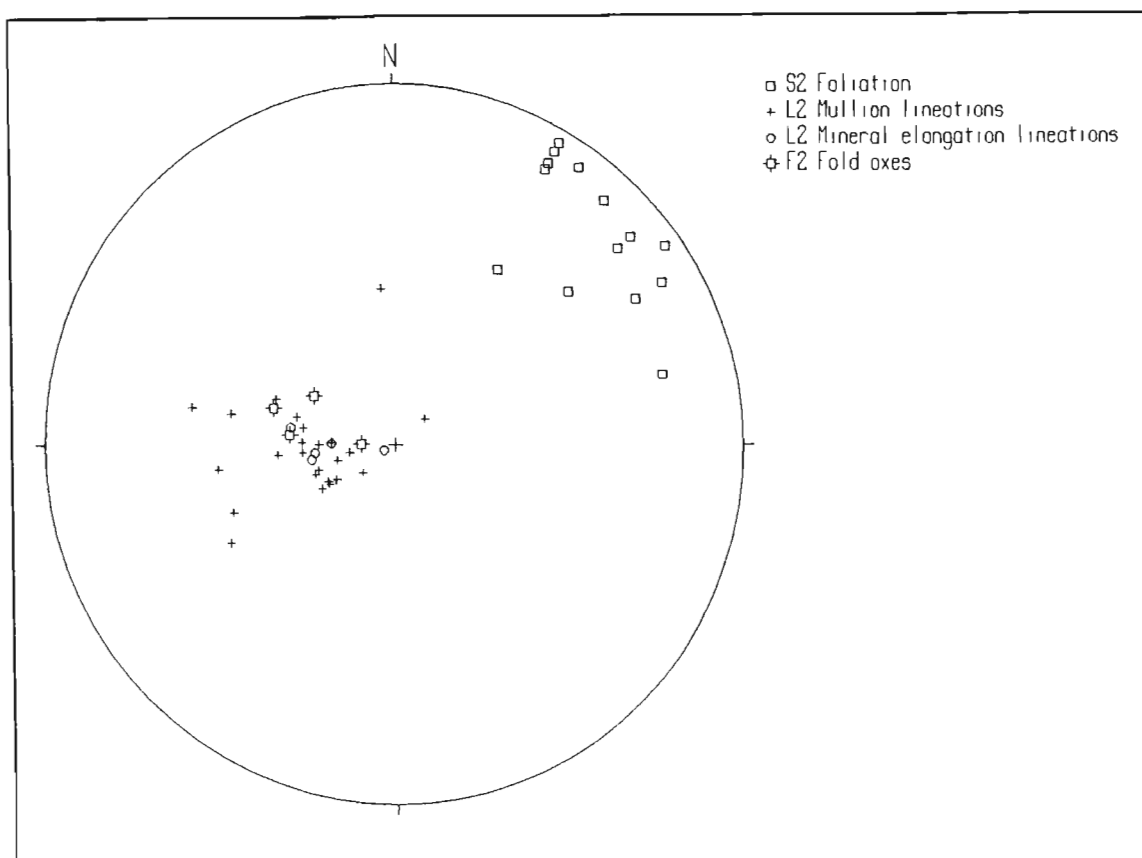


Figure 6.8: Equal area, stereographic projection of L_2 lineations (mullions: $n=23$; elongation: $n=5$), F_2 fold axes ($n=4$) and S_2 shear zone foliation ($n=14$) measured at locality M2.

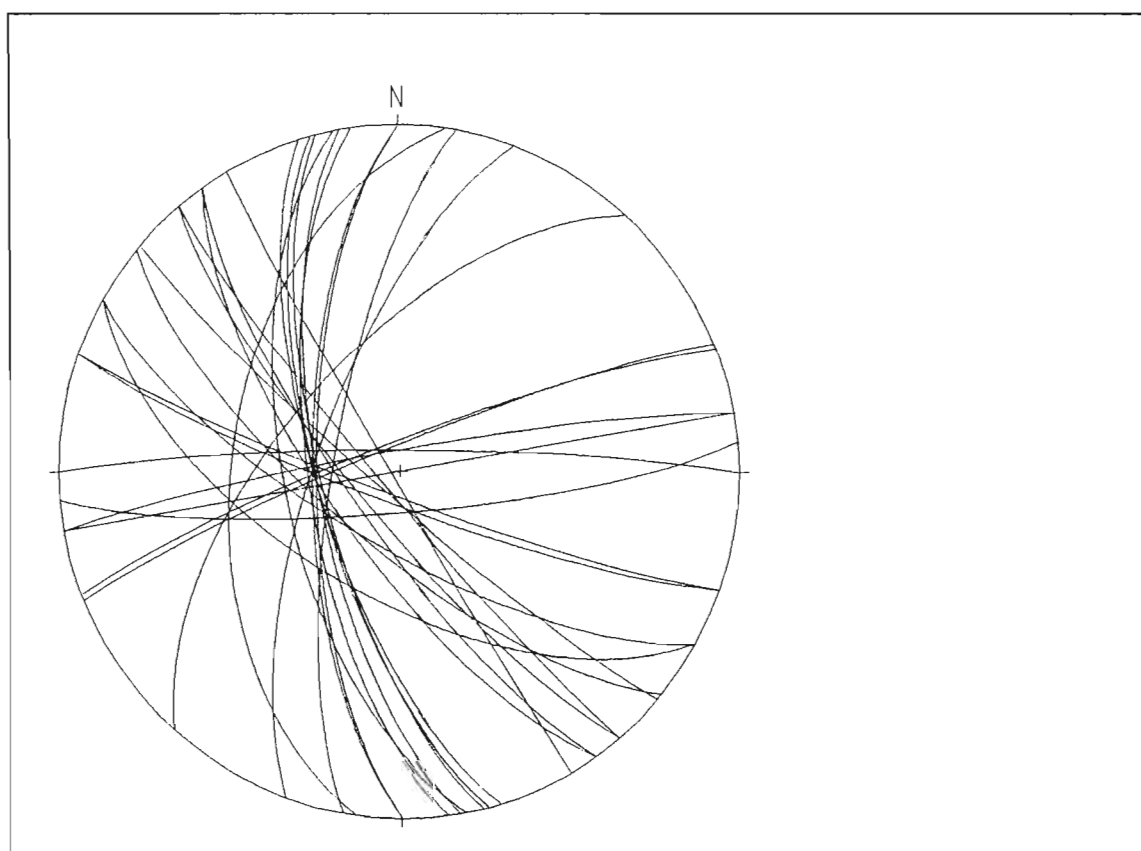


Figure 6.9: Equal area, stereographic projection of bedding and the bedding sub-parallel S_1 foliation ($n=30$) measured at locality M2.

measured at locality M2 (Figure 6.8). All of these linear features plunge to the WSW parallel to the L_2 mineral elongation lineations.

The D_2 structural elements observed in unit MQ in the Marydale area could conceivably be related to two deformation events (i.e. the folds were generated during an early event and were rotated as a result of movement on shear zones that developed during a later, separate, event). The parallelism of the mineral elongation lineations in both high- and low-strain zones suggest instead that the folds and the shear zones developed during one single progressive deformation. The shear zones were preferentially developed in the more incompetent micaceous quartzite and quartz-mica schist horizons. Initially, the fold axes in these high-strain zones would have been perpendicular to the movement direction. With subsequent deformation, the F_2 fold axes were rotated into parallelism with the mineral elongation lineations (movement direction).

At locality M3 (Figure 6.1), weakly foliated pegmatite veins from the tonalite cross-cut the S_2 foliation developed in a high-strain zone in unit MQ (Figure 6.2). Near the contact with unit MQ, the tonalite itself is strongly foliated. The foliation is defined by the preferred orientation of hornblende crystals and biotite. Narrow zones (20-30cm) of strongly foliated tonalite are separated by several metres of weakly foliated tonalite indicating that the deformation was heterogeneous in nature. The foliation in the tonalite strikes NNW and dips to the WSW, parallel to the S_2 foliation in the adjacent Spioenkop Formation rocks. A mineral lineation, defined by aligned hornblende crystals plunges to the WSW. S-C fabrics indicate an ENE vergent, thrust sense of movement. Thus, although pegmatite veins from the tonalite cross-cut the S_2 foliation in the Spioenkop Formation, the tonalite is interpreted to be a syn- D_2 intrusive (probably late-stage). Moving westward from the contact, the foliation decreases in intensity and is only developed in discrete zones bounded by weakly foliated rock. The contact between the tonalite and the Spioenkop Formation formed a zone of anisotropy along which strain was concentrated during the D_2 deformation.

In the area west of the Brulpan fault, an Uitdraai Formation quartzite horizon forms a prominent, arcuate topographic feature (Figure 6.1). At locality M4, the Uitdraai Formation quartzite and micaceous quartzite has a strong S_2 mylonitic foliation. Small scale F_2 folds with L_2 mullion lineations are developed in discrete zones. The mullion lineations are parallel to a strong mineral elongation lineation, indicating that this is a D_2 high-strain zone. Both the L_2 lineations and the S_2 foliation have been folded by an NW plunging, open, upright F_3 anticline. A weak, subvertical, axial planar cleavage is developed in the axial region of the F_3 fold. This S_3 cleavage crenulates the S_2 foliation. At locality M5, the geometry of D_2 fabric elements is characteristic of a high-strain zone. As indicated on Figure 6.1, the L_2 lineations plunge

to the south down the dip of the southward dipping S_2 foliation. The anomalous attitude of the D_2 fabric elements at this locality (in particular the southward plunge of the L_2 lineation) cannot be reconciled with the F_3 folding and is probably due to rotation caused by movement on the Brulpan fault.

6.2 The Prieska Poort area

The Uitdraai Formation was studied in two road-cuttings on the road between Prieska and Copperton (localities 6.2 and 6.3- Map 1). The observations made in each of these road-cuttings are documented below.

6.2.1 Locality 6.2

The Uitdraai Formation at locality 6.2 consists of light-purple coloured, siliceous quartzite with narrow (<5cm thick) brown quartz-mica schist layers. Bedding and a weakly developed, bedding sub-parallel S_1 foliation have been folded to produce F_2 folds with prominent L_2 mullion lineations. Figure 6.10 shows the orientations of S_1 and bedding planes measured at locality 6.2. The cluster of intersections (β -axes) defines the mean F_2 fold axis, that plunges at approximately 25° to the SSE. This is parallel to the measured L_2 mullion lineations at this locality (Figure 6.11).

This locality is a D_2 low-strain zone as it has gently SSE plunging F_2 folds. No S_2 foliation or L_2 mineral elongation lineations were observed. In thin section, the Uitdraai Formation quartzites have a very similar appearance to the Spioenkop Formation siliceous quartzites (unit Q) situated in the D_2 low-strain zone in the Marydale area (see Figure 6.6). The quartz grains are extensively recrystallised and contain stubby muscovite laths with no preferred orientation.

6.2.2 Locality 6.3

The road-cutting at this locality is approximately 200m in length and was mapped in section using a photo-mosaic. The cutting consists of intercalated grey siliceous quartzite, brown micaceous quartzite, biotite-muscovite-quartz-garnet \pm sillimanite schist and amphibolite of the Uitdraai Formation. Planar bedded heavy mineral bands can be recognised in the brown micaceous quartzite.

Locality 6.3 is situated in a D_2 high-strain zone. An S_1 foliation (sub-parallel to bedding) can be recognised that has been folded by F_2 folds. The orientations of bedding and S_1 foliation planes are shown

in Figure 6.12. Note that the mean F_2 fold axis defined by the cluster of β -axes plunges steeply to the WSW. The orientations of L_2 mullion lineations show some spread (Figure 6.13) and trend between WSW and north-west, in part sub-parallel to the cluster of β -axes shown on Figure 6.12.

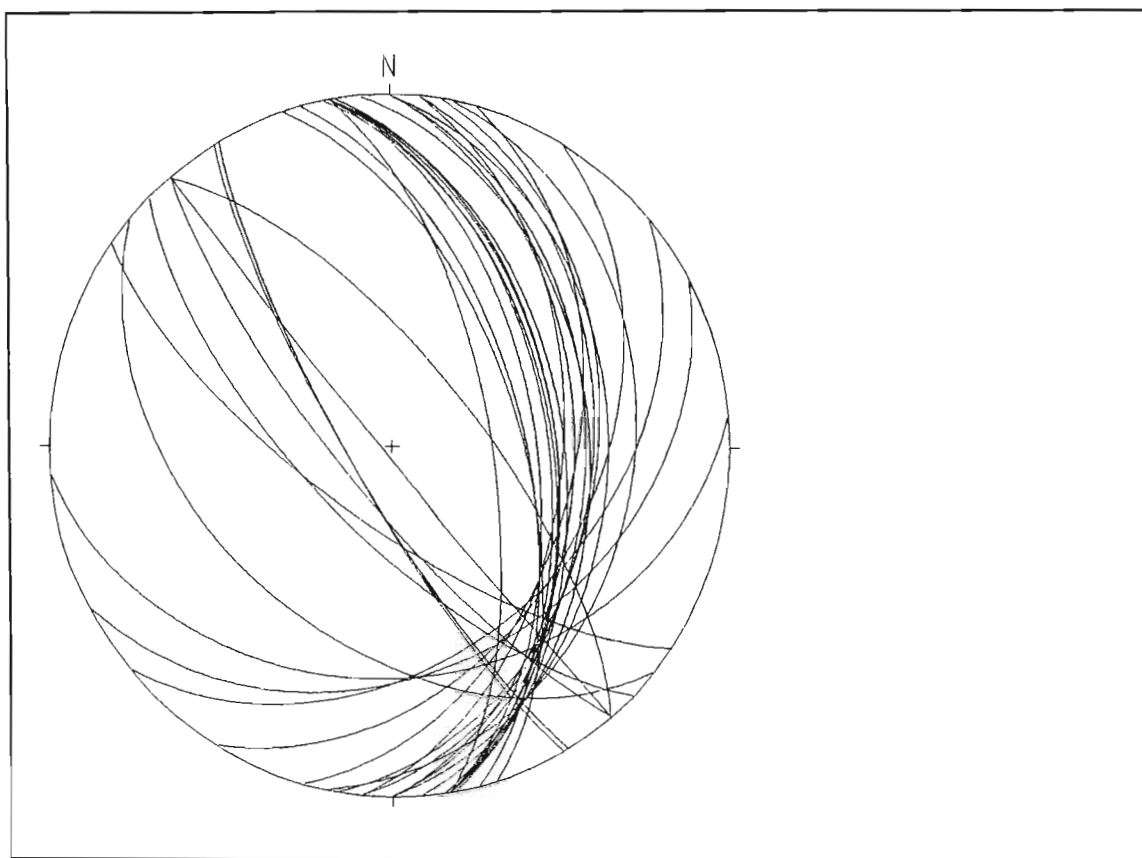


Figure 6.10: Equal area, stereographic projection of bedding and S_1 foliation planes ($n=29$) measured at locality 6.2.

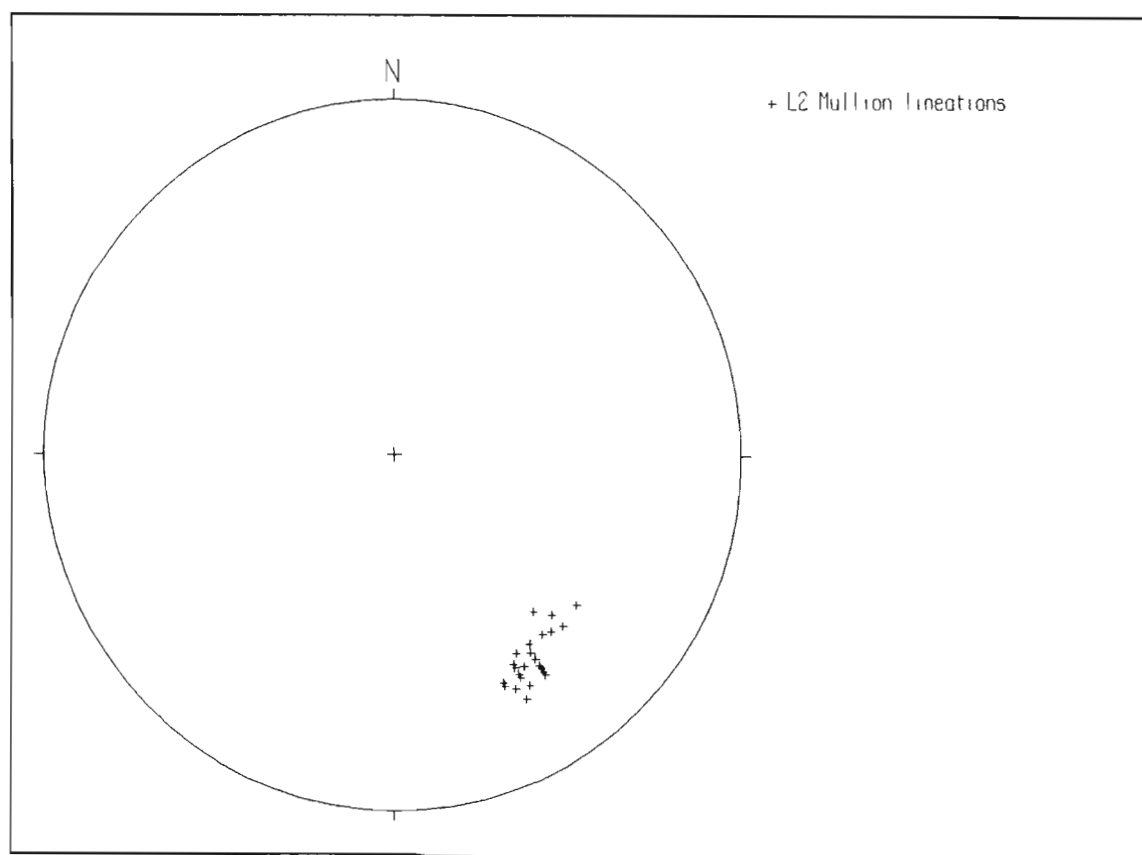


Figure 6.11: Equal area, stereographic projection of L_2 mullion lineations ($n=24$) measured at locality 6.2.

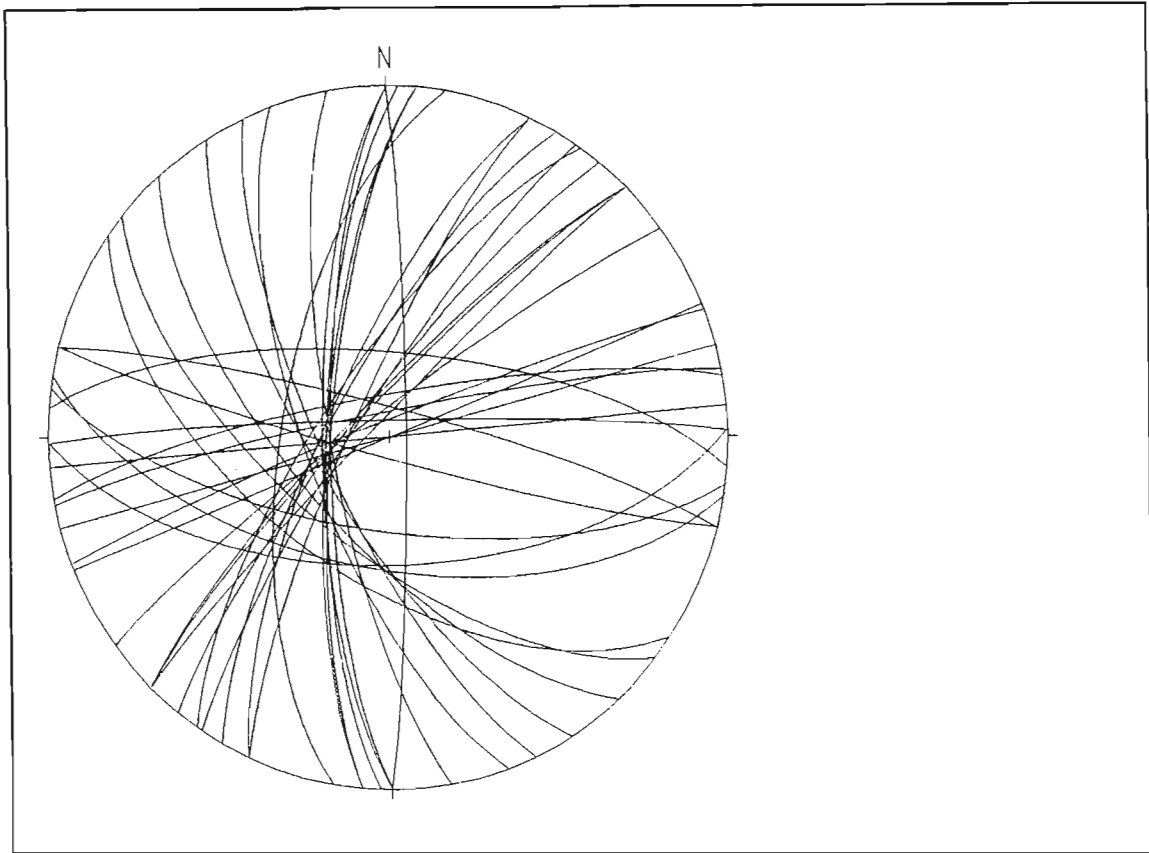


Figure 6.12: Equal area, stereographic projection of bedding and S_1 foliation planes ($n=37$) measured at locality 6.3.

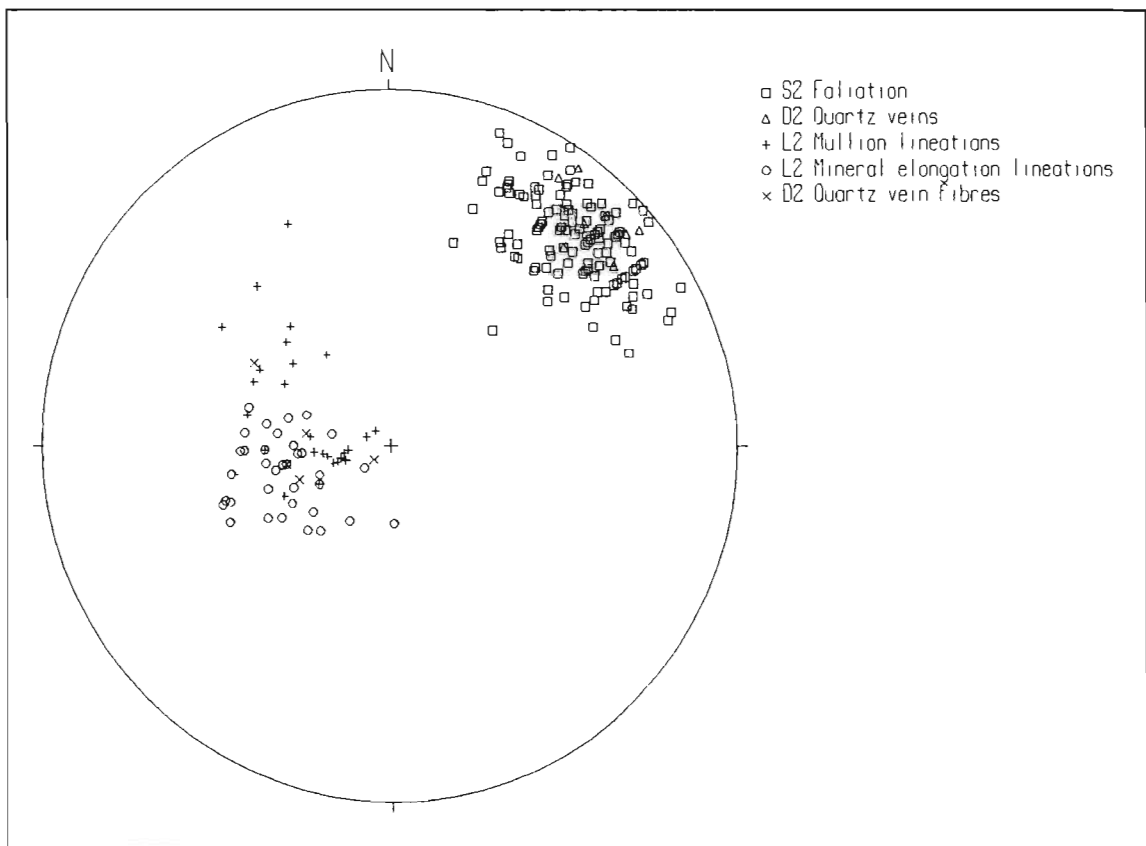


Figure 6.13: Equal area, stereographic projection of D_2 fabric elements and quartz veins measured at locality 6.3.
(S_2 Foliation $n=118$; D_2 quartz veins $n=7$; L_2 mullions $n=25$; L_2 elongation $n=34$; D_2 quartz fibres $n=5$)

A strong, steeply south-west dipping S_2 foliation (Figure 6.13) is developed in all lithotypes exposed in the road-cutting, with the exception of the siliceous grey quartzite. The S_2 foliation in the schistose rocks is defined by layers of biotite and muscovite studded with small subhedral garnets (Figure 6.14). The S_2 foliation in the micaceous quartzites is defined by tabular annealed quartz grains bounded by narrow layers of muscovite (very similar to Figure 6.7) and represents an annealed mylonite. The amphibolite is strongly foliated and comprises hornblende laths with a strong preferred orientation that anastomose around narrow “pods” of quartz and feldspar.

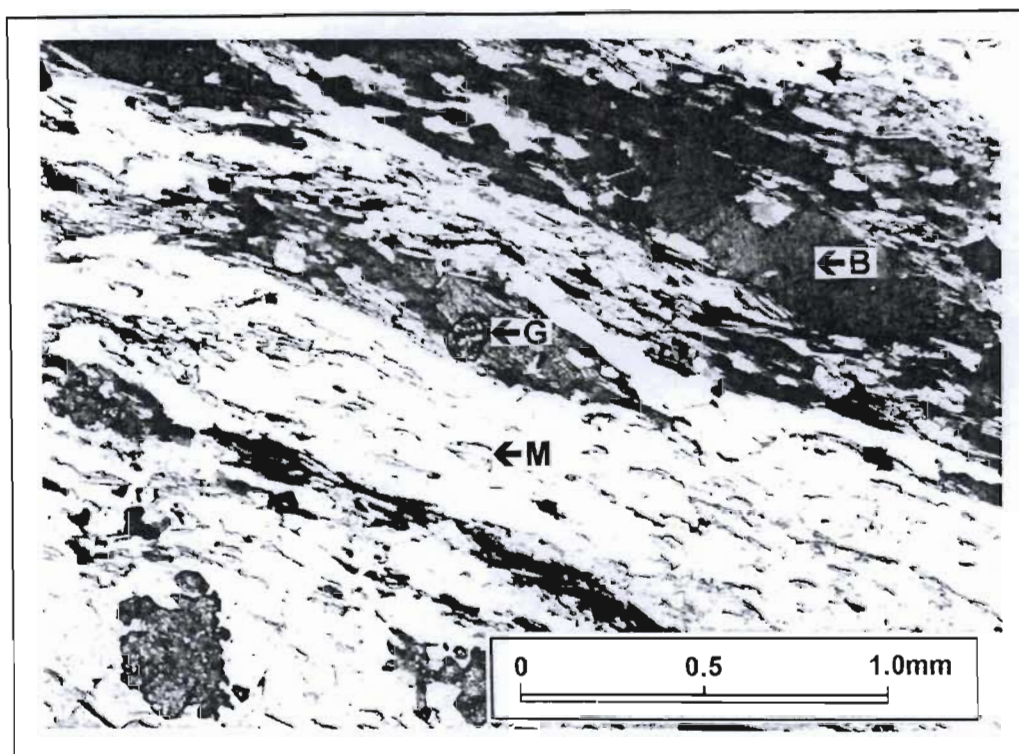


Figure 6.14: Photomicrograph of a sample of Uitdraai Formation schist from locality 6.3. B=biotite, G=garnet, M=muscovite. Transmitted, plane-polarised light.

Elongate quartz-mica aggregates define a L_2 mineral elongation lineation that plunges steeply to the WSW (Figure 6.13). Sillimanite porphyroblasts, up to 1cm in length are developed in discrete horizons within the schistose units. The long axes of these porphyroblasts are orientated parallel to the L_2 mineral elongation lineations and they are interpreted to have grown parallel to the movement direction during the D_2 deformation. S-C fabrics in association with the mineral elongation lineations imply an ENE vergent, thrust sense of movement.

The L_2 mullion lineations, and the F_2 fold axes have been partially, or completely, rotated into parallelism with the mineral elongation lineations during the D_2 deformation, thus accounting for the variation in attitude of the L_2 mullion lineations in Figure 6.13. In very high strain zones in the road-cutting (typically in the schistose horizons), sheath folds were observed (Figure 6.15). Fibrous quartz veins parallel to the

S₂ foliation are developed in the micaceous quartzite. The shear fibres in these quartz veins plunge to the WSW, parallel to the L₂ mineral elongation lineations (Figure 6.13). The quartz veining is thus syn-D₂ in age.

An anomalous anticline-syncline pair is developed in the grey siliceous quartzite horizon (Figure 6.16). These folds are upright, close structures with fold axes that plunge at shallow angles to the north-west, perpendicular to the L₂ mineral elongation lineations. The siliceous quartzite horizon is bounded by highly sheared micaceous quartzite in which mullion lineations plunge steeply to the WSW, parallel to the mineral elongation lineations. A thin section of the grey siliceous quartzite revealed that it consists of recrystallised quartz with a strong undulose extinction, but lacking a preferred orientation. The quartz grains contain small, stubby muscovite laths that show a weak preferred orientation. These observations indicate that although bounded by highly sheared rocks, in which attitude of fabric elements are characteristic of a D₂ high-strain zone, the competent siliceous grey quartzite represents a D₂ low-strain zone. The gently plunging folds in the grey siliceous quartzite are thus interpreted to be F₂ folds formed in a D₂ low-strain zone. The preferential partitioning of strain into more incompetent horizons demonstrates the heterogeneous nature of the deformation during the D₂ event.

Two NNW striking, subvertical faults were identified at this road-cutting. The faults are marked by narrow crush zones. Slickenlines on these both of these fault zones plunge at gentle angles to the NNW implying strike slip movement. Neither the movement sense nor the displacement on these faults could be determined.

6.3 The Blaauwputs area

Figure 6.17 is a geological map of the Blaauwputs area (locality 6.4) based on work during this study. The Brulpan fault, follows a NNW to northerly trend in this area and separates rocks of the Kaaie Group in the west from rocks of the Olifantshoek Supergroup and the Draghoender granite in the east.

A unit of interbedded volcanic and sedimentary rocks, exposed to the north of the Draghoender granite (Figure 6.17), was interpreted to be part of the Zeekoebaart Formation by Vajner (1974) and is indicated as such on the 1:250 000 geological survey map of the area (SAGS, 1995). Smit (1977) noted similarities between this unit and the Hartley Formation in the Boegoeberg dam area and interpreted it to be part of the Hartley Formation, an observation that was confirmed during this study. The Hartley Formation in this area consists of dark green, dominantly amygdaloidal mafic lava with bright green hyaloclastite



Figure 6.15: Plan view of a small scale sheath fold in the Uitdraai Formation. Locality 6.3.

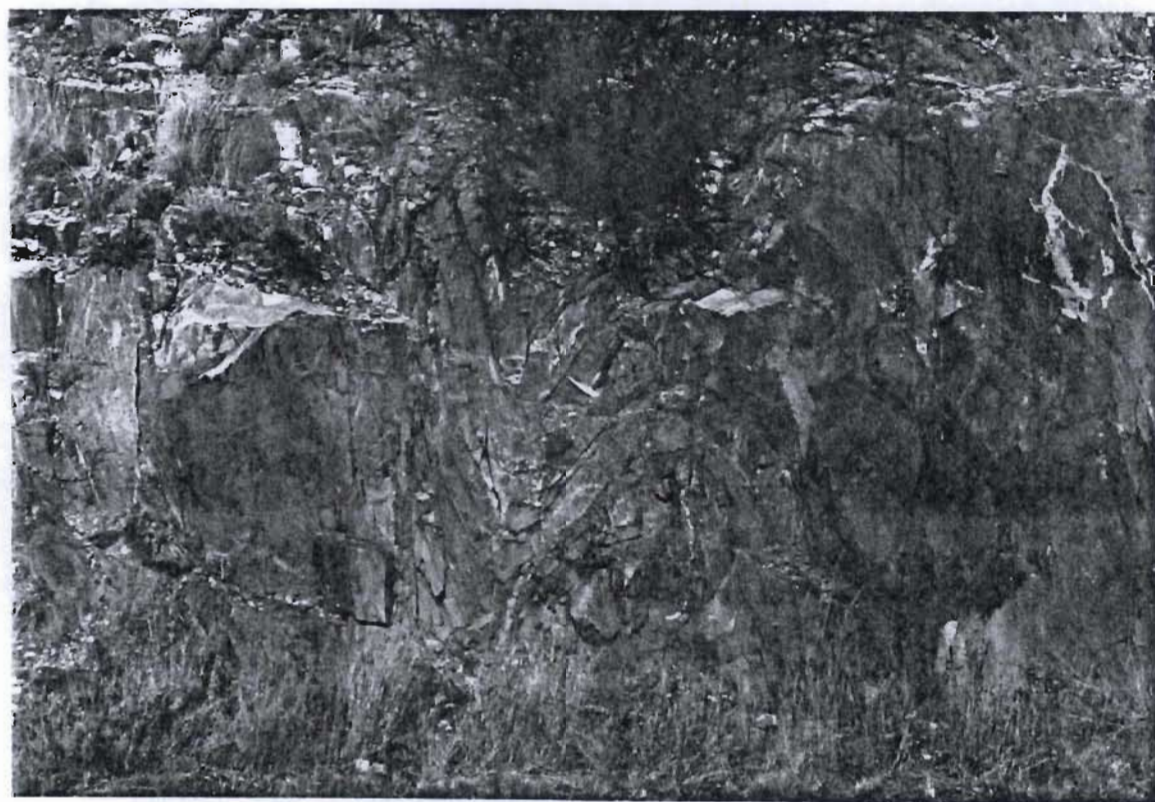


Figure 6.16: F_2 anticline-syncline pair in siliceous grey quartzite of the Uitdraai Formation. The plane of section is orientated approximately east-west. Locality 6.3.

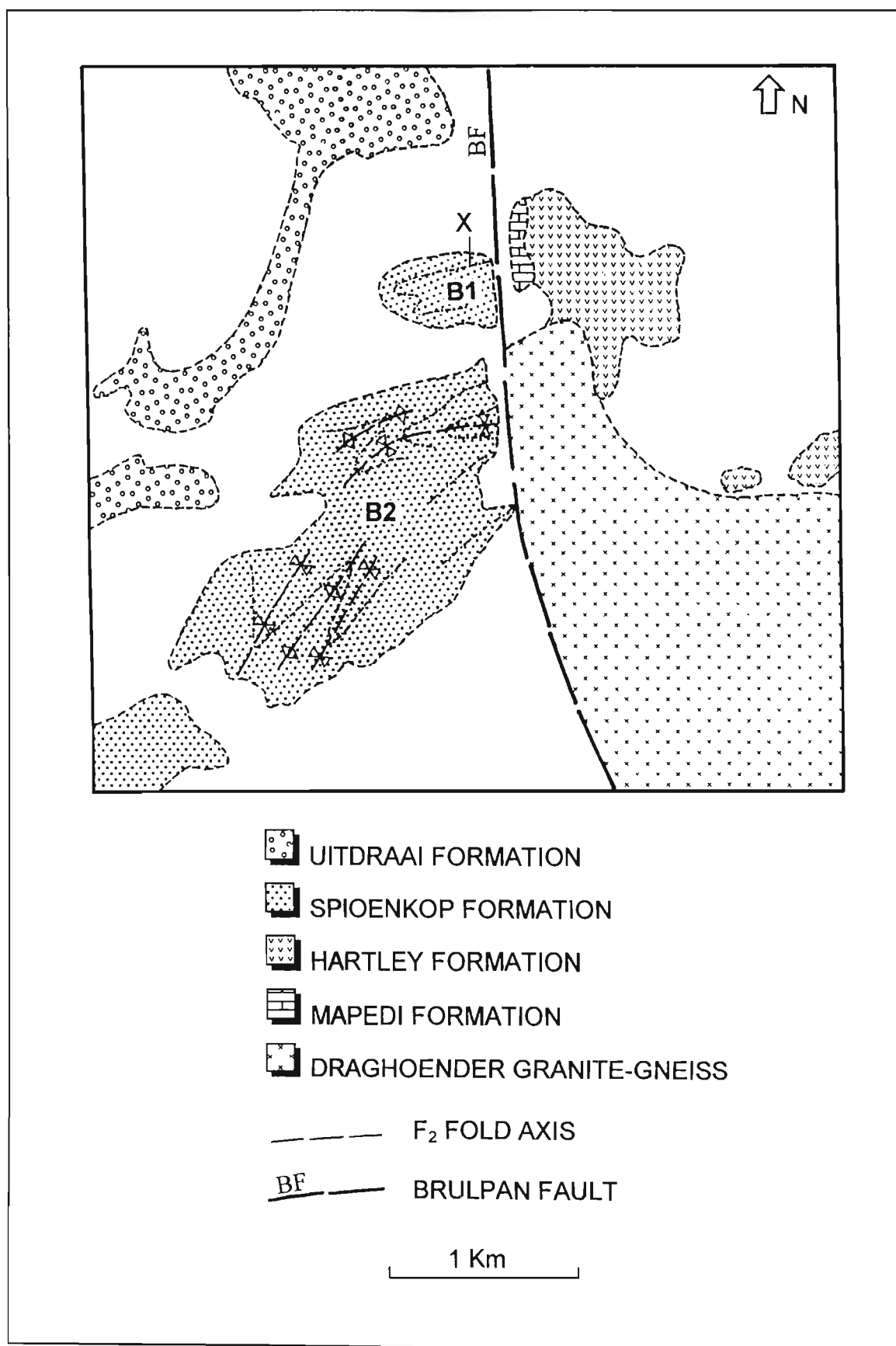


Figure 6.17: Geological map of the Blaauwputs area (Locality 6.4).

flow-top breccias and agglomerate layers. Welded tuff, grey-green quartzite, brown quartzite and meta-psammite horizons are interbedded with the lavas. The lavas are overlain along a sheared contact by a highly deformed dolomite unit. Vajner (1974) suggested that this unit is part of the Griqualand West Supergroup. SAGS (1995) interpreted the dolomite to be part of the ≈ 3.1 Ga Marydale Group. In this section, this dolomite is composed almost exclusively of dolomite ($\approx 85\%$) and quartz ($\approx 15\%$). The dolomite contains narrow layers of calcareous quartzite and is interpreted to represent a highly deformed equivalent of the impure, cross-bedded dolomites of the Mapedi Formation that were observed in the Boegoeberg dam area. The foliation in the contact zone between the Mapedi dolomite and the Hartley Formation strikes 355° and dips 35° to the west. S-C fabrics, in association with mineral elongation lineations that plunge 32° in direction 261° , imply west over east thrust sense of movement. The Mapedi Formation dolomites have thus been thrust over the Hartley Formation at this locality. These isolated outcrops of Mapedi and Hartley Formation strata are too small to include on Map 1.

Investigation of the Kaaiaen domain in the Blaauwputs area was concentrated on the two hills comprised of Spioenkop Formation rocks labelled B1 and B2 on Figure 6.17. The Spioenkop Formation that forms these hills comprises white siliceous quartzite interbedded with subordinate micaceous quartzite and quartz-mica schist. Narrow amphibolite layers occur sub-parallel to the primary layering. These amphibolites comprise hornblende, plagioclase, alkali feldspar and quartz with minor chlorite and epidote.

A number of fold closures, defined by form lines can be observed on Figure 6.17. In the field, it was evident that these closures are related to tight folds that are overturned to the south or south-east (Figure 6.18). The folds have rounded hinges and mullion lineations parallel to the fold axes. They are interpreted as F_2 folds. Figure 6.19 shows the orientations of L_2 mullion lineations measured on hills B1 and B2. The variation in trend of the mullion lineations from north-south to east-west is due to the change in orientation of F_2 folds visible on Figure 6.17. The change in trend is consistent with clockwise rotation of the folds due to apparent dextral sense, strike slip movement on the Brulpan fault.

At the locality marked X (Figure 6.17) mullion lineations are refolded around a small scale, open fold that plunges 65° in direction 340° . This probably represents a F_3 fold. Its NNW trend is similar to that of the F_3 folds observed in the Marydale area (i.e. it has not been significantly rotated by the Brulpan fault). The large amount of apparent clockwise rotation of F_2 folds into the Brulpan fault may be an artefact produced by truncation of an F_3 anticline by the Brulpan fault.



Figure 6.18: North-west trending F_2 fold that is overturned to the south-east. Location: southern slope of hill B2 (Figure 6.17).

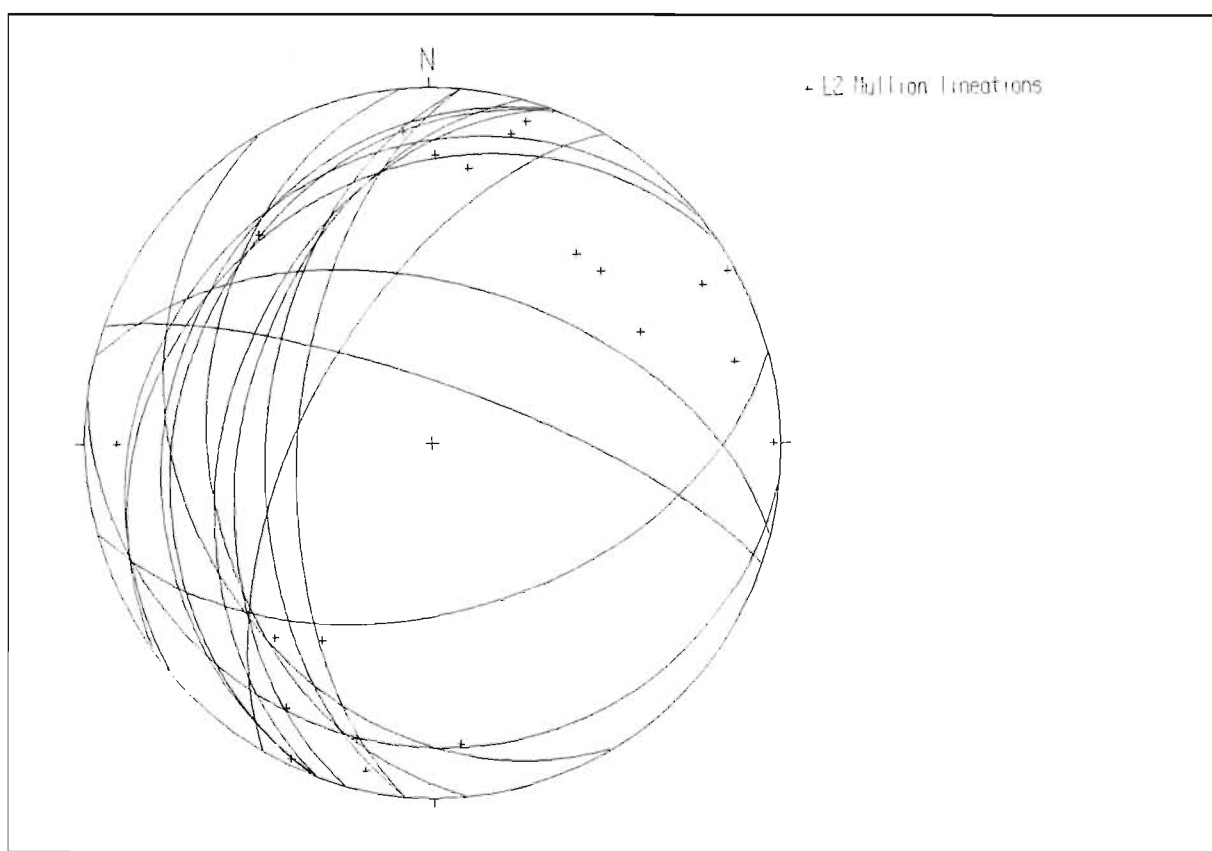


Figure 6.19: Equal area stereographic projection of bedding and S_1 foliation planes ($n=15$) and L_2 mullion lineations ($n=21$) measured in the Blaauwputs area.

6.4 Discussion

6.4.1 Correlation of structural elements observed in the Kaaian Domain

Table 6.1 lists the phases of deformation recognised by previous workers in the northern part of the Kaaian Domain and the south-western part of the Kheis belt (Stowe, 1983, 1986) and in the immediate vicinity of the Copperton shear zone (Humphreys and Van Bever Donker, 1987; Humphreys *et al.*, 1988). These workers have used different symbols for the various phases of deformation recognised in the area. In order to rationalise the symbology, deformation phases recognised by these workers have either been correlated with the Kheis orogeny (KD) or one of six phases of deformation that occurred during the extended Namaqua Orogeny (ND₁-ND₆).

During this study of the southern part of the Kaaian Domain four phases of deformation (D₁-D₃ and north to north-west striking faults) were recognised in rocks of the Kaaian Group and the Spioenkop Formation. Table 6.1 shows the proposed correlations between these deformation events and those recognised by previous workers.

	Kheis Orogeny	Extended Namaqua Orogeny					
This study	KD	ND ₁	ND ₂	ND ₃	ND ₄	ND ₅	ND ₆
This chapter	D ₁	D ₂	D ₃				Brulpan fault
Stowe (1983, 1986)	KF1 (NF1a)	KF2 (NF1b)	NF2	NF3	NF4	NNW striking shear-zones and faults	
Humphreys and Van Bever Donker (1987)	FK1	FN1 (FK2)	FN2	FN3	FN4	FN5a	FN5b
Humphreys <i>et al.</i> (1988)	FK1 (FN1a)	FN1b (FK2)	FN2	FN3	FN4	FN5	

Table 6.1: Correlation between the deformation phases recognised by previous workers and those documented in the southern part of the Kaaian Domain.

The D₁ event resulted in the development of isoclinal folds with sharp hinges and an axial planar S₁ foliation. Fold closures are seldom observed in the field, but the foliation is commonly developed, sub-parallel to bedding, in the more incompetent units of the Spioenkop and Uitdraai Formations. Stowe (1986) documented folds with similar geometry in the Groblershoop Formation and the Zonderhuis Formation (i.e. in the south-western part of the Kheis belt). They are the oldest structural elements recognised in these units and were considered by Stowe (1986) to be related to craton vergent deformation during the Kheis orogeny. Importantly, the D₁ fabric elements are absent from the 1240 Ma

Leerkrans Formation and the 1285 Ma Areachap Group (Stowe, 1986). Due to subsequent deformation during the D₂ and D₃ events, it was not possible to determine the original attitude and vergence of the D₁ structural elements in the areas mapped during this study. However, based on similarities between D₁ fabric elements in the southern part of the Kaaie domain and those described from the western part of the Kheis belt by Stowe (1986), the D₁ event is correlated here with the Kheis orogeny (KD).

The F₁ folds and S₁ foliation have been deformed during a D₂ deformation event. The D₂ deformation was characterised by the development of eastward vergent thrust sense shear zones and tight, overturned F₂ folds. The D₂ deformation was highly heterogeneous leading to the preferential partitioning of strain into the more incompetent lithotypes. This heterogeneous deformation has resulted in significant differences in the style and orientation of structural elements in high- and low-strain zones. F₂ folds are characterised by rounded hinges and a strong mullion lineation parallel to the fold axes. Vajner (1974) and Smit (1977) recognised these folds in the western part of the Kheis belt and the Kaaie domain but failed to identify the heterogeneous nature of the deformation. Stowe (1986) recognised folds with F₂ geometry and, associated craton vergent thrust sense shear zones, in the south-western part of the Kheis belt, the northern part of what is here termed the Kaaie domain, the Leerkrans Formation and the Areachap Group. Stowe (1986) and Humphreys *et al.* (1988) suggested that the D₂ deformation was related to an early phase of the extended Namaqua orogeny (ND₁) during which the Areachap Group volcanic arc was thrust over the south-western part of the Kheis belt and the Kaapvaal Craton.

D₂ low-strain zones, where not re-orientated by D₃ folding, are characterised by approximately NNW-SSE trending periclinal folds that are overturned to the east. Fold axes plunge at shallow angles to the NNW or SSE and are perpendicular to mineral elongation lineations that plunge to the WSW. D₂ low-strain zones are typically developed in competent quartzite units.

D₂ high-strain zones are developed in micaceous quartzite and quartz-mica schists of the Uitdraai and Spioenkop Formations. A strong WSW dipping mylonitic or schistose foliation has developed in these high strain zones. S-C fabrics in these high strain zones indicate a craton vergent, thrust sense of displacement. At most localities, F₂ fold axes have “sheared-out” limbs and have been rotated into parallelism with the WSW plunging mineral elongation lineations. In certain horizons, sheath folds have developed.

The NNW striking, WSW dipping, D₂ shear zones in the Uitdraai and Spioenkop Formations are parallel to those developed in the Draghoender granite along the western edge of the Marydale basement high.

Mineral elongation lineations in all of these shear zones plunge to the WSW and kinematic indicators imply an ENE, thrust sense of movement. The contact between the basement rocks and the meta-sedimentary rocks of the Kaaie domain was nowhere directly observed, but either side of the contact the rocks are highly strained. The contact is interpreted to be a major D_2 thrust sense shear zone and forms part of the Doornberg shear zone (Map 1), a zone of craton vergent, thrust sense shearing recognised by Coward and Potgieter (1983) in the area between Prieska and Copperton.

Mineral assemblages of hornblende-plagioclase-alkali feldspar-quartz in metamorphosed mafic sills and garnet-sillimanite-biotite-muscovite-quartz assemblages in schistose horizons of the Spioenkop and Uitdraai Formations are indicative of amphibolite facies metamorphism. The S_2 foliation is itself defined by these metamorphic minerals. At the isolated localities that were studied, the D_2 deformation was thus accompanied by amphibolite facies metamorphism. Based on field evidence, a hornblende-biotite tonalite exposed in the Marydale area is interpreted to be a syn- D_2 intrusion.

Unequivocal evidence for the D_3 deformation was only observed in the Marydale area, where fabric elements related to the D_2 deformation, are deformed by open, upright, NW trending F_3 folds. The only planar fabric associated with this deformation is a weak axial planar cleavage developed in the hinge zones of the F_3 folds. Vajner (1974) and Stowe (1986) noted that the F_3 folds become progressively tighter moving westwards across the Kaaie domain and into the Namaqua belt.

The north-west to north trending Brulpan fault zone was not directly observed during the present study. Similarly orientated faults in the Kaaie domain and the western part of the Kheis belt (e.g. the Doringberg fault) have a dextral strike-slip sense of displacement and post-date the D_3 event. The Brulpan Fault is interpreted to be a component of the late-Namaqua orogeny, dextral sense, strike-slip fault system.

As noted in Chapter 5, south-east vergent thrust sense shear zones associated with the Kheis orogeny (KD) and ENE vergent thrust sense shear zones are developed along the northern and western margins of the Marydale basement high respectively. Mineral elongation lineations in both sets of shear zones imply dip-slip movement which is incompatible with the two sets having developed during the same phase of deformation. Observations made in the southern part of the Kaaie domain indicate that ENE vergent thrusting (D_2) occurred along the western margin of the Marydale basement high during the earliest phase of the extended Namaqua orogeny (ND_1). The Kheis belt with its north-east structural trend is thus truncated by the NNW trending Doornberg shear zone and the northern part of the Brulpan fault.

6.4.2 Stratigraphic correlations

Table 6.2 outlines the proposed stratigraphic correlations between the Uitdraai and Spioenkop Formations and the Olifantshoek Supergroup.

Olifantshoek Supergroup	Kaaien Group	
Grobbershoop Formation		
Brulsand Formation	Uitdraai Formation	Spioenkop Formation
Matsap Formation		
Hartley Formation		
Lucknow Formation		
Mapedi Formation		

Table 6.2: Proposed stratigraphic correlations between the Olifantshoek Supergroup, the Uitdraai Formation and the Spioenkop Formation.

The rocks that comprise the southern part of the Kaaien domain have been subdivided into the Spioenkop and the Uitdraai Formations by SACS (1980). The Spioenkop Formation consists of siliceous white quartzite, micaceous quartzite and quartz-mica schists. The Uitdraai Formation consists of brown and purple siliceous quartzite, micaceous quartzite and quartz-mica schists. With the exception of planar bedded, heavy mineral layers consisting of recrystallised ore minerals, all sedimentary structures have been obliterated by the intense ND₁ deformation and associated amphibolite facies metamorphism . Both the Spioenkop Formation and the Uitdraai Formation have been intruded by mafic sills, now represented by amphibolites. Based on observations made during this study the following conclusions can be drawn:

•Given the similar lithotypes and deformation history of the Uitdraai Formation and the Spioenkop Formation, it seems illogical to consider the Spioenkop Formation to be the uppermost unit of the ≈3.0 Ga Marydale Group as suggested by SACS (1980), Coward and Potgieter (1983), Cornell *et al.* (1986), Stowe (1986) and Humphreys *et al.* (1988). The Spioenkop Formation has been thrust over the Archaean basement rocks of the Marydale high along the Doornberg shear zone (Map 1). Its stratigraphic position overlying the Marydale Group in the area between Copperton and Prieska should be regarded as allochthonous or par-allochthonous. It is suggested that the Spioenkop Formation should be considered to be part of the Kaaien Group as recommended by Scott (1987).

- The Uitdraai Formation (part of the Kaaie Group), in the southern part of the Kaaie domain, and the Olifantshoek Supergroup (in the Kheis belt) both consist of meta-sedimentary rocks that were deformed during the Kheis orogeny (D_1 equivalent to KD: Table 6.1). Mafic sills are common in both units.
- No coarse grained clastic material (conglomerates), metamorphosed mafic volcanics or impure dolomite (characteristic of the units in the lower part of the Olifantshoek Supergroup) was observed in the Uitdraai Formation or the Spioenkop Formation in the southern part of the Kaaie domain. A correlation between the Uitdraai and Spioenkop Formations and any of the stratigraphic units of the Olifantshoek Supergroup that underlie the Brulsand Formation is thus highly unlikely.
- Siliceous quartzites interbedded with more immature quartzites and meta-psammite horizons are the dominant lithology in the Brulsand Formation of the Olifantshoek Supergroup. The quartzites in the Brulsand Formation commonly exhibit planar bedded heavy mineral bands. It is suggested that the Uitdraai and Spioenkop Formations are equivalents of the Brulsand Formation.

7. THE MAGONDI BELT

7.1 Regional setting

The Magondi belt is a regionally north-east to north striking, north-west to west dipping, orogenic belt situated on the north-west margin of the Zimbabwe Craton (Figure 7.1). The south-east, or external, part of the Magondi belt (Figure 7.2) comprises rocks of the Magondi Supergroup (Deweras, Lomagundi and Piriwiri Groups), that were deposited along the margin of the Zimbabwe Craton and subsequently thrust to the south-east over the Craton during the Magondi orogeny (Treloar, 1988; Leyshon and Tennick, 1988). The internal part of the Magondi belt (forming the western and north-western sectors of the belt) comprises an imbricate thrust stack of Early Proterozoic basement granitoid-gneisses and Magondi Supergroup rocks (Figure 7.2) that are intruded by weakly deformed granitoids, the largest of which is the Urungwe granite (Treloar, 1988). Metamorphic grades vary from greenschist facies in the external part of the orogen, to upper amphibolite-granulite facies in the internal part (Treloar, 1988; Treloar and Kramers, 1989).

The Magondi belt is truncated, and structurally overprinted, in the north by the younger, Pan-African age Zambezi belt (Figure 7.1). Rocks of the Magondi Supergroup, that were deformed during the Magondi orogeny, are unconformably overlain in this area by meta-sediments of the Makuti Group (Figure 7.2). The Makuti Group post-dates the Magondi orogeny but was deformed and thrust southwards over the Magondi belt during the Zambezi orogeny (Treloar, 1988). The Urungwe Klippe (Figure 7.2) represents an erosional remnant of a shallow dipping thrust sheet of Makuti Group strata (Treloar, 1988). The Sijarira Group sediments overlie deformed strata of the Magondi belt with angular unconformity (Kirkpatrick, 1976; Treloar, 1988) but underlie the Urungwe Klippe. The Sijarira Group thus post-dates the Magondi orogeny but pre-dates the Zambezi orogeny. All of these units that were deformed during the Magondi and/or Zambezi orogenies are overlain, with angular unconformity, by the Karoo Supergroup in the north and west (Figure 7.2).

The Dett inlier (Figure 7.1) consists of high grade equivalents of the Magondi Group, exposed in an erosional window through the unconformably overlying Karoo Supergroup (Lockett, 1979).

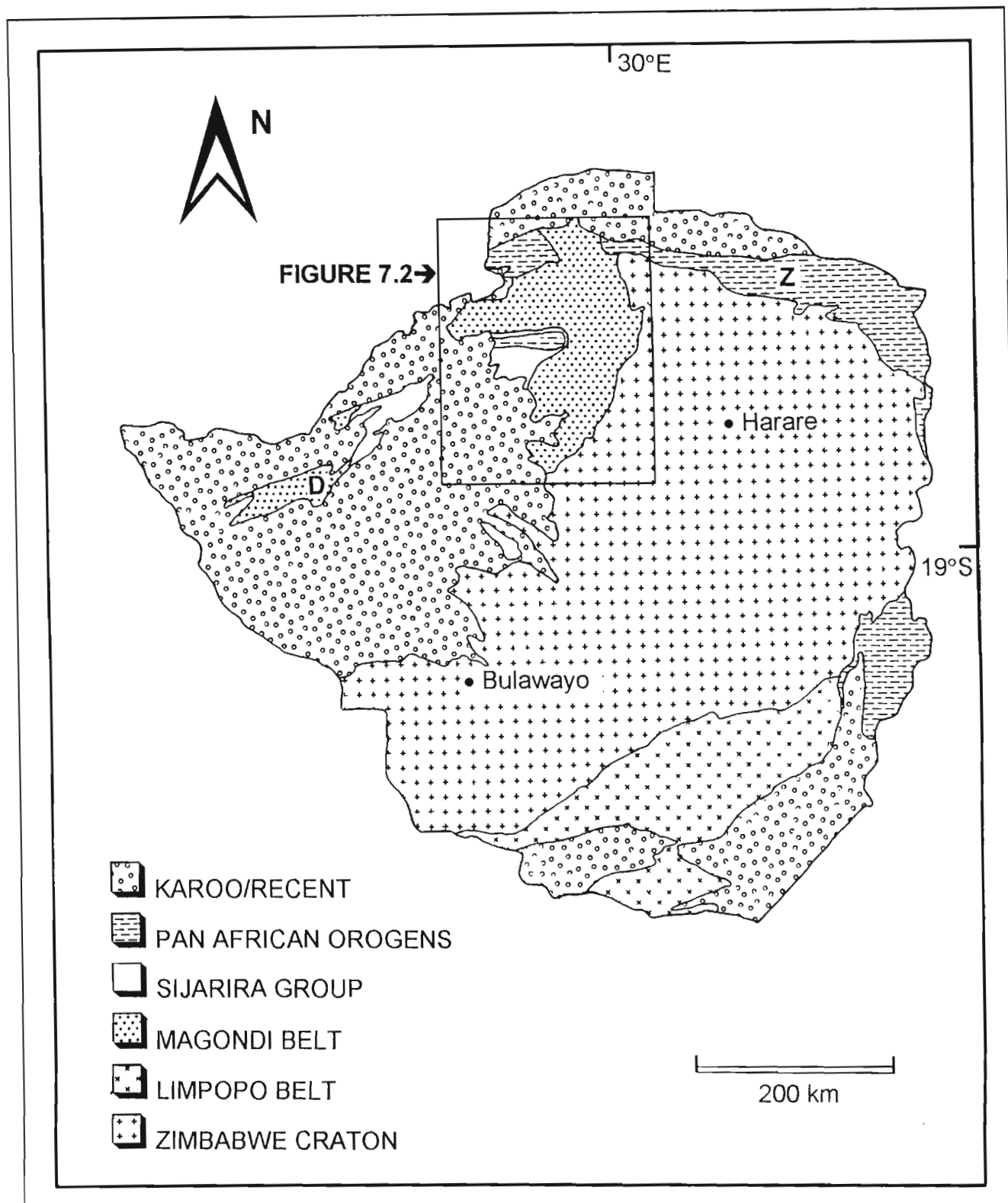


Figure 7.1: A simplified geological map of Zimbabwe (after Treloar, 1988). The area included in Figure 7.2 is outlined.

Z=Zambezi belt, D=Dett inlier.

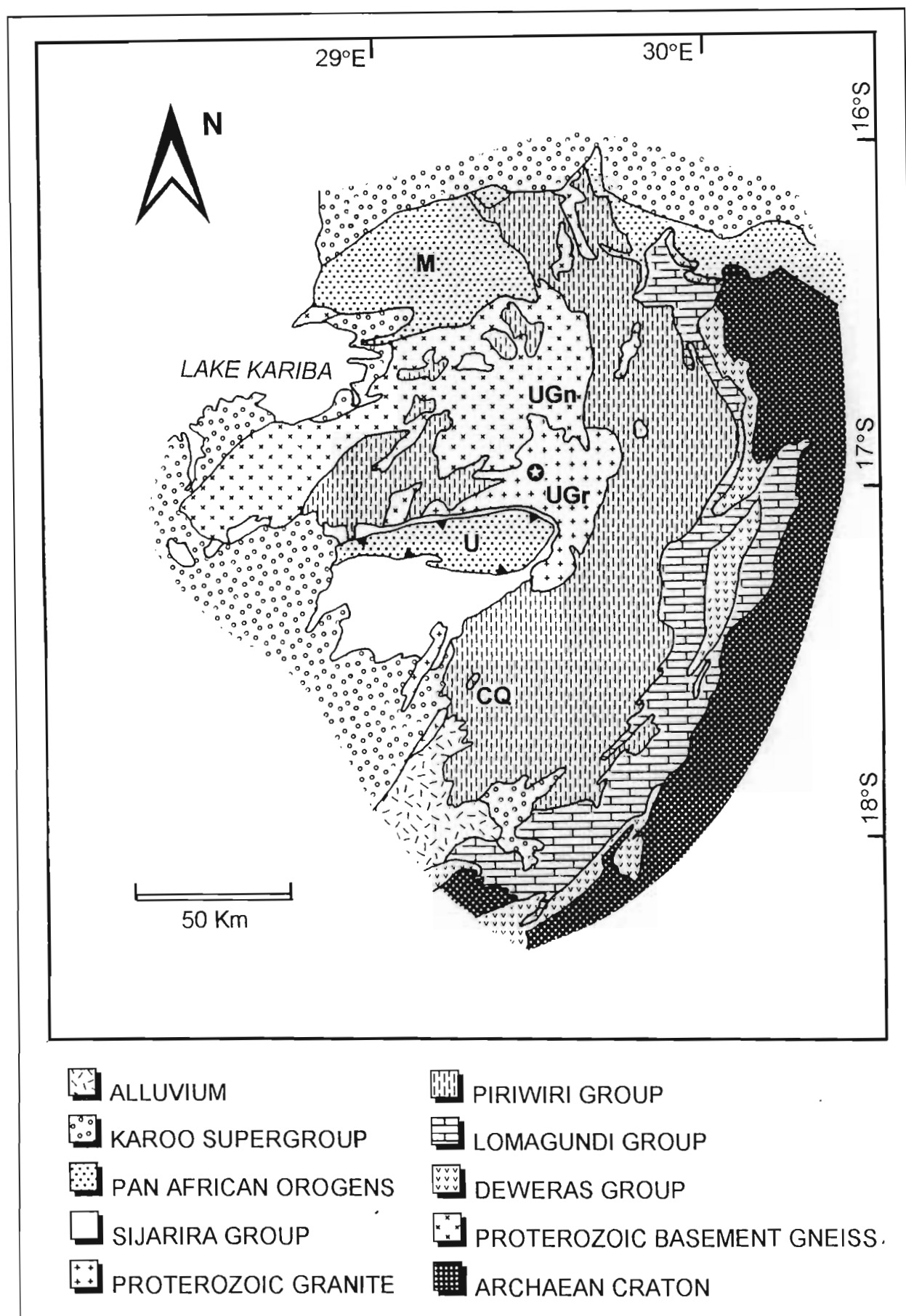


Figure 7.2: Simplified geological map of the Magondi belt (after Treloar, 1988). M=Makuti Group, U=Urungwe Klippe, UGr=Urungwe granite, UGn=Urungwe gneiss, CQ=Copper Queen granite dome, ★=Murereshi River locality.

7.2 Existing age constraints on the deposition of the Magondi Supergroup and the timing of the Magondi orogeny.

The depositional age of the Magondi Supergroup is very poorly constrained. A Rb-Sr whole rock age of 2170 ± 100 Ma is reported for a mafic lava horizon in the basal, Deweras Group (Treloar, 1988). Pb-Pb galena ages ranging between 2250 and 2100 Ma are reported from the Magondi Supergroup rocks that surround the Copper Queen granite dome (Leyshon, 1969; Treloar, 1988). These Pb-Pb ages may be unreliable constraints on the depositional/extrusion age of the Magondi Supergroup, as the origin of the Pb and Cu sulphides in the Copper Queen area (Figure 7.2) remains controversial (Leyshon, 1969; Treloar, 1988; Leyshon and Tennick, 1988; Master, 1991).

Vail *et al.* (1968) used K/Ar studies of metamorphic micas from the Magondi Supergroup rocks (in the external part of the Magondi belt) in an attempt to date the Magondi orogeny and calculated ages ranging from 1974 ± 70 to 1659 ± 50 Ma. A number of granitoid bodies, intruding the basement gneisses in the Lake Kariba area have been dated (Rb/Sr whole rock) at 1980 ± 80 Ma (Loney, 1969).

More recently, Treloar and Kramers (1989), using Rb-Sr whole rock geochronology obtained ages of 1890 ± 260 and 1780 ± 280 Ma, from charnockitic granite intrusions and leucocratic granite melt-segregations respectively, that occur in granulite facies Magondi Supergroup rocks in the internal part of the Magondi belt. Treloar and Kramers (1989) interpreted these ages, albeit with large errors, to represent crystallisation ages of granitic melts produced during the Magondi orogeny. Munyanyiwa *et al.* (1995) dated two charno-enderbites, that intrude the early Proterozoic basement gneisses in the internal part of the Magondi belt, and obtained ages of: 1932 ± 27 Ma and 1960 ± 39 Ma (conventional U-Pb zircon) and 1933 ± 4 and 1959 ± 3 Ma (single zircon Pb-Pb evaporation). Munyanyiwa *et al.* (1995) interpreted these ages to indicate that granulite facies metamorphism, during the Magondi orogeny, occurred between approximately 1960 and 1930 Ma.

7.3 The Urungwe granite

The Urungwe granite occurs in the internal part of the Magondi belt (Figure 7.2) and is intrusive into both the Early Proterozoic Urungwe basement gneiss and meta-sediments of the Piriwiri Group (Kirkpatrick, 1976). It is unconformably overlain in the south-west by the pre-Zambezi Sijarira Group (Kirkpatrick, 1976) and thus cannot be related to the Zambezi orogeny. Kirkpatrick (1976) recognised both porphyritic

and fine grained-varieties in the southern portion of the Urungwe granite and noted that feldspar phenocrysts in the porphyritic variety are locally aligned north-west/south-east.

Although covered by younger rocks in the south-west it can be seen that the Urungwe granite has an elongate map pattern, with a long axis in plan view orientated north-east/south-west, parallel to the structural trend of the Magondi belt (Figure 7.2). Treloar (1988) interpreted the Urungwe granite to be one of a suite of syn- to post-kinematic intrusions associated with the Magondi orogeny.

Rb-Sr (whole rock) dating of the Urungwe granite yielded an age of 2153 ± 125 Ma (Clifford *et al.*, 1967). Mineral ages of 1211 ± 40 Ma (Rb-Sr muscovite), 948 ± 40 Ma (K-Ar muscovite) and 843 ± 40 Ma (K-Ar biotite) were determined during the same study (Clifford *et al.*, 1967).

The Urungwe granite was studied and sampled adjacent to the Murereshi river (Figure 7.2). At this locality the Urungwe granite has a heterogeneously developed, north-east striking, steeply north-west dipping ($\approx 80^\circ$) foliation defined by biotite. The long axes of alkali feldspar phenocrysts are aligned parallel to the foliation planes (Figure 7.3). A weak mineral lineation defined by aggregates of quartz and biotite plunges down the plane of the foliation to the north-west. S-C fabrics imply a north-west over south-east thrust sense of movement. The orientation of the fabric elements, and the implied kinematics are consistent with the Urungwe granite being a syn-Magondi orogeny intrusive. This interpretation is also consistent with the elongate map pattern of the granitoid.

7.4 U-Pb Single zircon SHRIMP dating of the Urungwe granite

A sample taken from the Urungwe granite at the Murereshi river locality was selected for radiometric dating (using the U-Pb single zircon SHRIMP method), in order to determine the timing of the Magondi orogeny and to provide a minimum age constraint for the Magondi Supergroup. Zircons were separated from the sample, and analysed using the SHRIMP ion microprobe, at the Australian National University by R.A. Armstrong.

Zircons from the Urungwe granite are honey-coloured, generally euhedral, have pronounced long, sharp pyramidal terminations and short prism faces (Armstrong, 1997b). In section it was observed that many of the zircons have cores of inherited zircons. The cores are generally rounded and are surrounded by compositionally zoned overgrowths representing magmatic zircon (Armstrong, 1997b).

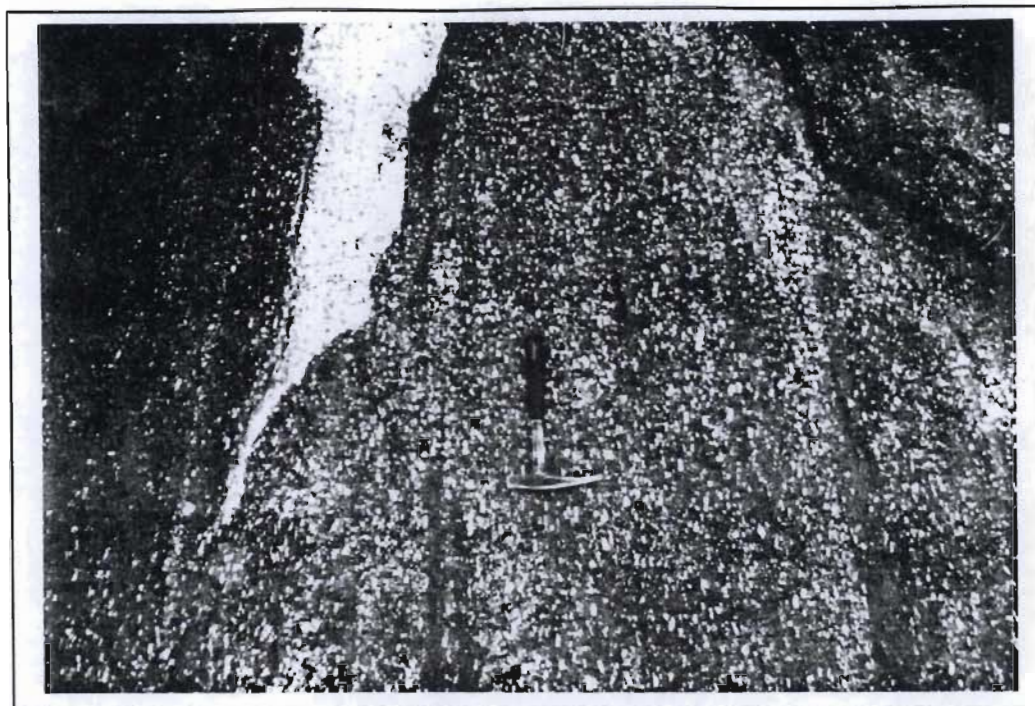


Figure 7.3: Foliated Urungwe granite at the Murereshi river locality. The foliation, defined by biotite and feldspar phenocrysts, strikes parallel to the handle of the hammer.

The U-Th-Pb SHRIMP results for the Urungwe granite are presented in Table 7.1 and are plotted on U-Pb Wetherill concordia diagrams in Figures 7.4 and 7.5. From these diagrams it can be seen that the analyses of structureless zircons (i.e. those with no core-rim relationships) and the rims of composite zircons (i.e. those with a central core) plot as a tightly clustered group, straddling the concordia, from which a $^{207}\text{Pb}/^{206}\text{Pb}$ age of 1997 ± 3 Ma is calculated (Figure 7.5). This age is interpreted to reflect the crystallisation age of the Urungwe granite. The older ages obtained from the zircon cores indicate that the granite has a complex and heterogeneous pattern of inheritance.

The 1997 ± 3 Ma U-Pb (single zircon SHRIMP) crystallisation age obtained for the syn-tectonic Urungwe granite is older than the ≈ 1960 - 1939 Ma Pb-Pb evaporation ages reported by Munyanyiwa *et al.* (1995) for syn-tectonic charno-enderbites (Munyanyiwa *et al.*, 1995). Pb-Pb evaporation radiometric ages are however minimum ages constrained by only one ratio. The SHRIMP age for the Urungwe granite does overlap, within error, the older of the two U-Pb conventional zircon ages (1960 ± 39 Ma) for the charno-enderbites that were reported by Munyanyiwa *et al.* (1995) and the Rb-Sr whole rock ages reported by Treloar and Kramers (1989) for similar charnokitic rocks that intrude the Piriwiri Group..

The 1997 ± 3 Ma U-Pb single zircon SHRIMP age for the syn-tectonic Urungwe granite is interpreted to be a refinement of previous age constraints on the Magondi orogeny. It also places a reliable minimum age constraint on the deposition/extrusion of the Magondi Supergroup. The Magondi Supergroup can thus be bracketed between ≈ 2.17 (Rb-Sr whole rock: Treloar, 1988) and 1.99 Ga.

Table 7.1: Summary of U-Pb SHRIMP analyses of zircons from the Urungwe granite.

Grain.spot	U/ppm	Th/ppm	Th/U	Pb*/ppm	204/206	% 1206	206/238	t	207/235	t	207/206	t	Ages (In Ma)				% CONC
													206/238	207/235	207/206	t	
Sample UG1																	
1.1	1068	42	0.04	394	0.000010	0.0150	0.3780	0.0074	6.407	0.130	0.1229	0.0005	2067	2033	1999	8	103
2.1	1422	56	0.04	525	0.000010	0.0150	0.3795	0.0125	6.401	0.215	0.1223	0.0004	2074	2032	1990	6	104
3.1	1307	42	0.03	467	0.000008	0.0120	0.3673	0.0093	6.224	0.168	0.1229	0.0007	2017	2008	1999	11	101
4.1	1236	33	0.03	487	0.000010	0.0150	0.3868	0.0077	6.540	0.133	0.1226	0.0003	2108	2051	1995	5	106
5.1	1169	49	0.04	406	0.000006	0.0090	0.3583	0.0085	6.055	0.147	0.1226	0.0003	1974	1984	1994	5	99
5.2	324	176	0.54	203	0.000006	0.0090	0.5397	0.0160	14.138	0.521	0.1900	0.0035	2782	2759	2742	31	102
6.1	1321	37	0.03	495	0.000007	0.0110	0.3852	0.0074	6.540	0.129	0.1231	0.0003	2101	2051	2002	4	105
7.1	1514	23	0.02	547	0.000016	0.0240	0.3733	0.0085	6.302	0.148	0.1225	0.0004	2045	2019	1992	6	103
8.1	1292	55	0.04	468	0.000017	0.0260	0.3711	0.0071	6.273	0.125	0.1226	0.0004	2034	2015	1995	6	102
9.1	849	46	0.05	288	0.000148	0.2240	0.3464	0.0071	5.823	0.125	0.1219	0.0005	1917	1950	1985	8	97
9.2	820	466	0.57	330	0.000058	0.0870	0.3684	0.0189	6.946	0.371	0.1368	0.0014	2022	2105	2187	18	93
10.1	1232	50	0.04	454	0.000010	0.0150	0.3780	0.0075	6.422	0.133	0.1232	0.0005	2067	2035	2004	7	103
10.2	167	172	1.03	88	0.000249	0.3770	0.4475	0.0119	9.972	0.287	0.1616	0.0013	2384	2432	2473	14	96
11.1	1511	173	0.11	519	0.000028	0.0430	0.3538	0.0105	5.946	0.193	0.1219	0.0012	1953	1968	1984	17	98
12.1	172	198	1.15	82	0.000010	0.0150	0.3784	0.0085	6.436	0.160	0.1234	0.0010	2069	2037	2005	15	103
12.2	1211	134	0.11	433	0.000042	0.0640	0.3670	0.0070	6.238	0.123	0.1233	0.0004	2015	2010	2004	6	101
13.1	1151	68	0.06	408	0.000026	0.0400	0.3642	0.0071	6.170	0.124	0.1229	0.0004	2002	2000	1998	5	100

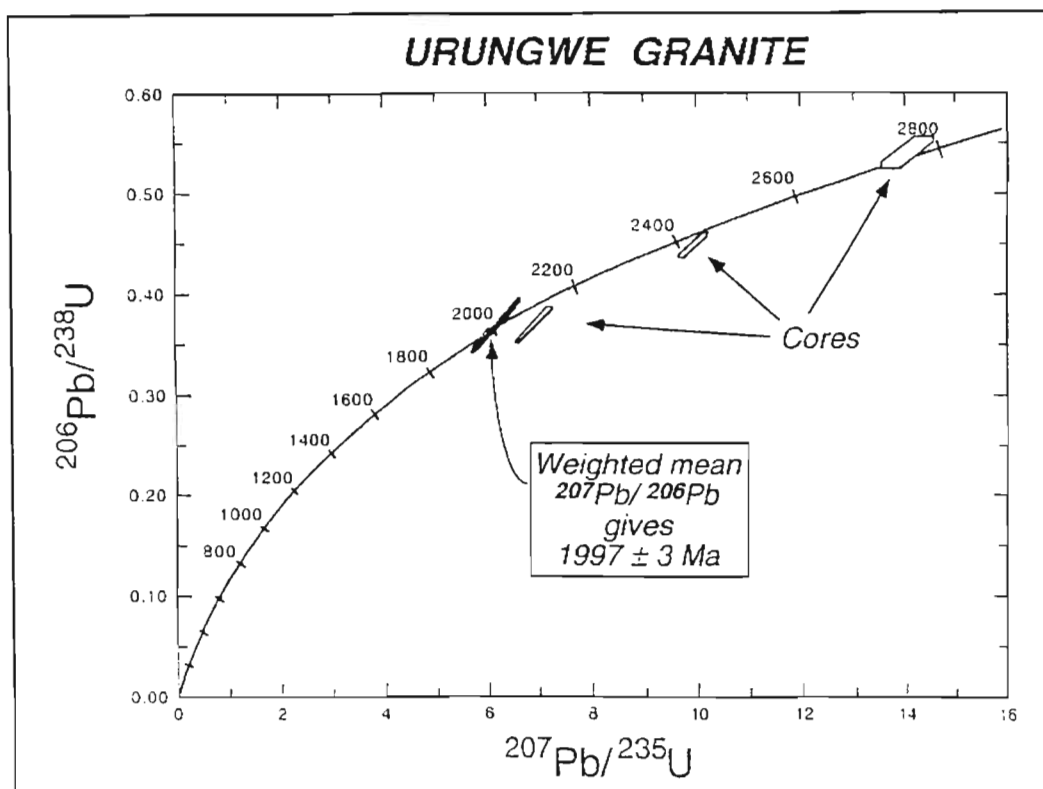


Figure 7.4: U-Pb concordia diagram of zircon analyses from the Urungwe granite. Analyses performed by R.A. Armstrong.

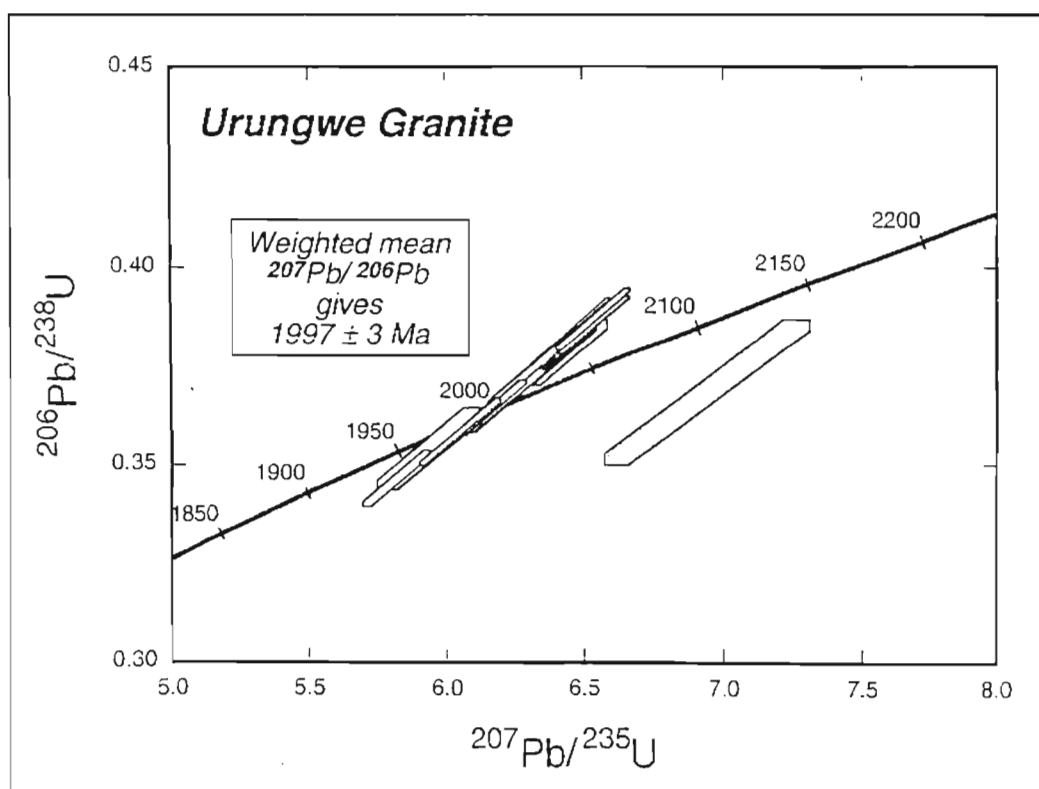


Figure 7.5: Enlarged portion of Figure 7.4 showing the group of concordant U-Pb analyses that define a crystallisation age of $1997 \pm 3 \text{ Ma}$ for the Urungwe granite.

8. DISCUSSION

In the discussion that follows, the observations made during this study are integrated with the existing geological data base. A chronological approach (oldest to youngest) is taken in discussing the geological evolution of the western margin of the Kaapvaal Craton, the Olifantshoek Supergroup depository, the Kheis belt and the Kaaien Domain.

8.1 The Marydale basement high

The Marydale basement high constitutes the westernmost exposure of the basement rocks that form the Kaapvaal Craton. Field relations indicate that the ≈ 3.0 Ga Marydale Group greenstones (Burger and Coertze, 1973; Barton *et al.*, 1986) are older than the Draghoender granite, as suggested by Vajner (1974). This is supported by a U-Pb single zircon SHRIMP age of 2853 ± 4 Ma for the Draghoender granite.

The relative ages of the Draghoender granite and the Skalkseput granite have not been unequivocally demonstrated in the field during this study, nor during a previous investigation by Vajner (1974). Numerous granitic veins that intrude the Draghoender granite may be related to intrusion of the Skalkseput granite. An attempt to date the Skalkseput granite at the type locality using the U-Pb SHRIMP method proved unsuccessful. A sample of the Skalkseput granite from a different locality has been dated at 2718 ± 8 Ma (Pers. comm. R.A. Armstrong: U-Pb single zircon SHRIMP). Provided that the Skalkseput granite comprises granitoid intrusions related to a single event, this radiometric age indicates that the Skalkseput granite is younger than the Draghoender granite.

The Marydale basement high is situated to the west of the margin of the early Kaapvaal crustal shield (Figure 8.1) of De Wit *et al.* (1992). Radiometric age constraints on the timing of granitoid intrusion in the Marydale area (≈ 2.9 -2.7 Ga) are consistent with those from the Kraaipan granite-greenstone terrain (Figure 8.1). In the Kraaipan granite-greenstone terrain the Kraaipan Group greenstones are intruded by the 2749 ± 3 Ma Mosita adamellite (Anhaeusser and Walraven, 1997: Pb-Pb zircon evaporation), the 2780.6 ± 1.8 Ma Gabarone granite and rhyolite complex (Grobler and Walraven, 1993: Pb-Pb single zircon evaporation) and the 2880 ± 2 Ma Schweizer-Reneke granite (Robb *et al.*, 1992: U-Pb single rutile and monazite). Radiometric age constraints from the Marydale and Kraaipan granite-greenstone terrain's therefore support the proposal by De Wit *et al.* (1992) that Late-Archaeon crustal growth of the Kaapvaal Craton occurred by terrane accretion along the western edge of the early crustal shield, between ≈ 3.1 and 2.65 Ga.

granite at the type locality on farm Skalkseput (Chapter 5). If the sample of Skalkseput granite dated by R.A. Armstrong forms part of the same intrusive suite as the granite that intrudes the Zeekoebaart Formation then the Zeekoebaart Formation must be older than 2718 ± 8 Ma.

Table 8.1 shows a generalised stratigraphic column and available radiometric age constraints for the Ventersdorp Supergroup. The minimum age of the Zeekoebaart Formation (2718 ± 8 Ma) is within error of the crystallisation ages of both the Makwassie and Alberton Formations. Suggesting a correlation with the Allanridge Formation (Pniel Group) is unlikely. On available data therefore the Zeekoebaart Formation may be an equivalent of the mafic lavas of the Klipriviersberg or Platberg Group, or (as is less likely given the 2.85 Ga age for the Draghoender Granite) an older stratigraphic unit such as the 3.07 Ga Dominion Group (Armstrong *et al.*, 1991: U-Pb single zircon SHRIMP).

Group	Formation	Lithology	Age
Pniel	Allanridge	Andesitic lava	
	Bothaville	Sediments	
Platberg	Rietgat	Lava and sediments	2709±4
	Makwassie	Qtz-fsp porphyry	
	Goedgenoeg	Andesitic lava	
	Kameeldoorns	Sediments	
Klipriviersberg	Edenville	Amygdaloidal and porphyritic lavas with subordinate tuffs	2714±8
	Loraine		
	Orkney		
	Alberton		
	Venterspost	Conglomerate	

Table 8.1: Generalised stratigraphy and age constraints for the Ventersdorp Supergroup. Age dates are U-Pb single zircon SHRIMP ages (in Ma) from Armstrong *et al.* (1991).

8.3 The Griqualand West Supergroup

The tectonic setting of the basin/s that formed the depository (or depositories) for the Griqualand West Supergroup, and possible correlations of individual units in the Griqualand West Supergroup with those in the roughly contemporaneous Transvaal Supergroup (Figure 8.1) remain uncertain (e.g. Button, 1976; Beukes, 1986; Harmer and Von Grunewaldt, 1991; Walraven and Martini, 1995; Altermann, 1996;

Cheney, 1996). A tuff in the basal unit of the Griqualand West Supergroup has been dated at 2643 ± 3 Ma (Pers. comm. R.A. Armstrong: U-Pb single zircon SHRIMP), roughly constraining the onset of Griqualand West Supergroup deposition. The basaltic lavas of the Ongeluk Formation, near the top of the Griqualand West Supergroup, have been dated at 2222 ± 13 Ma (U-Pb whole rock: Cornell *et al.*, 1996).

Along the south-western edge of the preserved Griqualand West basin, the basal Schmidtsdrif Subgroup unconformably overlies the Zeekoebaart Formation and the basement granitoids of the Marydale basement high. Two unconformities have been recognised within the Griqualand West Supergroup, one within in the Schmidtsdrif Subgroup and the other at the base of the Makganyene Formation (Visser, 1971; Beukes, 1986). On a regional scale (Map 1), the strike and dip of the strata above and below these unconformities is sub-parallel and they are best referred to as disconformities.

The Voelwater Subgroup has been considered by most workers to conformably overlie the Ongeluk Formation (e.g. Nel *et al.*, 1986; Gutzmer and Beukes, 1995) and has traditionally been included in the Griqualand West Supergroup (SACS, 1980). Observations in the Boegoeberg dam area indicate that the Voelwater Subgroup overlies the Griqualand West Supergroup with angular unconformity. The Voelwater Subgroup shall be discussed separately in section 8.5. In the sections that follow, the term Griqualand West Supergroup shall be used to refer to all rocks of the Griqualand West Supergroup of SACS (1980) that pre-date the Voelwater Subgroup. The Griqualand West Supergroup, as defined here, was deposited/extruded between approximately 2.65 Ga and 2.22 Ga.

8.4 Pre-Voelwater Subgroup folding of the Griqualand West Supergroup

An east-west orientated compressional event, producing approximately north-south trending periclinal folds (e.g. the Dimoten and Ongeluk-Witwater synclines- Map 1) in the Griqualand West Supergroup, occurred prior to deposition of the Voelwater Subgroup. These folds are very gentle, open upright structures in the eastern part of the preserved Griqualand West basin and become progressively tighter, but remain upright, moving towards the west and south-west. Observations in the Boegoeberg dam area indicate that layer-parallel slip played an important role in the development of these folds.

Visser (1944), Van Wyk (1980) and Beukes and Smit (1987) have shown that the folding occurred prior to the development of the Wolhaarkop and Manganore Formations that outcrop along the western (eroded) edge of the Maremane structure (Map 1). The observation that the Voelwater Subgroup was deposited after this folding event places an important constraint on the relative timing of the deformation.

The deformation can thus be considered to be post-Ongeluk Formation, pre-Voelwater Subgroup. The timing of this deformation is poorly constrained in terms of absolute ages. The 2222 ± 13 Ma, U-Pb whole rock age (Cornell *et al.*, 1996) for a lava horizon in the Ongeluk Formation provides a maximum age constraint on the deformation. The oldest, radiometrically dated, stratigraphic unit that post-dates the north-south trending folding is the 1928 ± 4 Ma Hartley Formation (Cornell *et al.*, 1998: U-Pb single zircon evaporation) of the Olifantshoek Supergroup. In terms of available radiometric ages the Pre-Voelwater folding of the Griqualand West Supergroup can thus be bracketed in a ≈ 300 Ma interval.

The observation that the folds become progressively more gentle and eventually “die out” to the east suggests that this early deformation was as a result of an eastward vergent compressional event. Any evidence in the west, for an orogen linked to this event, has been removed by the development of the Olifantshoek Supergroup depository and subsequent Kheis- and extended Namaqua- orogenesis.

8.5 The Voelwater Subgroup

Beukes (1978) subdivided the Voelwater Subgroup into the Hotazel, Mooidraai and Beaumont Formations. The development of the Hotazel and Mooidraai Formations of Beukes (1978) is restricted to the Kalahari manganese field (Black rock area: Map 1). The Voelwater Subgroup rocks examined during this study are correlated with the Beaumont Formation of Beukes (1978) and shall be referred to by this name in the section that follows.

The Beaumont Formation consists of hematite-rich banded ironstones, finely laminated hematite iron ore, ferruginous and siliceous chert, dolomite and minor phyllite. The Beaumont Formation overlies the Griqualand West Supergroup with angular unconformity but is disconformably overlain by the Olifantshoek Supergroup. In the areas studied, the Beaumont Formation overlies either the Ongeluk Formation or the Campbellrand Subgroup. In the Boegoeberg dam area, chert, banded ironstone and laminated hematite iron ore of the Beaumont Formation are preserved as lenses, overlying the Campbellrand Subgroup dolomites, below the basal Olifantshoek Supergroup unconformity.

The Wolhaarkop Formation breccia and the Manganore Formation banded ironstones and laminated iron ore occur as lenses in a similar stratigraphic position on the western edge of the Maremane structure (Map 1). The age and genesis of these units has long been the source of controversy. Most previous models have considered the Wolhaarkop Formation to be a residual chert breccia on an unconformity or a karstic slump feature. The overlying Manganore Formation has been interpreted to be an equivalent of either the

Postmasburg Group (Button, 1976), the Koegas Subgroup (Beukes, 1978) or the Asbestos Hills Subgroup (Visser, 1944; Van Wyk, 1980; Van Schalkwyk and Beukes, 1986). All of these correlations must be reconciled with the observation that elsewhere in the preserved Griqualand West basin (e.g. the eastern side of the Maremane structure) the Asbestos Hills Subgroup conformably overlies the Campbellrand Subgroup, the Koegas Subgroup conformably overlies the Asbestos Hills Subgroup (Beukes, 1986) and the base of the Postmasburg Group is marked by the Makganyene Formation diamictite of glacial origin (Visser, 1971).

Van Wyk (1980) and Van Schalkwyk and Beukes (1986) noted that the development of the Wolhaarkop and Manganore Formations must post-date the large north-south trending, periclinal folds such as the Ongeluk-Witwater syncline. These authors suggested that the Manganore Formation represents Asbestos Hills Subgroup banded ironstones that slumped into sinkholes in the underlying Campbellrand Subgroup dolomites prior to deposition of the Olifantshoek Supergroup, and were hematized by circulating fluids. Van Wyk (1980) and Van Schalkwyk and Beukes (1986) base their interpretation of the Manganore Formation as an Asbestos Hills correlate on bed for bed correlations, yet cite localised brecciation as evidence for sinkhole related slumping.

The development of sinkholes (collapse dolines) occurs as a result of sub-terrestrial chemical weathering of lithified carbonate rocks that contain structural or compositional inhomogeneities that allow groundwater to interact with the rock in discrete zones (LeGrand and LeMoreaux, 1975). The collapse of the roof of a cave, leading to the generation of a sinkhole, results in the deposition of a chaotic breccia on the floor of the sinkhole. Visser (1944) and later workers have noted that although locally brecciated, primary layering in the Manganore Formation is both recognisable and laterally continuous. This is inconsistent with the sinkhole model of Van Wyk (1980) and Van Schalkwyk and Beukes (1986) as one would expect primary layering in lithified Asbestos Hills Subgroup rocks to be chaotically disrupted by slumping/mass-wasting into an underlying cave.

It is suggested here that the Manganore Formation is a correlate of the Beaumont Formation. Both units were deposited subsequent to folding of the Griqualand West Supergroup (which they overlie with angular unconformity) but prior to deposition of the Olifantshoek Supergroup. Both units consist predominantly of hematite-rich, banded ironstones that locally contain hematite iron ore.

The Wolhaarkop Formation was probably deposited during a period of chemical weathering and erosion of the Griqualand West Supergroup, leading to the formation of a karst topography in the Campbellrand

Subgroup. The Wolhaarkop Formation breccia may represent a solution collapse breccia as suggested by Van Wyk (1980) and Van Schalkwyk and Beukes (1986). Locally, the Wolhaarkop Formation comprises a chert pebble conglomerate (Van Wyk, 1980), that was deposited on this unconformity prior to deposition of the banded ironstones. The depositional palaeo-environment of the Beaumont and Manganore Formations, and the genesis of the hematite ore bodies therein, remains unclear. The Beaumont and Manganore Formations are preserved as lenses in pre-depositional, palaeo-topographic lows (on the karstic weathering surface in the Campbellrand Subgroup) below the unconformity at the base of the Olifantshoek Supergroup.

If the Beaumont Formation represents a lateral equivalent of the Hotazel and Mooidraai Formations as suggested by Beukes (1983), then the Hotazel Formation should unconformably overlie the Ongeluk Formation lavas in the Kalahari Manganese Field. Most previous workers have interpreted the Hotazel Formation to conformably overlie the Ongeluk Formation (e.g. Nel *et al.*, 1986; Gutzmer and Beukes, 1985). If this interpretation is correct then the manganese-rich Hotazel Formation cannot be a Beaumont Formation correlate. It is worthwhile noting that Jennings (1986) interpreted the contact between the Hotazel Formation and the Ongeluk Formation as erosional and recognised pre-Hotazel Formation palaeo-topography at the Middelpaats mine situated south of Hotazel. The age and stratigraphic correlation of the Hotazel and Mooidraai Formations thus remains uncertain.

8.6 The Olifantshoek Supergroup depository

The Olifantshoek Supergroup overlies the Griqualand West Supergroup with angular unconformity and the Beaumont Formation with disconformity. In the Boegoeberg dam area (Map 1), the Olifantshoek Supergroup and the Beaumont Formation have an ENE strike and northerly dip. This trend is in strong contrast to the north-south striking, east-dipping trend of the Griqualand West Supergroup. It is unclear whether the Beaumont Formation represents some initial stage related to geological events that ultimately resulted in the evolution of the depository that hosted the Olifantshoek Supergroup.

Very few process related studies of the Olifantshoek Supergroup have been made in an attempt to explain the tectonic setting of its depository. Cooper (1978) suggested that the Olifantshoek Supergroup was deposited in a north-south striking, ensialic rift that developed as a result of “*an aborted attempt at continental drift*”. This interpretation was based on observations made in the Magondi belt and the apparent alignment of the Magondi belt with the Kheis belt. Hartnady *et al.* (1985) and Stowe (1986) suggested that the Olifantshoek Supergroup was deposited as a series of clastic wedges that prograded

westwards from the Kaapvaal Craton but gave no indication of the tectonic setting of the depository. Cornell (1987) suggested that the Olifantshoek Supergroup represents a "*miogeosynclinal sequence deposited after rifting*" that reflects the "*early stages of the development of a north-south trending passive continental margin*". The term "miogeosyncline" is defined in Howell (1995) as: "*An archaic term for the thick, nonvolcanic, carbonate- and clastic-rich strata along a continental margin*" and is clearly misused in this context. Nevertheless, these suggestions by Cornell (1987) are the first reference to the possibility that the Olifantshoek Supergroup depository might be related to rifting of the Kaapvaal Craton, or its margin, and not an ensialic basin. Cheney *et al.* (1990) correlated the Olifantshoek Supergroup with the geographically separated Soutpansberg, Waterberg and Palapye Groups and considered each Group to represent an erosional remnant of much larger basin that once covered large tracts of the combined Kaapvaal-Zimbabwe Craton.

Any attempt to analyse the tectonic setting of the Olifantshoek Supergroup depository is severely hindered by the poor exposure, uncertain internal stratigraphy and regional correlation of the units exposed in the western part of the Kheis belt (viz.: the Groblershoop Formation, the Kaaie Group and the Zonderhuis Formation). The rocks in this area have been strongly deformed during the Kheis orogeny and the stratigraphy has been imbricated by several thrust sense shear zones (Stowe, 1986). To the west and north-west of these units of uncertain stratigraphic correlation the Kheis belt is covered by Kalahari sand. In the south-west, the Kheis belt is truncated by the Namaqua belt.

In the eastern part of the Kheis belt, that formed the focus of this investigation, the stratigraphy and broad sedimentological characteristics of the Olifantshoek Supergroup have been ascertained with a reasonable amount of confidence. What shall be attempted here is to determine the tectonic setting of the Olifantshoek Supergroup *sensu stricto*. As the distribution of the units of uncertain stratigraphic correlation in the western part of the Kheis belt is largely structurally controlled, possible correlations of these units will be evaluated in the discussion dealing with the Kheis orogeny (section 8.8).

The Mapedi Formation is the lowermost unit of the Olifantshoek Supergroup and overlies the Griqualand West Supergroup with angular unconformity. The basal conglomerate or shale of the Mapedi Formation, and the immediately overlying clastic sediments, were deposited in a fluvio-deltaic palaeo-environment (Beukes and Smit, 1987, this study). These sediments are conformably overlain by a mafic lava horizon. Conformably overlying the mafic lavas are a series of clastic and carbonate sediments that record a conformable transition from a fluvio-deltaic to a shallow marine palaeo-environment (i.e. a marine transgression).

The base of the Lucknow Formation is marked by a disconformity, upon which high energy fluvial sediments are preserved, indicating a rapid fall in alluvial base level. In places large amounts, or all, of the Mapedi Formation has been removed at this disconformity. The preserved part of the Mapedi Formation may therefore represent only a small amount of the original succession. The Lucknow Formation fluvial sediments are disconformably overlain by the basal conglomerate or agglomerate of the Hartley Formation. The basal agglomerate has a tuffaceous matrix and volcanic clasts in places and is interpreted to be a debris flow. In the Boegoeberg dam area the Hartley Formation rests disconformably on the Mapedi Formation or the Voelwater Subgroup, indicating that the Lucknow Formation and large parts of the Mapedi Formation have been eroded. In the Korannaberge, a sedimentary breccia developed at the base of the Hartley Formation is interpreted to be a talus slope deposit. This implies that localised uplift (i.e. some tectonic control) and mass-wasting of the underlying strata occurred prior to extrusion of the Hartley Formation lavas (see Appendix 1 for Hartley Formation lava geochemistry). The Hartley Formation volcanism was localised, and in places the Matsap Formation disconformably overlies older units of the Olifantshoek Supergroup or the Voelwater Subgroup. At these localities a basal conglomerate is developed. As the Matsap Formation conformably overlies the Hartley Formation elsewhere, this conglomerate is regarded as a lateral equivalent of the Hartley Formation. Where developed, the Hartley Formation consists of basaltic lavas (Cornell, 1987), pyroclastics and clastic sediments. Pillow lavas are developed in places indicating sub-aqueous extrusion for at least some of the lava flows. The proportion of clastic sediments increases towards the top of the unit.

The Matsap and Brulsand Formations record an overall transition from a high energy fluvial, to a shallow marine siliclastic palaeo-environment (i.e. a marine transgression). The upper part of the Hartley Formation, and the Fuller member (Matsap Formation), contain thick, poorly sorted conglomerate units indicative of a proximal, high energy environment. The amount of coarse grained material (conglomerate) decreases upwards through the Ellies Rus and Glen Lyon members. Quartzites in the Verwater member (Brulsand Formation) contain sedimentary structures (herring-bone cross bedding, desiccation cracks) indicative of an intertidal environment. The interpretation of the Top Dog member (Brulsand Formation) as a shallow marine, high energy siliclastic deposit is based on the maturity of the quartzites, indications of upper flow regime conditions (thick planar bedded heavy mineral bands) and its stratigraphic position overlying the intertidal Verwater member. The Groblershoop Formation pelitic schists with quartzite intercalations may represent deeper water marine sediments related to this second marine transgression.

Mafic (basaltic) volcanism in association with high energy, proximal fluvial sediments, is typical (but not diagnostic) of the initial basin-fill of depositories that develop in response to rifting of the continental

lithosphere (e.g. Bond *et al.*, 1985, Thompson *et al.*, 1987, Dalziel *et al.*, 1987). Both ancient (e.g. the Canadian Cordillera) and more recent (e.g. the north-west Atlantic) continental rift successions have been recognised for many years yet debate still continues as to the precise mechanism that causes extension and rifting of the continental lithosphere. Two basic models for rifting have been proposed, these are commonly termed the “active” and “passive” mechanisms (Allen and Allen, 1990). The proponents of active rifting (e.g. Burke and Dewey, 1973) argue that thermal effects generated by mantle plumes cause thinning of the continental lithosphere and subsequent isostatic uplift. The extensional forces necessary for the generation of the rift are created by the doming associated with this uplift. Passive rifting models (e.g. McKenzie, 1978) involve thinning of the continental lithosphere as a result of regional tensional forces exerted by lithospheric plate configurations and plate boundary phenomenon (i.e. caused by plate tectonics). These tensional forces cause failure of the continental lithosphere, initiation of rifting, and allow passive upwelling of hot material from the asthenosphere. “Active” and “passive” rift mechanisms represent idealised end members. In reality the development of rifts may be characterised by aspects of each (Allen and Allen, 1990).

In the simplest scenario (regardless of the mechanism that initiates rifting), continental rift-related basins can be regarded as having a two stage development. The initial *rift stage* is characterised by extensional faulting. At the end of rifting, extensional faulting ceases and the rift system subsides in response to cooling and thermal contraction of the lithosphere. This second stage is referred to as the *thermal subsidence* or *post-rift stage*.

Extensional faulting during the rift stage of basin development results in the formation of half-graben, typically linked to listric normal faults that extend into the basement rocks (Thompson *et al.*, 1987; Allen and Allen, 1990). The development of these structures results in localised, rapid falls in alluvial base level and the deposition of proximal conglomerates and immature fluvial clastic sediments. Typically, fault blocks are stripped of stratigraphy and the conglomerates in the half-graben are characterised by clasts derived from the adjacent fault block (Thompson *et al.*, 1987). The rift stage is often characterised by relatively abrupt lateral facies and thickness variations, the presence of mafic volcanics and volcanoclastic conglomerates (Bond *et al.*, 1985).

The Olifantshoek Supergroup shows an overall proximal to distal facies polarity, moving westwards from the Kaapvaal Craton. Thus if the Olifantshoek Supergroup was deposited in a rift related setting, it is reasonable to assume that most extensional faults associated with the rifting would have had an approximately north-south trend

The Mapedi Formation records a transition from a shallow water, high energy fluvio-deltaic palaeo-environment to a shallow marine, high energy palaeo-environment. The Lucknow Formation, Hartley Formation and Fuller member contain high energy fluvial clastics such as thick conglomerate horizons, and in the case of the Hartley Formation volcanoclastic debris flows also. The sedimentary breccia observed at the base of the Hartley Formation in the Korannaberge may represent a talus slope deposit caused by extensional faulting prior to extrusion of the Hartley Formation lavas. No direct evidence for extensional faulting that occurred pre-and syn-Olifantshoek Supergroup deposition was observed but it is likely that any north-south trending extensional faults would have been reactivated (inverted) as thrusts during the Kheis orogeny. Clasts in the conglomerate and debris flow volcanoclastics of the Olifantshoek Supergroup are almost entirely derived from underlying strata of the Olifantshoek Supergroup and the Voelwater Subgroup. The numerous disconformities, recording rapid falls in alluvial base level, provide additional evidence of deposition in a fault controlled, extensional setting. North-south trending, subvertical normal faults in the Black Rock area post-date the Mapedi and Lucknow Formations but pre-date the Kheis orogeny (Gutzmer and Beukes, 1995). These faults could conceivably be related to rifting during deposition of the Hartley Formation and Fuller member.

Further evidence for a rift related origin for the Olifantshoek Supergroup comes from palaeocurrent analysis of the Volop Group by Jansen (1983). Palaeocurrent directions for the Fuller member (measured by Jansen *op cit.* at several localities along the strike of the Korannaberge-Langberge) are indicative of a mean southerly palaeocurrent, but locally show variations in sediment transport direction that vary from east to west. The mean southerly directed palaeocurrent vector, perpendicular to the regional east-west facies polarity suggests that the Fuller member was deposited in a fault controlled setting analogous to the Tanganyika basin in the East African rift. In the Tanganyika basin, sediment input in the rift is derived largely from the rift flanks, yet overall sediment transport is parallel to the rift in an axial river (Allen and Allen, 1990).

Continental rifting is the initial stage of a sequence that can lead to rupture of the continental crust and generation of a new ocean basin. Sedimentation during the thermal subsidence stage typically records a transition from the high energy, fluvial palaeo-environment of the rift stage to marine sedimentation as the new ocean basin is developed (Allen and Allen, 1990). After deposition of the high energy fluvial sediments and volcanics of the Fuller Member a gradual marine transgression occurred. Palaeocurrent directions in the Ellies Rus member indicate a polymodal, south to westerly directed sediment transport direction (Jansen, 1983). The Glen Lyon member and Brulsand Formation show a westerly (or east-west in the case of the intertidal Verwater member) palaeocurrent, with little variation in direction either

locally or along the strike of the Korannaberge-Langberge (Jansen, 1983). The change in palaeocurrent direction from southerly (Fuller member) to westerly is consistent with fault controlled sedimentation being replaced by sedimentation in a gradually subsiding basin (deepening westwards) that developed during a thermal subsidence phase.

It is therefore suggested that the Olifantshoek Supergroup was deposited in a north-south trending continental rift-passive margin setting. Multiple rifting events each showing a rift- and thermal subsidence- stage are common in the evolution of passive continental margins that develop as a result of the rifting of continental lithosphere (e.g. Thompson *et al.*, 1987). The Mapedi Formation is interpreted to represent the volcanics and sediments deposited during an early rifting event. The lower fluvial sediments and the mafic lava represent the rift stage. The rift stage was followed by a marine transgression in response to thermal subsidence. Renewed extension and consequent drop in alluvial base levels led to erosion of large parts of the Mapedi Formation. The Lucknow Formation, Hartley Formation and Fuller member were deposited during the rift stage of this event. The gradual marine transgression that occurred subsequent to Fuller member deposition is interpreted to represent the thermal subsidence stage associated with the development of a north-south trending, passive continental margin along the western margin of the Kaapvaal Craton.

The age and duration of the rifting and deposition of the Olifantshoek Supergroup is poorly constrained. The onset of crustal extension must have occurred after ≈ 2222 Ma (the age of the Ongeluk Formation) but prior to ≈ 1928 Ma (the age of the Hartley Formation). The upper limit on Olifantshoek Supergroup deposition is defined by the onset of Namaqua orogenesis at ≈ 1.2 Ga.

Continental rifting often occurs along favourably aligned, pre-existing structural weaknesses in the continental crust (Park, 1990). The geometry of early structural elements in the Kraaipan greenstone belt (Figure 8.1) and magnetic anomalies in the western part of the Kaapvaal Craton suggest that the Archaean basement rocks in this area have an approximately north-south structural grain (Vearncombe, 1986; De Wit *et al.*, 1992). It is probable therefore that rifting of the Kaapvaal Craton occurred along north-south orientated structural discontinuities that resulted from accretionary tectonics during the Mid- to Late-Archaean.

8.7 The significance of the mafic intrusions

In all the areas investigated during this study, spanning the entire length of the Kheis belt, gabbro-norite sills were observed in the Olifantshoek Supergroup. The sills post-date the Olifantshoek Supergroup, but intruded prior to the Kheis orogeny. A gravity survey across the Kheis belt by Geerthsen *et al.* (1991) identified the presence of a significant gravity high, situated below the Olifantshoek Supergroup, that was inconsistent with the surface geology. Geerthsen *et al.* (1991) suggested that the causative body of this geophysical anomaly was a large mafic intrusion. The gabbro-norite sills observed at surface may therefore represent satellite intrusions related to a large mafic intrusion that occurs, at depth, below the Olifantshoek Supergroup.

8.8 The Kheis orogeny

The Kheis belt comprises rocks of the Griqualand West Supergroup, the Olifantshoek Supergroup, the Kaaiaen Group and the Zonderhuis Formation that have been deformed during a craton-vergent orogenic event, termed the Kheis orogeny. Observations from the Marydale basement high indicate that the basement rocks were deformed during this event. Structural elements produced during the Kheis orogeny include folds, brittle-ductile thrust sense shear zones (that juxtapose older strata over younger strata) and bedding sub-parallel, thrust sense shear zones.

Linear orogenic belts such as the Kheis belt develop in response to regional compression resulting from the interaction of two plates along a destructive plate boundary. In any collisional event involving one or more stable cratons or shields comprised of continental crust (such as the Kaapvaal Craton), it is usual to find that the folds and thrusts are directed outwards from the internal zone, or hinterland, of the orogenic belt towards one of the adjacent stable cratons or shields. A continental crustal block towards or over which the folds and thrusts verge is termed the foreland.

Most of the terminology utilised in the description of fold and thrust belts has been developed by workers in the North American Cordillera. In this region, a distinction is made between “thin-skinned” and “thick-skinned” thrust belts. In thin-skinned thrust belts, thrusting is confined to non-crystalline supra-crustal “cover rocks”. In thick-skinned fold and thrust belts both crystalline basement rocks and cover rocks are involved in the deformation.

Although it is useful to distinguish between belts characterised by thin- and thick-skinned tectonics, it has been demonstrated that both thin-skinned and thick-skinned deformation occurs within a single orogenic belt (e.g. Hatcher and Hooper, 1992). The internal zone of an orogen is characterised by thick-skinned tectonics (basement rocks are thrust over younger cover rocks). Thin skinned deformation typically occurs in the external part of an orogen. In literature dealing with the North American Cordillera (e.g. Evenchick, 1992), that part of an orogen characterised by thin-skinned deformation, is referred to as a foreland fold and thrust belt. The lowermost thrust in a foreland fold and thrust belt typically links up with a basal detachment situated at the contact between the cover rocks and the underlying basement rocks.

The Kheis belt is characterised by structural repetition of the Griqualand West Supergroup, the Olifantshoek Supergroup and supra-crustal rocks of uncertain correlation leading Stowe (1986) to suggest that the Kheis belt is a thin-skinned foreland fold and thrust belt, analogous to those described from the North American Cordillera. There are however, several significant differences between the geometry of the Kheis belt and the classic geometry of “Cordilleran type” foreland fold and thrust belts. These will be discussed in the paragraphs that follow.

In Cordilleran type foreland fold and thrust belts, the lowermost thrust in a fold and thrust belt, referred to as the sole thrust, follows the contact between the crystalline basement rocks and the overlying cover rocks and is often referred to as a basal detachment or décollement. At the external margin of the fold and thrust belt the sole-thrust typically steepens or “ramps”, cutting up through the overlying cover rocks, but does not necessarily reach the palaeo-surface.

Beukes and Smit (1987) noted that no eastward vergent thrusts could be recognised east of the Blackridge thrust and suggested that it represents the sole thrust to the Kheis fold and thrust belt. McClay (1992) defines a sole thrust as “*The lowermost thrust common to a thrust system*”. Implicit in this definition is that all overlying thrusts are geometrically, kinematically and mechanically linked to the sole thrust. Thrust systems can occur on any scale and do not necessarily refer to an entire fold and thrust belt (McClay, 1992).

In the Boegoeberg dam area, a zone of overturned- to upright- folds occurs in the immediate footwall of the Blackridge thrust system. East and south of this folded zone, no Kheis-age thrusts, folds or foliation were observed in the Griqualand West Supergroup. Thus observations made during this study support the suggestion made by Beukes and Smit (1987) that the Blackridge thrust is the easternmost thrust that

developed during the Kheis orogeny. Does this imply that the Blackridge thrust is linked to a basal detachment at the interface between the basement and the cover-rocks? Not necessarily.

In the Boegoeberg dam area (Map 2), the Blackridge thrust branches into a complex imbricate system. The lowermost thrust in this system dips steeply to the north-west and cuts down stratigraphy into the Zeekoebaart Formation and the Archaean granitoids of the Marydale basement high (Map 1) implying basement involvement, during thrusting, in the external margin of the Kheis fold and thrust belt. This is inconsistent with the Blackridge thrust system linking at depth with a basal detachment at the interface between the basement and the cover-rocks.

Two classical models have been proposed to account for the interactive development of folds and faults in thrust systems: the fault-bend and fault-propagation models (Suppe, 1983, 1985). In both, folding is essentially a result of propagation of the thrust. Both models assume that layer thickness remains constant during thrusting and the resultant folding. This leads to the development of folds with kink-band geometry. In these classic models the folds are only formed in the hangingwall of the thrust. Any folds that underlie the thrust plane are interpreted to be fault bend folds formed in the hanging-wall of a deeper thrust. Although these models do not account for every observed structure, they have been successfully applied in foreland fold and thrust belts in the North American Cordillera.

The fold and thrust geometry of the Kheis belt cannot be reconciled with either of the classic models of fold and thrust interaction. The folds in the eastern part of the Kheis belt have rounded hinges and formed mainly by a process of flexural slip. The folds are upright except in the immediate hanging- and foot-wall of a brittle-ductile thrust sense shear zone (where they are overturned towards the craton). West dipping, thrust sense shear zones cutting across east-dipping fold limbs were observed in the Korannaberge-Langberge mountain chain. This suggests that upright folds formed as a result of layer-parallel shortening during the initial stages of the Kheis orogeny. Continued shortening resulted in the development of west-dipping, brittle-ductile thrust sense shear zones and the overturning of originally upright folds. The fold and thrust geometry in the eastern part of the Kheis belt indicates that the Kheis belt was deformed by a different mechanism to the classical models of Suppe (1983, 1986) invoked for the North American Cordillera.

These observations imply that the Kheis belt cannot be modelled in terms of a simple thrust system with a basal detachment situated at the basement-cover interface. What other mechanisms can be invoked to explain “Kheis type” fold and thrust geometry at the external margin of an orogenic belt? Perhaps the

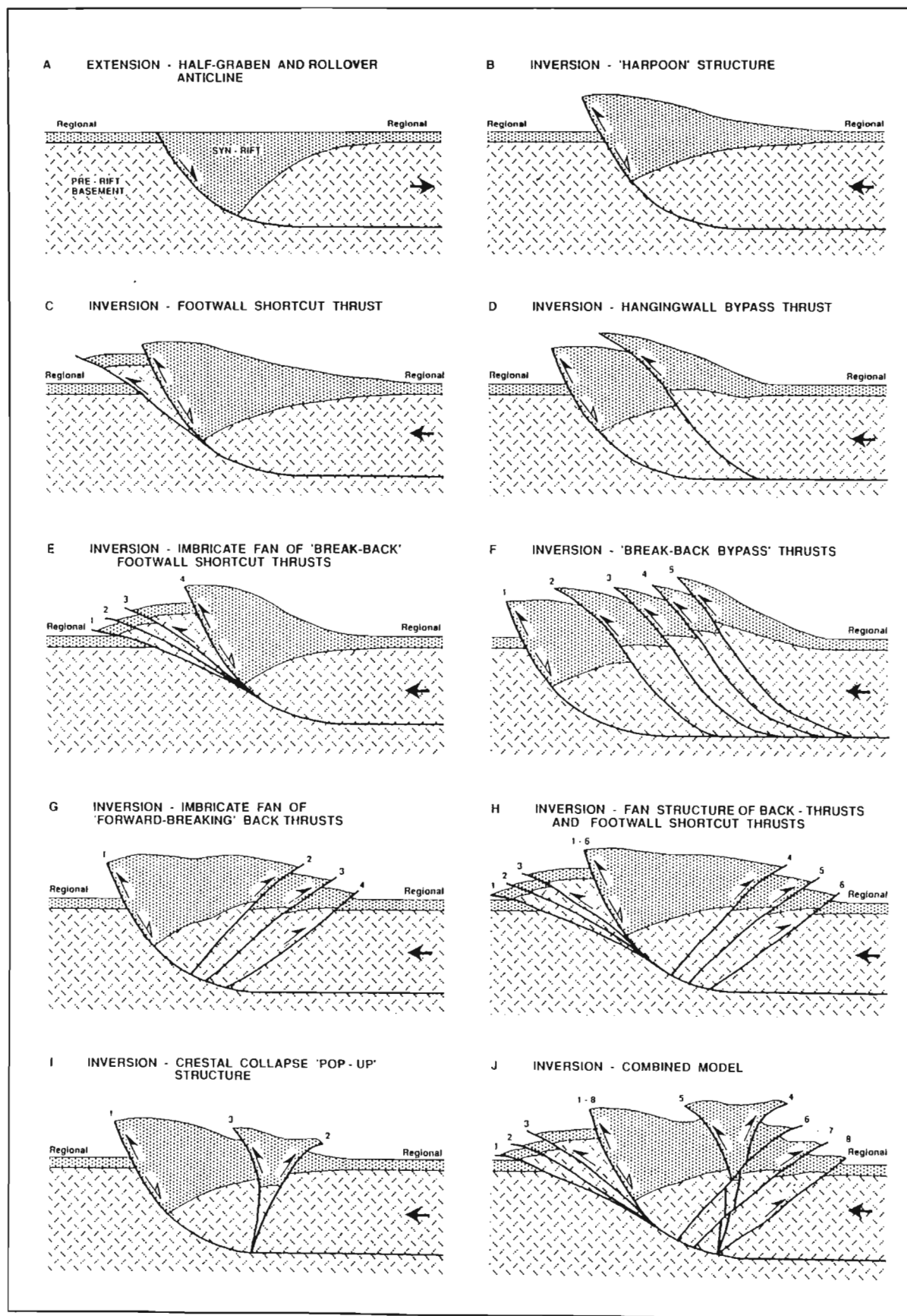
answer lies in the previous history of the western edge of the Kaapvaal Craton. The Olifantshoek Supergroup formed in a continental rift-passive margin setting. During rifting, extensional faults develop. These faults deform both the pre-rift supracrustals as well as the basement rock of the rifted shield or craton and typically dip away from the continental margin. Does inversion tectonics provide the answer?

The architecture of thrust systems in inverted extensional basins is often influenced, and in many cases strongly controlled, by pre-existing extensional fault geometries (McClay and Buchanan, 1992). In such cases the thrust faults have geometries and trajectories that are significantly different to those found in typical “Cordilleran type” foreland fold and thrust belts. Invariably, the geometry of a fold and thrust belt formed by basin inversion is far more complex than that observed in Cordilleran type belts. The development of fold and thrust belts in pre-existing extensional basins is a relatively new concept and as yet no “unifying” model has been proposed. This is advantageous as the documented geometry of inverted basins is thus geologically controlled and not model dependant. What is clear from the literature (McClay and Buchanan, 1992) is that a large variety of geometries can exist in inverted extensional basins. Some of the features that typically occur in inverted extensional basins are shown in Figure 8.2.

The observed fold and thrust geometry of the eastern part of the Kheis belt is very similar to that documented from the Variscan fold and thrust belt in south Wales by Powell (1989). The Variscan fold and thrust belt (Figure 8.3) comprises a “two-stage rift”-passive margin sequence, that has been thrust over Precambrian and lower-Palaeozoic basement rocks. Deformation during the orogenic event that produced the fold and thrust belt was largely controlled by pre-existing extensional faults that developed during rifting.

On the right-hand side of Figure 8.3, rift related strata unconformably overlie the basement rocks and dip towards the hinterland (hintward dipping) at shallow angles. This part of the section is equated with the shallow hintward dipping, Olifantshoek Supergroup rocks that unconformably overlie the Griqualand West Supergroup in the footwall of the Blackridge thrust (Map 1). The Johnston thrust system is a low angle, short-cut thrust system (Figure 8.2; Figure 8.3) developed in the footwall of a reactivated extensional fault (the Benton fault). The Blackridge thrust shows similar, shallow hintward dipping, geometry along most of the Kheis belt (Beukes and Smit, 1987). However, in the Boegoeberg dam area, the Blackridge thrust system dips steeply to the north-west. In this area, the Blackridge thrust system cuts down section through the Griqualand West Supergroup into the basement rocks of the Marydale basement high, yet remains sub-parallel to the trend of the overlying Olifantshoek Supergroup. This may indicate the position where a shallow dipping, short-cut thrust fault system (the Blackridge thrust) links up with a

Figure 8.2: Conceptual models for thrust faults developed by the inversion of an extensional listric fault (from: McClay and Buchanan, 1992).



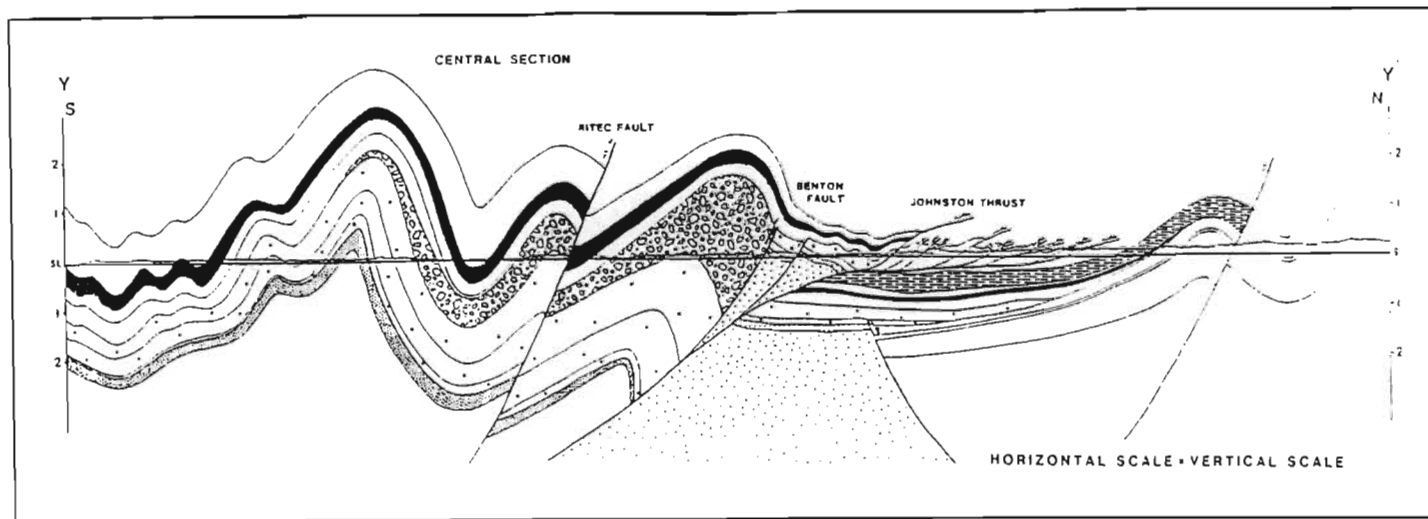


Figure 8.3: Cross section of the Variscan fold and thrust belt, south west Wales. (from: Powell, 1989).

steeply dipping, reactivated extensional fault (i.e. an equivalent structural relationship to that illustrated by the zone where Johnston thrust links up with the Benton fault in Figure 8.3). This would explain the awkward geometry of the cross-sections of the Boegoeberg dam area (Figures 4.19, 4.20).

In the area east of Olifantshoek (Map 1, Figure 3.21), the Korannaberg thrust dips at a shallow angle to the west, sub-parallel to bedding in the Beaumont Formation (Voelwater Subgroup), along the contact between the Beaumont Formation and the Ongeluk Formation. This apparent younger-over-older thrusting probably represents a sheared unconformity between the Beaumont Formation and the Ongeluk Formation that has been preferentially utilised by the Korannaberg thrust. In the area north of Olifantshoek, the Korannaberg thrust cuts up-section (i.e. “ramps”). The Korannaberg thrust in the Traverse 4 area comprises three branches that are interpreted to link-up down section (Map 1). The close association between the sedimentary breccia (fault scarp deposit?) at the base of the Hartley Formation and the central splay of the Korannaberg thrust suggests that the steepening of the Korannaberg thrust system in this area may be due to inversion of pre-existing extensional faults.

In the Olifantshoek Supergroup, folds are overturned in either the hanging- and foot-wall, or just the hangingwall, of major thrust sense shear zones. In this aspect, the style of deformation differs from that of the Variscan fold and thrust belt, where folds are only overturned in the hangingwall of reactivated normal faults. The observation that in the Kheis belt, at least some of the folds pre-date the thrusts, suggests that the folds formed during the early stages of the orogeny and were subsequently sheared along thrust sense shear zones to form overturned anticline-syncline pairs.

With the exception of the central part of the Traverse 1 area, no major thrust sense shear zones were observed in the Matsap and Brulsand Formations that form the Korannaberge-Langberge mountain chain. Both small-scale and large-scale folds in this area are upright to slightly west inclined, open to close structures (Figures 3.20; 3.21), that exhibit very similar geometry to that those developed in the hangingwall of the Ritec fault in the Variscan fold and thrust belt (Figure 8.3).

It is important to note that even in a fold and thrust belt in which the thrust geometry has been controlled by pre-existing listric normal faults the basal thrust must link up with a detachment zone at depth. The Blackridge thrust cuts down into the Skalkseput granite, therefore the basal detachment of the Kheis belt must be rooted within the basement rocks of the Kaapvaal Craton.

Thus the geometry of the eastern part of the Kheis belt exhibits features consistent with deformation during the Kheis orogeny being largely controlled by pre-existing normal faults. What about the western part of the Kheis belt?

The only regional study of the western part of the Kheis belt that incorporates observations regarding the overall structural framework is that of Stowe (1986). Stowe (1986) divided the western part of the Kheis belt into two terranes: the Skeurberg terrane in the east and the Diepklip terrane in the west. Although the use of the term “terrane” is not recommended here because of its genetic implications it shall be retained for descriptive purposes.

The eastern boundary of the Skeurberg terrane was taken to be a thrust sense shear zone developed at the contact between the Brulsand Formation and the Groblershoop Formation. This shear zone is exposed at locality 7.1 (Map 1) but is not indicated as a thrust for reasons that follow. At locality 7.1 highly sheared meta-basite (possibly equivalent to the gabbro-norite sills in the Boegoeberg dam area) separates mylonitised Brulsand Formation quartzites in the footwall from Groblershoop Formation schists in the hangingwall. Tight, overturned folds occur in discrete zones in the Brulsand Formation. The foliation in the shear zone strikes north-east and dips steeply to the north-west, sub-parallel to the lithological layering in the quartzites. Mineral elongation lineations plunge down the dip of the foliation to the north-west. S-C fabrics indicate a north-west over south-east, thrust sense of movement. As the foliation is bedding sub-parallel, this shear zone probably represents a sheared sedimentary contact (that was intruded by a mafic sill prior to the Kheis orogeny) between the Brulsand Formation and the overlying Groblershoop Formation schists. The bedding sub-parallel thrust sense shear zone does not cause

duplication of stratigraphy and as such is not indicated as a thrust on Map 1. The shear zone nevertheless represents a high strain zone.

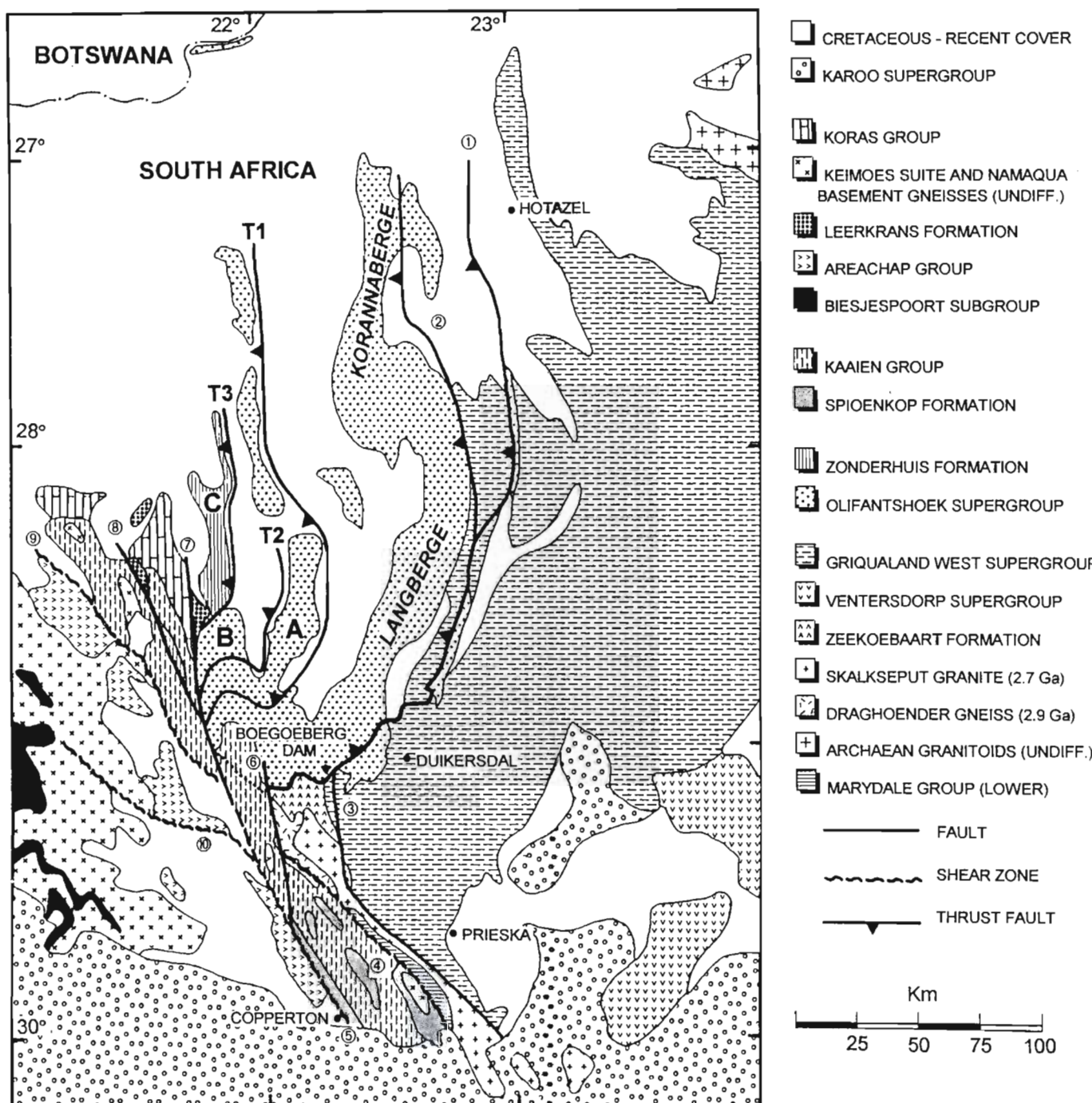
A quartzite unit, included in the Groblershoop Formation by SACS (1980), that forms a prominent range of hills called the Skurweberge (Map 1), has been thrust over schists of the Groblershoop Formation (Stowe, 1986). Stowe (1986) termed this unit the Skeurberg quartzite. The Skeurberg quartzite is indicated on Figure 8.4 as thrust sheet A, it has been thrust over schists of the Groblershoop Formation along thrust T1. Moen (1980) considered the Skeurberg quartzite to be part of the Groblershoop Formation and correlated it with the Uitdraai Formation (Kaaie Group) of SACS (1980). Moen (1980) noted that the Skeurberg quartzite comprises grey quartzite, with thick planar bedded heavy mineral layers, interbedded with “sericitic sandstone”. Similar lithotypes (quartzite with planar bedded heavy mineral bands and meta-psammite) form the Brulsand Formation along the western edge of the Korannaberg-Langberge.

In the study of the quartzites that outcrop in the Molopo River area (Map 1) it was noted that these rocks are very similar to the Brulsand Formation quartzites exposed on the western flanks of the Korannaberg-Langberge. The Molopo River outcrops occur along strike of the Skeurberg quartzite.

U-Pb (single zircon SHRIMP) dating of detrital zircons from the Skeurberg quartzite indicates that this unit must be younger than ≈ 1850 Ma (Pers. comm. R.A. Armstrong). The Matsap and the Brulsand Formations overlie the 1928 ± 4 Ma Hartley Formation. All of these units were deformed during the Kheis orogeny, prior to the ≈ 1.2 Ga extended Namaqua orogeny. The Brulsand Formation and the Skeurberg quartzite were thus deposited in the same, albeit very broad, time interval. It is suggested here that the Skeurberg quartzite may be an equivalent of the Brulsand Formation that has been thrust over the Groblershoop Formation schists during the Kheis orogeny. The Skeurberg quartzite is therefore shown as part of the Groblershoop Formation on Map 1 (i.e. a unit of uncertain internal stratigraphy and correlation).

The contact between the Skeurberg quartzite and the overlying rocks of thrust sheet B is marked by a west dipping, thrust sense shear zone (Stowe, 1986) labelled T2 on Figure 8.4. Thrust sheet B (Figure 8.4) has been interpreted by SACS (1980), Moen (1980) and Stowe (1986) to be part of the Groblershoop Formation as it is dominated by schistose rocks with narrow quartzite intercalations. If the Skeurberg quartzite is a correlate of the Brulsand Formation, as suggested here, then thrust T2 may represent a

Figure 8.4: Simplified geological map of the south-western part of the Kaapvaal Craton, the Kheis belt, the Kaaiken domain and the eastern part of the Namaqua belt. ①= Blackridge thrust; ②= Korannaberg thrust; ③= Doringberg fault; ④= Doornberg s.z.; ⑤= Copperton s.z.; ⑥= Brulpan fault; ⑦= Brakbos fault; ⑧= Dagbreek fault; ⑨= Straussberg s.z.; ⑩= Boven-Rugzeer s.z. The approximate eastern boundary of Kheis belt is marked by ①. The boundary between the Kheis belt and Kaaiken domain is formed by ④, ⑥, dotted line and ⑦. The boundary between the Kaaiken domain and the Namaqua belt is marked by ⑤ and ⑨. T1, T2 and T3 refer to thrusts discussed in the text. A, B and C refer to the thrust sheets bounded by these thrusts.



bedding sub-parallel shear zone developed along an originally sedimentary contact between the Brulsand Formation and Groblershoop Formation schist (analogous to that exposed at locality 7.1).

Thrust T3 (Figure 8.4) was taken by Stowe (1986) to form the boundary between the Skeurberg terrane and the Diepklip terrane. The Diepklip terrane consists of rocks of the Zonderhuis Formation. The Zonderhuis Formation has been included in the Wilgenhoutsdrif Group of SACS (1980), stratigraphically underlying the Leerkrans Formation. The inclusion of the Zonderhuis Formation and the Leerkrans Formation into one Group by SACS (1980) was based on the interpretation by Moen (1980) that the Leerkrans Formation conformably overlies the Zonderhuis Formation. Stowe (1986) observed that while structural elements related to both the Kheis and extended Namaqua orogenies can be recognised in the Zonderhuis Formation, only Namaqua age structures are developed in the Leerkrans Formation. The Zonderhuis Formation is thus older than the Leerkrans Formation and any contact between the two units should be viewed as being either tectonic or an angular unconformity.

The Zonderhuis Formation in the Diepklip terrane has a north-south trend and is interpreted to form part of the Kheis belt. It has been highly strained and bedding is seldom observed, but where developed it strikes north-south, sub-parallel to a strongly developed, steeply west dipping foliation (Moen, 1980). Due to its highly deformed nature the internal stratigraphy of the Zonderhuis Formation in this area cannot be determined with any certainty (Moen, 1980). The Zonderhuis Formation is comprised of rocks that, based on descriptions by Moen (1980) and observations made during this study, bear a striking similarity to the lower part of the Olifantshoek Supergroup. Table 8.2 shows possible correlations. It is suggested that the Zonderhuis Formation represents highly deformed equivalents of the Mapedi Formation (and possibly the Voelwater Subgroup and Hartley Formation) that have been thrust over rocks of the Groblershoop Formation along thrust T3 (Figure 8.4).

From the lithostratigraphic evidence presented by Moen (1980) and the structural observations of Stowe (1986) it thus appears that the Skeurberg and Diepklip “terrane” of Stowe (1986) represent a series of west dipping, thrust bounded sheets of Olifantshoek Supergroup strata. The quartzite unit that forms the prominent range of mountains known as the Skurweberge is probably an equivalent of the Brulsand Formation. The Zonderhuis Formation is probably an equivalent of the Mapedi Formation (and possibly the Hartley Formation and Voelwater Subgroup). The intervening low lying areas are underlain by poorly exposed Groblershoop Formation pelitic schists with quartzite intercalations.

Zonderhuis Formation (Moen, 1980).	Possible Olifantshoek Supergroup equivalents (this study)
Light-green to grey siliceous quartzite.	<i>Mapedi Formation</i> : Green to grey, siliceous quartzite is characteristic of the upper part of the Mapedi Formation.
Green and brown phyllites interbedded with siliceous quartzite.	<i>Mapedi Formation</i> : Interbedded green coloured, brown weathering phyllites and siliceous quartzite were observed in the Map 2 and Voelwater areas.
Conglomerate containing clasts of white quartzite and red jasper.	<i>Mapedi Formation</i> : The Mapedi Formation contains conglomerate with quartzite and ferruginous chert (jasper) clasts.
Dolomite, limestone, argillaceous carbonate, calcareous quartzite.	<i>Mapedi Formation</i> : Dolomite was observed in the Olifantshoek area. Interbedded impure dolomite and calcareous quartzite occurs in the Boegoeberg dam area.
Amygdaloidal mafic lava	<i>Mapedi Formation?</i> <i>Hartley Formation?</i>
Red ferruginous chert	<i>Voelwater Subgroup?</i>
Serpentine	?

Table 8.2: Possible correlations between the Zonderhuis Formation rocks described by Moen (1980) and the Olifantshoek Supergroup.

The thrust sense shear zones that bound these thrust sheets of Olifantshoek Supergroup strata dip to the west at approximately 50° (Stowe, 1986). The internal structure of the thrust sheets is dominated by isoclinal folds, on all scales, with sharp hinges (chevron type) that are overturned to the east. The limbs of these folds are typically sheared out along small scale, thrust sense shear zones (Stowe, 1986). This style of deformation is completely different to that observed in the Olifantshoek Supergroup in the eastern part of the Kheis belt. This heterogeneity of deformation style has led workers such as Vajner (1974) and Moen (1980) to suggest that the rocks west of the Korannaberge-Langberge are unrelated to the Olifantshoek Supergroup and that the deformation elements were formed during the extended Namaqua orogeny. As noted by Stowe (1986) the intensity of deformation in the Kheis belt increases towards the west. An almost identical scenario has been documented from the Kechika Trough in the western Rocky Mountains of northern Canada by McClay *et al.* (1989). The Kechika Trough is an extensional basin that was inverted during the Columbian Laramide orogeny. A cross section of the resultant fold and thrust belt geometry is shown in Figure 8.5. Note the similarity between the style of deformation in the forward part of the belt with that of the eastern part of the Kheis belt. A short-cut thrust fault system such as the Blackridge thrust system is not developed in the Kechika Trough.

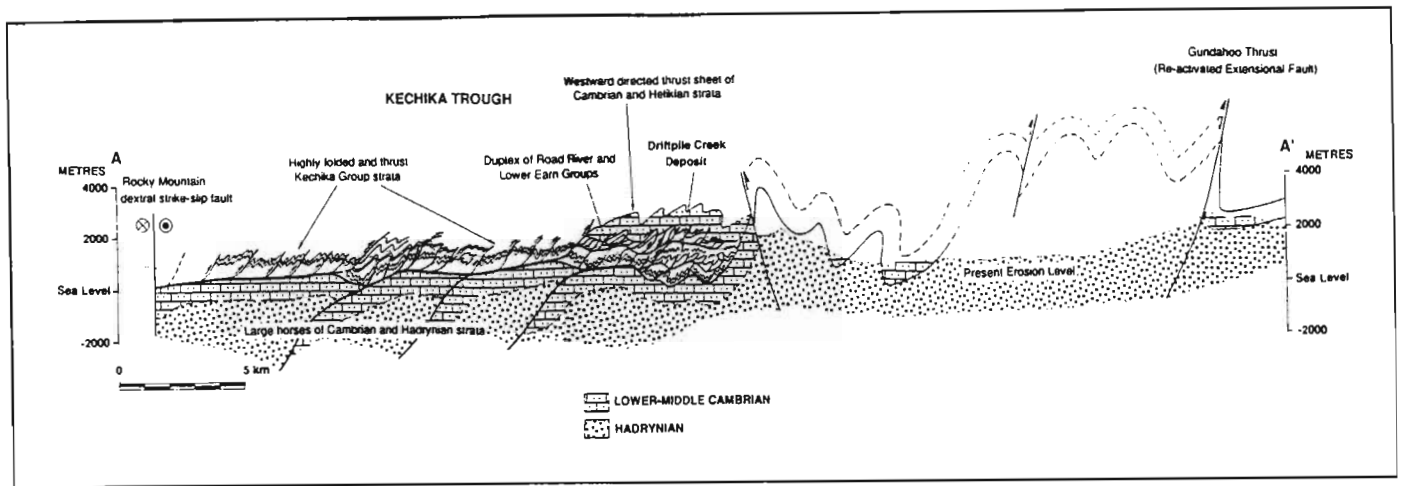


Figure 8.5: Fold and thrust geometry of the Kechika trough, western Canadian Rocky mountains. The forward part of the fold and thrust belt exhibits geometry similar to the eastern part of the Kheis belt. The western part of the belt exhibits similar features to those described by Stowe (1986) for the western part of the Kheis belt. (From: McClay *et al.*, 1989).

The western part of the inverted Kechika Trough is characterised by intense deformation, chevron folds on all scales, and numerous hinterland dipping thrust sheets (McClay *et al.*, 1989). A similar description is applicable to the western part of the Kheis belt. Thus the geometry of both the eastern and western sections of the Kheis belt is compatible with that of a foreland fold and thrust belt where deformation has largely been controlled by re-activation of extensional faults.

No description of a fold and thrust belt is complete without at least an estimate of the amount of crustal shortening that has been accommodated by the deformed strata. Beukes and Smit (1987) concluded that 35-55 km of crustal shortening has occurred as a result of displacement on the Blackridge thrust. This estimate was based on the bow-and-arrow rule of Elliot (1976) and the arcuate trace of the Blackridge thrust. It must be noted that this method should only be used to estimate thrust fault displacement when the ends of the thrust fault can be demonstrated to be terminal ends (tip points) with negligible displacement (Elliot, 1976). The northern extension of the Blackridge thrust (north of the Black Rock area) is unknown, the southern extension of the Blackridge thrust is truncated by the NNW striking zone of Namaqua shearing and faulting along the western edge of the Marydale basement high. In addition, the bow and arrow rule of Elliot (1976) was based on observations pertaining to thin skinned "Cordilleran type" fold and thrust belts. The Blackridge thrust is interpreted here to be a footwall short-cut thrust fault and as such, the amount of crustal shortening estimated to have occurred as a result of movement on the Blackridge thrust by Beukes and Smit (1987) is deemed unreliable.

Due to the numerous disconformities and complex structural relationships in the Boegoeberg dam and Traverse 1 areas, problems that are compounded by the lack of sub-surface geological control, no attempt has been made to estimate crustal shortening in these parts of the Kheis belt. A rough estimate of the minimum amount of shortening that has occurred *as a result of folding* along the eastern part of the Kheis belt has been calculated by extrapolating the contact between the Hartley Formation and Fuller member along the length of the cross-section for Traverse 2 and the Lucknow Formation-Hartley Formation contact along the length of the Traverse 3 cross-section (Figure 8.6). Simple line-length restoration of these folded contacts (assuming originally horizontal strata) implies that 28-32% of crustal shortening occurred as a result of folding. This represents an absolute minimum as it excludes: (a) shortening that resulted from movement on bedding sub-parallel thrust sense shear zones and (b) shortening that occurred as a result of stratigraphic duplication along brittle-ductile thrust sense shear zones.

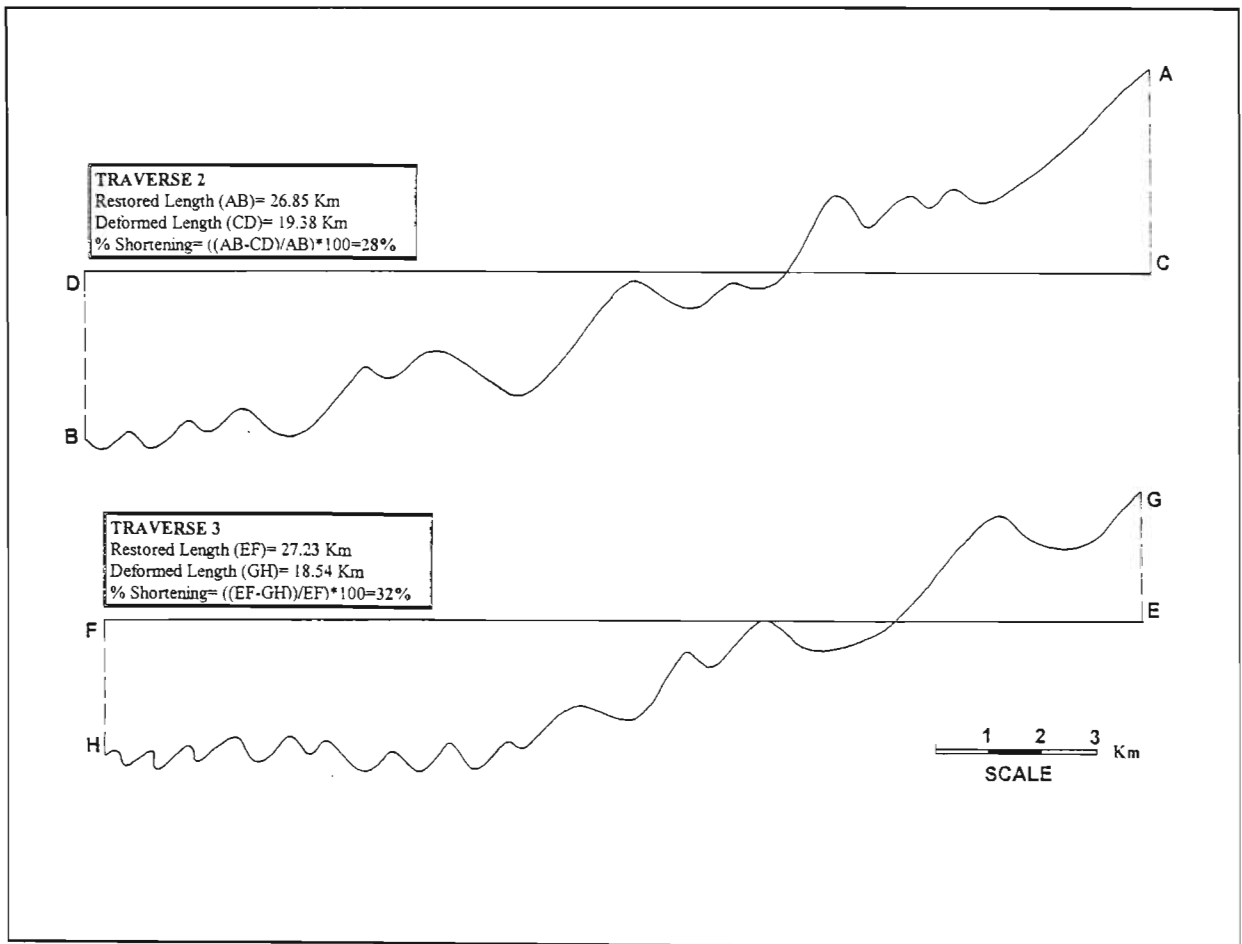


Figure 8.6: Trace of the Hartley Formation-Fuller member contact extrapolated along the length of the cross-section of Traverse 2 (Figure 3.20) and a similarly constructed section for the Lucknow Formation-Hartley Formation contact for Traverse 3 (Figure 3.21). Restored and deformed lengths of these contacts are indicated.

8.9 The extended Namaqua orogeny

The structural trend of the Kheis belt is truncated in the south-west by the combined Brulpan Fault-Doornberg shear zone (Figure 8.4). To the west of these structures, the meta-sediments of the Kaaie Group (Uitdraai, Dagbreek and Sultanaoord Formations) and Spioenkop Formation have a north-west to NNW structural trend, parallel to that of the eastern part of the Namaqua belt (Map 1). The term Kaaie domain refers to this linear zone of Olifantshoek Supergroup equivalents of uncertain stratigraphic correlation, that have been strongly overprinted during the extended Namaqua orogeny such that they have a dominant north-west to NNW structural trend. The lineaments forming the western and eastern margins of the Kaaie domain are indicated on Figure 8.4.

Both the Uitdraai Formation and the Spioenkop Formation were deformed during the Kheis orogeny but structural elements related to the Kheis orogeny have been strongly overprinted and re-orientated by ENE vergent thrust sense shear zones that developed during the ND₁ phase of the extended Namaqua orogeny. The Uitdraai and Spioenkop Formations comprise lithotypes very similar to the Brulsand Formation of the Olifantshoek Supergroup. Recent U-Pb single zircon SHRIMP dating of detrital zircons from the Uitdraai Formation indicate a maximum depositional age of ≈ 1850 Ma (Pers. comm. R.A. Armstrong), similar to that of the Skeurberg quartzite (interpreted here to be an equivalent of the Brulsand Formation). The Uitdraai and Spioenkop Formations may therefore represent highly deformed equivalents of the Brulsand Formation.

In the north, the Kaaie domain comprises rocks of the Dagbreek and Sultanaoord Formations (Map 1). The Dagbreek Formation consists of quartz-mica schist and quartzite with amphibolite and serpentinite layers (Moen, 1980). It is highly deformed, especially in the western part of the Kaaie domain. The Sultanaoord Formation is exposed in an antiformal structure situated south-east of Sultanaoord (Map 1), where it overlies the Dagbreek Formation. It consists of massive white quartzites interbedded with red-weathering phyllite and schist (Moen, 1980). The Sultanaoord Formation is overlain along a sheared contact by the Zonderhuis Formation. U-Pb SHRIMP dating of detrital zircons from the Sultanaoord Formation yielded a maximum age of ≈ 1850 Ma, similar to that of the Uitdraai Formation and the Skeurberg quartzite (Pers. comm. R.A. Armstrong). It is therefore possible that the Dagbreek Formation and the overlying Sultanaoord Formation represent highly deformed equivalents of the Olifantshoek Supergroup.

Structural elements related to three Namaqua deformation events have been documented in the southern part of the Kaaiken domain. During the first of these (ND₁) the Uitdraai and Spioenkop Formations were thrust towards the ENE over rocks of the Marydale basement high. Fabric elements of similar geometry have been documented from the northern part of the Kaaiken domain and the Areachap Group (Stowe, 1986; Humphreys *et al.*, 1988). These workers suggest that this deformation was related to accretion of the Areachap Group volcanic arc onto the combined Kheis belt-Kaapvaal Craton.

These early craton-vergent shear zones are refolded by upright, open, north-west to NNW trending ND₂ folds. The youngest Namaqua deformation structures that have been recognised are north-west to NNW striking, dextral sense strike slip faults such as the Doringberg fault.

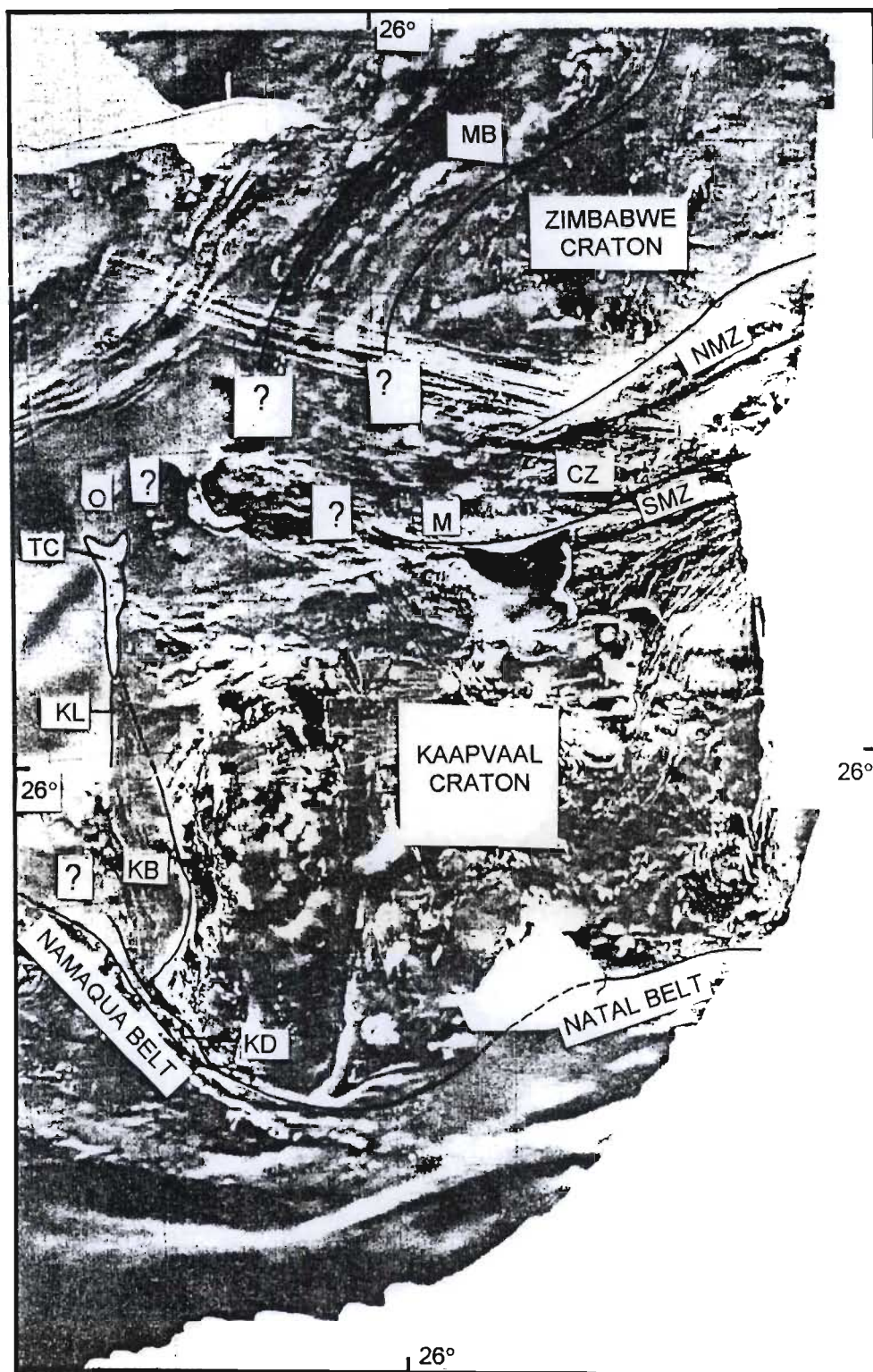
8.10 Correlations between the Kheis belt, the Okwa basement complex and the Magondi belt.

A regional aero-magnetic image of southern Africa is useful in defining the boundaries of the Kheis belt (Figure 8.7). Consistent with observations made during this study, the Kheis belt can be seen to be truncated in the south by the north-west trending Namaqua belt. The Kaaiken domain, that part of the Kheis belt that was strongly overprinted during the extended Namaqua orogeny, is indicated on Figure 8.7.

Any possible extension of the Kheis belt is indistinct in the west and north-west (Figure 8.7), as this area forms part of the Rehoboth domain (Stowe *et al.*, 1984; Thomas *et al.*, 1993), an area covered by rocks of the Karoo Supergroup, Kalahari Group and windblown sand. The Kalahari line (Figure 8.7) is a linear magnetic anomaly marked in part by the Tshane mafic/ultramafic complex (Hutchins and Reeves, 1980). Hartnady *et al.* (1985) suggested that this lineament marks a “*pre-Namaqua rifted continental margin*”. What is apparent from Figure 8.7 is that the lineaments defining the structural trend of the Kheis belt are truncated by the Kalahari line. This implies that the causative magnetic body that defines the Kalahari line (formed in part by the Tshane mafic/ultramafic complex) post-dates the Kheis orogeny and cannot be related to rifting during Olifantshoek Supergroup deposition. Its position may however have been influenced by pre-existing structural inhomogeneities related to the rifting along the western margin of the Kaapvaal Craton during Olifantshoek Supergroup deposition.

The northern extension of the Kheis belt is unclear from Figure 8.7. Two schools of thought exist as regards the northern continuation of the Kheis belt. Stowe *et al.* (1984) and Hartnady *et al.* (1985) argue

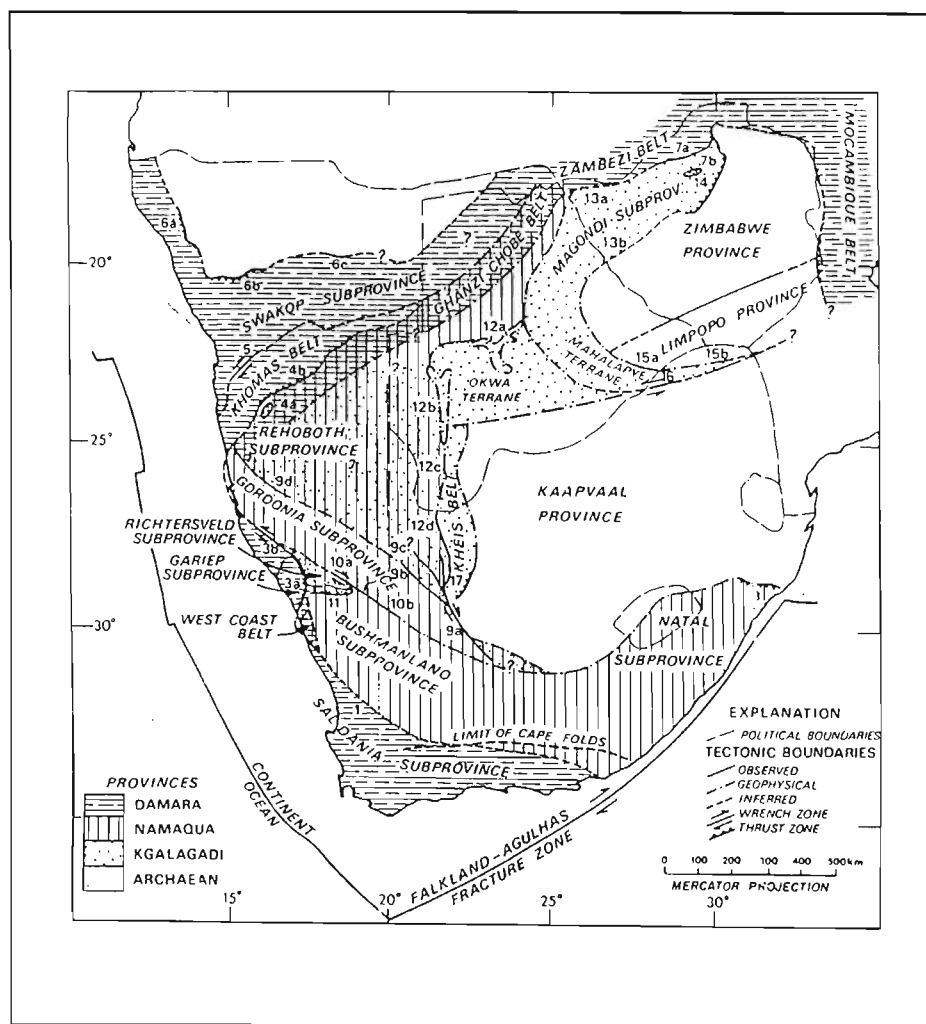
Figure 8.7: Airborne magnetic image of the eastern part of southern Africa. KB=Kheis belt, KD=Kaaia domain, KL=Kalahari line, TC=Tshane complex, O=Okwa basement complex, MB=Magondi belt, NMZ=Northern marginal zone (Limpopo belt), CZ=Central zone (Limpopo belt), SMZ=Southern marginal zone (Limpopo belt), M=Mahalapye plutonic block. Data courtesy of GEODASS. Image produced by CORNER GEOPHYSICS (Namibia).



that the Kheis belt should be considered to be a Subprovince of a larger, Eburnian age Province (the Kgalagadi Province) that includes the Magondi Subprovince (belt) and the Okwa basement complex (terrane) (Figure 8.8). Carney *et al.* (1994) interpret the Magondi belt to be the north-eastern part of a continuous orogenic belt that includes the Okwa basement complex and the Kheis belt (Figure 8.9).

Implicit in the interpretation of Stowe *et al.* (1984) is the separation of the Magondi belt from the Kheis belt by the Okwa basement complex, indicating that the Kheis and Magondi belts do not form a continuous orogenic belt along the western margin of the combined Kaapvaal-Zimbabwe Cratons (Figure 8.8). Based on regional aero-magnetic imagery, Stowe *et al.* (1984) interpreted the Magondi belt to have an arcuate structural trend that wraps around the western edge of the Zimbabwe craton and links up with the Mahalapye plutonic block (terrane) in eastern Botswana (Figure 8.8).

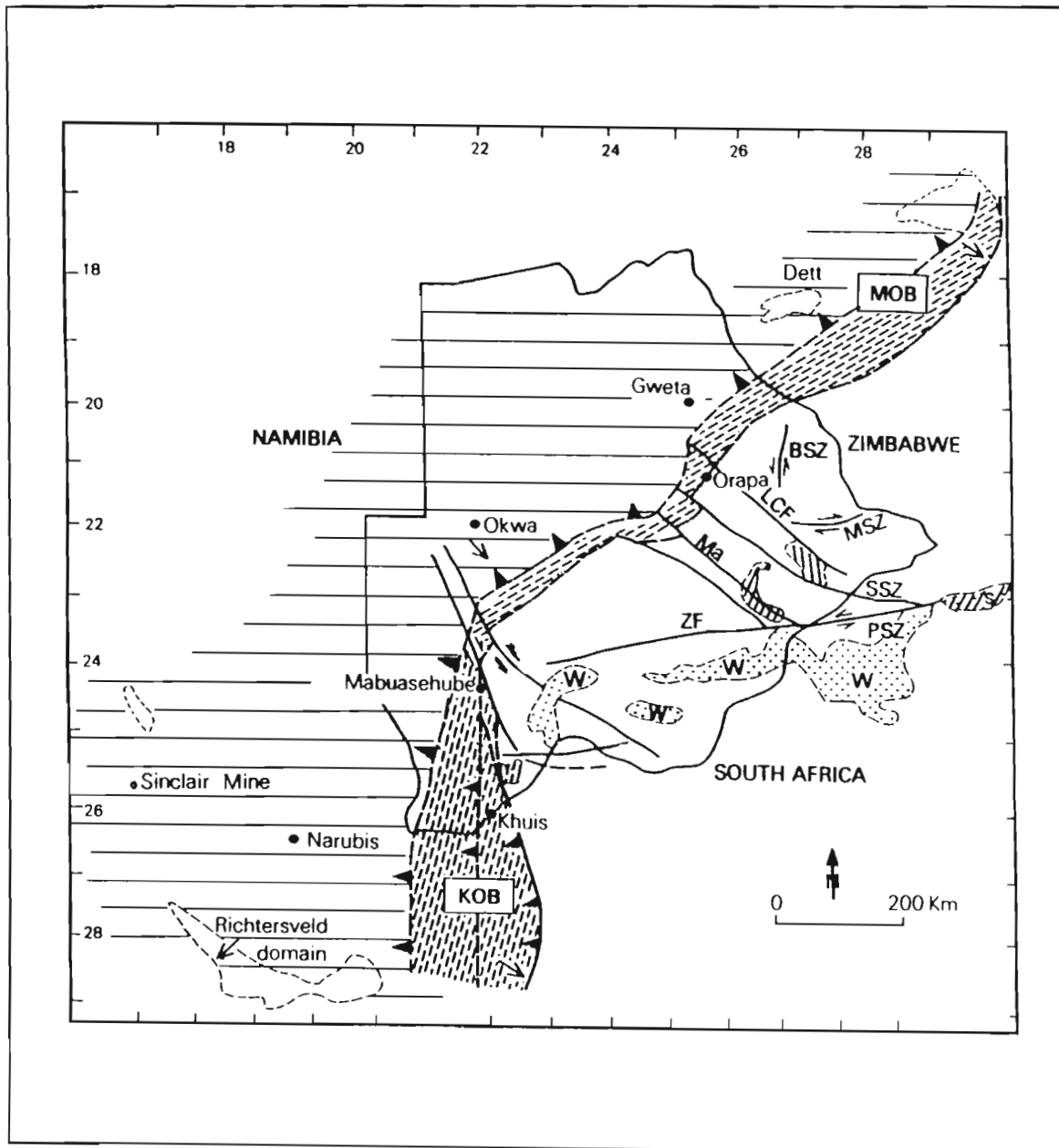
Figure 8.8: An interpretation of the crustal architecture of southern Africa. From: Stowe *et al.* (1984).



The Mahalapye plutonic block (Figure 8.7), situated at the western edge of the Central Zone (part of the Limpopo belt), consists of granitoid-gneisses equivalent to those in the Central Zone, that have undergone partial melting to produce migmatites during a tectonometamorphic event that occurred subsequent to the

≈2.65 Ga Limpopo orogeny (Ermanovics, 1980; Hisada and Paya, 1997). Unfoliated granitoids that intrude both the migmatites and the gneiss have been dated at 2007 ± 45 Ma (U-Pb single zircon SHRIMP) and may be related to this tectonometamorphic event (Pers. comm. S. McCourt and R.A. Armstrong, 1997).

Figure 8.9: Interpretation of the Kheis belt (KOB), Okwa basement complex (situated in the vicinity of Okwa) and the Magondi belt (MOB) as one continuous orogen. From: Carney *et al* (1994).



The Magondi belt is a regionally north-east to north striking, west dipping fold and thrust belt situated on the western margin of the Zimbabwe craton (Figure 8.7). The south eastern, or external, part of the Magondi belt comprises a volcano-sedimentary succession (the Magondi Supergroup); deposited along the western margin of the Zimbabwe craton; that was thrust to the south-east over the craton during the Magondi orogeny (Treloar, 1988). The north-western, or internal, part of the Magondi belt comprises an

imbricate thrust stack of basement gneisses and amphibolite-granulite facies Magondi Supergroup rocks that are intruded by weakly deformed syn-tectonic granitoids such as the Urungwe granite (Kirkpatrick, 1976; Treloar, 1988; this study).

A U-Pb single zircon SHRIMP age of 1997 ± 3 Ma for the syn-tectonic Urungwe granite constrains the timing of the Magondi orogeny and provides a minimum age constraint on deposition of the Magondi Supergroup. The Magondi Supergroup was therefore deposited, and deformed during the Magondi orogeny, prior to extrusion of the 1928 ± 4 Ma Hartley Formation (Cornell *et al.*, 1998) lavas of the Olifantshoek Supergroup. Any direct correlation between the Kheis belt and the Magondi belt is thus invalid. Geophysical imagery (Figure 8.7) indicates that the Kheis belt and the Magondi belt do not form a continuous orogen as suggested by Carney *et al.* (1994), but rather that the Magondi belt follows an arcuate trend around the edge of the Zimbabwe Craton as suggested by Stowe *et al.* (1984). The 1997 ± 3 Ma age for the Magondi orogeny is within error of the 2007 ± 45 Ma age for the unfoliated granites in the Mahalapye plutonic block. It is possible that Magondi orogenesis was responsible for “reworking” of the Limpopo belt granulites, at ≈ 2000 Ma, in the Mahalapye plutonic block.

The Okwa basement complex (Figure 8.7) has been interpreted to represent a fragment of an allochthonous terrane that was accreted onto the western edge of the combined Kaapvaal-Zimbabwe Craton during the “Kheis-Magondi” orogeny (Carney *et al.*, 1994). The Okwa basement complex (OBC) comprises porphyritic felsites, granite and granite-gneiss. A Rb-Sr whole rock age-date of 1813 Ma from the granite-gneisses, considered to be a crystallisation age by Key and Rundle (1981), has subsequently been re-interpreted as a metamorphic age (Carney *et al.*, 1994). Granites in the OBC have recently been dated at 2055 ± 4 Ma (Pers. comm. L.V. Ramokate: U-Pb zircon TIMS: Thermal ionisation mass-spectrometry). If the 1813 Ma date represents the age of metamorphism and formation of the north-east/south-west trending foliation in the OBC, as suggested by Carney *et al.* (1994), then it is possible that deformation and metamorphism in the OBC is related to the Kheis orogeny (which is poorly constrained between 1928 Ma and 1200 Ma). This is highly speculative however, and is not supported by any geological or geophysical data. A 1813 Ma metamorphic age for the OBC precludes the possibility of it being an extension of the ≈ 2000 Ma Magondi belt.

9. CONCLUSION

- The ≈ 3.0 Ga Marydale Group greenstones were intruded by granitoids between ≈ 2.9 and 2.7 Ga.
- The Zeekoebaart Formation is older than the 2718 ± 8 Ma Skalkseput granite. It is unlikely that the Zeekoebaart Formation is a correlate of the $< 2709 \pm 4$ Ma Pniel Group, but it may be an equivalent of the Platberg Group, Klipriviersberg Group or an older stratigraphic unit.
- The ≈ 2.65 - 2.22 Ga Griqualand West Supergroup unconformably overlies the Zeekoebaart Formation and the basement rocks of the Marydale basement high.
- The Griqualand West Supergroup was deformed during an east-west orientated compressional event, that produced north-south trending periclinal folds, prior to deposition of the Voelwater Subgroup, the Wolhaarkop Formation and the Manganore Formation.
- The Voelwater Subgroup is correlated with the Manganore Formation.
- The Olifantshoek Supergroup was deposited in an extensional basin that developed in response to rifting of the Kaapvaal Craton, thermal subsidence and the development of a passive margin. The rift had north-south orientated axis and probably developed along pre-existing structural weaknesses inherited from a period of Mid- to Late-Archaean accretionary tectonics. Deposition of the Olifantshoek Supergroup is poorly constrained between ≈ 2.2 - 1.2 Ga
- The Olifantshoek Supergroup was intruded by gabbro-norite sills prior to the Kheis Orogeny.
- Subsequent to deposition of the Olifantshoek Supergroup, both it and the underlying rocks of the Kaapvaal Craton were deformed in a craton vergent orogenic event termed the Kheis Orogeny. The cause of this event is unclear as only the eastern, external part of the Kheis belt is exposed. The timing of the Kheis orogeny is poorly constrained between ≈ 1.9 - 1.2 Ga.
- Inversion of north-south trending extensional faults, that developed during the rift-stage of the Olifantshoek Supergroup depository, occurred during the Kheis Orogeny. The resultant fold and thrust geometry of the Kheis belt was largely controlled by inversion tectonics.

- In the area east of the Korannaberge, the Blackridge thrust is a shallow dipping, short-cut thrust fault. In the Boegoeberg dam area the dip of the Blackridge thrust steepens and it cuts down stratigraphy into the basement rocks of the Kaapvaal Craton. This steepening is interpreted to be a result of linking of the short-cut thrust fault with an inverted rift-related extensional fault. No Kheis-age thrusts are developed east of the Blackridge thrust. The Blackridge thrust, the basal thrust of the Kheis belt, therefore roots along a detachment situated within the basement rocks of the Kaapvaal Craton.
- The Kaaiken Group, Spioenkop Formation and Zonderhuis Formation are all correlated with the Olifantshoek Supergroup. The geographic distribution of these units is largely controlled by structural elements that developed during Kheis- and extended Namaqua- Orogenesis.
- North-west to NNW trending faults and shear zones, that developed in response to accretionary tectonics during the 1.2-1.0 Ga extended Namaqua Orogeny, truncate the structural trend of the Kheis belt. A north-west to NNW trending zone of Olifantshoek Supergroup rocks, that have been structurally and metamorphically overprinted during the extended Namaqua Orogeny, occurs along the eastern margin of the Namaqua belt.
- The Magondi Supergroup was deposited, and deformed during the ≈ 2 Ga Magondi orogeny, prior to the deposition of most of the Olifantshoek Supergroup. The Kheis belt cannot be correlated with the Magondi belt.

ACKNOWLEDGEMENTS

Professor Steve McCourt supervised this project and, notwithstanding a schedule that few people would cope with, always found the time to make field visits and discuss problems. Steve, for your enthusiasm, scientific input and encouragement over the past four years I am deeply grateful.

Financial and logistical support from Anglo American Prospecting Services (AAPS) is gratefully acknowledged. Dr Dawie Strydom (AAPS), who took a keen interest in the project, is thanked for his time spent in discussion and in the field.

Errol Smart (AAPS) spent four months assisting with the fieldwork and logistics during the first field-season. Errols' boundless enthusiasm, coupled with his unrivalled ability as a devils advocate, helped make the fieldwork both enjoyable and challenging.

Hennie Van Den Berg kindly allowed access to ground owned by ISCOR.

Carol Lathy, Don and Caroline McIvor from SAMANCOR (Hotazel) and Gerhard and Suella Steenkamp from ISCOR (Wegdraai) are thanked for their hospitality and bottomless cooler-boxes.

Dr Richard Armstrong (Australian National University - Canberra) deserves a special vote of thanks for the time spent discussing radiometric age constraints and for the helpful manner in which he conducted the age determinations for this study.

I am very grateful to Dr Hubert Munyanyiwa (University of Zimbabwe - Harare) for showing me key outcrops in the Magondi Belt, including the Urungwe granite that was dated during this study.

The staff members of the Geology Department at the University of Durban-Westville all assisted with different aspects of the project. Thanks especially to Ashwin Sudamah who had the unenviable task of making thin-sections of grungy, lower greenschist facies rocks.

On a personal note, the encouragement from my family and friends helped immeasurably during the write-up of this project. I'd especially like to thank: my parents, Claire Hilliard, Sumesh Manthre, Eric and Bridget Clark, Juan and Sue Hugo, Louis Van Wyk, Ewan Burgers and Rob Gardiner.

REFERENCES

- Allen, P.A., Allen, J.R. (1990) Basin analysis. Blackwell, London. 451pp.
- Altermann, W., Halbich, I.W. (1990) Thrusting, folding and stratigraphy along the southwestern margin of the Kaapvaal Craton. *S. Afr. J. Geol.* 93: 553-566.
- Altermann, W., Halbich, I.W. (1991) Structural history of the southwestern corner of the Kaapvaal Craton and the adjacent Namaqua realm: new observations and a reappraisal. *Precambrian Res.* 52: 133-166.
- Altermann, W. (1996) Sedimentology, geochemistry and palaeogeographic implications of volcanic rocks in the Upper Archaean Campbell Group, western Kaapvaal craton, South Africa. *Precambrian Res.* 79: 73-100.
- Anhaeusser, C.R., Walraven, F. (1997) Polyphase crustal evolution of the Archaean Kraaipan granite-greenstone terrane, Kaapvaal Craton, South Africa. Economic Geology Research Unit Information Circular 313, University of the Witwatersrand, Johannesburg, 27pp.
- Armstrong, R.A. (1987) Geochronological studies on Archaean and Proterozoic formations of the foreland of the Namaqua front and possible correlations on the Kaapvaal Craton. Ph.D. thesis (Unpubl.), University of the Witwatersrand, Johannesburg. 274pp.
- Armstrong, R.A. (1997a) An Ion Microprobe (SHRIMP) U-Pb zircon geochronological study of various lithotypes from the western margin of the Kaapvaal Craton, South Africa. Unpubl. Rep. Precise radiogenic isotope services. 11pp.
- Armstrong, R.A. (1997b) Ion Microprobe (SHRIMP) U-Pb dating of zircons from the Urungwe granite. Unpubl. Rep. Precise radiogenic isotope services. 4pp.
- Armstrong, R.A., Compston, W., Retief, E.A., Williams, I.S., Welke, H.J. (1991). Zircon ion microprobe studies bearing on the age and evolution of the Witwatersrand triad. *Precambrian Res.* 53: 243-266.
- Ashwal, L.D., Andreoli, M.A.G., Page, T., Armstrong, R.A., Tucker, R.D. (1997) Geology and geochronology of High temperature granulites, Vaalputs area, central Namaqualand, South Africa. Abstract Volume: Tectonics division of the Geological Society of South Africa XIII Anniversary Conference, University of the Witwatersrand, Johannesburg.
- Barton, E.S., Burger, A.J. (1983) Reconnaissance isotopic investigations in the Namaqua Mobile Belt and implications for Proterozoic crustal evolution-Upington Geotraverse. *Spec. Publ. Geol. Soc. S. Afr.* 10: 173-191.
- Barton, E.S., Armstrong, R.A., Cornell, D.H., Welke, H.J. (1986) Feasibility of total-rock Pb-Pb dating of metamorphosed banded iron formation; the Marydale Group, southern Africa. *Chem. geol.* 59: 255-271.
- Barton, E.S., Altermann, W., Williams, I.S., Smith, C.B. (1994) U-Pb zircon age for a tuff in the Campbell Group, Griqualand West Sequence, South Africa: Implications for Early Proterozoic rock accumulation rates. *Geology.* 22: 343-346.
- Berthé, D., Choukroune, P., Jegonzo, P. (1979) Ortho-gneiss, mylonite and non-coaxial deformation of granites: the example of the South Armorican shear zone. *J. Str. Geol.* 1: 31-42.
- Beukes, N.J. (1978) Die karbonaatgesteentes en ysterformasies van die Ghaap-Groep van die Transvaal-Supergroep in Noord-Kaapland. Ph.D. thesis (unpubl.), Raandse Afrikaans University, Johannesburg. 580pp.
- Beukes, N.J. (1979) Litostratigrafiese onderverdeling van die Schmidtsdrif-Subgroep van die Ghaap-Groep in Noord-Kaapland. *Trans. geol. Soc. S. Afr.* 82: 313-327.
- Beukes, N.J. (1980a) Lithofacies and stratigraphy of the Kuruman and Griquatown Iron-formations, Northern Cape Province, South Africa. *Trans. geol. Soc. S. Afr.* 83: 69-86.

- Beukes, N.J. (1980b) Stratigrafie en litofasies van die Campbellrand-Subgroep van die Proterofitiese Ghaap-Groep, Noord-Kaapland. *Trans. geol. Soc. S. Afr.* 83: 141-170.
- Beukes, N.J. (1983) Palaeoenvironmental setting of iron-formations in the depositional basin of the Transvaal Supergroup, South Africa. In: *Iron formation facts and problems*. Trendall, A.F., Morris, R.C. (Eds). Elsevier, Amsterdam. 558pp.
- Beukes, N.J. (1984) Sedimentology of the Kuruman and Griquatown Iron-formations, Transvaal Supergroup, South Africa. *Precambrian Res.* 24: 47-84.
- Beukes, N.J. (1986) The Transvaal Sequence in Griqualand West. In: *Mineral deposits of southern Africa*. Anhaeusser, C.R., Maske, S (Eds). *Geol. Soc. S. Afr. Johannesburg*. 819-828.
- Beukes, N.J., Smit, C.A. (1987) New evidence for thrust faulting in Griqualand West, South Africa: implications for stratigraphy and age of red beds. *S. Afr. J. Geol.* 90: 378-394.
- Boardman L.G. (1941) The geology of the manganese deposits on Aucampsrust, Postmasburg. *Trans. geol. Soc. S. Afr.* 43: 27-36.
- Bond, G.C., Christie-Blick, N., Kominz, M.A., Devlin, W.J. (1985) An early Cambrian rift to post-rift transition in the Cordillera of western North America. *Nature*. 315: 742-746.
- Botha, B.J.V., Grobler, N.J., Linstrom, W., Smit, C.A. (1976) Stratigraphic correlation between the Kheis and Matsap Formations and their relation to the Namaqualand Metamorphic Complex. *Trans. geol. Soc. S. Afr.* 79: 304-311.
- Botha, B.J.V., Grobler, N.J., Linstrom, W., Smit, C.A. (1977) Major structural features of the area between the Langeberge range and Kenhardt, Northern Cape Province. *Trans. geol. Soc. S. Afr.* 80: 101-109.
- Botha, B.J.V., Smit, C.A., Linstrom, W., Grobler, N.J. (1979) Metamorphic zonation in the Matsap, Kheis and Namaqua domains east and west of the Kaaie Hills, northern Cape Province. *Trans. geol. Soc. S. Afr.* 82: 55-66.
- Burke, K., Dewey, J.F. (1973) Plume generated triple junctions: key indicators in applying plate tectonics to old rocks. *J. Geol. Chicago*. 81: 406-433.
- Burger, A.J., Coertze, F.J. (1973) Radiometric age measurements on rocks from southern Africa to the end of 1971. *Bull. geol. Soc. S. Afr.* 58. 46pp.
- Button, A. (1976) Transvaal and Hammersley basins- review of basin development and mineral deposits. *Minerals Sci. and Engineering*. 8: 262-293.
- Carney, J.N., Aldiss, D.T., Lock, N.P. (1994) The geology of Botswana. Geological Survey Department, Republic of Botswana. *Bulletin* 37. 113pp.
- Cheney, E.S., Barton, J.M., Brandl, G. (1990) Extent and age of the Soutpansberg sequences of southern Africa. *S. Afr. J. Geol.* 93: 664-675.
- Cheney, E.S. (1996) Sequence stratigraphy and plate tectonic significance of the Transvaal succession of southern Africa and its equivalent in Western Australia. *Precambrian Res.* 79: 3-24.
- Clifford, T.N., Rex, D.C., Snelling, N.J. (1967) Radiometric data for the Urungwe and Mwami granites of Rhodesia. *Earth Planet. Sci. Lett.* 2: 5-12.
- Cooper, M.R. (1978) The sedimentary environment of the Deweras Group in Rhodesia. *Nature*. 272: 810-812.
- Compston, W., Williams, I.S., Kirschvink, J.L., Zhang, Z., Ma, G. (1992) Zircon U-Pb ages for the Early cambrian time scale. *J. Geol. Soc. London*. 149: 171-184.
- Cornell, D.H., Hawkesworth, C.J., Van Calsteren, P., Scott, W.D. (1986) Sm-Nd study of Precambrian crustal development in the Prieska-Copperton region, Cape Province. *Trans. geol. Soc. S. Afr.* 89: 17-28.

- Cornell, D.H. (1987) Stratigraphy and petrography of the Hartley Basalt Formation, northern Cape Province. *S. Afr. J. Geol.* 90: 7-24.
- Cornell, D.H., Kroner, A., Humphreys, H., Griffin, G. (1990) Age of origin of the polymetamorphosed Copperton Formation, Namaqua-Natal Province, determined by single grain zircon Pb-Pb dating. *S. Afr. J. Geol.* 93: 709-716.
- Cornell, D.H., Schutte, S.S., Eglinton, B.L. (1996) The Ongeluk basaltic andesite formation in Griqualand West, South Africa: submarine alteration in a 2222 Ma Proterozoic sea. *Precambrian Res.* 76: 101-123.
- Cornell, D.H., Walraven, F., Armstrong, R.A. (1998) Geochronology of the Hartley basalt formation. *J. Afr. Earth Sci.* 26:5-27
- Coward, M.P., Potgieter, R. (1983) Thrust zones and shear zones of the margin of the Namaqua and Kheis mobile belts, southern Africa. *Precambrian Res.* 21: 39-54.
- Crampton, D. (1974) A note on the age of the Matsap Formation of the northern Cape Province. *Trans. geol. Soc. S. Afr.* 77: 71-72.
- De Wit, M.J., Roering, C., Hart, R.J., Armstrong, R.A., De Ronde, C.E.J., Green, R.W.E., Tredoux, M., Peberdy, E., Hart, R.A. (1992) Formation of an Archaean continent. *Nature.* 357: 553-562.
- Dalziel, I.W.D., Storey, B.C., Garrett, S.W., Grunow, A.M., Herrod, L.D.B., Pankhurst, R.J. (1987) Extensional tectonics and fragmentation of Gondwanaland. In: *Continental Extensional Tectonics*. Coward, M.P., Dewey, J.F., Hancock, P.L. (Eds.). Spec. Publ. Geol. Soc. London. 13: 433-441.
- Elliot, D. (1976) The motion of thrust sheets. *J. Geophys. Res.* 81: 949-963.
- Ermanovics, I.F. (1980) The geology of the Mokgware Hills area. Geological Survey Department, Republic of Botswana. *Bulletin* 13. 86pp.
- Evenchick, C.A. (1992) The Skeena fold belt: a link between the Coast Plutonic Complex, the Omineca belt and the Rocky Mountain fold and thrust belt. In: *Thrust Tectonics*. McClay, K.R. (Ed.). Chapman and Hall, London. 365-375.
- Geerthsen, K., Maher, M.J., Meyer, R. (1991) The western edge of the Griqualand West Basin- A geophysical perspective. *S. Afr. J. Geol.* 94: 96-103.
- Geringer, G.J., Botha, B.J.V., Pretorius, J.J., Ludick, D.J. (1986) Calc-alkaline volcanism along the eastern margin of the Namaqua Mobile Belt, South Africa - A possible middle Proterozoic volcanic arc. *Precambrian Res.* 33: 139-170.
- Geringer, G.J., Botha, B.J.V., Slabbert, M.J. (1988) The Keimoes Suite-a composite granitoid batholith along the eastern margin of the Namaqua mobile belt, South Africa. *S. Afr. J. Geol.* 91: 465-476.
- Grobbelaar, W.S., Beukes, N.J. (1986) The Bishop and Glosam manganese mines and the Beeshoek iron ore mine of the Postmasburg area. In: *Mineral deposits of southern Africa*. Anhaeusser, C.R., Maske, S. (Eds). Geol. Soc. S. Afr., Johannesburg. 957-961.
- Grobler, D.F., Walraven, F. (1993) Geochronology of the Gaberone Granite Complex extensions in the area north of Mafikeng, South Africa. *Chem. Geol.* 105: 319-337.
- Gutzmer, J., Beukes, N.J. (1995) Fault-controlled metasomatic alteration of early Proterozoic sedimentary manganese ores in the Kalahari Manganese field, South Africa. *Econ. Geol.* 90: 823-844.
- Harmer, R.E., Von Grunewaldt, G. (1991) A review of magmatism associated with the Transvaal Basin- implications for its tectonic setting. *S. Afr. J. Geol.* 94: 104-122.
- Hartnady, C.J.H., Joubert, P., Stowe, C.W. (1985) Proterozoic crustal evolution in southwestern Africa. *Episodes.* 8: 236-245.
- Hatcher, R.D., Hooper, R.J. (1992) Evolution of crystalline thrust sheets in the internal parts of mountain chains. In: *Thrust Tectonics*. McClay, K.R. (Ed.). Chapman and Hall, London. 217-233.
- Hisada, K., Paya, B.K. (1997) Phase analysis of migmatites in the Mahalapye Plutonic Block, eastern Botswana. *Abstract Volume: Intraplate Magmatism and tectonics of southern Africa*, Dept. of Geology, University of Zimbabwe, Harare.

- Hoffman, P.F. (1989). Precambrian geology and tectonic history of North America. In: The Geology of North America Vol. A: The Geology of North America - an overview. The Geological Society of America. 447-511
- Howell, D.G. (1995) Principles of terrane analysis. Chapman and Hall, London. 245pp.
- Humphreys, H.C., Van Bever Donker, J.M. (1987) Aspects of deformation along the Namaqua Province eastern boundary, Kenhardt District, South Africa. *Precambrian Res.* 36: 39-63.
- Humphreys, H.C., Van Bever Donker, J.M., Scott, W.D., Van Schalkwyk, L. (1988) The early deformational history of the eastern Namaqua Province: new evidence from Prieska Copper Mines. *S. Afr. J. Geol.* 91: 174-183.
- Humphreys, H.C., Schlegel, G.C.J., Stowe, C.W. (1991) High-pressure metamorphism in garnet-hornblende-muscovite-plagioclase-quartz schists from the Kheis belt. *S.Afr. J. Geol.* 94: 170-173.
- Hutchins, D.G., Reeves, C.V. (1980) Regional geophysical exploration of the Kalahari in Botswana. *Tectonophysics.* 69: 210-220.
- Jackson, C., Harris, R.W. (1997). Microstructural evidence for extensional reactivation of the Hartbees River Thrust belt, northeastern Namaqua Tectonic Province. Abstract Volume: Tectonics division of the Geological Society of South Africa XIII Anniversary Conference, University of the Witwatersrand, Johannesburg.
- Jansen, E. (1983) Die stratigrafie en sedimentologie van die Volop-Groep, Olifantshoek-opeenvolging. M.Sc. thesis (unpubl), Randse Afrikaans University, Johannesburg. 138pp.
- Jennings, M. (1986) The Middleplaats manganese ore deposit, Griqualand West. In: Mineral deposits of southern Africa. Anhaeusser, C.R., Maske, S. (Eds.). *Geol. Soc. S. Afr.* 979-983.
- Kent, L.E. (1971) Annals of the Geological Survey of South Africa: 1968-1969. Pretoria. 141pp.
- Key, R.M., Rundle, C.C. (1981) The regional significance of new isotopic ages from Precambrian windows through the Kalahari Beds in northwestern Botswana. *Trans. geol. Soc. S. Afr.* 84: 51-66.
- Kirkpatrick, I.M. (1976) The Geology of the Country around Tengwe, Lomagundi District. Rhodesia Geological Survey. Bulletin 75. 176pp.
- Kober, B. (1986) Whole grain evaporation for $^{207}\text{Pb}/^{206}\text{Pb}$ age investigations on single zircons using a double filament thermal ion source. *Contr. Min. Petrology.* 93: 482-490.
- LeGrand, H.E., LaMoreaux, P.E. (1975) Hydrogeology and Hydrology of Karst. In: Hydrogeology of Karstic Terrains. Burger, A., Dubertret, L. (Eds.). International Association of Hydrogeologists, Paris. 9-19.
- Leyshon, P.R. (1969) The geology of the country around the Copper Queen. Rhodesian Geological Survey. Bulletin 66. 174pp.
- Leyshon, P.R., Tennick, F.P. (1988) The Proterozoic Magondi Mobile belt in Zimbabwe- a review. *S. Afr. J. Geol.* 91: 114-131.
- Locket, N.H. (1979) The geology of the country around Dett, Wankie district. *Rhod. Geol. Surv. Bull.* 85.
- Loney, P.E. (1969) The geology of the Kariba district, Rhodesia, with special reference to geochronology and amphibolite petrochemistry. Ph. D thesis (Unpubl.) Leeds Univ. 110pp.
- Master, S. (1991) Stratigraphy, tectonic setting and mineralisation of the Early Proterozoic Magondi Supergroup, Zimbabwe: A review. Economic Geology Research Unit Information Circular 238, University of the Witwatersrand, Johannesburg. 75pp.
- McClay, K.R., Insley, W.W., Anderton, R. (1989) Inversion of the Kechika Trough, Northeastern British Columbia, Canada. In: Inversion Tectonics. Cooper, M.A., Williams, G.D. (Eds). *Spec. Publ. Geol. Soc. London.* 235-257.
- McClay K.R., Buchanan, P.G. (1992) Thrust faults in inverted extensional basins. In: Thrust Tectonics. McClay, K.R. (Ed.) Chapman and Hall, London. 93-104.

- McClay, K.R. (1992) Glossary of thrust tectonics terms. In: *Thrust Tectonics*. McClay, K.R. (Ed.). Chapman and Hall, London. 419-433.
- McCourt, S. (1995) The crustal architecture of the Kaapvaal crustal block South Africa, between 3.5 and 2.0 Ga. *Mineralium Deposita*. 30: 89-97.
- McKenzie, D.P. (1978) Some remarks on the development of sedimentary basins. *Earth Planet. Sci. Letters*. 40: 25-32.
- Moen, H.F.G. (1980) Petrology and geological setting of the Wilgenhoutsdrif formation, Northern Cape Province. M.Sc thesis (Unpubl.), Univ. Orange Free State, Bloemfontein. 287pp.
- Munyanyiwa, H., Kroner, A., Jaeckel, P. (1995) U-Pb and Pb-Pb single zircon ages from the Magondi mobile belt, northwest Zimbabwe. *S. Afr. J. Geol.* 98: 52-57.
- Nel, C.J., Beukes, N.J., De Villiers, J.P.R. (1986) The Mamatwan manganese mine of the Kalahari manganese field. In: *Mineral deposits of southern Africa*. Anhaeusser, C.R., Maske, S. (Eds.). Geol. Soc. S. Afr. 963-978.
- Park, R.G. (1990) *Geological structures and moving plates*. Blackie, London.
- Pettijohn, F.J., Potter, P.E., Siever, R. (1972) *Sand and sandstone*. Springer-Verlag, New York.
- Powell, C.M. (1989) Structural controls on Palaeozoic basin evolution and inversion in southwest Wales. *J. Geol. Soc. London*. 146: 439-446.
- Quinquis, H., Audren, C.L., Brun, J.P., Cobbold, P.R. (1978) Intense progressive shear in Ile de Groix blueschists and compatibility with subduction or obduction. *Nature*. 273: 43-45.
- Ramsay, J.G. (1980) The crack-seal mechanism of rock deformation. *Nature*. 248: 135-139.
- Ramsay, J.G., Huber, M.I. (1987) *The techniques of modern structural geology - Vol 2: Folds and Fractures*. Academic Press, London. 700pp.
- Robb, L.J., Davis, D.W., Kamo, S.L., Meyer, F.M. (1992) Ages of altered granites adjoining the Witwatersrand Basin, with implications for the origin of gold and uranium. *Nature*. 357, 672-680.
- Robb, L.J., Armstrong, R.A., Waters, D.J. (1997) Timing of metamorphism and crustal growth in Namaqualand: Evidence from single zircon U-Pb Geochronology. Abstract Volume: Tectonics division of the Geological Society of South Africa XIII Anniversary Conference, University of the Witwatersrand, Johannesburg.
- Roering, C., Berlenbach, J., Schweitzer, J.K. (1989) Guidelines for the classification of fault rocks. COMRO. Johannesburg. 22pp.
- Rogers, A.W., Du Toit, A.L. (1908) Report on the geology of parts of Prieska, Hay, Britstown, Carnarvon and Victoria West. Annual Rep. Geological Commission of the Cape of Good Hope. 14: 8-108.
- SACS: South African Committee For Stratigraphy (1980) *Stratigraphy of South Africa. Part 1 (Comp. L.E. Kent). Lithostratigraphy of the Republic of South Africa, South West Africa/Namibia and the Republics of Bophuthatswana, Transkei and Venda: Handb. geol. Surv. S. Afr., 8. 690pp.*
- SACS: South African Committee for Stratigraphy (1994) Sequences bite the dust. *Geobulletin (Quarterly bulletin of the Geological Society of South Africa)*. 37: 17.
- SAGS: South African Geological Survey (1977) 1:250 000 Geological Series Sheet 2822 Postmasburg. Compiled by H.F.G. Moen. Government Printer, Pretoria.
- SAGS: South African Geological Survey (1979) 1:250 000 Geological Series Sheet 2722 Kuruman. Compiled by H.F.G. Moen. Government Printer, Pretoria.
- SAGS: South African Geological Survey (1984) *Geological map of the Republics of South Africa, Transkei, Bophuthatswana, Venda and Ciskei and the Kingdoms of Lesotho and Swaziland*. Compiled by D.J.L. Visser. Government Printer, Pretoria.

- SAGS: South African Geological Survey (1995) 1:250 000 Geological Series Sheet 2922 Prieska. Compiled by S.J. Malherbe and H.F.G. Moen. Government Printer, Pretoria.
- Schlegel, G.C.J. (1986) Metamorphic and structural evolution of the Kheis tectonic Province. M.Sc. thesis (unpubl.). University of Cape Town. 217pp.
- Schlegel, G.C.J. (1988) Contribution to the metamorphic and structural evolution of the Kheis Tectonic Province, northern Cape, South Africa. *S. Afr. J. Geol.* 91: 27-37.
- Schlütte, S.S. (1993) Ongeluk volcanism in relation to the Kalahari manganese field. Ph.D thesis (Unpubl.) University of Natal, Durban. 255pp.
- Scott, W.D. (1987) A lithostratigraphic and metamorphic profile across the Kaapvaal-Namaqua boundary, North-West Cape Province. M.Sc. thesis (Unpubl.), University of Stellenbosch. 215pp.
- Smit, C.A. (1977) Die geologie rondom Groblershoop, met spesiale verwysing na die verband tussen die Namakwalandse Mobiele Gordel en die Kheis-Matsapgesteentes. Ph.D. thesis (Unpubl.). University of the Orange Free State, Bloemfontein. 390pp.
- Stowe, C.W. (1983) The Upington geotraverse and its implications for craton margin tectonics. *Spec. publ. geol. Soc. S. Afr.* 10: 147-171.
- Stowe, C.W., Hartnady, C.J.H., Joubert, P. (1984) Proterozoic tectonic Provinces of southern Africa. *Precambrian Res.* 25: 229-231.
- Stowe, C.W. (1986) Synthesis and interpretation of structures along the north-eastern boundary of the Namaqua Tectonic Province, South Africa. *Trans. geol. Soc. S. Afr.* 89: 185-198.
- Streckeisen, A. (1976) To each plutonic rock its own name. *Earth Sci. Rev.* 12: 1-33.
- Sumner, D.Y., Bowring, S.A. (1996) U-Pb geochronologic constraints on deposition of the Campbellrand Subgroup, Transvaal Supergroup, South Africa. *Precambrian Res.* 79: 25-35.
- Suppe, J. (1983) Geometry and kinematics of fault-bend folding. *American Journal of Science.* 283: 648-721.
- Suppe, J. (1985) Principles of structural geology. Prentice-Hall, New Jersey. 537pp.
- Tankard, A.J., Jackson, M.P.A., Eriksson, K.A., Hobday, D.K., Hunter, D.R., Minter, W.E.L. (1982) Crustal evolution of Southern Africa. Springer Verlag, New York. 523pp.
- Thomas, R.J., Von Veh, M.W., McCourt, S. (1993) The tectonic evolution of southern Africa: an overview. *J. African earth. Sci.* 16: 5-24.
- Thomas, R.J., Cornell, D.H., Moore, J.M., Jacobs, J. (1994) Crustal evolution of the Namaqua-Natal Metamorphic Province, southern Africa. *S. Afr. J. Geol.* 97: 8-14.
- Thompson, B., Mercier, E., Roots, C. (1987) Extension and its influence on Canadian Cordilleran passive-margin evolution. In: *Continental Extensional Tectonics*. Coward, M.P., Dewey, J.F., Hancock, P.L. (Eds.). *Spec. Publ. Geol. Soc. London.* 13: 409-417.
- Treloar, P.J. (1988) The geological evolution of the Magondi Mobile Belt, Zimbabwe. *Precambrian Res.* 38: 55-73.
- Treloar, P.J., Kramers, J.D. (1989) Metamorphism and geochronology of granulites and migmatitic granulites from the Magondi mobile belt, Zimbabwe. *Precambrian Res.* 45: 277-289.
- Trendall, A.F., Compston, W., Williams, I.S., Armstrong, R.A., Arndt, N.T., McNaughton, N.J., Nelson, D.R., Barley, M.E., Beukes, N.J., De Laeter, J.R., Retief, E.A., Torne, A.M. (1990) Precise zircon U-Pb chronological comparison of the volcano-sedimentary sequences of the Kaapvaal and Pilbara Cratons between about 3.1 and 2.4 Ga. Abstract volume: Third International Archaean symposium, Perth. 81-83.

- Vail, J.R., Snelling, N.H., Rex, D.C. (1968) Pre-Katangan geochronology of Zambia and adjacent parts of central Africa. *Can. J. Earth Sci.* 5: 621-628.
- Vajner, V. (1974). The tectonic development of the Namaqua Mobile Belt and its foreland in parts of the Northern Cape. Chamber of Mines Precambrian Research Unit. Bulletin 14. University of Cape Town. 201pp.
- Van Schalkwyk, J.F., Beukes, N.J. (1986) The Sishen iron ore deposit, Griqualand West. In: Mineral deposits of southern Africa. Anhaeusser, C.R., Maske, S. (Eds.). *Geol. Soc. S. Afr.* 931-956.
- Van Wyk, J.P. (1980) Die geologie van die gebied Rooinekke-Matsap-Wolhaarkop in Noord-Kaapland met spesiale verwysing na die Koegas Subgroep en die Transvaal Supergroep. M.Sc. thesis (Unpubl), Randse Afrikaans University, Johannesburg. 159pp.
- Vearncombe, J.R. (1986) Structure of veins in a gold-pyrite deposit in banded iron formation, Amalia greenstone belt, South Africa. *Geol. Mag.* 123: 601-609.
- Visser, D.J.L. (1944) Stratigraphic features and tectonics of portions of Bechuanaland and Griqualand West. *Trans. geol. Soc. S. Afr.* 47: 197-254.
- Visser, J.N.J. (1971) The deposition of the Griquatown glacial member in the Transvaal Supergroup. *Trans. geol. Soc. S. Afr.* 74: 187-199.
- Walraven, F., Martini, J. (1995) Zircon Pb-evaporation age determinations of the Oak Tree Formation, Chuniespoort Group, Transvaal Sequence: implications for Transvaal-Griqualand West basin correlations. *S. Afr. J. Geol.* 98: 58-67.
- Wilson, G. (1953) Mullion and rodding structures in the Moine series of Scotland. *Geol. Assoc. Proc.* 64: 118-151

LIST OF FIGURES

Figure 1.1: The crustal architecture of southern Africa (modified after Thomas *et al.*, 1993). The study area is indicated in colour. 2

Figure 1.2: Simplified geological map of the SW part of the Kaapvaal Craton, the Kheis belt and the eastern part of the Namaqua belt. ①= Blackridge thrust; ②= Korannaberg thrust; ③= Doringberg fault; ④= Doornberg s.z (shear zone); ⑤= Copperton s.z.; ⑥= Brulpan fault; ⑦= Brakbos fault; ⑧= Dagbreek fault.; ⑨= Straussberg s.z.; ⑩= Boven-Rugzeer s.z. The approximate eastern boundary of the Kheis belt is marked by ①. The boundary between the Kheis belt and the Kaaiken domain is formed by ④, ⑥, dotted line and ⑦. The boundary between the Kaaiken domain and the Namaqua belt is marked by ⑤ and ⑨. An additional copy of this Figure is located in the front map-pocket. 3

Figure 2.1: Geological map of the Maremane structure and surrounding area (From: Van Schalkwyk and Beukes, 1986). 19
The Maremane structure (termed the Maremane dome by Beukes and Smit, 1987) comprises the eastern limb (east dipping) of a periclinal anticline that developed in the Griqualand West Supergroup (indicated as Transvaal Sequence above) prior to deposition of the Olifantshoek Supergroup. The western limb of this anticline is not exposed due to deposition of the Olifantshoek Supergroup on an angular unconformity and the development of westward dipping thrust faults.

Figure 3.1: Cross section of the Ongeluk Formation, Voelwater Subgroup, Mapedi Formation and Lucknow Formation exposed on farm Voelwater 480. 38

Figure 3.2: Composite stratigraphic column for the Hartley Formation in the Traverse 2-3 areas. 41

Figure 3.3: The Neylan bed conglomerate, situated at the base of the Hartley Formation. locality 3.4- Map 1. 43

Figure 3.4: Photomicrograph of a sample of Hartley Formation lava exposed in a quarry on the western part of the Olifantshoek allotment area (Traverse 3). P=plagioclase, M=magnetite, Q=quartz filled amygdale. Cross-polarised transmitted light. 43

Figure 3.5: Welded tuff (a preserved ignimbrite deposit) in the Hartley Formation on farm Pudukhush 533- Traverse 2. 44

Figure 3.6: The sedimentary breccia developed at the base of the Hartley Formation on farm Mooihoek 306 (Traverse 1). 44
The clast assemblage is dominated by clasts of white to light-green siliceous quartzite of the Mapedi Formation. Rare clasts of Voelwater Subgroup jasper are also present (see immediately below compass).

Figure 3.7: A sedimentary contact between the basal conglomerate of the Fuller member and ferruginous chert of the Voelwater Subgroup (farm Groenwater 304- Traverse 1). 44

Figure 3.8: Polymict conglomerate band in the Fuller member (farm Drogepoort 345- Traverse 1). The clast assemblage comprises jasper, ferruginous chert, siliceous chert, banded ironstone, vein quartz and siliceous white quartzite and was probably derived from the underlying Mapedi Formation, Lucknow Formation and Voelwater Subgroup. 46

Figure 3.9: Planar bedded heavy mineral layers in the Fuller member (farm Watermeyer 576- Traverse 2). The dark bands are comprised of rounded opaque heavy minerals and zircon grains up to 0.4mm in diameter. The lighter bands consist of quartzite. 47

Figure 3.10: Trough cross-bedded quartzite in the Ellies Rus member (farm Watermeyer 576- Traverse 2). 50

Figure 3.11: Desiccation cracks developed in a mud drape on a ripple-marked quartzite horizon of the Verwater member (farm Inglesby 580- Traverse 2). 50

Figure 3.12: Photomicrograph of a sample of Verwater member quartzite from farm Schaapkloof 584 (Traverse 3). Note the sub-rounded grains. The quartz grains exhibit weak undulose extinction and minor recrystallisation along grain boundaries. The phyllosilicates in the matrix are muscovite and chlorite. Transmitted cross-polarised light. 52

Figure 3.13: Mature quartzite with low angle cross-bedding. Top Dog member (farm Lukin 581- Traverse 2). 52

Figure 3.14: An unfoliated core-stone from the gabbronorite sill exposed on farm Watermeyer 576. 54

Figure 3.15: Photomicrograph of the groundmass of sample PS0716. P=plagioclase, C=Clinopyroxene, O=orthopyroxene, B=biotite rimming magnetite. 54

Figure 3.16: Equal area, stereographic projection (π -diagram) of bedding plane (n=182) and fold axes (n=7) orientations in the Traverse 2 area. 57

Figure 3.17: Equal area, stereographic projection (π -diagram) of bedding plane (n=133) and fold axes (n=2) orientations in the Traverse 3 area. 57

Figure 3.18: 3rd order folds in the Ellies Rus member (Traverse 2). The field of view of the photograph is approximately 50×75m. East is to the left of the photograph. 58

Figure 3.19: Shallow southward plunging 3rd order fold in the Glen Lyon member (Traverse 2). East is to the right of the photograph. 58

Figure 3.20: Geological cross-section from Y to Y' of Traverse 2. The horizontal and vertical scales are equal. 60

Figure 3.21: Geological cross section from Z to Z' of Traverse 3. The horizontal and vertical scales are equal. 61

Figure 3.22: Equal area, stereographic projection (π -diagram) of bedding plane (n=52) orientations for the Traverse 4 area. 62

Figure 3.23: Equal area, stereographic projection (π -diagram) of bedding plane (n=125) orientations for the Traverse 1 area. 62

Figure 3.24: Geological cross section from X to X' of the Traverse 1 area. Horizontal and vertical scales are equal. 63

Figure 3.25: Flexural-slip shear zone geometry in a 3rd order fold. 64

Figure 3.26: Phyllonite developed along a bedding parallel, flexural-slip shear zone. The sub-rounded minerals (with pressure shadows) labelled "Z" are detrital zircons. Transmitted cross-polarised light. 65

Figure 3.27: Axial planar cleavage developed in the axial region of a 2nd order fold. Top Dog member (farm Mutsistan 523- Traverse 2). 66

Figure 3.28: Equal area, stereographic projection (π -diagram) of the orientations of planar and linear fabric elements measured in the Traverse 1 area. (Axial planar cleavage: n=5; West dipping shear zones: n=56; East dipping shear zones: n=2; Mineral elongation lineations: n=41). 67

Figure 3.29: Equal area, stereographic projection (π -diagram) of the orientations of planar and linear fabric elements measured in the Traverse 2 area (Axial planar cleavage: n= 15; West dipping shear zones: n=42; East dipping shear zones: n=12; Mineral elongation lineations: n=29) 68

Figure 3.30: Equal area, stereographic projection (π -diagram) of the orientations of planar and linear fabric elements measured in the Traverse 3 area (Axial planar cleavage: n=15; West dipping shear zones: n=26; East dipping shear zones: n=3; Mineral elongation lineations: n=18). 69

Figure 3.31: Equal area, stereographic projection (π -diagram) of the orientations of planar and linear fabric elements measured in the Traverse 4 area (Axial planar cleavage: n=2; West dipping shear zones: n=20; East dipping shear zones: n=3; Mineral elongation lineations: n=17). 70

Figure 3.32: Photomicrograph of a sample of Fuller member quartzite with a well developed axial planar cleavage. 71

Figure 3.33: A westward dipping, bedding sub-parallel shear zone, developed in an argillaceous horizon bounded by siliceous quartzite. S-C fabrics indicate west over east thrust sense of movement. East is to the right of the photograph. Ellies Rus member, farm Gamayana 532- Traverse 2. 72

Figure 3.34: A west dipping thrust sense shear zone cutting across an east dipping fold limb. A bedding plane (solid line labelled S_0) and cross-bedding (dashed line) are marked on the rock. East is to the right of the photograph as indicated. Ellies Rus member quartzite, farm Watermeyer 576- Traverse 2. 73

Figure 3.35: Protomylonite developed in a west dipping, thrust sense shear zone. Transmitted cross-polarised light. 74

Figure 3.36: Mylonitised Fuller member quartzite. East is to the right of the photograph. S-C fabrics indicate a west over east, thrust sense of movement. 73

Figure 3.37: Photomicrograph of the mylonite shown in Figure 3.34. Transmitted cross-polarised light. 73

Figure 3.38: Equal area, stereographic projection (π -diagram) of the orientations of bedding (n=21) and axial planar cleavage (n=6) measured on the anticline at locality 3.6. 75

Figure 3.39: Equal area, stereographic projection (π -diagram) of planar and linear fabric elements measured east of locality 3.6 in the Molopo River area (Axial planar cleavage: n=14; Mineral elongation lineations: n=5; West dipping shear zones: n=4). 76

Figure 3.40: Composite stratigraphic column of the Voelwater Subgroup and the Olifantshoek Supergroup for the Korannaberge-Langberge area. Note that the thickness of units indicated in the hatched column is not to scale. 78

Figure 4.1: Summary stratigraphic column of the Boegoeberg Dam area. 81

Figure 4.2: Geological map of farm Geelbeksdam and the surrounding area. Modified after Vajner (1974). 83

Figure 4.3: Field log of the stratigraphy of the Schmidtsdrif Subgroup on Geelbeksdam. The insert shows the textural variations within an individual lava flow in the Schmidtsdrif Subgroup. ZF= Zeekoebaart Formation. CRS= Campbellrand Subgroup. 84

Figure 4.4: Voelwater Subgroup banded ironstone comprising alternating hematite rich and siliceous chert layers. (Farm 312- Map 2). 88

Figure 4.5: Cross-section of the lens of Voelwater Subgroup rocks exposed at locality L2 (farm Bovenzeekoebaart 313). 89

Figure 4.6: Photomicrograph of finely laminated iron ore from the Voelwater Subgroup. The primary layering is defined by a subtle change in the hematite grain size and by layers of gangue minerals. Plane-polarised reflected light. 90

Figure 4.7: Lucknow Formation quartzite overlying banded ironstones of the Voelwater Subgroup. View is southwards from locality L4. 90

Figure 4.8: Cross-bedded impure dolomite of the Mapedi Formation (Farm Zeekoebar 9- Map 2). 95

Figure 4.9: Agglomerate developed at the base of the Hartley Formation. Locality L1- Farm Bovenzeekoebaart 313. 95

Figure 4.10: Pillow lava in the Hartley Formation. Farm Zeekoebaart 306. This outcrop is only weakly foliated, but the pillows have been elongated parallel to a north-west plunging mineral elongation lineation (approximately parallel to the handle of the hammer). 97

Figure 4.11: Photomicrograph of sample PS0791. Transmitted cross-polarised light. C=Clinopyroxene, O=Orthopyroxene, P=Saussurite, G=Graphic quartz-feldspar intergrowth.

Figure 4.12: Equal area, stereographic projection (π -diagram) of bedding plane orientations (n=153) of the Griqualand West Supergroup measured in the Map 2 area.

Figure 4.13: Small scale fold in Campbellrand Subgroup dolomite. Note the small shear zone dislocating the chert band in the core of the fold.

Figure 4.14: Equal area stereographic projection of small scale, pre-Olifantshoek Supergroup fold axes orientations (n=14) measured in the Map 2 area.

Figure 4.15: Tracing of a polished slab of Asbestos Hills Subgroup banded ironstone cut perpendicular to the fold axial plane. Extension parallel to the fold axial surface is indicated by the growth direction of the asbestos fibres.

Figure 4.16: Equal area, stereographic projection of fold axes (n=17) and axial planar cleavage (n=6) that developed in rocks of the Olifantshoek Supergroup during the Kheis orogeny (Map 2 area).

Figure 4.17: Equal area, stereographic projection of Olifantshoek Supergroup bedding planes (n=307) measured in the Map 2 area.

Figure 4.18: Equal area projection of Voelwater Subgroup bedding planes (n=24) measured in the Map 2 area.

Figure 4.19: Cross-section from A-C for the Map 2 area. Horizontal and vertical scales are equal.

Figure 4.20: Cross-section from D-F for the Map 2 area. Horizontal and vertical scales are equal.

Figure 4.21: Equal area stereographic projection (π -diagram) of foliation planes (n=325) from bedding sub-parallel shear zones and brittle-ductile thrust sense shear zones that developed during the Kheis orogeny. Map 2 area.

Figure 4.22: Equal area stereographic projection of mineral elongation and stretching lineations (n=155) that formed during the Kheis orogeny in the Map 2 area.

Figure 4.23: Photomicrograph of a Matsap Formation meta-psammite (proto-mylonite) from a bedding sub-parallel thrust sense shear zone. The "s" and "c" planes are indicated. Transmitted, cross-polarised light.

Figure 4.24: A highly strained conglomerate layer in the Matsap Formation. A stretching lineation defined by the long axes of elongated pebbles plunges obliquely down the plane of the foliation. Farm Zeekoebaart 306.

Figure 4.25: Photomicrograph of a mylonite from the Hartley Formation. Transmitted cross-polarised light.

Figure 4.26: Tight overturned folds in a bedding sub-parallel thrust sense shear zone developed in Voelwater Subgroup banded ironstones. The compositional banding dips north-west. Farm Zeekoebaart 306.

Figure 4.27: Photomicrograph of a sample of strongly foliated Voelwater Subgroup banded ironstone (Farm Zeekoebaart 306). S=Specularite, C=Crystalline hematite, Q=Quartz. Transmitted cross-polarised light.

Figure 4.28: A bedding sub-parallel shear zone in banded ironstone of the Asbestos Hills Subgroup. S-C fabrics indicate a north-west over south-east thrust sense of movement. South-east is to the right of the photograph.

Figure 4.29: Photomicrograph of Cu-mineralised veining developed at locality P1 (farm Zeekoebaart 306). Reflected plane-polarised light. Ch=Chalcocite, B=Bornite, C=Covellite Q=Quartz, S=Siderite.

Figure 4.30: Extensional quartz-specularite veins in banded chert of the Voelwater Subgroup. Viewed in cross-section. South is to the right of the photograph. Locality: Farm 312.

Figure 4.31: Plan view of the extensional veins illustrated in Figure 4.28. Quartz fibres have grown parallel to the extension direction.

Figure 4.32: View (looking south-east from locality D3- farm Bovenzeekoebaart 313) of the brittle-ductile thrust sense shear zone along which the Asbestos Hills Subgroup (AHS) has been thrust over the Mapedi Formation (MF) and the Campbellrand Subgroup (CS).

Figure 4.33: Sheath folds developed in banded ironstones of the Voelwater Subgroup. Locality D10- farm 312.

Figure 4.34: Small scale NNW plunging Namaqua folds developed in mylonitised Mapedi Formation quartzite (north is to the left of the photograph). A sub-vertical cleavage, axial planar to the small scale folds, crenulates the mylonitic foliation. Farm Bovenzeekoebaart 313- located in the brittle-ductile thrust sense shear zone north of locality D5.

Figure 4.35: Equal area, stereographic projection (π -diagram) of Namaqua fold axes (n=23) and cleavage (n=16) orientations for the Map 2 area

Figure 4.36: Fault breccia developed in Mapedi Formation quartzite along the western branch of the Doringberg fault. Locality D6-farm Bovenzeekoebaart 313.

Figure 4.37: Slickensided fault plane bounding the breccia shown in Figure 4.36. Note the gentle plunge of the slickenlines.

Figure 4.38: The western branch of the Doringberg fault at locality D7 (farm Bovenzeekoebaart 313). North is to the left of the photograph. The fault breccia zone (BZ) truncates a brittle-ductile thrust sense shear zone (TF), formed during the Kheis orogeny that has thrust dolomites of the Campbellrand Subgroup (CS) over banded ironstones of the Asbestos Hills Subgroup (AHS).

Figure 4.39: Lithostratigraphic column of the Griqualand West and Olifantshoek Supergroups in the Boegoeberg dam area. The disconformity at the base of the Makganyene Formation and the thickness of the Koegas Subgroup are based on observations by Beukes (1986) and Vajner (1974). The thickness of units in the hatched column is not to scale.

Figure 5.1: U-Pb concordia diagram of SHRIMP analyses of zircons from the Draghoender granite (Analyses performed by R.A. Armstrong).

Figure 5.2: The contact between the Zeekoebaart Formation (ZF) and the Skalkseput granite (SG). Locality 5.4.

Figure 5.3: The coarse grained pegmatoidal rock developed at the contact between the Skalkseput granite and the Zeekoebaart Formation. Note the lava xenolith (X) within the granite.

Figure 5.4: U-Pb concordia diagram of SHRIMP analyses of zircons from the Skalkseput granite (Analyses by R.A. Armstrong).

Figure 5.5: U-Pb concordia diagram of SHRIMP analyses of zircons from the Zeekoebaart Formation. (Analyses by R.A. Armstrong).

Figure 6.1: Geological map of the Marydale area.

Figure 6.2: A weakly foliated pegmatite vein cutting across strongly foliated quartzite and micaceous quartzite of the Spioenkop Formation. The vein passes under the pencil. (Locality M3- Figure 6.1).

Figure 6.3: Small scale F_1 folds with angular hinge zones that are refolded by a steeply plunging F_2 fold. Locality M2- Figure 6.1.

Figure 6.4: Equal area stereographic projection (β -diagram) of the orientations of bedding and S_1 foliation ($n=29$) measured in the D_2 low strain zone formed by unit Q.

Figure 6.5: Equal area, stereographic projection of L_2 lineations (mullions: $n=15$; elongation: $n=5$) from the low strain zone formed by unit Q.

Figure 6.6: Photomicrograph of a sample of siliceous quartzite from unit Q (low strain zone). Note the lack of foliation. Cross-polarised, transmitted light.

Figure 6.7: Photomicrograph of an annealed mylonite developed in a micaceous quartzite horizon at locality M2 (Unit MQ- high strain zone). Cross-polarised, transmitted light.

Figure 6.8: Equal area, stereographic projection of L_2 lineations (mullions: $n=23$; elongation: $n=5$), F_2 fold axes ($n=4$) and S_2 shear zone foliation ($n=14$) measured at locality M2.

Figure 6.9: Equal area, stereographic projection of bedding and the bedding sub-parallel S_1 foliation ($n=30$) measured at locality M2. 15

Figure 6.10: Equal area, stereographic projection of bedding and S_1 foliation planes ($n=29$) measured at locality 6.2. 15

Figure 6.11: Equal area, stereographic projection of L_2 mullion lineations ($n=24$) measured at locality 6.2. 15

Figure 6.12: Equal area, stereographic projection of bedding and S_1 foliation planes ($n=37$) measured at locality 6.3. 15

Figure 6.13: Equal area, stereographic projection of D_2 fabric elements and quartz veins measured at locality 6.3. 15
(S_2 Foliation $n=118$; D_2 quartz veins $n=7$; L_2 mullions $n=25$; L_2 elongation $n=34$; D_2 quartz fibres $n=5$)

Figure 6.14: Photomicrograph of a sample of Uitdraai Formation schist from locality 6.3. B=biotite, G=garnet, M=muscovite. Transmitted, plane-polarised light. 15

Figure 6.15: Plan view of a small scale sheath fold in the Uitdraai Formation. Locality 6.3. 15

Figure 6.16: F_2 anticline-syncline pair in siliceous grey quartzite of the Uitdraai Formation. The plane of section is orientated approximately east-west. Locality 6.3. 15

Figure 6.17: Geological map of the Blaauwputs area (Locality 6.4). 15

Figure 6.18: North-west trending F_2 fold that is overturned to the south-east. Location: southern slope of hill B2 (Figure 6.17). 16

Figure 6.19: Equal area stereographic projection of bedding and S_1 foliation planes ($n=15$) and L_2 mullion lineations ($n=21$) measured in the Blaauwputs area. 16

Figure 7.1: A simplified geological map of Zimbabwe (after Treloar, 1988). The area included in Figure 7.2 is outlined. Z=Zambezi belt, D=Dett inlier. 16

Figure 7.2: Simplified geological map of the Magondi belt (after Treloar, 1988). M=Makuti Group, U=Urungwe Klippe, UGr=Urungwe granite, UGn=Urungwe gneiss, CQ=Copper Queen granite dome, ★=Murereshi River locality. 16

Figure 7.3: Foliated Urungwe granite at the Murereshi river locality. The foliation, defined by biotite and feldspar phenocrysts, strikes parallel to the handle of the hammer. 17

Figure 7.4: U-Pb concordia diagram of zircon analyses from the Urungwe granite. Analyses performed by R.A. Armstrong. 17

Figure 7.5: Enlarged portion of Figure 7.4 showing the group of concordant U-Pb analyses that define a crystallisation age of 1997 ± 3 Ma for the Urungwe granite. 17

Figure 8.1: Regional features of the Late-Archaean crustal block comprising the Kaapvaal Craton, the Zimbabwe Craton and the Limpopo belt (modified after McCourt, 1995) 17

Figure 8.2: Conceptual models for thrust faults developed by the inversion of an extensional listric fault (from: McClay and Buchanan, 1992). 19

Figure 8.3: Cross section of the Variscan fold and thrust belt, south west Wales. (from: Powell, 1989). 19

Figure 8.4: Simplified geological map of the south-western part of the Kaapvaal Craton, the Kheis belt, the Kaaiken domain and the eastern part of the Namaqua belt. ①= Blackridge thrust; ②= Korannaberg thrust; ③= Doringberg fault; ④= Doornberg s.z.; ⑤= Copperton s.z.; ⑥= Brulpan fault; ⑦= Brakbos fault; ⑧= Dagbreek fault.; ⑨= Straussberg s.z.; ⑩= Boven-Rugzeer s.z. The approximate eastern boundary of Kheis belt is marked by ①. The boundary between the Kheis belt and Kaaiken domain is formed by ④, ⑥, dotted line and ⑦. The boundary between the Kaaiken domain and the Namaqua belt is marked by ⑤ and ⑨. T1, T2 and T3 refer to thrusts discussed in the text. A, B and C refer to the thrust sheets bounded by these thrusts. 19

Figure 8.5: Fold and thrust geometry of the Kechika trough, western Canadian Rocky mountains. The forward part of the fold and thrust belt exhibits geometry similar to the eastern part of the Kheis belt. The western part of the belt exhibits similar features to those described by Stowe (1986) for the western part of the Kheis belt. (From: McClay *et al.*, 1989). 19

Figure 8.6: Trace of the Hartley Formation-Fuller member contact extrapolated along the length of the cross-section of Traverse 2 (Figure 3.20) and a similarly constructed section for the Lucknow Formation-Hartley Formation contact for Traverse 3 (Figure 3.21). Restored and deformed lengths of these contacts are indicated. 19

Figure 8.7: Airborne magnetic image of the eastern part of southern Africa. KB=Kheis belt, KD=Kaaiken domain, KL=Kalahari line, TC=Tshane complex, O=Okwa basement complex, MB=Magondi belt, NMZ=Northern marginal zone (Limpopo belt), CZ=Central zone (Limpopo belt), SMZ=Southern marginal zone (Limpopo belt), M=Mahalapye plutonic block. Data courtesy of GEODASS. Image produced by CORNER GEOPHYSICS (Namibia). 20

Figure 8.8: An interpretation of the crustal architecture of southern Africa. From: Stowe *et al.* (1984). 20

Figure 8.9: Interpretation of the Kheis belt (KOB), Okwa basement complex (situated in the vicinity of Okwa) and the Magondi belt (MOB) as one continuous orogen. From: Carney *et al.* (1994). 20

LIST OF TABLES

	Page
Table 2.1: An overview of the stratigraphy of the study area including available age constraints and proposed correlations of units of uncertain stratigraphic position.	11
1: The Zonderhuis Formation is the lower part of the Wilgenhoutsdrif Group. The Leerkrans Formation (upper Wilgenhoutsdrif Group) has been excluded from this table.	
2: Scott (1987) proposed that the Spioenkop Formation be correlated with the Kaaiken Group. SAGS (1995) interpret the Spioenkop Formation to have a Mokolian metamorphic age (2070-1180Ma) but an uncertain depositional age.	
Table 2.2: The lithostratigraphy of the Marydale Group after SACS (1980).	12
Table 2.3: Stratigraphic subdivisions of the Zeekoebaart Formation (after Vajner, 1974).	14
Table 2.4: The stratigraphy of the Griqualand West Supergroup after Beukes (1986) and Beukes and Smit (1987). See text for source of age data and analytical techniques.	16
Table 2.5: Lithostratigraphy of the Olifantshoek Supergroup after Visser (1944).	21
Table 2.6: Lithostratigraphy of the Olifantshoek Supergroup after SACS (1980).	21
Table 2.7: Lithostratigraphy of the Volop Group after SACS (1980).	25
Table 2.8: The lithostratigraphy of the Kaaiken Group after SACS (1980).	27
Table 2.9: Correlation between the deformation phases recognised by previous workers and those used in this study.	32
Table 3.1: Composite stratigraphic column for the Voelwater Subgroup and Olifantshoek Supergroup rocks that form the Korannaberge and Langberge.	37
Table 3.2: Modal analyses of samples PS0715 and PS0716.	53
Table 4.1: Modal analysis of sample PS0791 from locality L8 (Boegoeberg Water Reserve).	100
Table 5.1: U-Th-Pb data from ion microprobe analyses of zircons from the Draghoender granite, the Skalkseput granite and the Zeekoebaart Formation. Uncertainties given at the one sigma level (Analyses performed by R.A. Armstrong).	133
Table 5.2: Stratigraphic subdivisions of the Zeekoebaart Formation (after Vajner, 1974).	138
Table 6.1: Correlation between the deformation phases recognised by previous workers and those documented in the southern part of the Kaaiken Domain.	162

Table 6.2: Proposed stratigraphic correlations between the Olifantshoek Supergroup, the Uitdraai Formation and the Spioenkop Formation. 165

Table 7.1: Summary of U-Pb SHRIMP analyses of zircons from the Urungwe granite. 173

Table 8.1: Generalised stratigraphy and age constraints for the Ventersdorp Supergroup. Age dates are U-Pb single zircon SHRIMP ages (in Ma) from Armstrong *et al.* (1991). 177

Table 8.2: Possible correlations between the Zonderhuis Formation rocks described by Moen (1980) and the Olifantshoek Supergroup. 197

LIST OF MAPS

MAP 1: Geological map of the Kheis belt

MAP 2: Geological map of the Boegoeberg ~~dam~~ area

TRAVERSE 1

TRAVERSE 2

TRAVERSE 3

TRAVERSE 4

LEGEND FOR TRAVERSES 1-4